The Dissertation Committee for Ping-Hui Szu Certifies that this is the approved version of the following dissertation:

The Biosynthesis of TDP-D-Desosamine: Characterization and Mechanistic Studies of DesII, a Radical *S*-Adenosylmethionine-dependent Enzyme

Committee:

Hung-wen Liu, Supervisor

Eric V. Anslyn

Walter L. Fast

Brent L. Iverson

Christian P. Whitman

The Biosynthesis of TDP-D-Desosamine: Characterization and Mechanistic Studies of DesII, a Radical *S*-Adenosylmethionine-dependent Enzyme

by

Ping-Hui Szu, B.S.

Dissertation

Presented to the Faculty of the Graduate School of

The University of Texas at Austin

in Partial Fulfillment

of the Requirements

for the Degree of

Doctor of Philosophy

The University of Texas at Austin

May 2008

Dedication

To my parents

Acknowledgements

First, and foremost, I would like to thank Professor Ben Liu for the opportunity to work in his lab at the University of Texas at Austin. His continuous support and encouragement during my Ph.D. studies were also greatly appreciated. Some of the assays presented in this dissertation are technically challenging due to the oxygen sensitivity of the [4Fe-4S] cluster of DesII. I appreciate Ben's infinite patience and encouragement that allowed me to persist and not to abandon this project at any point.

My project, like others in the Liu lab, was quite challenging. It was the first radical SAM enzyme project in the group. This provided a tremendous opportunity to learn new techniques and new chemistry. This work would not have been possible without the initial assistance from Dr. Feng Yan. Feng has an unusually broad and deep background in mechanistic enzymology, particularly in radical enzymology. He was instrumental in guiding me through the anaerobic techniques, EPR studies, and analogue design work. When I was writing my dissertation this spring, Feng had already left for his postdoc at the University of California at San Francisco. However, he still made time in his busy schedule to read my dissertation and provide critical comments. Dr. Wei-luen (Allen) Yu guided me through all of the molecular biology work. When I started my Ph.D. work, I had no background in molecular biology. Allen was always extremely

patient and always happy to answer my questions. He taught me numerous techniques from beginning to end. Dr. Yung-nan Liu provided initial guidance in protein purification. Dr. Xiaotao Pu's suggestions concerning the synthesis of the labeled substrate and the fluorinated substrate analogue were also deeply appreciated. Dr. Jeff Munos and Mr. Chris Thibodeaux provided great kinetics input.

Our collaborators, Professor Sheryl Tsai and Mr. Pete Smith at the University of California at Irvine, provided invaluable assistance in crystallographic studies of E_1 and E_3. This collaboration has sparked my interest in the power of structural biology, which I am going to pursue in my postdoctoral training. Sheryl also offered many constructive suggestions during my search for a postdoctoral position. For EPR spectroscopic studies, Professor Ah-Lim Tsai at the University of Texas-Houston Medical School, taught me how to operate the EPR instrument and provided important insight on interpreting EPR data.

A very special thanks goes to Professor Christian Whitman, who was the committee chair for my qualifier exam in the spring of 2004. Chris worked closely with me during my exam preparation and provided great advice on how to write a good grant proposal. He was also key in helping me to improve my English writing skills. He was extremely patient and always happy to answer my questions. I indeed benefited from the process. As a non-native speaker, I also obtained a lot of assistance from Chris during the course of my Ph.D. studies. Additionally, my coworkers including Dr. William Kittleman and Mrs. Jess White-Philip also provided considerable assistance in writing. William offered many helpful suggestions during the course of writing my dissertation. Jess was always happy to teach me how to speak good English. I deeply appreciate that Jess read

through this 200-page dissertation and corrected all grammatical errors. Many thanks goes to the rest of my coworkers in the Liu group for their day-to-day help. I would also like to thank my doctoral committee including Professor Eric Anslyn, Professor Walter Fast, Professor Brent Iverson, and Professor Christian Whitman. Late April is indeed a very busy time to schedule a defense. I appreciate that all of my committee members made their time available. Their valuable suggestions for my dissertation were also very much appreciated.

I deeply appreciate that my undergraduate advisor, Professor Yung-Son Hon at National Chung-Cheng University in Taiwan, strongly encouraged me to come to the US to pursue my PhD. Finally, I would like to thank my parents for their unending support and encouragement during my Ph.D. studies. Although we have been on different sides of the globe for six years, my mother always called to encourage me before all of my important events. My parents' continuous encouragement and support made me stronger and more confident.

The Biosynthesis of TDP-D-Desosamine: Characterization and Mechanistic Studies of DesII, a Radical *S*-Adenosylmethionine-dependent Enzyme

Publication No._____

Ping-Hui Szu, Ph.D.

The University of Texas at Austin, 2008

Supervisor: Hung-wen Liu

D-Desosamine, a 3-(dimethylamino)-3,4,6-trideoxyhexose found in a number of macrolide antibiotics including methymycin, neomethymycin, pikromycin, and narbomycin produced by *Streptomyces venezuelae*, plays an essential role in conferring biological activities to its parent aglycones. The proteins encoded by the *desI* and *desII* genes in the methymycin/pikromycin biosynthetic gene cluster have been proposed to catalyze C-4 deoxygenation in D-desosamine biosynthesis. DesI is a pyridoxal 5′-phosphate-dependent C4-aminotransferase and catalyzes a transamination reaction converting thymidine diphosphate (TDP)-4-keto-6-deoxy-D-glucose to TDP-4-amino-4,6-dideoxy-D-glucose. DesII, which contains a [4Fe-4S] cluster binding motif, CXXXCXXC, has been identified as a member of the radical *S*-adenosylmethionine (SAM) enzyme superfamily by sequence analysis. To study the catalytic function of DesII, the *desII* gene was heterologously overexpressed in *Escherichia coli* and the DesII

protein was purified to near homogeneity. Biochemical studies clearly established that the substrate for DesII is TDP-4-amino-4,6-dideoxy-D-glucose, and DesI and DesII function independently to carry out C-4 deoxygenation. DesII requires a $[4Fe\text{-}4S]^{1+}$ center and *S*-adenosylmethionine for activity. Accordingly, the originally proposed mechanism for C-4 deoxygenation in which DesI and DesII function together was revised. Two possible mechanisms have subsequently been proposed for the DesII reaction. The DesII catalysis is likely initiated by the formation of a 5'-deoxyadenosyl radical followed by the C-3 hydrogen atom abstraction. In the first possible route, the key step is a radical-induced deamination followed by the readdition of ammonia to the resulting cation radical intermediate, which is effectively a 1,2-amino shift, to form an aminol radical. Alternatively, the reaction may involve deprotonation of the 3-hydroxyl group to yield a ketyl radical anion to facilitate the β-elimination of the ammonia group. Interestingly, DesII is flexible towards TDP-D-quinovose and TDP-3-amino-3,6-dideoxy-D-glucose. A possible biological reducing system, flavodoxin, flavodoxin reductase, and NADPH, for the reduction of the $[4Fe\text{-}4S]^{2+}$ cluster, was also identified. Deuterium incorporation into SAM using C-3 deuterium-labeled substrate provides solid evidence for C-3 hydrogen atom abstraction by the 5'-deoxyadenosyl radical in the proposed mechanism. TDP-3-fluoro-3,6-dideoxy-D-glucose serves as a competitive inhibitor for DesII, which is in favor of deprotonation of the C-3 hydroxyl group being involved in DesII catalysis.

Table of Contents

List of Tables

List of Figures

Chapter 1: Background and Significance

1.1 DEOXY SUGARS IN MACROLIDE ANTIBIOTICS

Deoxy sugars are an essential class of carbohydrates which exist ubiquitously in Nature as mono-, di-, tri-, and even tetradeoxy species, often contributing to a diverse repertoire of biological activities (*1, 2*). For example, D-desosamine (**1-1**), a 3-(dimethylamino)-3,4,6-trideoxyhexose found in a number of macrolide antibiotics including methymycin (**1-2**), neomethymycin (**1-3**), pikromycin (**1-4**), and narbomycin (**1-5**) produced by *Streptomyces venezuelae*, plays an essential role in conferring biological activities to its parent aglycones (*3*) (Figure 1-1). In the following sections, a brief discussion including some examples of deoxy sugars found in macrolide antibiotics and a brief introduction of the formation of desosamine from the pikromycin biosynthetic pathway are presented.

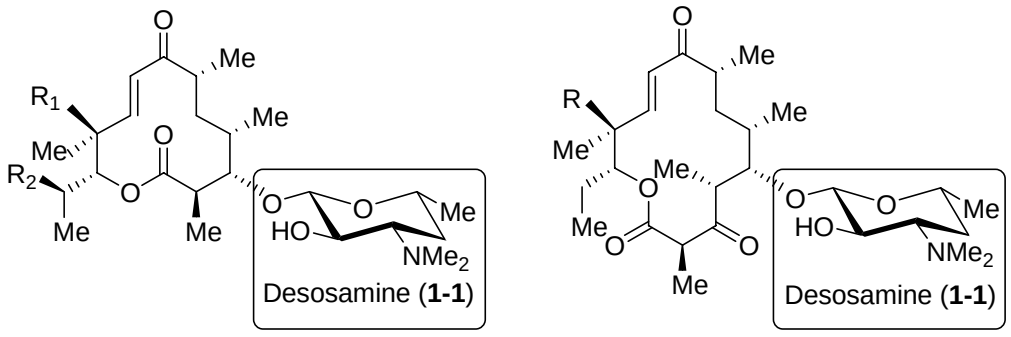

R_1=OH, R_2=H: methymycin (**1-2**)
R_1=H, R_2=OH: neomethymycin (**1-3**)

R=OH: pikromycin (**1-4**)
R=H: narbomycin (**1-5**)

Figure 1-1. Macrolide antibiotics produced by *Streptomyces venezuelae*.

1.1.1 Occurrence and Importance

Macrolide antibiotics are an important group of compounds due to their potent activity against gram-positive bacteria (*4*). The ring size of the aglycone lactone can vary, but generally contains either 12, 14, or 16 atoms. Examples include methymycin (**1-2**), a 12-membered ring macrolide, pikromycin (**1-4**), erythromycin A (**1-6**), and oleandomycin (**1-7**), which are 14-membered ring macrolides, and tylosin (**1-8**) and spiramycin (**1-9**), which are 16-membered ring macrolides (*1*) (Figure 1-2). Deoxysugars are commonly found as prominent structural components in macrolide antibiotics. For example, methymycin, pikromycin, erythromycin A, and oleandomycin share a common sugar moiety, D-desosamine. Erythromycin A carries a second sugar, L-cladinose (**1-10**). Oleandomycin also contains an additional sugar, L-oleandrose (**1-11**). Tylosin and spiramycin both have L-mycarose (**1-12**) and D-mycaminose (**1-13**), whereas tylosin also carries D-mycinose (**1-14**) and spiramycin contains D-forosamine (**1-15**), which is a tetradeoxy sugar (*1*).

Macrolide antibiotics inhibit bacterial protein biosynthesis by blocking the 50S ribosome through specific binding with the 23S ribosomal subunit and various other proteins (*5*). The deoxyhexose moieties of macrolides are essential for their interactions with the peptidyl transferase cavity of 23S ribosomal RNA. In fact, the crystal structures of the 50S ribosomal subunit of the eubacterium *Deinococcus radiodurans* complexed with the clinically useful antibiotic, erythromycin, revealed that 2'-hydroxyl group of the desosamine moiety forms hydrogen bonds with nitrogen atoms of adenosine 2058 and 2059 in the peptidyl transferase cavity. Additionally, the protonated form of 3'-dimethylamino group of desosamine was found to interact with the backbone oxygen of

guanosine 2505 in the peptidyl transferase cavity through ionic interactions (*6*). Understanding the formation of deoxysugars in detail in combination with the current knowledge of the macrolide aglycone biosynthesis (*7*, *8*) could provide an entirely new vantage point for biosynthetic engineering of glycosylated natural products in the future.

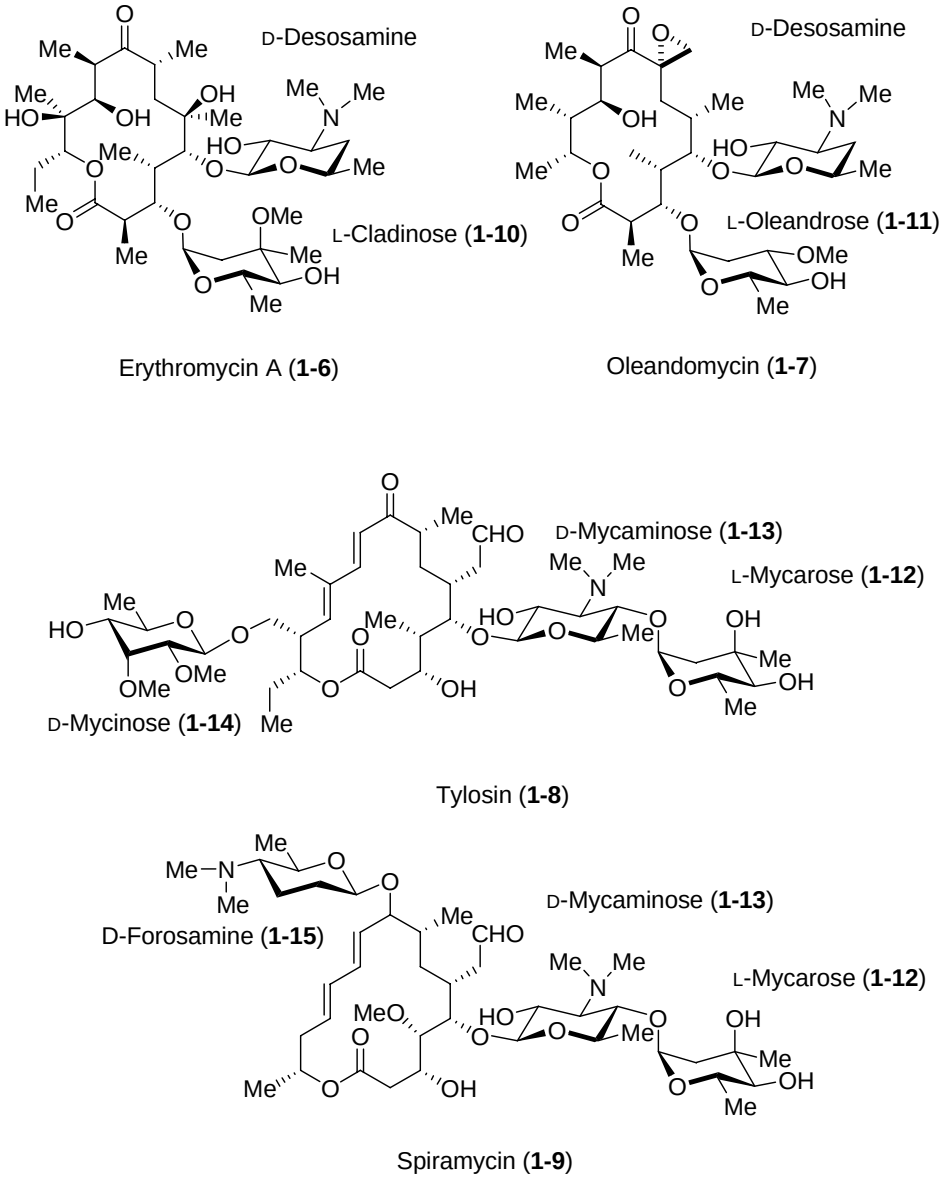

Figure 1-2. Structures of macrolide antibiotics, erythromycin A, oleandomycin, tylosin, and spiramycin.

1.1.2 Desosamine Biosynthesis

(a)

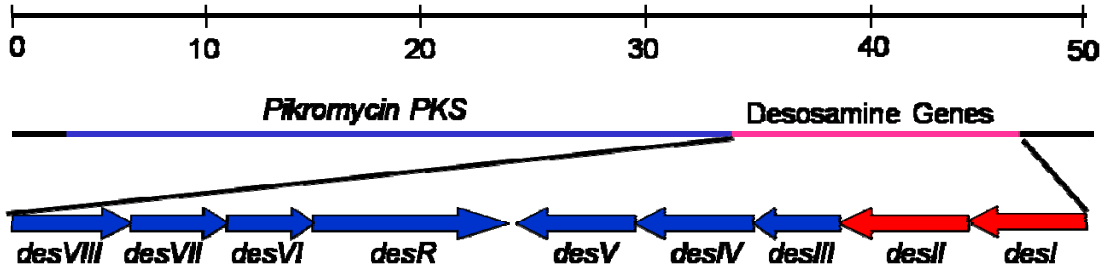

(b)

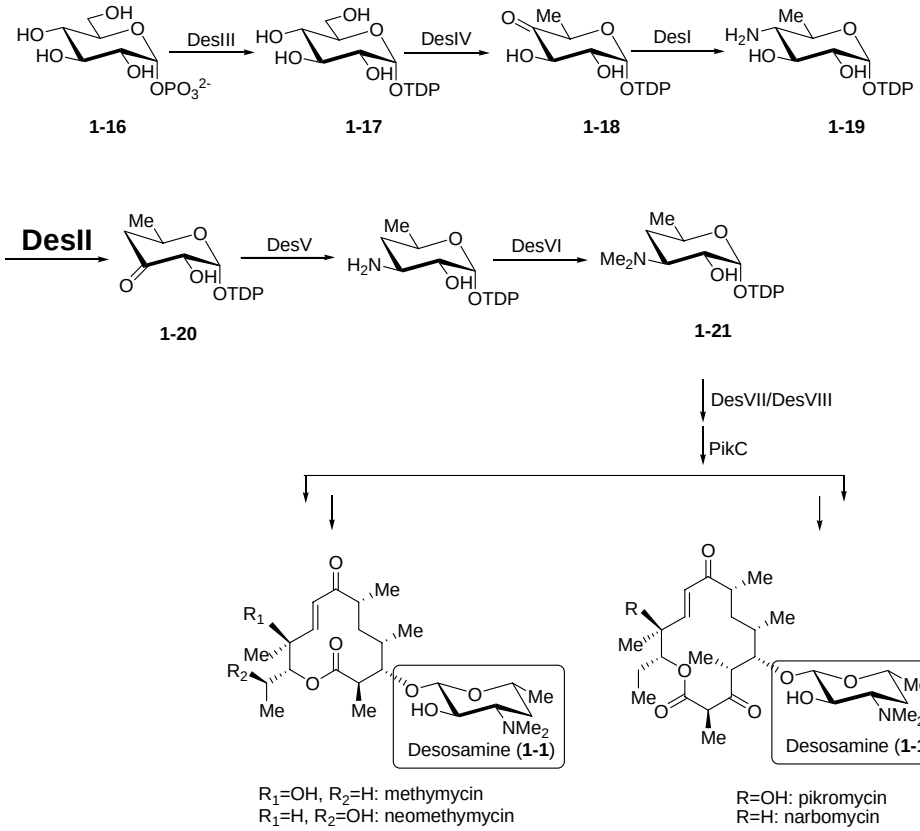

Figure 1-3. (a) Desosamine biosynthetic gene cluster from *Streptomyces venezuelae*. (b) TDP-D-desosamine pathway in the biosynthesis of methymycin neomethymycin, pikromycin, and narbomycin in *S. venezuelae*.

Previous studies on the pikromycin/methymycin biosynthetic gene cluster from *Streptomyces venezuelae* have determined that the desosamine biosynthetic gene cluster is a 13-kb stretch of DNA and contains nine open reading frames (*3*) (Figure 1-3a). Among the nine open reading frames, eight (*desI-desVIII*) were suggested to be directly involved in desosamine biosynthesis. Immediately upstream of the desosamine biosynthetic genes is a cluster of polyketide synthase genes (*pikA*), which encode proteins involved in macrolide formation. Organized into four multifunctional proteins in addition to a type II thioesterase (TEII), PikA consists of six catalytic modules, each containing a unique set of covalently linked catalytic domains. Pikromycin polyketide synthase has the unusual ability to efficiently generate two macrolactone products of differing ring size, biosynthesizing both 12 and 14-membered rings. Methymycin (**1-2**) and neomethymycin (**1-3**) are derived from the 12-membered ring macrolactone 10-deoxymethynolide, whereas pikromycin (**1-4**) and narbomycin (**1-5**) are derived from the 14-membered ring macrolactone, narbonolide (*3*). The D-desosaminyl glycosyltransferase, DesVII, along with its auxiliary protein DesVIII catalyzes the glycosyltransfer reaction, which confers the antibiotic activity to pikromycin (*9, 10*). The biosynthesis of TDP-D-desosamine (TDP = thymidine diphosphate) involves six enzymes starting from the coupling of glucose-1-phosphate (**1-16**) with thymidine triphosphate (TTP) catalyzed by α-D-glucose-1-phosphate thymidylyltransferase (DesIII) to generate TDP-D-glucose (**1-17**) (Figure 1-3b). The subsequent C-6 deoxygenation is catalyzed by a nicotinamide adenine dinucleotide (NAD^+)-dependent nucleotidyldiphosphohexose (NDP-hexose) 4,6-dehydratase (DesIV), affording **1-18**. The key step in desosamine biosynthesis, C-4 deoxygenation, is catalyzed by DesI and DesII, which are a pyridoxal 5′-phosphate

(PLP)-dependent C-4 aminotransferase and a radical *S*-adenosylmethionine (SAM)-dependent C-4 deaminase, respectively (*11, 12*). The enzymatic mechanisms for C-6 deoxygenation and C-4 deoxygenation are presented in the next section. Subsequently, DesV catalyzes a PLP-dependent C-3 aminotransfer reaction, followed by C-3 *N*,*N*-dimethylation catalyzed by DesVI, an *N*,*N*-dimethyltransferase, to generate TDP-D-desosamine (**1-21**) (*13*). This C-3 *N*,*N*-dimethylamino group exhibits an important function to confer the biological activity of desosamine in macrolide antibiotics (*6*).

1.2 Mechanisms of Enzymatic Carbon-Oxygen Bond Cleavage in Deoxyhexose Biosynthesis

Carbon-oxygen bond cleavage is one of the most important reactions in biological systems. Diverse approaches are applied to achieve this carbon-oxygen bond cleavage at various positions of the hexose ring (*14-16*). A few representative enzymes and their respective reactions are presented in Table 1-1. Previous deoxy sugar biosynthetic studies have determined that a common biosynthetic precursor for most deoxyhexoses is a nucleotidyldiphospho-4-hexulose. The modes of different deoxygenation reactions are determined by the position of the carbon-oxygen bond to be cleaved, i.e., whether it is α or β to the 4-keto group (Figure 1-4). A brief review of the current knowledge of deoxygenation mechanisms at C-2, C-3, C-4, and C-6 involved in the generation of the corresponding deoxysugars is presented in the following section. Insights into these enzymatic processes may be useful for the development of rational strategies to generate new deoxy sugars. Such a biosynthetic approach to produce novel glycoconjugates offers

an opportunity to optimize the pharmacological properties of the parent secondary metabolites.

Reaction	Representative Enzyme
C2 Deoxygenation	**TylX3**
C3 Deoxygenation	**E_1/E_3**
C6 Deoxygenation	**E_{od}**

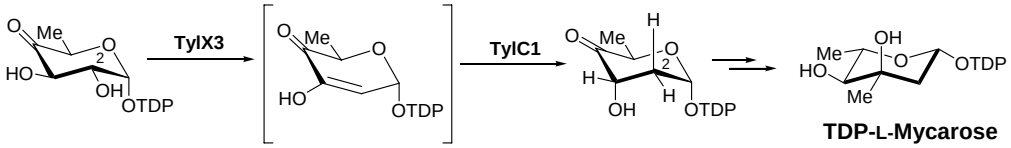

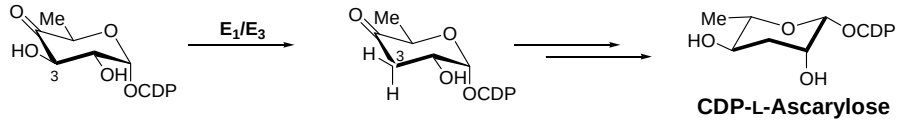

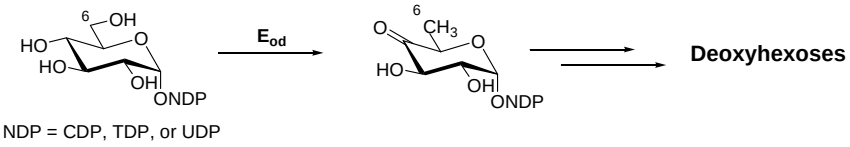

Table 1-1. The C2, C3, and C6 deoxygenation and their representative enzymes.

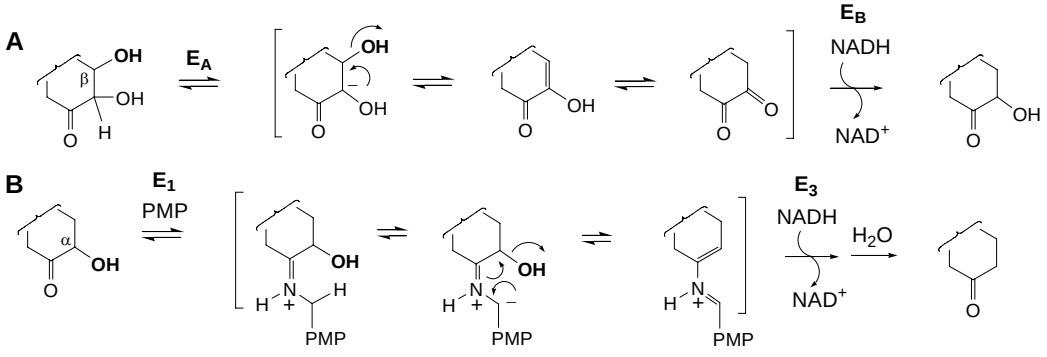

Figure 1-4. A prototypical mechanism for α-deoxygenation and β-deoxygenation of a ketosugar substrate.

1.2.1 CARBON-OXYGEN BOND CLEAVAGE AT THE C-6 POSITION

The C-6 deoxygenation, catalyzed by a nicotinamide adenine dinucleotide (NAD^+)-dependent nucleotidyldiphosphohexose (NDP-hexose) 4,6-dehydratase (E_{od}), is the first committed step in the biosynthetic pathways of most deoxyhexoses (*14-16*) (Figure 1-5). E_{od} is a member of the short-chain dehydrogenase/reductase (SDR) family (*17*) and converts an NDP-hexose (**1-22**) to a corresponding NDP-4-keto-6-deoxyhexose (**1-25**). Enzymes in the SDR family contain a conserved protein fold that binds a nicotinamide adenine dinucleotide cofactor (either NAD^+ or $NADP^+$, denoted $NAD(P)^+$) which plays an essential role in catalysis.

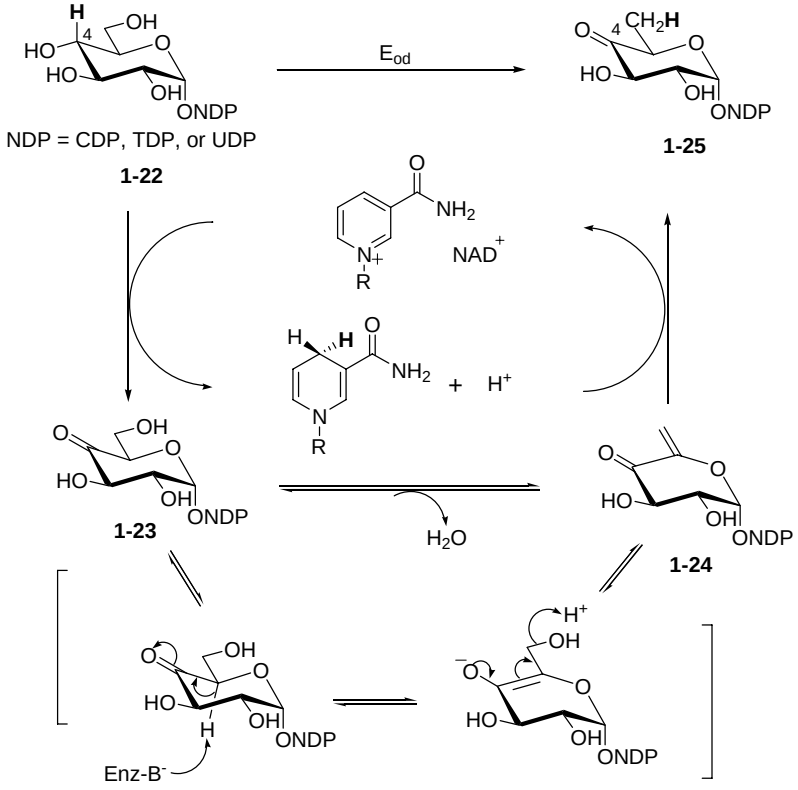

Figure 1-5. The mechanism of the C6 deoxygenation catalyzed by E_{od}.

The enzymatic reaction of C-6 deoxygenation involves three sequential steps (i.e., an oxidation-dehydration-reduction process) as shown in Figure 1-5. First, oxidation occurs regiospecifically at the C4 hydroxyl group, converting the substrate NDP-D-glucose (**1-22**) to a 4-ketosugar intermediate (**1-23**) with concomitant reduction of NAD^+. Subsequently, proton abstraction at C-5 triggers the elimination of water to generate a 4-keto-$\Delta^{5,6}$-glucoseen intermediate (**1-24**), which is then reduced by NADH to give the product, NDP-6-deoxy-4-keto-glucose (**1-25**). Interestingly, the nicotinamide cofactor is regenerated at the end of enzyme turnover. It serves as a true prosthetic group in this case, in contrast to most NAD(P)-dependent enzymes where it serves as a co-substrate. Based on the crystal structure of TDP-D-glucose 4,6-dehydratase (RmlB) from *Salmonella enterica serovar* Typhimurium, the conserved tyrosine 167 was identified as the active-site base involved in deprotonation of the C-4 hydroxyl group. The conserved aspartic acid 134 and glutamic acid 135 function as the general acid and base to catalyze the dehydration step (*18*). The C-6 deoxygenation generates a C-4 ketosugar, and the C-4 keto group activates the pyranose ring for the subsequent modifications in the biosynthesis of many unusual sugars.

1.2.2 Carbon-oxygen bond cleavage at the C-2 position

2-Deoxyhexoses are commonly found as prominent structural components in bacterial secondary metabolites, such as polyketide and aminoglycoside antibiotics. Examples include L-rhodinose in aromatic polyketide antibiotic granaticin B (*19*), mycarose in macrolide antibiotic tylosin (*20*), and *N*-methyl-L-glucosamine found in aminoglycoside antibiotic streptomycin (*21*) (Figure 1-6).

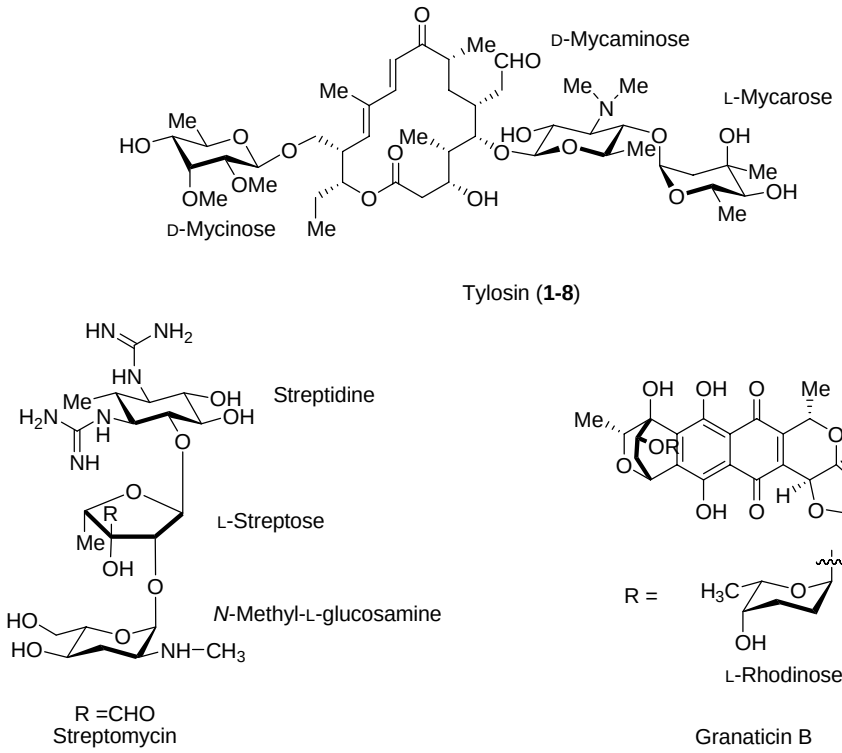

Figure 1-6. Examples of antibiotics containing 2-deoxysugars, such as tylosin, streptomycin, and granaticin B.

The C-2 deoxygenation catalyzed by TylX3 in the TDP-L-mycarose biosynthetic pathway of *Streptomyces fradiae* is analogous to the reaction mechanism for C-6 deoxygenation reaction sequence *(20)* (Figure 1-7). This reaction sequence proceeds through α-proton abstraction followed by β-carbon-oxygen bond cleavage. The formation of the C-4 keto group in TDP-4-keto-6-deoxy-glucose (**1-18**) lowers the pK_a of the adjacent C-3 hydrogen, which facilitates the deprotonation at C-3, and the subsequent elimination of the C-2 hydroxyl group to give **1-27**. TylX3 requires a Zn^{2+} ion for catalysis and there are three possible roles for this metal cation. First, Zn^{2+} could activate an active-site-bound water, which serves as a base in C-3 deprotonation. Second, it could

function as a Lewis-acid to facilitate the elimination of the C-2 hydroxyl group. Third, it may stabilize the enediolate intermediate **1-26**.

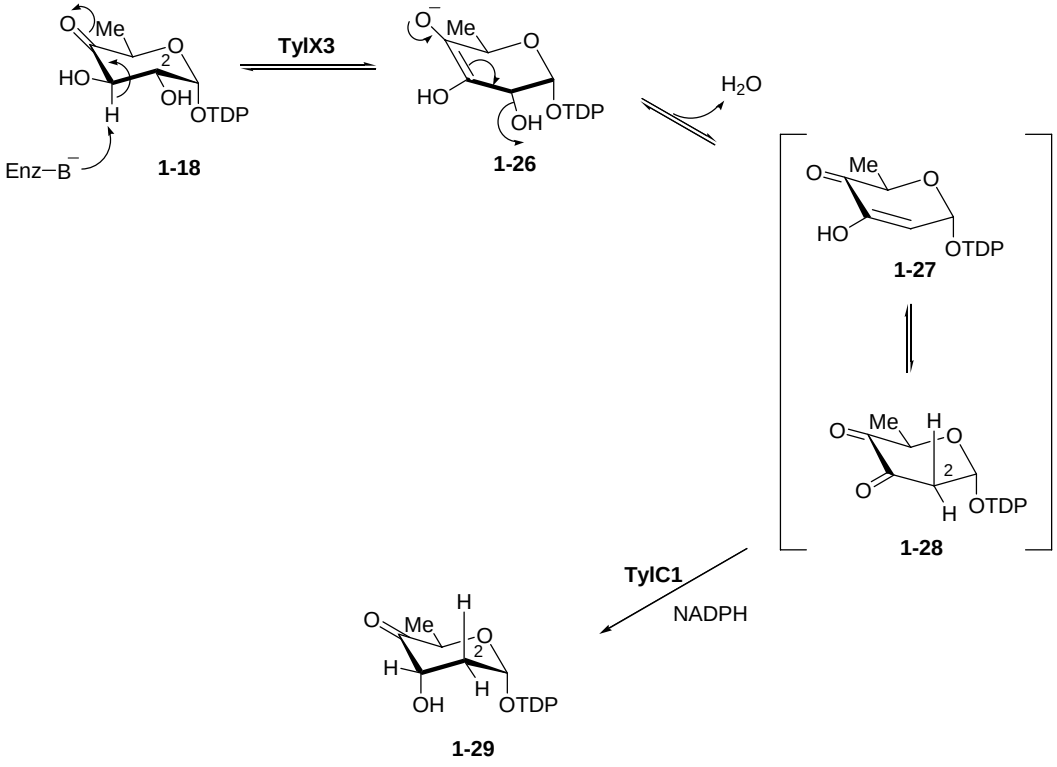

Figure 1-7. The mechanism of the C2 deoxygenation catalyzed by TylX3.

Tautomerization of **1-27** generates the labile 3,4-diketone **1-28**, which is reduced in the presence of the next enzyme in the pathway, the NADPH-dependent C3-ketoreductase, TylC1, to afford the 2,6-dideoxyhexose **1-29**. The joint action between TylX3 and TylC1 is necessary to prevent the release of the unstable intermediates (**1-27**/**1-28**) in the biosynthetic pathway. However, evidence from the yeast two hybrid assay and gel filtration chromatography suggested such a TylX3 and TylC1 complex was not formed.

1.2.3 Carbon-oxygen bond cleavage at the C-3 position

The mechanism of C-3 deoxygenation in the biosynthesis of 3,6-didexysugars (such as **1-30**, Figure 1-8) is more complicated than either C2 or C6 deoxygenation. Since the scissile carbon-oxygen bond is adjacent to the 4-keto group, the carbon-oxygen bond cleavage cannot be assisted by the activation of the hydrogen positioned α to the 4-keto group. Thus, a different strategy must be applied to achieve C3 deoxygenation. Significant efforts have been devoted to the elucidation of the enzymatic mechanism underlying C3 deoxygenation. The 3,6-dideoxyhexoses, found predominantly in the *O*-antigen of lipopolysaccharides (LPS) (*22*), have been shown to be the major antigenic determinants of some Gram-negative bacteria (*23*). In Nature, CDP-6-deoxy-L-*threo*-D-*glycero*-4-hexulose-3-dehydrase (E_1), along with its reductase (E_3), catalyze the C-3 deoxygenation of CDP-4-keto-6-deoxy-D-glucose (**1-31**) in the presence of NADH to form CDP-4-keto-3,6-dideoxy-D-glucose (**1-30**) in the 3,6-dideoxyhexose biosynthetic pathway (Figure 1-8) (*16*). Product **1-30** is the common precursor for at least four of the seven naturally occurring 3,6-dideoxyhexoses, namely abequose (**1-32**), ascarylose (**1-33**), paratose (**1-34**), and tyvelose (**1-35**, Figure 1-8) (*16*). The importance of 3,6-dideoxyhexoses to the pathogenicity of the Gram-negative carriers makes E_1 an appealing target for antibiotic development against the host Gram-negative bacteria. Crystal structural studies of E_1 currently underway may facilitate the development of E_1-targeting antibiotics (*24*).

As shown in Figure 1-8, E_1 alone catalyzes the reversible dehydration of **1-31** via Schiff-base formation with the cofactor pyridoxamine 5'-phosphate (PMP) to give **1-36**, followed by 1,4-dehydration to give **1-37**. Reduction of the dehydrated product **1-37** by

the reductase E_3 forms **1-39**, which after hydrolysis yields the product **1-30** and regenerates PMP (*25, 26*). Both E_1 and E_3 contain a [2Fe-2S] cluster, and E_3 also contains a tightly bound flavin adenine dinucleotide (FAD) in the active site (*27*). The E_1-E_3 mechanism is intriguing because it involves two single-electron transfers from NADH-reduced E_3 to E_1 via the respective [2Fe-2S] clusters to reduce **1-37** (*16*). During this process, the PMP cofactor of E_1 participates directly in the single-electron redox chemistry by stabilizing an unpaired electron spin in the electron-transfer reduction (*28, 29*). While the reaction catalyzed by lysine aminomutase also involves a PLP-stabilized radical (*30*), the formation of a cofactor-based radical (**1-38**) makes the E_1 reaction unique.

The E_1 sequence is homologous to those in the PLP-containing aspartate aminotransferase (AAT) superfamily (*31*). Several of these AAT family enzymes, such as E_1, serve as dehydrases or aminotransferases in the nucleotide sugar biosynthetic pathways (*32-35*). However, E_1 contains a [2Fe-2S] cluster in addition to PMP (*36*), distinguishing E_1 from these other enzymes. This unusual structural feature is even more intriguing because the cysteine ligands of the iron-sulfur cluster have a C-X_{57}-C-X_1-C-X_7-C motif, which is unique among [2Fe-2S]-containing enzymes (*37*). In the absence of an E_1 structure, the unusual dehydration-radical reduction mechanism catalyzed by E_1 is not fully understood. Thus, current efforts have been focused on the determination of the crystal structure of E_1, which can help verify the configuration of this unique [2Fe-2S] cluster and visualize the path of the electron relay from the iron-sulfur center to the PMP-coenzyme site. These studies will provide the structural basis to elucidate the distinct PMP-radical mechanism observed in E_1.

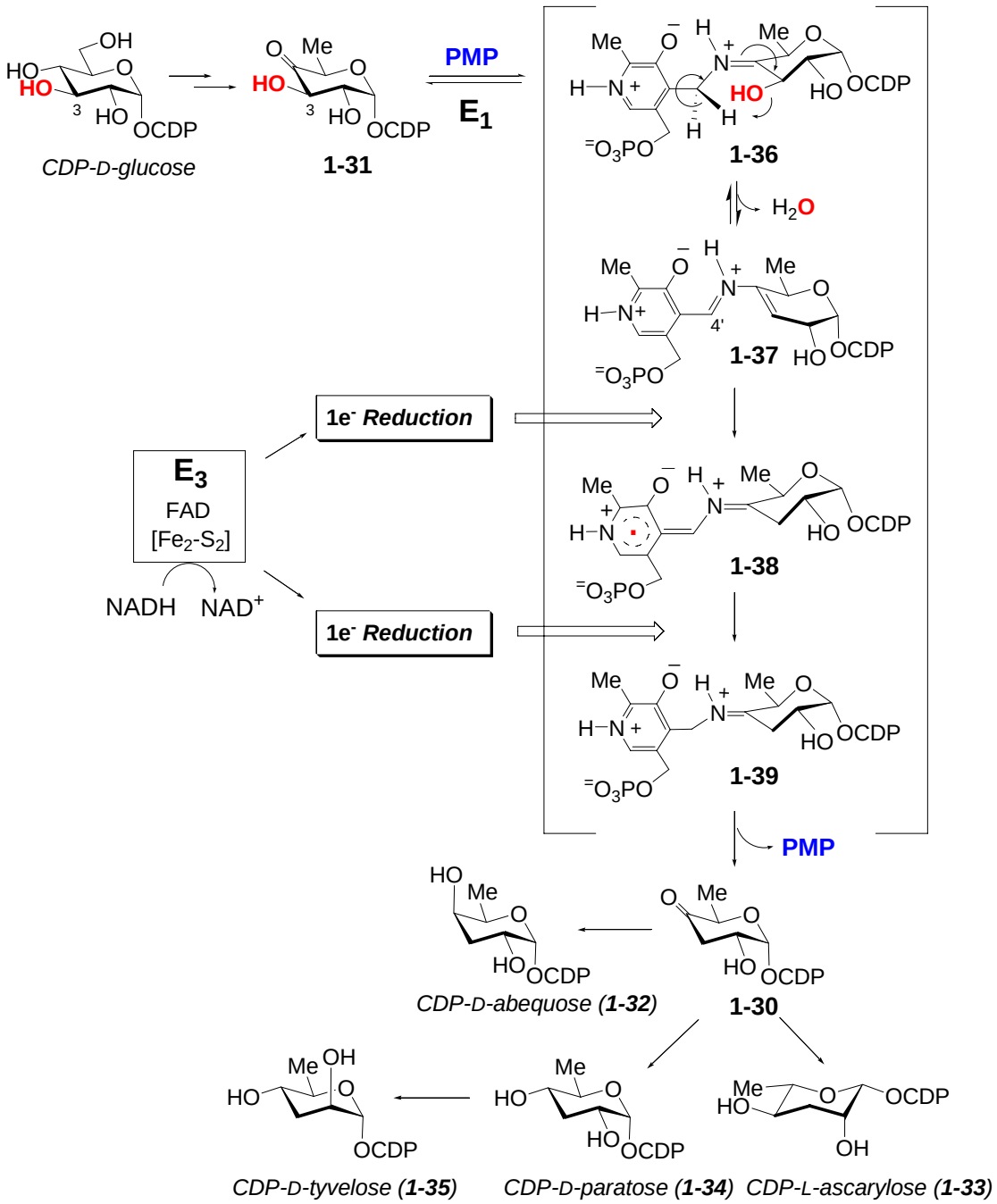

Figure 1-8. The mechanims of the C3 deoxygenation catalyzed by E_1/E_3.

1.2.4 Carbon-oxygen bond cleavage at the C-4 position

Compared to the deoxygenation mechanisms at C-2, C-3, and C-6, very little is known about the C-4 deoxygenation involved in the biosynthesis of desosamine from *Streptomyces venezuelae*. It was originally proposed that the C-4 deoxygenation follows a strategy similar to that applied in the C-3 deoxygenation catalyzed by E_1 and E_3 as previously described (*36, 38*). This possibility is supported by the fact that the translated sequences of two genes, *desI* and *desII*, which are assigned to encode proteins involved in the C-4 deoxygenation in the desosamine biosynthetic gene cluster (*3, 39*), are similar to B_6-dependent enzymes and those containing an iron-sulfur center, respectively. However, later characterization of the purified DesI protein showed that it catalyzes the C-4 transamination of **1-18** (Figure 1-3b) to generate TDP-4-amino-4,6-dideoxy-D-glucose (**1-19**) in the presence of pyridoxal 5′-phosphate (PLP) and L-glutamate (*11*). Further sequence analysis revealed that DesII, which contains a [4Fe-4S] consensus motif (CXXXCXXC), belongs to the recently identified radical *S*-adenosylmethionine (SAM) enzyme superfamily (*40*). These two observations prompted a revision of the proposed biosynthetic pathway for TDP-D-desosamine. As depicted in Figure 1-9, the DesI/DesII reaction may be initiated by the incorporation of a nitrogen-containing functional group from PMP at C-4 (such as **1-40**), followed by the radical-induced 1,2-nitrogen shift (**1-40→1-41→1-43→1-44**) to yield an aminol intermediate (such as **1-45**). Subsequent elimination of an ammonium ion would afford the predicted product **1-20**. The regeneration of PMP may be facilitated by the transamination activity of DesI in the presence of L-glutamate.

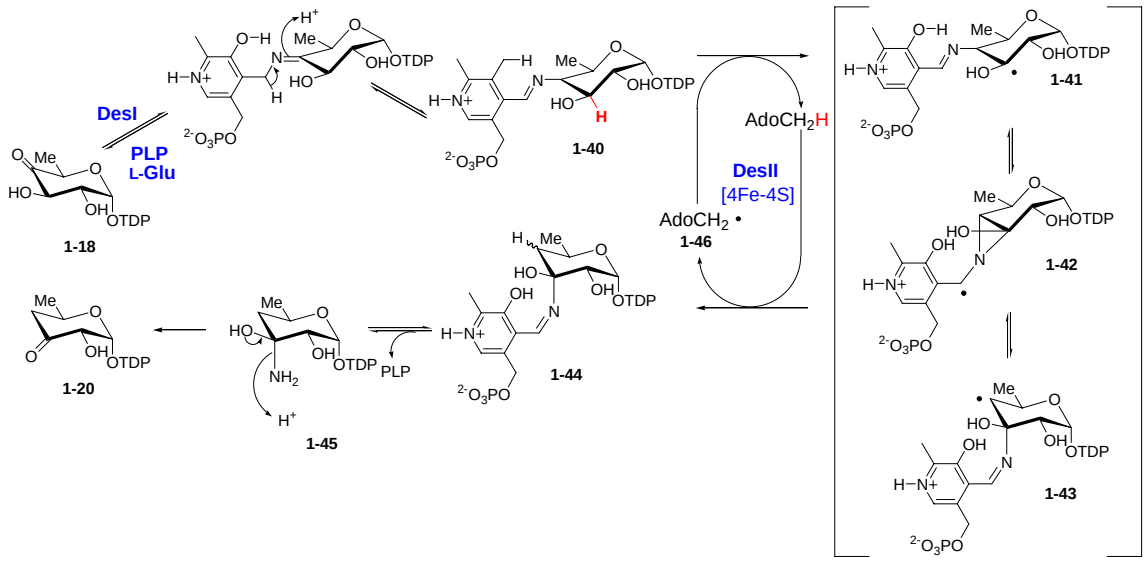

Figure 1-9. The original mechanims of C4 deoxygenation catalyzed by DesI and DesII.

The key mechanistic components of this reaction are reminiscent of those used in the reaction catalyzed by lysine 2,3-aminomutase (LAM), which is a [4Fe-4S]-containing enzyme that requires PLP and SAM for activity (*41-43*). Catalysis by LAM is triggered by the abstraction of a hydrogen atom from the lysine-PLP adduct by the 5′-deoxyadenosyl radical ($AdoCH_2$•, **1-46**, Figure 1-9), which is formed by the reductive cleavage of SAM through the reduced [4Fe-4S] center (*44*). A more detailed discussion regarding the reaction catalyzed by LAM is presented in section 1.3.3. A similar abstraction of a hydrogen atom, induced by the 5′-deoxyadenosyl radical (**1-46**), from **1-40** at C-3 to give **1-41** may also be the key event of the C-4 deoxygenation reaction. However, the recent biochemical characterization of DesII has demonstrated that DesII can recognize the DesI product (**19**, Figure 1-10) as a substrate, which suggests that DesI and DesII function independently to achieve the C-4 deoxygenation (*12*). A revised

mechanistic proposal was necessary to account for these observations. In these revised mechanisms, DesI and DesII function as a C-4 aminotransferase and C-4 deaminase, respectively. Similarly, the generation of the 5'-deoxyadenosyl radical (**1-46**, Figure 1-10) in the first part of the reaction is facilitated by the reduced $[4Fe\text{-}4S]^{+}$. The chemical transformation is likely triggered by a hydrogen atom abstraction at C-3 of the substrate (**1-19**) by the 5'-deoxyadenosyl radical, followed by two possible routes (A and B). In route A, the amine migration is similar to the proposed mechanisms for B_{12}-dependent ethanolamine ammonia-lyase (*45*). In route B, deprotonation of the 3-hydroxyl group of **1-47** yields a ketyl radical anion **1-48**, whose resonance form facilitates the β-elimination of the 4-amino group to generate enol radical **1-49** (*46*). A detailed discussion regarding the revised mechanisms is presented in Chapter 3.

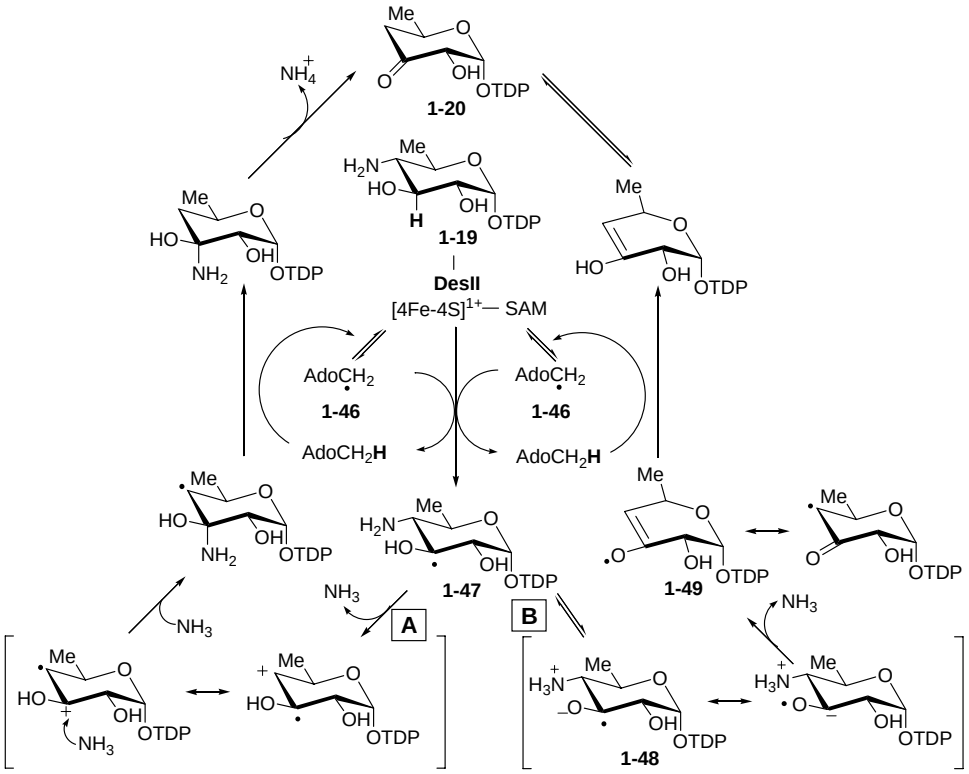

Figure 1-10. The revised mechanims of C4 deoxygenation catalyzed by DesI and DesII.

1.3 RADICAL *S*-ADENOSYLMTEHIONINE (SAM) ENZYME SUPERFAMILY

The radical *S*-adenosylmethionine (SAM) enzyme superfamily includes more than 2800 proteins. These enzymes catalyze a variety of radical reactions, such as isomerization, protein radical formation, sulfur insertion, ring formation, anaerobic oxidation, and unusual methylations (*40, 42*). They function in the biosynthesis of DNA precursors, cofactors, vitamins, herbicides, and antibiotics, and also participate in various biodegradation pathways. A partial list of radical SAM enzymes and their biological functions are presented in Table 1-2. The enzymes in this superfamily share a conserved sequence motif, CXXXCXXC, which coordinates a required [4Fe-4S] cluster. In addition to this conserved sequence motif, this class of enzymes also contains a glycine-rich sequence, which resembles the SAM binding site in the SAM-dependent methyltransferases. In fact, a SAM cofactor is always required for catalysis. The roles of the [4Fe-4S] cluster and the SAM cofactor in the enzymatic reactions, and the interaction between the [4Fe-4S] cluster and SAM will be discussed in section 1.3.1. In the following sections, a brief review of radical SAM-dependent enzymes which have been characterized in detail to date is presented. Examples include lysine 2,3-aminomutase, which catalyzes the interconversion of L-lysine and L-β-lysine, anaerobic ribonucleotide reductase-activase and pyruvate formate lyase-activase which activate the radical enzymes by glycyl radical formation, biotin synthase and lipoyl synthase, which catalyze sulfur insertion reaction (*41*).

Protein	Function	Reference
LAM	Amino group rearrangement	Ruzicka *et al.* (*47*)
BlsG	Amino group rearrangement	Cone *et al*. (*48*)
Eam	Amino group rearrangement	Ruzicka *et al*. (*49*)
SplB	Spore photoproduct lyase	Rebeil *et al*. (*50*)
DesII	Desosamine biosynthesis	Zhao *et al*. (*11*)
Littorine mutase	Alkaloid biosynthesis	Ollagnier *et al. (51)*
PFL activase	Formation of glycyl radical	Wong *et al*. (*52*)
ARR activase	Formation of glycyl radical	Eliasson *et al.* (*53*)
Glycerol dehydrase activase	Formation of glycyl radical	O′Brien *et al. (54)*
Hydroxyphenylacetate Decarboxylase activase	Formation of glycyl radical	Yu *et al*. (*55*)
BioB	Sulfur insertion	Duin *et al*. (*56*)
LipA	Sulfur insertion	Reed *et al*. (*57*)
BchE	Bacteriochlorophyll biosynthesis	Suzuki *et al*. (*58*)
HemN	Coproporphyrinogen III oxidase	Akhtar *et al*. (*59*)
MoaA	Molybdopterin biosynthesis	Rieder *et al*. (*60*)
MiaB	Methylthiolation of tRNA	Esberg *et al*. (*61*)
TYW1	Wybusine biosynthesis in $tRNA^{Phe}$	Noma *et al*. (*62*)
ThiH	Biogenesis of thiazole in thiamine	Begley *et al*. (*63*)
PqqE	Pyrroloquinoline quinine biosynthesis	Goodwin *et al*. (*64*)
NifB	Nitrogenase FeMoCo maturation	Allen *et al*. (*65*)
AtsB	Formylglycine formation in sulfatase	Fang *et al*. (*66*)
ExsD	Succinoglycan production	Becker *et al*. (*67*)
SpcY	Spectinomycin biosynthesis	Lyutzkanova *et al*. (*68*)
AlbA	Subtilosin biosynthesis	Zhang *et al*. (*69*)
SanA	Nicomycin biosynthesis	Möhrle *et al*. (*70*)
BcpD	Bialaphos biosynthesis	Thompson & Seto (*71*)
MitD/MmcD	Mitomycin biosynthesis	Mao *et al*. (*72*)
OxsB	Oxetanocin biosynthesis	Morita *et al*. (*73*)
Fms7	Fortimicin biosynthesis	Kuzuyama *et al.* (*74*)
Fom3	Fosfomycin biosynthesis	Kuzuyama *et al.(75)*
CloN6	Chorobicin biosynthesis	Westrich *et al.* (*76*)
Nclk-binding	Cdk5 activator binding	Ching *et al*. (*77*)
Best5	Interferon inducible protein	Grewal *et al*. (*78*)
HydE/HydG	Cofactor Maturation/[FeFe] hydrogenase	Posewitz *et al*. (*79*)
AviX12	Epimerization in Avilamycin A	Boll *et al*. (*80*)
Elp3	Elongator complex function	Paraskevopoulou *et al*. (*81*)

Table 1-2. Examples of radical SAM enzymes and their respective functions.

1.3.1 The [4Fe-4S] cluster in the radical SAM enzymes

Spectroscopic characterization, including selenium X-ray absorption spectroscopy (XAS) of lysine 2,3-aminomutase (*44*) and electron nuclear double resonance (ENDOR) of lysine 2,3-aminomutase (*44*) and pyruvate formate lyase activase (*82*), and the crystal structure of biotin synthase (*83*), have shown that the three conserved cysteine residues coordinate three of the four irons of the [4Fe-4S] cluster. Additionally, it has shown that SAM, which is the fourth ligand of the cluster, binds as an N/O chelate to the unique fourth iron position through its amino nitrogen and carboxylate oxygen (Figure 1-11).

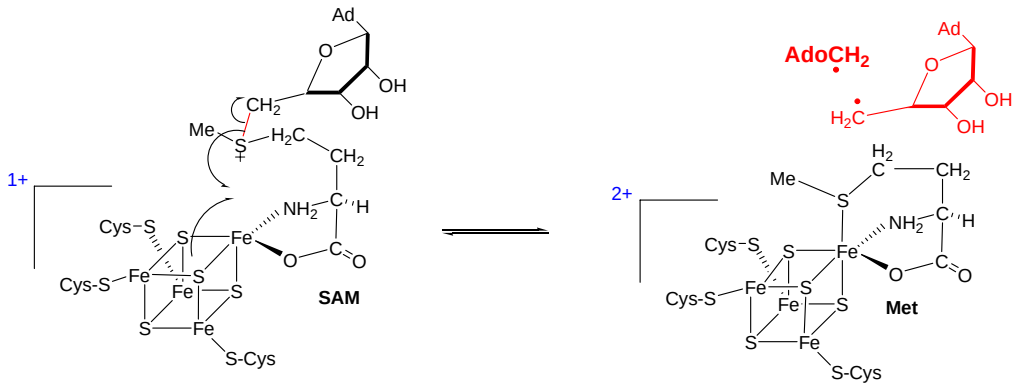

Figure 1-11. The reductive cleavage of SAM by the [4Fe-4S] center in lysine 2,3-aminomutase (*44*).

As the midpoint redox potential of the $[4Fe\text{-}4S]^{1+/2+}$ clusters in radical SAM enzymes is very negative (about -500 mV), it would appear to be difficult to reduce the oxidized $[4Fe\text{-}4S]^{2+}$ cluster under physiological conditions. Studies on the reduction potential of the $[4Fe\text{-}4S]^{1+/2+}$ cluster in lysine 2,3 aminomutase have demonstrated that the binding of SAM to the [4Fe-4S] cluster elevates the reduction potential by 86 mV compared to that of dihydrolipoate (*84*). This difference accounts for the SAM-dependent reduction of the

[4Fe-4S] in the presence of dithionite as previously reported for this enzyme. Under physiological conditions, however, a possible reducing system involving flavodoxin, flavodoxin reducatse, and NADPH has been reported for pyruvate formate lyase-activase, anaerobic ribonucleotide reductase-activase, and biotin synthase (*41*). Four different oxidation states of the iron-sulfur cluster have been observed in LAM including $[4Fe\text{-}4S]^{3+}$, a minor component in the purified enzyme, $[3Fe\text{-}4S]^{1+}$, an oxidation product of $[4Fe\text{-}4S]^{3+}$, $[4Fe\text{-}4S]^{2+}$, the major component in purified enzyme, and $[4Fe\text{-}4S]^{1+}$, which is generated after SAM-dependent reduction with dithionite (*41*) (Table 1-3). Among them, only the reduced $[4Fe\text{-}4S]^{1+}$ cluster is catalytically active but is very sensitive to the oxygen. Its sensitivity to oxygen made the mechanistic studies of this class of enzymes technically challenging so that only a handful of radical SAM enzymes have been characterized to date. Thus far, it is known that the $[4Fe\text{-}4S]^{1+}$ cluster donates one electron to the carbon-sulfur bond in SAM to induce the homolytic cleavage of this bond to generate the 5′-deoxyadenosyl radical and methionine (*41*). The 5′-deoxyadenosyl radical intermediate initiates subsequent radical reactions, which is discussed in a brief review of five radical SAM enzymes in Section 1.3.3 to 1.3.8.

Oxidation State	EPR (g value)	Significance
$[4Fe\text{-}4S]^{3+}$	2.007	Minor component of purified enzyme
$[3Fe\text{-}4S]^{+}$	2.015	Oxidation product of $[4Fe\text{-}4S]^{3+}$
$[4Fe\text{-}4S]^{2+}$	EPR silent	Major component of purified enzyme
$[4Fe\text{-}4S]^{+}$	1.96	Catalytic form

Table 1-3. Four oxidation states of the iron-sulfur cluster observed in LAM (*41*).

1.3.2 Comparison of *S*-Adenosylmethionine (SAM) with adenosylcobalamin

S-Adenosylmethionine (SAM) has long been known as a methyl group donor in biological systems. SAM methylates a series of biologically important molecules, such as DNA, hormones, neurotransmitters, and signal transduction systems by nucleophilic substitution. Recently, however, a new class of enzymatic reactions utilizing SAM as a cofactor has been discovered, where SAM serves as the initiator of various enzymatic radical reactions. Adenosylcobalamin (coenzyme B_{12} or AdoCbl) is known to catalyze a range of enzymatic radical reactions which are initiated by generation of the 5′-deoxyadenosyl radical (*85*). Adenosylcobalamin and SAM share the adenosyl moiety in common but have few chemical properties in commom. The structure of SAM, however, is not as complex as adenosylcobalamin. In contrast to the weak carbon-cobalt bond in AdoCbl, the carbon-sulfur bonds (about 60 kcal mol^{-1} bond dissociation energy) in SAM are quite strong, and thus they cannot be homolytically cleaved simply by binding to the enzyme. The electron transfer from the reduced $[4Fe\text{-}4S]^{1+}$ cluster to this carbon-sulfur bond facilitates its homolytic cleavage to generate the 5′-deoxyadenosyl radical and methionine. Although much has been learned about the role of SAM as a radical initiator in the past two decades (*41-43*), many questions remain unclear, especially regarding to the interaction between the [4Fe-4S] cluster and SAM. Perhaps the progress on protein crystallography will provide insights into these questions by thorough examination of the crystal structures of this class of enzymes.

1.3.3 Lysine 2,3-aminomutase

Lysine 2,3-aminomutase (LAM) was the first radical SAM enzyme to be characterized and is the most extensively studied example in this superfamily (*41-43*). In

the late 1960s and early 1970s, H. A. Barker investigated the lysine metabolism in *Clostridium* species and discovered this enzyme, lysine 2,3-aminomutase (*86*). This enzyme catalyzes the first step in the metabolism of lysine to acetate, the interconversion of L-lysine and L-β-lysine (*47, 87*) (Figure 1-12).

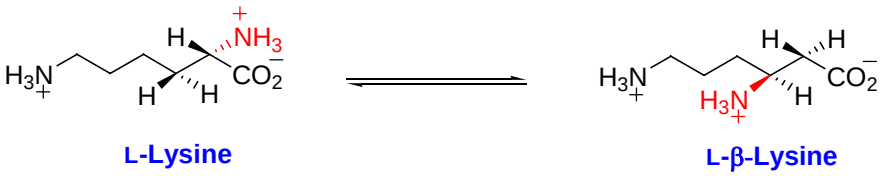

Figure 1-12. The reaction catalyzed by lysine 2,3-aminomutase.

The interconversion of L-lysine and L-β-lysine resembles coenzyme B_{12}-dependent rearrangements. Adenosylcobalamin, however, was not required for activity. LAM was active only under anaerobic conditions and contained pyridoxal 5′-phosphate (PLP) and iron. The addition of ferrous iron and PLP increased its activity. Interestingly, the addition of SAM was absolutely required for LAM catalysis. This discovery shed new light onto SAM's function in enzyme reactions, including novel enzymatic rearrangements that were later recognized as radical-based reactions. PLP is known to stabilize carbanions but had never before been proposed in a radical mechanism. In addition to the SAM cofactor, the involvement of PLP introduced more complications to the reaction mechanism. A working hypothesis involving both SAM and PLP cofactors in the reaction mechanism is outlined in Figure 1-13a, where the reductive cleavage of SAM to generate the 5′-deoxyadenosyl radical is omitted. The catalysis is initiated by the formation of an external aldimine **1-50** between the α-amino group of lysine and the PLP

cofactor, followed by an aza-allylic isomerization to form **1-53**. Abstraction of the C-3 hydrogen from the Schiff base **1-50** by the 5′-deoxyadenosyl radical leads to the radical **1-51** and 5′-deoxyadenosine. This is followed by a 1,2-nitrogen shift from C-2 to C-3 (i.e., **1-51→1-52→1-53**). Pairing of the unpaired electron in **1-51** with a π-electron of the imine bond forms an azacyclopropylcarbinyl radical intermediate **1-52**. Subsequent C4-N bond cleavage gives this C-2-centered radical **1-53**. Abstraction of a hydrogen atom from the methyl group of 5′-deoxyadenosine by the C-2-centered radical **1-53** produces the Schiff base **1-54** and regenerates the 5′-deoxyadenosyl radical. Hydrolysis of the Schiff base **1-54** releases the product, L-β-lysine. Three radical intermediates in the proposed mechanism have been characterized by electron paramagnetic resonance (EPR) spectroscopy in the presence of natural substrate, substrate analogue, or cofactor analogue. Product radical **1-53** is the only radical stable enough to be detected by EPR spectropsopy when L-lysine is the substrate (*88-91*). Radical stability can be attributed to delocalization of the unpaired electron by the carboxyl group. Second, the substrate radical **1-51** was identified and characterized by using substrate analogue, 4-thia-L-lysine, which was stabilized by the adjacent 4-thia group, making it the most stable radical intermediate under steady state conditions (*92, 93*). Third, 5′-deoxyadenosyl radical was identified and characterized using *anhydro*SAM (*an*SAM,), which is an allylic analogue of the 5'-deoxyadenosyl radical and generated an allylic radical via reductive cleavage of *an*SAM (*94, 95*) (Figure 13b). The allylic radical was stable enough to be detected by EPR spectroscopy.

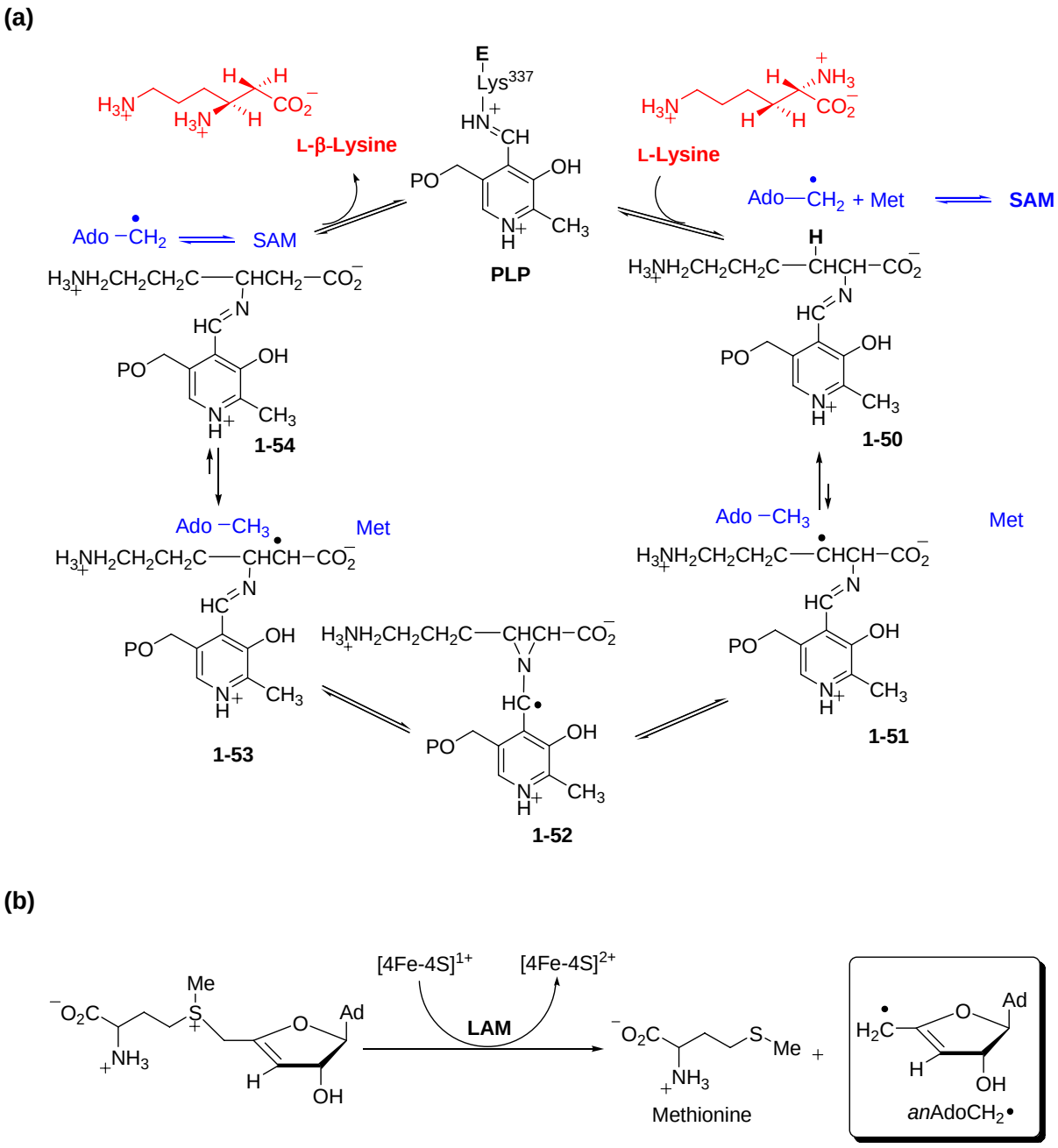

Figure 1-13. (a) The radical mechanism of lysine 2,3-aminomutase (LAM). (b) Characterization of an allylic analogue of the 5'-deoxyadenosyl radical in LAM using EPR spectroscopy.

1.3.4 Pyruvate Formate-Lyase Activase

Pyruvate formate-lyase (PFL) catalyzes the reaction of pyruvate with coenzyme A to generate formate and acetyl-CoA (*96*) (Figure 1-14).

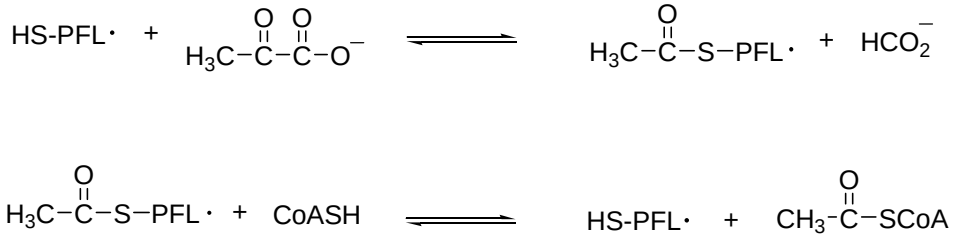

Figure 1-14. The reaction catalyzed by pyruvate formate-lyase (PFL).

This reaction is completely reversible. The rate constants for the forward and backward reactions were 770 and 260 sec^{-1}, respectively (*96*). Purified PFL from *Escherichia coli* is a homodimer and does not contain any metals or cofactors. The enzyme is not catalytically active when purified under aerobic conditions, and is activated under anaerobic conditions by the function of another enzyme, pyruvate formate-lyase activating enzyme (PFL-activase) (*96, 97*). The Knappe group has demonstrated that the activation of PFL proceeds with the formation of a stable radical on the enzyme (*98*), which accounts for one radical spin per homodimer (*99*). This unpaired electron has later been assigned to be on the α-carbon of Gly734 (*100*). One interesting feature of this glycyl radical on PFL is that the α-hydrogen undergoes free solvent exchange as demonstrated in the EPR experiments performed in deuterium oxides, in which the 15-G doublet splitting vanished (*100, 101*). The Kozarich group has shown that the exchange process was assisted by Cys419 by a combination of mechanism-based inactivation studies and site-directed mutagenesis (*102, 103*). In mechanism-based inactivation

studies, in addition to Cys419, the role of Cys418 in the reaction mechanism was also identified. Although the reaction mechanism catalyzed by PFL is not entirely understood, it is generally believed that the reaction involves an *S*-acetylated enzyme intermediate (such as **1-59**) and proceeds by a ping-pong mechanism (*96*) (Figure 1-15). One possible mechanism for the first half-reaction is shown in Figure 1-15. The glycyl radical (**1-55**) is transferred to Cys418 via the thiyl radical intermediate on Cys419 (**1-56**). Subsequently, the thiyl radical intermediate of Cys418 (**1-57**) serves as a thiyl nucleophile to form a C−S bond to the C2 of pyruvate. The tetrahedral radical intermediate (**1-58**) then collapses into a thioester (**1-59**) and a formyl radical, which abstracts a hydrogen atom from Cys419, leading to the formation of formate and the regeneration of the glycyl radical (**1-60**).

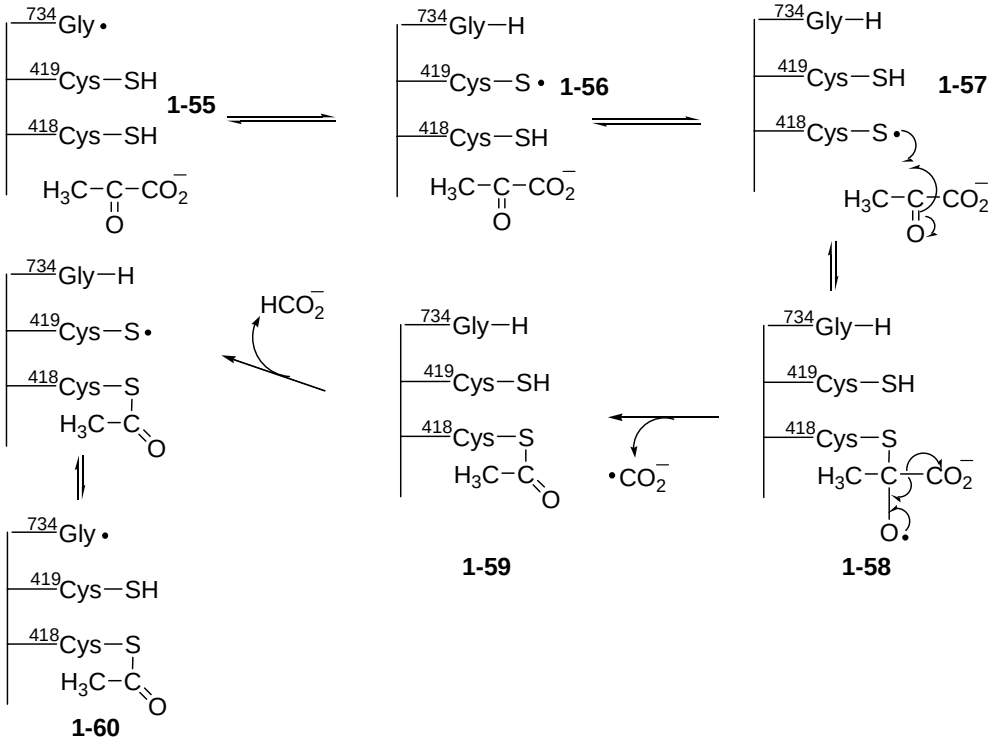

Figure 1-15. The radical mechanism for the acetylation reaction of PFL.

Finally, coenzyme A is acetylated by the acetyl group transferred from Cys418 (Figure 1-16).

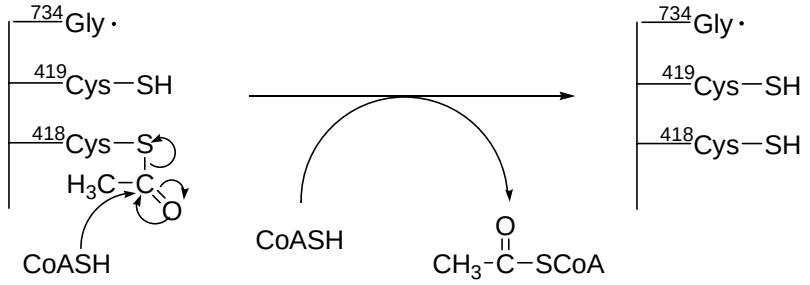

Figure 1-16. The conversion of *S*-acetyl-PFL and CoA to acetyl-CoA and PFL.

PFL-activase, a 28-kDa monomeric protein, catalyzes the formation of the glycyl radical in PFL. The reaction requires SAM, pyruvate, and an external electron source, which can be provided by either NADPH via the flavodoxin/flavodoxin reductase system or by chemical reductants, such as 5'-deazaflavin or dithionite (*97, 104*). The 5'-deoxyadenosyl radical generated by the reductive cleavage of SAM stereospecifically abstracts the *pro-S* hydrogen of Gly734 to generate the glycyl radical and 5'-deoxyadenosine (*105*) (Figure 1-17). Previous studies have shown that one equivalent of SAM is homolytically cleaved to generate 5'-deoxyadenosine and methionine (*98, 106*), thus SAM serves as a cosubstrate in this reaction, which is different from its role as a coenzyme in the reaction catalyzed by LAM.

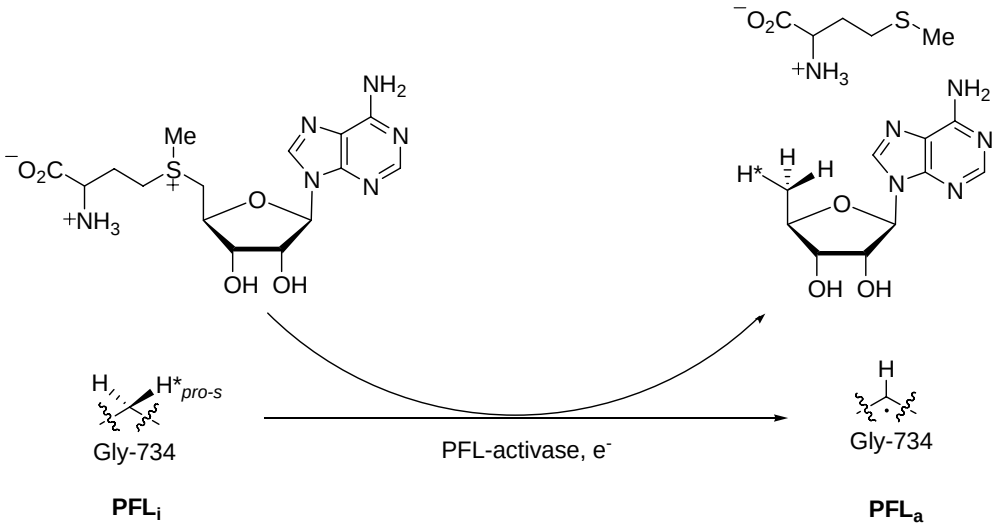

Figure 1-17. The activation of PFL by PFL-activase.

1.3.5 Anaerobic Ribonucleotide Reductase Activase

Ribonucleotide reductases (RNRs), which are ubiquitous in Nature, catalyze the essential *de novo* synthesis of deoxynucleotides. Four different classes of ribonucleotide reductases have been identified on the basis of the cofactor requirements as presented in Table 1-4 (*107*).

	Class Ia	Class Ib	Class II	Class III
Oxygen dependence	Aerobic	Aerobic	Aerobic/ Anaerobic	Anaerobic
Structure	$\alpha_2\beta_2$	$\alpha_2\beta_2$	$\alpha(\alpha_2)$	$\alpha_2\beta_2$
Genes	*nrdAB*	*nrdEF*		*nrdDG*
Radicals	Y…C	Y…C	AdB12…C	SAM..G..C
Metal Site	Fe-O-Fe	Fe-O-Fe	Co	Fe-S
Substrate	NDP	NDP	NDP/NTP	NTP
Reductant	Thioredoxin Glutaredoxin	NrdH-redoxin Glutaredoxin	Thioredoxin	Formate

Table 1-4. Four classes of ribonucleotide reductase.

The reaction mechanism of ribonucleotide reductases (Figure 1-18), however, is believed to be identical for the three classes (*107*). Class I RNRs are the most abundant and can be found in eukaryotes and various microorganisms, such as aerobically grown *E.coli*. Class I RNRs contain a diferric center adjacent to a tyrosine residue, which is transformed to a tyrosyl radical upon hydrogen atom abstraction by the diferric center in the presence of O_2 and a reductant. Class I RNRs can be further divided into two subclasses (class Ia and Ib) on the basis of their reductant sources, sequence similarity, and allosteric properties (*108*). Class II RNRs contain an adenosylcobalamin as a cofactor. Another form of RNRs produced by anaerobically grown *E. coli* is named anaerobic ribonucleotide reductase (ARR or Class III RNR), whose activase is a member of the radical SAM enzyme superfamily.

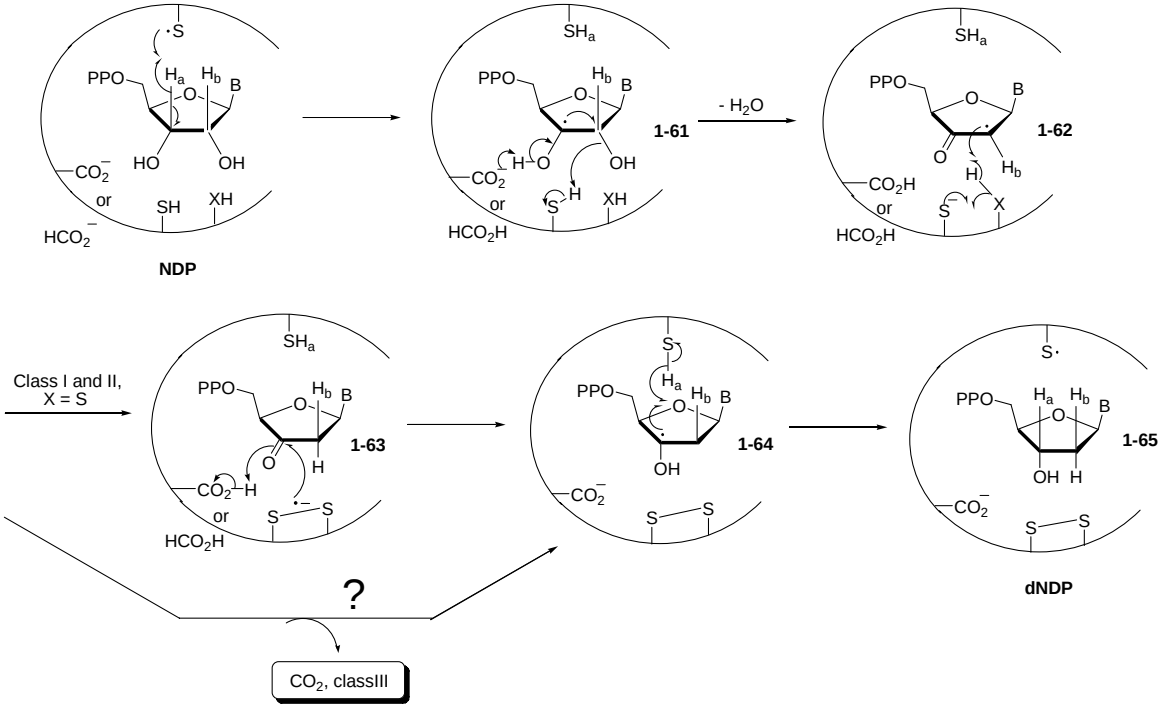

Figure 1-18. Proposed mechanism for all classes of ribonucleotide reductases (RNRs).

All classes of enzymes are believed to use a thiyl radical derived from a cysteine residue on the protein to initiate the subsequent radical reactions, but the strategy applying different cofactors to generate the thiyl radical varies between classes (*107, 108*). Herein, the mechanism for generation of the thiyl radical in ARR (or Class III RNR) is presented, along with the proposed enzymatic mechanism for all RNRs is presented.

Anaerobic ribonucleotide reductase (ARR), a 160-kDa α_2-homodimeric enzyme, catalyzes the C-2 deoxygenation of ribonucleotides using formate as a reductant (*109*) (Figure 1-19).

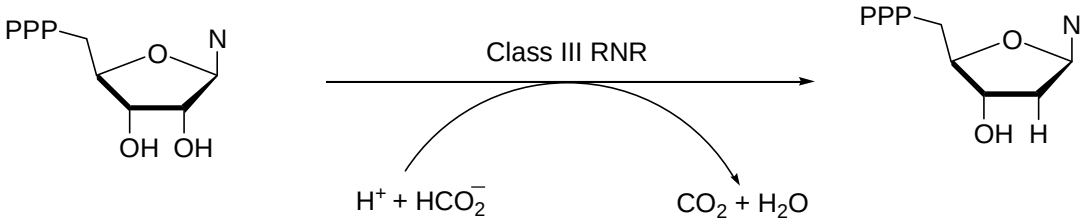

Figure 1-19. The reaction catalyzed by class III ribonucleotide reductase.

Sequence analysis revealed that ARR and pyruvate formate lyase share some sequence similarity, especially with respect to the glycine radical site (*110*). Subsequent EPR experiments provided the evidence for the presence of a protein radical on ARR. This radical was later localized to Gly681 (*111*). The glycyl radical serves as an initiator of catalysis via the thiyl radical at the active site, and plays the same role as that of the tyrosyl radical in the Class I enzyme. ARR is isolated in an inactive form and activation under anaerobic conditions requires SAM, a reducing system composed of NADPH, flavodoxin, flavodoxin reductase, and a protein component named β, which was later

named anaerobic ribonucleotide reductase-activase (ARR-activase) (*112-114*). The function of SAM in ARR-activase was identified in a manner similar to that described above for lysine 2,3-aminomutase and PFL-activase (*115*). 5'-Deoxyadenosyl radical generated by the reductive cleavage of SAM abstracts an α-hydrogen atom of Gly681 followed by the hydrogen abstraction of the active-site cysteine residue (Cys290 in *E. coli*) on ARR to generate the thiyl radical (*112*). Subsequently, the thiyl radical abstracts a hydrogen atom at C-3 of ribonucleotides to generate the C-3-centered radical intermediate **1-61** (Figure 1-18). After the elimination of water, a ketyl radical **1-62** is yielded. Reduction of **1-63** generates a 2'-deoxynucleotide radical **1-64**, which is subsequently reduced to give the dNDP product (**1-65**) and regenerate the thiyl radical. Interestingly, the external reductant used by ARR is formate, which is different from those used in class I and II RNRs (Figure 1-19). Class I and II RNRs use a couple of active-site cysteines as reductants which are regenerated by thioredoxin and thioredoxin reductase. The strategy of formate oxidation to CO_2 is not well understood. Density functional theory (DFT) calculations suggested that the reaction mechanism may involve a formyl radical intermediate (**1-66**) as shown in Figure 1-20 (*116*), but more experiments are needed to verify this mechanistic proposal.

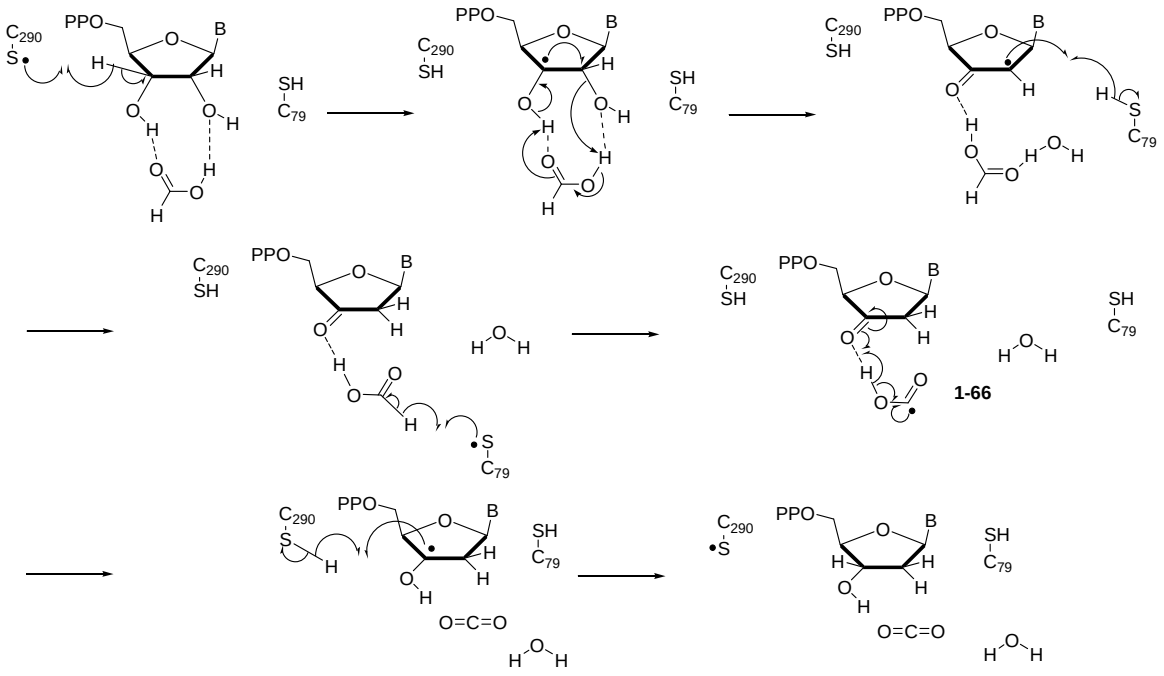

Figure 1-20. The proposed mechanism of class III ribonucleotide reductase using formate as a reductant.

1.3.6 Biotin Synthase

Biotin is an essential vitamin for humans. In plants and most bacteria, biotin is biosynthesized from pimeloyl CoA (**1-67**) and L-alanine by four enzymes, including BioF (i.e., 7-keto-8-amino-pelargonic acid synthase, KAPA synthase), BioA (i.e., 7,8-diamino-pelargonic acid synthase, DAPA synthase), BioD (i.e., dethiobiotin synthase), and BioB (i.e., biotin synthase) (Figure 1-21) (*117*).

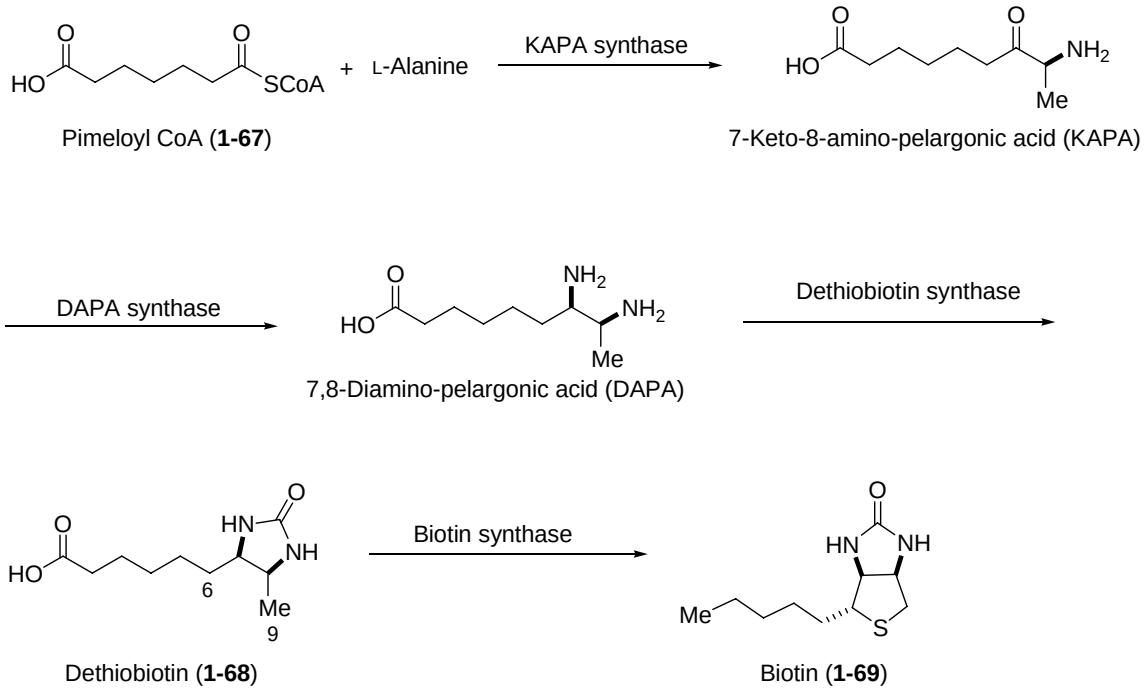

Figure 1-21. Four conserved steps in the biotin biosynthetic pathway found in plants, eubacteria and archaea.

Biotin synthase catalyzes the last step of the biotin biosynthesis and converts dethiobiotin (**1-68**) to biotin (**1-69**). This step is the most chemically difficult step in the pathway and involves the abstraction of two unreactive hydrogen atoms at carbons 6 and 9 of dethiobiotin (**1-68**) followed by the insertion of a sulfur atom between carbons 6 and 9 (Figure 1-22).

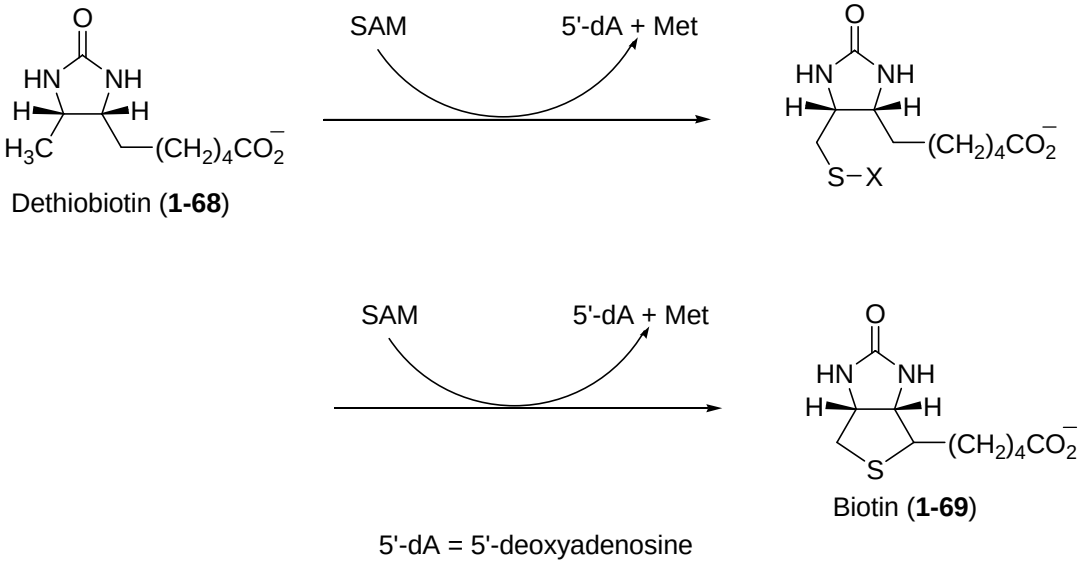

Figure 1-22. The reaction catalyzed by biotin synthase.

E. coli biotin synthase is a 39-kDa homodimeric protein. When purified aerobically, it usually contains approximately one [2Fe-2S] cluster per polypeptide but this is not the active form of the enzyme. Upon anaerobic reconstitution in the presence of excess iron, sulfide, and a reducing agent, the active form of the enzyme contains one $[2Fe\text{-}2S]^{2+}$ and one $[4Fe\text{-}4S]^{2+}$ cluster per polypeptide. The catalysis requires a SAM cofactor and a reducing system consisting of flavodoxin, flavodoxin reductase and NADPH (*118*). The crystal structure of *E. coli* biotin synthase containing the SAM cofactor and the substrate, dethiobiotin (**1-68**) has been solved to 3.4 Å resolution. This achievement should be noted as it was the first crystal structure of any of the radical SAM enzymes to be determined (*83*). The protein is homodimeric and each monomer adopts an $(\alpha/\beta)_8$ barrel (TIM barrel) fold. In addition to cofactor and substrate binding in the active site, a [2Fe-2S] cluster and a [4Fe-4S] cluster which flank the two organic substrates were also

observed in the active site. The [4Fe-4S] cluster is coordinated by three highly conserved cysteine residues (Cys53, Cys57, and Cys60) and the α-amino and α-carboxylate groups of SAM; the [2Fe-2S] cluster is coordinated by three cysteine residues, Cys97, Cys128, and Cys188 and an atypical metal ligand, arginine 260. However, mutagenic studies later suggested that Arg260 is not crucial for the catalysis of biotin synthase (*119*). The origin of sulfur in biotin has been a controversial issue for many years. Recent biophysical studies including UV-vis, EPR, Mössbauer, and resonance Raman spectroscopies have suggested that the sulfur atoms in biotin were derived from the [2Fe-2S] cluster (*120-122*). Accordingly, the current working model for the reaction mechanism catalyzed by BS is shown in Figure 1-23 (*120*). The 5'-deoxyadenosyl radical derived from the reductive cleavage of SAM abstracts a hydrogen atom at carbon 9 of dethiobiotin (**1-68**) to generate 5'-deoxyadenosine, methionine, and a C-9-centered substrate radical **1-70**, which subsequently attacks a bridging μ-sulfido atom of the [2Fe-2S] cluster to generate the sulfur-containing intermediate **1-71**. The hydrogen atom abstraction at C-9 occurs prior to that at C-6, which was proven by feeding experiments where 9-mercapto dethiobiotin was transferred into biotin by *B. sphaericus*, while the two epimers of 6-mercapto dethiobiotin were not (*123*). In the next step, the 5'-deoxyadenosyl radical derived from another molecule of SAM abstracts the 6-*pro-S* hydrogen atom of the 9-mercaptodethiobiotin intermediate **1-71** to generate the C-6-centered radical intermediate **1-72** (*124*). Attack of the C-6 radical on the sulfur atom of intermediate **1-72** leads to the formation of the thiophane ring in biotin (**1-69**) with concomitant reduction of the coordinated Fe^{III} species to Fe^{II}. Biotin synthase from *E. coli* is the most extensively

studied radical SAM enzyme that catalyzes sulfur insertion (*125*). Another example, lipoyl synthase, will be presented in the next section.

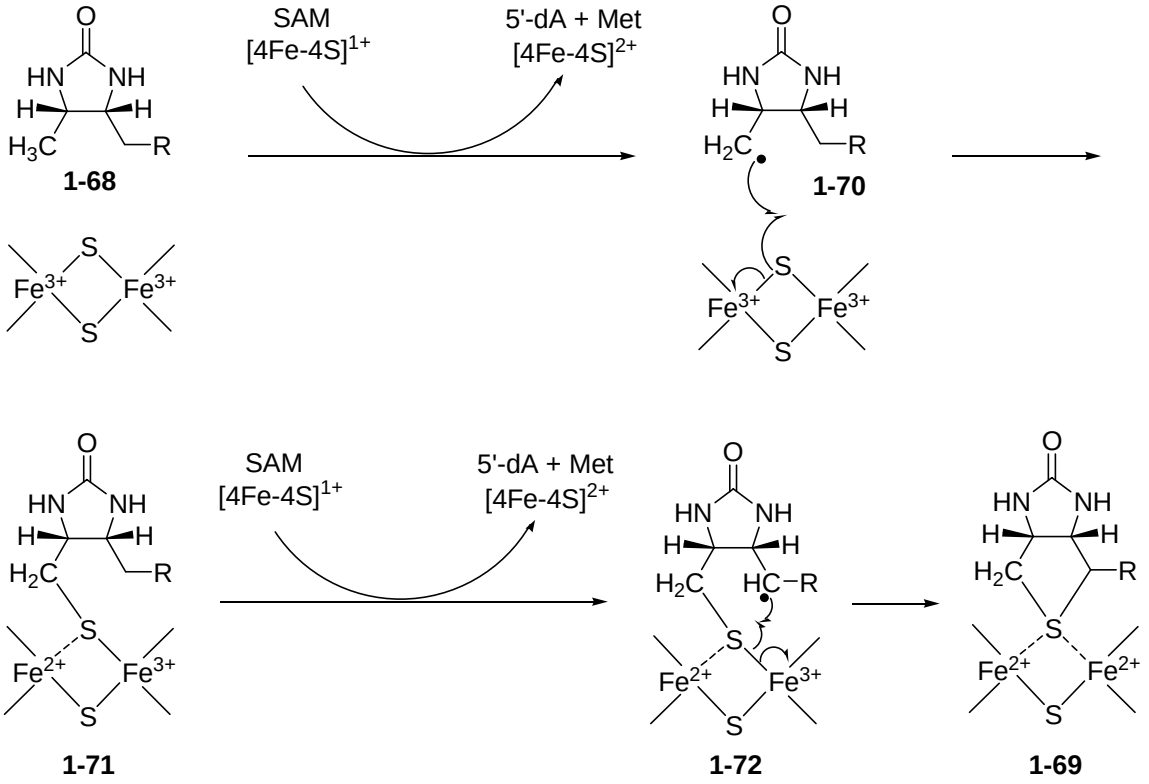

Figure 1-23. The radical mechanism of the sulfur insertion catalyzed by biotin synthase.

1.3.7 Lipoyl Synthase

Lipoyl synthase catalyzes the final step in the *de novo* biosynthesis of the lipoyl cofactor. Studies demonstrating the activity of the purified lipoyl synthase were hampered until the discovery of the enzyme's true substrate (*126*). The reaction catalyzed by lipoyl synthase involves the insertion of two sulfur atoms into carbon-hydrogen bonds at carbons 6 and 8 of an *n*-octanoyl chain attached to a specific lysine residue of a lipoyl-carrying protein (LCP) (*127*) (Figure 1-24). Three LCPs are known in *E. coli*: the H

protein of the glycine cleavage system, and the E_2 subunits of the pyruvate and α-ketoglutarate dehydrogenase complexes (*128*).

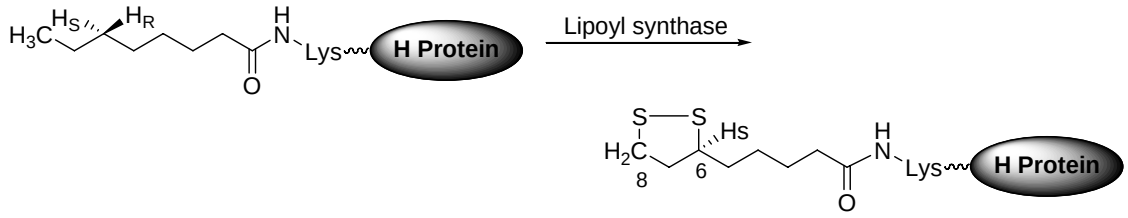

Figure 1-24. The reaction catalyzed by lipoyl synthase.

Previous *in vivo* feeding experiments revealed that the sulfur insertion at C-8 likely occurs prior to that at C-6. Because [8-$^2H_2$]- *n*-octanoyl-LCP was a comparable precursor for the biosynthesis of lipoic acid, while the corresponding [6-$^2H_2$] species was a much poorer precursor (*129*). However, a recent analysis of the reaction components before the completion of turnover using HPLC and NMR spectroscopy showed that the reaction mixture contained 6-mercaptooctanoylated intermediate but not 8-mercaptooctanoylated intermediate. These results suggested that the sulfur insertion occurred at C-6 prior to at C-8 (*130*). Thus, the reaction sequence of the sulfur insertion remains elusive and a detailed kinetic analysis is needed to resolve this controversy. *E. coli* lipoyl synthase contains eight cysteine residues, six of which are conserved in two different motifs. The first motif, CXXXCXXC, coordinates the [4Fe-4S] cluster, which is a highly conserved region in radical SAM enzymes, whereas the second motif, CX_4CX_5C, is only found in lipoyl synthase. Studies involving site-directed mutagenesis in combination with the iron and sulfur content determination, and UV-vis, EPR, and Mössbauer spectroscopies demonstrated that these three cysteine residues in the second motif coordinate an

additional [4Fe-4S] cluster (*131*). Thus it was believed that lipoyl synthase contains two [4Fe-4S] clusters per polypeptide. However, the precise role of the second [4Fe-4S] cluster in lipoyl synthase has not been established. Similar configurations and Mössbauer parameters preclude further studies to distinguish between these two clusters. Based on known sulfur origin in biotin synthase, it has been suggested that the second [4Fe-4S] cluster serves as the direct sulfur source. In contrast to biotin synthase, appreciably fewer experiments have been carried out to support this hypothesis for lipoyl synthase (*132*). Only recent labeling experiments have shown that lipoyl synthase itself serves as the direct source of sulfur atoms in lipoic acid, and that both sulfur atoms derive from the same lipoyl synthase polypeptide (*132*). Accordingly, a working model for the reaction catalyzed by lipoyl synthase is shown in Figure 1-25 (*127, 129, 130, 132*). A 5'-deoxyadenosyl radical derived from the reductive cleavage of SAM abstracts the *pro*-R hydrogen atom from C-6 of the substrate, *n*-octanoyllysine (**1-73**), to generate the C-6-centered substrate radical intermediate **1-74**. The substrate radical attacks one of the bridging μ-sulfido atom of the [4Fe-4S] cluster coordinated by the CX_4CX_5C motif with inversion of configuration to generate the sulfur-containing intermediate **1-75**. In the second half-reaction, a 5'-deoxyadenosyl radical derived from another molecule of SAM removes a hydrogen atom from C-8 of **1-75** to generate a C-8 alkyl radical **1-76**, which attacks another bridging μ-sulfido atom of the [4Fe-4S] cluster with concomitant reduction of Fe^{III} to Fe^{II} to yield **1-77**. The addition of two protons to **1-77** leads to the dissociation of the product **1-78**, the reduced form of the lipoyl cofactor. Although both the reaction mechanisms of biotin synthase and lipoyl synthase involve a radical initiated

sulfur insertion reaction, there are two differences in the reaction mechanism between them (*129*). First, the *pro-R* hydrogen is abstracted at C-6 of the *n*-octanoyl chain in lipoyl synthase, whereas the *pro-S* hydrogen at C-6 of dethiobiotin is removed in biotin synthase. Second, the sulfur insertion occurs with the inversion of configuration in lipoyl synthase, in contrast to the retention of the configuration in biotin synthase.

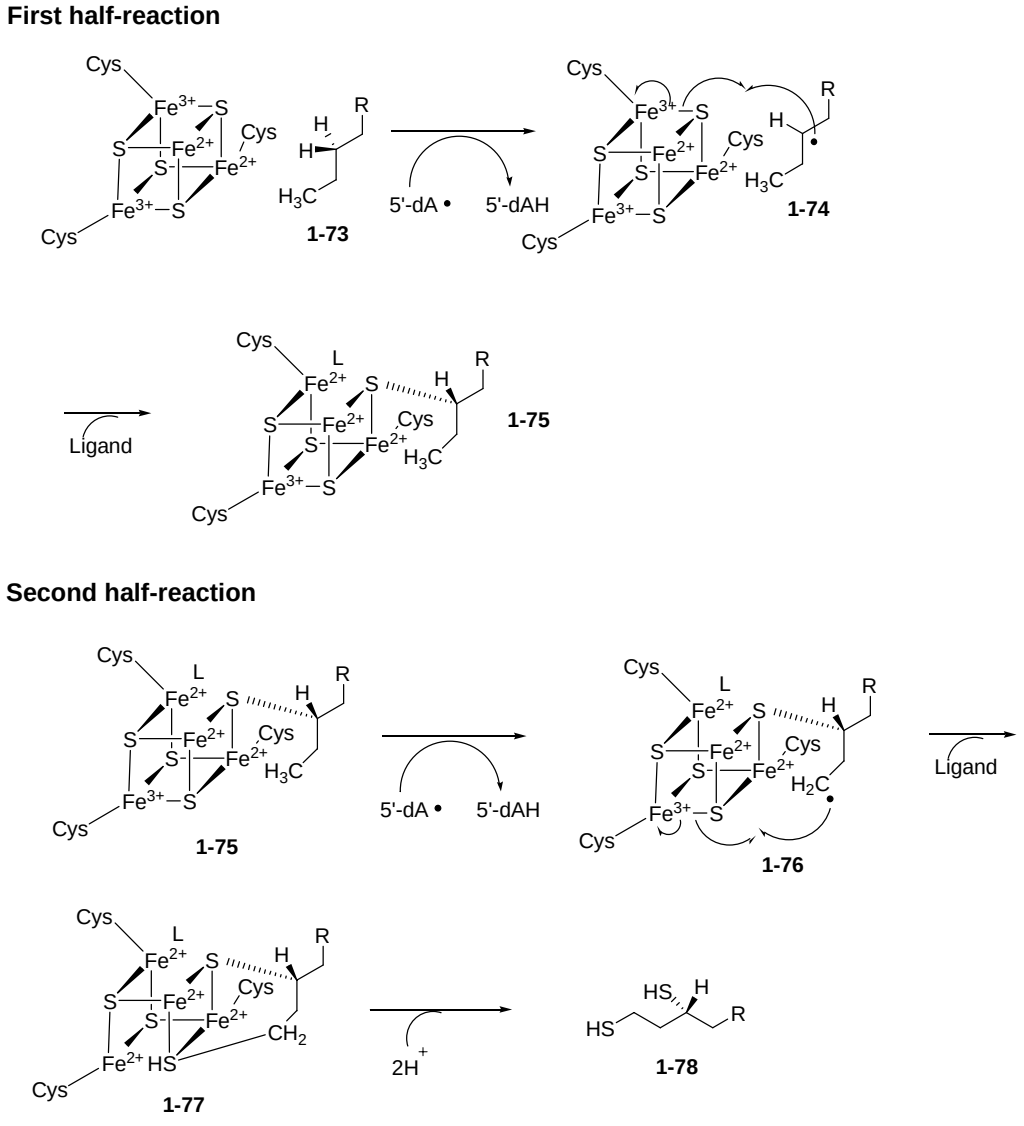

Figure 1-25. The radical mechanism of sulfur insertion catalyzed by lipoyl synthase.

1.4 THESIS STATEMENT

The dissertation focuses on the characterization and mechanistic studies of DesII involved in the biosynthesis of TDP-D-desosamine (**1-21**, Figure 1-3a) from the pikromycin biosynthetic pathway of *Streptomyces venezuelae*. DesII is directly responsible for the production of a key intermediate, TDP-3-keto-4,6-dideoxy-D-glucose (**1-20**, Figure 1-3a), in the biosynthesis of TDP-D-desosamine. DesII has been identified as a member of the radical *S*-adenosylmethionine (SAM) enzyme superfamily by sequence analysis. Previous genetic studies indicated that DesII is involved in C-4 deoxygenation. It was later confirmed that DesII catalyzes the oxidative deamination of TDP-4-amino-4,6-dideoxy-D-glucose (**1-19**, Figure 1-3a) to generate TDP-3-keto-4,6-dideoxy-D-glucose (**1-20**, Figure 1-3a). DesII is the first radical SAM enzyme involved in secondary metabolism to be characterized at the enzymatic level. Based on biochemical characterization, the originally proposed mechanisms were revised and two possible mechanisms have been suggested to account for these results.

The dissertation describes the biochemical characterization of DesII (Chapter 2) and mechanistic studies of DesII (Chapter 3). The characterization studies included the overexpression of the *desII* gene in *E. coli* and the purification of the DesII protein to near homogeneity. In addition, an anaerobic reconstitution method was developed to reconstitute the oxygen-sensitive [4Fe-4S] cluster *in vitro*. The [4Fe-4S] cluster was characterized by the determination of iron and sulfur content, UV-vis, and EPR spectroscopies. An HPLC assay demonstrated that DesII converts TDP-4-amino-4,6-dideoxy-D-glucose (**1-19**, Figure 1-3a) to TDP-3-keto-4,6-dideoxy-D-glucose (**1-20**, Figure 1-3a) in the presence of cofactor, SAM. The steady-state kinetic parameters of the

DesII-catalyzed reaction were determined using this HPLC assay. A possible *in vivo* reducing system, flavodoxin (from *E. coli*), flavodoxin reductase (from *E. coli*), and NADPH, for the reduction of $[4Fe\text{-}4S]^{2+}$ cluster, was identified. Additionally, the substrate specificity of DesII was also investigated. Preliminary testing of the culture conditions in M9 minimal media and iron-depleted media paved the way for future spectroscopic studies, such as Mössbauer and ENDOR spectroscopies. The mechanistic studies included the synthesis of TDP-3-deutero-4-amino-4,6-dideoxy-D-glucose to study the first step, C3 hydrogen atom abstraction by 5'-deoxyadenosyl radical (i.e., **1-19→1-47** Figure 1-10), in the proposed mechanism. Additionally, TDP-3-fluoro-3,6-dideoxy-D-glucose was synthesized to study whether deprotonation of the 3-hydroxyl group (i.e., **1-47→1-48**, Figure 1-10) is a part of the reaction mechanism. This analogue contains a hydroxyl group at C-4 similar to TDP-D-quinovose, which is a competent substrate with a comparable activity as the natural substrate.

The results presented in this dissertation clearly establish that DesI and DesII function independently to carry out the C-4 deoxygenation in the biosynthesis of TDP-D-desosamine. DesI functions as a PLP-dependent C-4 aminotransferase, and DesII functions as a C-4 deaminase. Moreover, DesII requires a $[4Fe\text{-}4S]^{1+}$ center and *S*-adenosylmethionine (SAM) for activity. Accordingly, the originally proposed mechanism for C-4 deoxygenation where DesI and DesII function together was revised. Additionally, DesII is flexible towards TDP-D-quinovose and TDP-3-amino-4,6-dideoxy-D-glucose (TylB product) from the macrolide antibiotic tylosin biosynthetic pathway. The initial mechanistic studies provide clarification of the newly revised mechanisms. The availability of various substrate analogues sets the stage for further investigation of the

proposed mechanisms and the possible trapping of the radical intermediates by rapid freeze-quench EPR spectroscopy.

Currently, only a handful of radical SAM enzymes have been characterized and all are involved in unusual biotransformations (*41-43*). The fact that DesII is responsible for a radical-induced deamination illustrates the catalytic versatility of this class of enzymes. Its cooperation with a transaminase (DesI) to carry out an overall deoxygenation reaction underscores Nature's ingenuity in devising strategies for carbon-oxygen bond scission.

1.5 REFERENCE

1. Thorson, J. S., Hosted, T. J., Jr., Jiang, J., Biggins, J. B., and Ahlert, J. (2001) Nature's carbohydrate chemists: the enzymatic glycosylation of bioactive bacterial metabolites, *Curr. Org. Chem. 5*, 139-167.

2. Kren, V., and Martinkova, L. (2001) Glycosides in medicine: "the role of glycosidic residue in biological activity", *Curr. Med. Chem. 8*, 1303-1328.

3. Xue, Y., Zhao, L., Liu, H.-w., and Sherman, D. H. (1998) A gene cluster for macrolide antibiotic biosynthesis in *Streptomyces venezuelae*: architecture of metabolic diversity, *Proc. Natl. Acad. Sci. USA. 95*, 12111-12116.

4. Walsh, C. T. (2003) *Antibiotics: Actions, Origins, Resistance*, American Society of Microbiology Press, Washington, DC.

5. Poehlsgaard, J., and Douthwaite, S. (2005) The bacterial ribosome as a target for antibiotics, *Nat. Rev. Microbiol. 3*, 870-881.

6. Schlunzen, F., Zarivach, R., Harms, J., Bashan, A., Tocilj, A., Albrecht, R., Yonath, A., and Franceschi, F. (2001) Structural basis for the interaction of antibiotics with the peptidyl transferase centre in eubacteria, *Nature 413*, 814-821.

7. Khosla, C., Tang, Y., Chen, A. Y., Schnarr, N. A., and Cane, D. E. (2007) Structure and mechanism of the 6-deoxyerythronolide B synthase, *Annu. Rev. Biochem. 76*, 195-221.

8. Smith, S., and Tsai, S.-C. (2007) The type I fatty acid and polyketide synthases: a tale of two megasynthases, *Nat. Prod. Rep. 24*, 1041-1072.

9. Borisova, S. A., Zhao, L., Melancon, C. E., III , Kao, C.-L., and Liu, H.-w. (2004) Characterization of the glycosyltransferase activity of DesVII: analysis of and implications for the biosynthesis of macrolide antibiotics, *J. Am. Chem. Soc. 126*, 6534-6535.

10. Borisova, S. A., Zhang, C., Takahashi, H., Zhang, H., Wong, A. W., Thorson, J. S., and Liu, H.-w. (2005) Substrate specificity of the macrolide-glycosylating enzyme pair DesVII/DesVIII: opportunities, limitations, and mechanistic hypotheses, *Angew. Chem. Int. Ed. 45*, 2748-2753.

11. Zhao, L., Borisova, S., Yeung, S.-M., and Liu, H.-w. (2001) Study of C-4 deoxygenation in the biosynthesis of desosamine: evidence implicating a novel mechanism, *J. Am. Chem. Soc. 123*, 7909-7910.

12. Szu, P.-h., He, X., Zhao, L., and Liu, H.-w. (2005) Biosynthesis of TDP-D-desosamine: Identification of a strategy for C4 deoxygenation, *Angew. Chem. Int. Ed. 44*, 6742-6746.

13. Chen, H., Yamase, H., Murakami, K., Chang, C.-w., Zhao, L., Zhao, Z., and Liu, H.-w. (2002) Expression, purification, and characterization of two *N*,*N*-dimethyltransferases, TylM1 and DesVI, involved in the biosynthesis of mycaminose and desosamine, *Biochemistry 41*, 9165-9183.

14. He, X. M., and Liu, H.-w. (2002) Mechanisms of enzymatic C-O bond cleavages in deoxyhexose biosynthesis, *Curr. Opin. Chem. Biol. 6*, 590-597.

15. Thibodeaux, C. J., Melancon, C. E., III , and Liu, H.-w. (2007) Unusual sugar biosynthesis and natural product glycodiversification, *Nature 446*, 1008-1016.

16. He, X., H.-w. (2002) Formation of unusual sugars: mechanistic studies and biosynthetic applications, *Annu. Rev. Biochem. 71*, 701-754.

17. Oppermann, U., Filling, C., Hult, M., Shafqat, N., Wu, X., Lindh, M., Shafqat, J., Nordling, E., Kallberg, Y., Persson, B., and Jornvall, H. (2003) Short-chain dehydrogenases/reductases (SDR): the 2002 update. , *Chem. Biol. Interact. 143-144*, 247-253.

18. Allard, S. T. M., Beis, K., Giraud, M.-F., Hegeman, A. D., Gross, J. W., Wilmouth, R. C., Whitfield, C., Graninger, M., Messner, P., Allen, A. G., Maskell, D. J., and Naismith, J. H. (2002) Toward a structural understanding of the dehydratase mechanism, *Structure 10*, 81-92.

19. Draeger, G., Park, S.-H., and Floss, H. G. (1999) Mechanism of the 2-deoxygenation step in the biosynthesis of the deoxyhexose moieties of the antibiotics granaticin and oleandomycin, *J. Am. Chem. Soc. 121*, 2611-2612.

20. Chen, H., Agnihotri, G., Guo, Z., Que, N. L. S., Chen, X. H., and Liu, H.-w. (1999) Biosynthesis of mycarose: isolation and characterization of enzymes involved in the C-2 deoxygenation *J. Am. Chem. Soc. 121*, 8124-8125.

21. Flatt, P. M., and Mahmud, T. (2007) Biosynthesis of aminocyclitol-aminoglycoside antibiotics and related compounds, *Nat. Prod. Rep. 24*, 358-392.

22. Liu, H.-w., and Thorson, J. S. (1994) Pathways and mechanisms in the biogenesis of novel deoxy sugars by bacteria, *Annu. Rev. Microbiol. 48*, 223-256.

23. Lindberg, B. (1990) Components of bacterial polysaccharides, *Adv. Carbohydr. Chem. Biochem. 48*, 279-318.

24. Smith, P., Lin, A., Szu, P.-H., Liu, H.-w., and Tsai, S. C. (2006) Biosynthesis of a 3,6-dideoxyhexose: crystallization and x-ray diffraction of CDP-6-deoxy-L-threo-D-glycero-4-hexulose-3-dehydrase (E_1) for ascarylose biosynthesis, *Acta Cryst. F62*, 231-234.

25. Burns, K. D., Pieper, P. A., Liu, H.-w., and Stankovich, M. T. (1996) Characterization of the spectral and thermodynamic properties of CDP-6-deoxy-L-threo-D-glycero-4-hexulose-3-dehydrase reductase (E_3) and CDP-6-deoxy-L-threo-D-glycero-4-hexulose-3-dehydrase (E_1), *Biochemistry 35*, 7879-7889.

26. Gassner, G. T., Johnson, D. A., Liu, H.-w., and Ballou, D. P. (1996) Kinetics of the reductive half reaction of the iron-sulfur flavoenzyme CDP-6-deoxy-L-threo-D-glycero-4-hexulose-3-dehydrase reductase, *Biochemistry 35*, 7752-7761.

27. Chen, X. M. H., Ploux, O., and Liu, H.-w. (1996) Biosynthesis of 3,6-dideoxyhexoses: *in vivo* and *in vitro* evidence for protein-protein interaction between CDP-6-deoxy-L-threo-D-glycero-4-hexulose-3-dehydrase (E_1) and its reductase (E_3). *Biochemistry 35*, 16412-16420.

28. Johnson, D. A., Gassner, G. T., Bandarian, V., Ruzicka, F. J., Ballou, D. P., Reed, G. H., and Liu, H.-w. (1996) Kinetic characterization of an organic radical in the ascarylose biosynthetic pathway, *Biochemistry 35*, 15846-15856.

29. Chang, C.-W. T., Johnson, D. A., Bandarian, V., Zhou, H., LoBrutto, R., Reed, G. H., and Liu, H.-w. (2000) Characterization of a unique coenzyme B_6 radical in the ascarylose biosynthetic pathway, *J. Am. Chem. Soc. 122*, 4239-4240.

30. Agnihotri, G., and Liu, H.-w. (2001) PLP and PMP radicals: a new paradigm in coenzyme B_6 chemistry, *Bioorg. Chem. 29*, 234-257.

31. Jansonius, J. N. (1998) Structure, evolution and action of vitamin B_6-dependent enzymes, *Curr. Opin. in Struct. Biol. 8*, 759-769.

32. Christen, P., and Mehta, P. K. (2001) From cofactor to enzymes. The molecular evolution of pyridoxal-5'-phosphate-dependent enzymes, *Chem. Rec. (New York, NY) 1*, 436-447.

33. Eads, J. C., Beeby, M., Scapin, G., Yu, T. W., and Floss, H. G. (1999) Crystal structure of 3-amino-5-hydroxybenzoic acid (AHBA) synthase, *Biochemistry 38*, 9840-9849.

34. Schneider, G., Kack, H., and Lindqvist, Y. (2000) The manifold of vitamin B_6 dependent enzymes, *Structure 8*, R1-6.

35. Thorson, J. S., Stanley, F. L., and Liu, H.-w. (1993) Biosynthesis of 3,6-dideoxyhexoses: new mechanistic reflections upon 2,6-dideoxy, 4,6-dideoxy, and amino sugar construction, *J. Am. Chem. Soc. 115*, 6993-6994.

36. Thorson, J. S., and Liu, H.-w. (1993) Characterization of the first PMP dependent iron-sulfur containing enzyme which is essential for the biosynthesis of 3,6-dideoxyhexoses, *J. Am. Chem. Soc. 115*, 7539-7540.

37. Agnihotri, G., Liu, Y.-n., Paschal, B. M., Liu, H.-w. (2004) Identification of an unusual [2Fe-2S]-binding motif in the CDP-6-deoxy-D-glycero-L-threo-4-hexulose-3-dehydrase from Yersinia pseudotuberculosis: implication for C-3 deoxygenation in the biosynthesis of 3,6-dideoxyhexoses., *Biochemistry 43*, 14265-14274.

38. Miller, V. P., Thorson, J. S., Ploux, O., Lo, S. F., and Liu, H.-w. (1993) Cofactor characterization and mechanistic studies of CDP-6-deoxy-$\Delta^{3,4}$-glucoseen reductase: Exploration into a novel enzymic carbon-oxygen bond cleavage event, *Biochemistry 32*, 11934-11942.

39. Zhao, L., Sherman, D. H., and Liu, H.-w. (1998) Biosynthesis of desosamine: Molecular evidence suggesting b-glucosylation as a self-resistance mechanism in methymycin/neomethymycin producing strain, *Streptomyces venezuelae*, *J. Am. Chem. Soc. 120*, 9374-9374.

40. Sofia, H. J., Chen, G., Hetzler, B. G., Reyes-Spindola, J. F., and Miller, N. E. (2001) Radical SAM, a novel protein superfamily linking unresolved steps in familiar biosynthetic pathways with radical mechanisms: functional characterization using new analysis and information visualization methods, *Nucleic Acids Research 29*, 1097-1106.

41. Frey, P. A., and Magnusson, O. T. (2003) *S*-adenosylmethionine: A wolf in sheep's clothing, or a rich man's adenosylcobalamin?, *Chem. Rev. 103*, 2129-2148.

42. Frey, P. A., Hegeman, A. D., and Ruzicka, F. J. (2008) The radical SAM superfamily, *Crit. Rev. Biochem. Mol. Biol. 43*, 63-88.

43. Frey, P. A. (2001) Radical mechanisms of enzymatic catalysis, *Annu. Rev. Biochem. 70*, 121-148.

44. Chen, D., Walsby, C., Hoffman, B. M., and Frey, P. A. (2003) Coordination and mechanism of reversible cleavage of *S*-adenosylmethionine by the [4Fe-4S] center in lysine 2,3-aminomutase, *J. Am. Chem. Soc. 125*, 11788-11789.

45. Bandarian, V., and Reed, G. H. (1999) *Ethanolamine ammonia-lyase*.

46. Kim, J., Hetzel, M., Boiangiu, C. D., and Buckel, W. (2004) Dehydration of (*R*)-2-hydroxyacyl-CoA to enoyl-CoA in the fermentation of α-amino acids by anaerobic bacteria, *FEMS Microbiol. Rev. 28*, 455-468.

47. Ruzicka, F. J., Lieder, K. W., and Frey, P. A. (2000) Lysine 2,3-aminomutase from *Clostridium subterminale SB4*: Mass spectral characterization of cyanogens bromide-treated peptides and cloning, sequencing, and expression of the gene kamA in *Escherichia coli*, *J. Bacteriol. 182*, 469-476.

48. Cone, M. C., Yin, X., Grochowski, L. L., Parker, M. R., and Zabriskie, T. M. (2003) The Blasticidin S biosynthesis gene cluster from *Streptomyces griseochromogenes*: Sequence analysis, organization, and initial characterization, *ChemBioChem 4*, 821-828.

49. Ruzicka, F. J., and Frey, P. A. (2007) Glutamate 2,3-aminomutase: a new member of the radical SAM superfamily of enzymes, *Biochim. Biophys. Acta. 1774*, 286-296.

50. Rebeil, R., Sun, Y., Chooback, L., Pedraza-Reyes, M., Kinsland, C., Begley, T. P., and Nicholson, W. L. (1998) Spore photoproduct lyase from *Bacillus subtilis* spores is a novel iron-sulfur DNA repair enzyme which shares fratures with proteins such as class III anaerobic ribonucleotide reductases and pyruvate-formate lyases, *J. Bacteriol. 180*, 4879-4885.

51. Ollagnier, S., Kervio, W., and Rétey, J. (1998) The role and source of 5'-deoxyadenosyl radical in a carbon skeleton rearrangement catalyzed by a plant enzyme, *FEBS Lett. 437*, 309-312.

52. Wong, K. K., Murray, B. W., Lewisch, S. A., Baxter, M. K., Ridky, T. W., Ulissi-DeMario, L., and Kozarich, J. W. (1993) Molecular properties of pyruvate formate-lyase activating enzyme, *Biochemistry 32*, 14102-14110.

53. Eliasson, R., Fontecave, M., Jornvall, H., Krook, M., Pontis, E., and Reichard, P. (1990) The anaerobic ribonucleoside triphosphate reductase from *Escherichia coli* requires *S*-adenosylmethionine as a cofactor, *Proc. Natl. Acad. Sci. USA 87*, 3314-3318.

54. O'Brien, J. R., Raynaud, C., Croux, C., Girbal, L., Soucaille, P., and Lanzilotta, W. N. (2004) Insight into the mechanism of the B_{12}-independent glycerol dehydratase from *Clostridium butyricum*: preliminary biochemical and structural characterization, *Biochemistry 43*, 4635-4645.

55. Yu, L., Blaser, M., Andrei, P. I., Pierik, A. J., and Selmer, T. (2006) 4-Hydroxyphenylacetate decarboxylases: properties of a novel subclass of glycyl radical enzyme systems, *Biochemistry 45*, 9584-9592.

56. Duin, E. C., Lafferty, M. E., Crouse, B. R., Allen, R. M., Sanyal, I., Flint, D. H., and Johnson, M. K. (1997) [2Fe-2S] to [4Fe-4S] cluster conversion in *Escherichia coli* biotin synthase, *Biochemistry 36*, 11811-11820.

57. Reed, K. E., and Cronan Jr., J. E. (1993) Lipoic acid metabolism in *Escherichia coli*: sequencing and functional characterization of the *lipA* and *lipB* genes, *J. Bacteriol. 175*, 1325-1336.

58. Suzuki, J. Y., Bollivar, D. W., and Bauer, C. E. (1997) Genetic analysis of chlorophyll biosynthesis, *Annu. Rev. Genet. 31*, 61-89.

59. Akhtar, M. (1994) The modification of acetate and propionate side chains during the biosynthesis of haem and chlorophills: mechanistic and stereochemical studies, *Ciba Found. Symp. 180*, 131-155.

60. Rieder, C., Eisenreich, W., O'Brien, J., Richter, G., Götze, E., Boyle, P., Blanchard, S., Bacher, A., and Simon, H. (1998) Rearrangement reactions in the biosynthesis of molybdopterin: an NMR study with multiply $^{13}C/^{15}N$ labeled precursors, *Eur. J. Biochem. 255*, 24-36.

61. Esberg, B., Leung, H. -C. E., Tsui, H. -C. T., Björk, G. R. and Winkler, M. E. (1999) Identification of the *miaB* gene, involved in methylthiolation of isopentenylated A37 derivatives in the tRNA of *Salmonella typhymurium Escherichia coli*, *J. Bacteriol. 181*, 7256-7265.

62. Noma, A., Kirino, Y., Icheuchi, Y., and Suzuki, T. (2006) Biosynthesis of wybutosine, a hypermodified nucleoside in eukaryotic phenylalanine tRNA, *EMBO J. 25*, 2142-2215.

63. Begley, T. P., Xi, J., Kinsland, C., Taylor, S., and McLafferty, F. (1999) The enzymology of sulfur activation during thiamin and biotin biosynthesis, *Curr. Opin. Chem. Biol. 3*, 623-629.

64. Goodwin, P. M., and Anthony, C. (1998) The biochemistry, physiology, and genetics of PQQ and PQQ-containing enzymes, *Adv. Microbiol. Physiol. 40*, 1-80.

65. Allen, R. M., Chatterjee, R., Ludden, P. W., and Shah, V. K. (1995) Incorporation of iron and sulfur from NitB cofactor into the iron-molybdenum cofactor of nitrogenase, *J. Biol. Chem. 270*, 26890-26896.

66. Fang, Q., Peng, J., and Dierks, T. (2004) Post-translational formylglycine modification of bacterial sulfatases by the radical *S*-adenosylmethionine protein AtsB, *J. Biol. Chem. 279*, 14570-14578.

67. Becker, A., Küster, H., Niehaus, K., and Pühler, A. (1995) Extension of the *Rhizobium meliloti* succinoglycan biosynthesis gene cluster: identification of the

exsA gene encoding an ABC transporter protein, and the *exsB* gene which probably codes for a regulator of succinoglycan biosynthesis, *Mol. Gen. Genet. 249*, 487-497.

68. Lyutzkanova, D., Distler, J., and Altenbuchner, J. (1997) A spectinomycin resistance determinant from the spectinomycin producer *Streptomyces flavopersicus*, *Microbiology 143*, 2135-2143.

69. Zhang, G., Yan, L. Z., Vederas, J. C., and Zuber, P. (1999) Genes of the sbo-alb locus of *Bacillus subtilis* are required for production of the antilisterial bacteriocin subtilosin, *J. Bacteriol. 181*, 7346-7355.

70. Möhrle, V., Roos, U., and Bormann, C. (1995) Identification of cellular proteins involved in nikkomycin production in *Streptomyces tendae Tü901*, *Mol. Microbiol. 15*, 561-571.

71. Thompson, C. J., and Seto, H. (1995) *Bialaphos: Genetics and Biochemistry of Antibiotic Production*, Vol. 28, Butterworth-Heinemann.

72. Mao, U., Varoglu, M., and Sherman, F. H. (1999) Molecular characterization and analysis of the biosynthetic gene cluster for the antitumor antibiotic mitomycin C from *Streptomyces lavendulae* NRRL2564, *Chem. Biol. 6*, 251-263.

73. Morita, M., Tomita, K., Ishizawa, M., Takagi, K., Kawamura, F., Takahashi, H., and Morino, T. (1999) Cloning of oxetanocin A biosynthetic and resistance genes that reside on a plasmid of *Bacillus megaterium* strain NK84-0128, *Biosc. Biotechnol. Biochem. 63*, 563-566.

74. Kuzuyama, T., Seki, T., Dairi, T., Hidaka, T., and Seto, H. (1995) Nucleotide sequence of fortimicin KL1 methyltransferase gene isolated from *Micromonospora olivasterospora*, and comparison of its deduced amino acid sequence with those of methyltransferases involved in the biosynthesis of bialaphos and fosfomycin, *J. Antibiot. 48*, 1191-1193.

75. Kuzuyama, T., Hidaka, T., Kamigiri, K., Imai, S., and Seto, H. (1992) Studies on the biosynthesis of fosfomycin. 4. The biosynthetic origin of the methyl group of fosfomycin, *J. Antibiot. 45*, 1812-1814.

76. Westrich, L., Heide, L., and Li, S. M. (2003) CloN6, a novel methyltransferase catalysing the methylation of the pyrrole-2-carboxyl moiety of clorobiocin, *ChemBioChem 4*, 768-773.

77. Ching, Y. P., Qi, Z., and Wang, J. H. (2000) Cloning of three neuronal Cdk5 activator binding proteins, *Gene 242*, 285-294.

78. Grewal, T. S., Genever, P. G., Brabbs, A. C., Birch, M., and Skerry, T. M. (2000) Best5: a novel interferon-inducible gene expressed during bone formation, *FASEB J. 14*, 523-531.

79. Posewitz, M. C., King, P. W., Smolinski, S. L., Zhang, L., Seibert, M., and Ghirardi, M. L. (2004) Discovery of two novel radical *S*-adenosylmethionine proteins required for the assembly of an active [Fe] hydrogenase, *J. Biol. Chem. 279*, 25711-25720.

80. Boll, R., Hofmann, C., Heitmann, B., Hauser, G., Glaser, S., Koslowski, T., Friedrech, T., and Bechthold, A. (2006) The active conformation of avilamycin A is conferred by AviX12, a radical AdoMet enzyme, *J. Biol. Chem. 281*, 14756-14763.

81. Paraskevopoulou, C., Fairhurst, S. A., Lowe, D. J., Brick, P., and Onesti, S. (2006) The Elongator subunit Elp3 contains a Fe_4S_4 cluster and binds *S*-adenosylmethionine, *Mol. Microbiol. 59*, 795-806.

82. Walsby, C. J., Ortillo, D., Broderick, W. E., Broderick, J. B., and Hoffman, B. M. (2002) An anchoring role for FeS clusters: Chelation of the amino acid moiety of *S*-adenosylmethionine to the unique iron site of the [4Fe-4S] cluster of pyruvate formate-lyase activating enzyme, *J. Am. Chem. Soc. 124*, 11270-11271.

83. Berkovitch, F., Nicolet, Y., Wan, J. T., Jarrett, J. T., and Drennan, C. L. (2004) Crystal structure of biotin synthase, an *S*-adenosylmethionine-dependent radical enzyme, *Science 303*, 76-80.

84. Hinckley, G. T., and Frey, P. A. (2006) Cofactor dependence of reduction potentials for $[4Fe\text{-}4S]^{2+/1+}$ in lysine 2,3-aminomutase, *Biochemistry 45*, 3219-3225.

85. Reed, G. H. (2004) Radical mechanisms in adenosylcobalamin-dependent enzymes, *Curr. Opin. Chem. Biol. 8*, 477-483.

86. Chirpich, T. P., Zappia, V., Costilow, R. N., and Barker, H. A. (1970) Lysine 2,3-aminomutase. Purification and properties of a pyridoxal phosphate and *S*-adenosylmethionine-activated enzyme, *J. Biol. Chem. 245*, 1778-1789.

87. Song, K. B., and Frey, P. A. (1991) Molecular properties of lysine-2,3-aminomutase, *J. Biol. Chem. 266*, 7651-7655.

88. Ballinger, M. D., Frey, P. A., and Reed, G. H. (1992) Structure of a substrate radical intermediate in the reaction of lysine 2,3-aminomutase, *Biochemistry 31*, 10782-10789.

89. Ballinger, M. D., Reed, G. H., and Frey, P. A. (1992) An organic radical in the lysine 2,3-aminomutase reaction, *Biochemistry 31*, 949-953.

90. Chang, C. H., Ballinger, M. D., Reed, G. H., and Frey, P. A. (1996) Lysine 2,3-aminomutase: rapid mix-quench electron paramagnetic resonance studies establishing the kinetic competence of a substrate-based radical intermediate, *Biochemistry 35*, 11081-11084.

91. Ballinger, M. D., Frey, P. A., Reed, G. H., and LoBrutto, R. (1995) Pulsed electron paramagnetic resonance studies of the lysine 2,3-aminomutase substrate radical: Evidence for participation of pyridoxal 5'-phosphate in a radical rearrangement, *Biochemistry 34*, 10086-10093.

92. Wu, W., Lieder, K. W., Reed, G. H., and Frey, P. A. (1995) Observation of a second substrate radical intermediate in the reaction of lysine 2,3-aminomutase: A radical centered on the β-carbon of the alternative substrate, 4-thia-L-lysine, *Biochemistry 34*, 10532-10537.

93. Miller, J., Bandarian, V., Reed, G. H., and Frey, P. A. (2001) Inhibition of lysine 2,3-aminomutase by the alternative substrate 4-thialysine and characterization of the 4-thialysyl radical intermediate, *Arch. Biochem. Biophys. 387*, 281-288.

94. Magnusson, O. T., Reed, G. H., and Frey, P. A. (1999) Spectroscopic evidence for the participation of an allylic analogue of the 5'-deoxyadenosyl radical in the reaction of lysine 2,3-aminomutase, *J. Am. Chem. Soc. 121*, 9764-9765.

95. Magnusson, O. T., Reed, G. H., and Frey, P. A. (2001) Characterization of an allylic analogue of the 5'-deoxyadenosyl radical: an intermediate in the reaction of lysine 2,3-aminomutase, *Biochemistry 40*, 7773-7782.

96. Knappe, J., Blaschkowski, H. P., Groebner, P., and Schmitt, T. (1974) Pyruvate formate-lyase of *Escherichia coli*. Acetyl-enzyme intermediate, *Eur. J. Biochem. 50*, 253-263.

97. Knappe, J., Schacht, J., Moeckel, W., Hoepner, T., Vetter, H., Jr., and Edenharder, R. (1969) Pyruvate formate-lyase reaction in *Escherichia coli*. The enzymic system converting an inactive form of the lyase into the catalytically active enzyme, *Eur. J. Biochem. 11*, 316-327.

98. Knappe, J., Neugebauer, F. A., Blaschkowski, H. P., and Gaenzler, M. (1984) Post-translational activation introduces a free radical into pyruvate formate-lyase, *Proc. Natl. Acad. Sci. USA. 81*, 1332-1335.

99. Himo, F. (2000) Stability of protein-bound glycyl radical: a density functional theory study, *Chem. Phys. Lett. 328*, 270-276.

100. Wagner, A. F. V., Frey, M., Neugebauer, F. A., Schaefer, W., and Knappe, J. (1992) The free radical in pyruvate formate-lyase is located on glycine-734, *Proc. Natl. Acad. Sci. USA. 89*, 996-1000.

101. Unkrig, V., Neugebauer, F. A., and Knappe, J. (1989) The free radical of pyruvate formate-lyase. Characterization by EPR spectroscopy and involvement in catalysis as studied with the substrate-analogue hypophosphite, *Eur. J. Biochem. 184*, 723-728.

102. Parast, C. V., Wong, K. K., and Kozarich, J. W. (1995) Electron paramagnetic resonance evidence for a cysteine-based radical in pyruvate formate-lyase inactivated with mercaptopyruvate, *Biochemistry 34*, 5712-5717.

103. Parast, C. V., Wong, K. K., Lewisch, S. A., and Kozarich, J. W. (1995) Hydrogen exchange of the glycyl radical of pyruvate formate-lyase is catalyzed by cysteine 419, *Biochemistry 34*, 2393-2399.

104. Conradt, H., Hohmann-Berger, M., Hohmann, H. P., Blaschowski, H. P., and Knappe, J. (1984) Pyruvate formate-lyase (inactive form) and pyruvate formate-lyase activating enzyme of *Escherichia coli*: isolation and structural properties, *J. Arch. Biochem. Biophys. 228*, 133-142.

105. Frey, M., Rothe, M., Wagner, A. F. V., and Knappe, J. (1994) Adenosylmethionine-dependent synthesis of the glycyl radical in pyruvate formate-lyase by abstraction of the glycine C-2 *pro-S* hydrogen atom. Studies of [^{2}H]glycine-substituted enzyme and peptides homologous to the glycine 734 site, *J. Biol. Chem. 269*, 12432-12437.

106. Knappe, J. S., T. 1976, 71, 1110. (1976) A novel reaction of *S*-adenosyl-L-methionine correlated with the activation of pyruvate formate-lyase, *Biochem. Biophys. Res. Commun. 71*, 1110-1117.

107. Stubbe, J., and van der Donk, W. A. (1998) Protein radicals in enzyme catalysis, *Chem. Rev. 98*, 705-762.

108. Jordan, A., and Reichard, P. (1998) Ribonucleotide reductases, *Annu. Rev. Biochem. 67*, 71-98.

109. Mulliez, E., Ollagnier, S., Fontecave, M., Eliasson, R., and Reichard, P. (1995) Formate is the hydrogen donor for the anaerobic ribonucleotide reductase from *Escherichia coli*, *Proc. Natl. Acad. Sci. USA. 92*, 8759-8762.

110. Sun, X., Harder, J., Krook, M., Jornvall, H., and Sjoberg, B.-M. (1993) A possible glycine radical in anaerobic ribonucleotide reductase from *Escherichia coli*: Nucleotide sequence of the cloned *nrdD* gene, *Proc. Natl. Acad. Sci. USA. 90*, 577-581.

111. Mulliez, E., Fontecave, M., Gaillard, J., and Reichard, P. (1993) An iron-sulfur center and a free radical in the active anaerobic ribonucleotide reductase of *Escherichia coli*, *J. Biol. Chem. 268*, 2296-2299.

112. Harder, J., Eliasson, R., Pontis, E., Ballinger, M. D., and Reichard, P. (1992) Activation of the anaerobic ribonucleotide reductase from *Escherichia coli* by *S*-adenosylmethionine, *J. Biol. Chem. 267*, 25548-25552.

113. Sun, X., Eliasson, R., Pontis, E., Andersson, J., Buist, G., Sjoeberg, B.-M., and Reichard, P. (1995) Generation of the glycyl radical of the anaerobic *Escherichia coli* ribonucleotide reductase requires a specific activating enzyme, *J. Biol. Chem. 270*, 2443-2446.

114. Bianchi, V., Haggaard-Ljungquist, E., Pontis, E., and Reichard, P. (1995) Interruption of the ferredoxin (flavodoxin) $NADP^+$ oxidoreductase gene of *Escherichia coli* does not affect anaerobic growth but increases sensitivity to paraquat, *J. Bacteriol. 177*, 4528-4531.

115. Ollagnier, S., Mulliez, E., Schmidt, P. P., Eliasson, R., Gaillard, J., Deronzier, C., Bergman, T., Graslund, A., Reichard, P., and Fontecave, M. (1997) Activation of the anaerobic ribonucleotide reductase from *Escherichia coli*. The essential role of the iron-sulfur center for *S*-adenosylmethionine reduction, *J. Biol. Chem. 272*, 24216-24223.

116. Cho, K. B., Himo, F., Graslund, A., and Siegbahn, P. E. M. J. (2001) The substrate reaction mechanism of class III anaerobic ribonucleotide reductase, *J. Phys. Chem. B 105*, 6445-6452.

117. Webb, M. E., Marquet, A., Mendel, R. R., Rebeille, F., and Smith, A. G. (2007) Elucidating biosynthetic pathways for vitamins and cofactors, *Nat. Prod. Rep. 24*, 988-1008.

118. Sanyal, I., Cohen, G., and Flint, D. H. (1994) Biotin synthase: purification, characterization as a [2Fe-2S] cluster protein, and *in vitro* activity of the *Escherichia coli bioB* gene product, *Biochemistry 33*, 3625-3631.

119. Broach, R. B., and Jarrett, J. T. (2006) Role of the $[2Fe\text{-}2S]^{2+}$ cluster in biotin synthase: mutagenesis of the atypical metal ligand arginine 260, *Biochemistry 45*, 14166-14174.

120. Ugulava, N. B., Sacanell, C. J., and Jarrett, J. T. (2001) Spectroscopic changes during a single turnover of biotin synthase: destruction of a [2Fe–2S] cluster accompanies sulfur insertion, *Biochemistry 40*, 8352–8358.

121. Jameson, G. N. L., Cosper, M. M., Hernández, H. L., Johnson, M. K., and Huynh, B. H. (2004) Role of the [2Fe–2S] cluster in recombinant *Escherichia coli* biotin synthase, *Biochemistry 43*, 2022–2031.

122. Tse Sum Bui, B., Mattioli, T. A., Florentin, D., Bolbach, G., and Marquet, A. (2006) *Escherichia coli* biotin synthase produces selenobiotin. Further evidence of the involvement of the $[2Fe–2S]^{2+}$ cluster in the sulfur insertion step, *Biochemistry 45*, 3824-2834.

123. Marquet, A., Frappier, F., Guillerm, G., Azoulay, M., Florentin, D., and Tabet, J. C. (1993) Biotin biosynthesis: synthesis and biological evaluation of the putative intermediate thiols, *J. Am. Chem. Soc. 115*, 2139-2145.

124. Frappier, F., Jouany, M., Marquet, A., Olesker, A., and Tabet, J. C. (1982) On the mechanism of the conversion of dethiobiotin to biotin in *E. coli*. Studies with deuterated precursors using tandem mass spectroscopic (MS-MS) techniques, *J. Org. Chem. 47*, 2257-2261.

125. Booker, S. J., Cicchillo, R. M., and Grove, T. L. (2007) Self-sacrifice in radical *S*-adenosylmethionine proteins, *Curr. Opin. Chem. Biol. 11*, 543-552.

126. Zhao, S., Miller, J. R., Jiang, Y., Marletta, M. A., and Cronan, J. E. J. (2003) Assembly of the covalent linkage between lipoic acid and its cognate enzymes, *Chem. Biol. 10*, 1293-1302.

127. Cicchillo, R. M., Iwig, D. F., Jones, A. D., Nesbitt, N. M., Baleanu-Gogonea, C., Souder, M. G., Tu, L., and Booker, S. J. (2004) Lipoyl synthase requires two equivalents of *S*-adenosyl-L-methionine to synthesize one equivalent of lipoic acid, *Biochemistry 43*, 6378-6386.

128. Cronan, J. E., Zhao, X., and Jiang, Y. (2005) Function, attachment and synthesis of lipoic acid in *Escherichia coli*, *Adv. Microb. Physiol. 50*, 103–146.

129. Parry, R. J. (1983) Biosynthesis of some sulfur-containing natural products. Investigations of the mechanism of carbon–sulfur bond formation, *Tetrahedron 39*, 1215-1238.

130. Douglas, P., Kriek, M., Bryant, P., and Roach, P. L. (2006) Lipoyl synthase inserts sulfur atoms into an octanoyl substrate in a stepwise manner, *Angew. Chem. 118*, 5321-5323.

131. Cicchillo, R. M., Lee, K.-H., Baleanu-Gogonea, C., Nesbitt, N. M., Krebs, C., and Booker, S. J. (2004) *Escherichia coli* lipoyl synthase binds two distinct [4Fe–4S] clusters per polypeptide, *Biochemistry 43*, 11770-11781.

132. Cicchillo, R. M., and Booker, S. J. (2005) Mechanistic investigations of lipoic acid biosynthesis in *Escherichia coli*: Both sulfur atoms in lipoic acid are contributed by the same lipoyl synthase polypeptide, *J. Am. Chem. Soc. 127*, 2860-2861.

Chapter 2: Characterization of DesII in the Biosynthesis of TDP-D-desosamine from *Streptomyces venezuelae*

2.1 INTRODUCTION

D-Desosamine (**2-1**), a 3-(dimethylamino)-3,4,6-trideoxyhexose found in a number of macrolide antibiotics including methymycin (**2-2**), neomethymycin (**2-3**), pikromycin (**2-4**), and narbomycin (**2-5**) produced by *Streptomyces venezuelae*, plays an essential role in conferring antibiotic activities to their parent aglycones (*1, 2*) (Figure 2-1). Although numerous strategies for C-O bond cleavage have been elucidated as described in Chapter 1, little is known about C-4 deoxygenation in desosamine biosynthesis (*3, 4*). Characterization of the enzymes involved in this transformation is essential to fully establish the reaction sequence involved in desosamine biosyntheis.

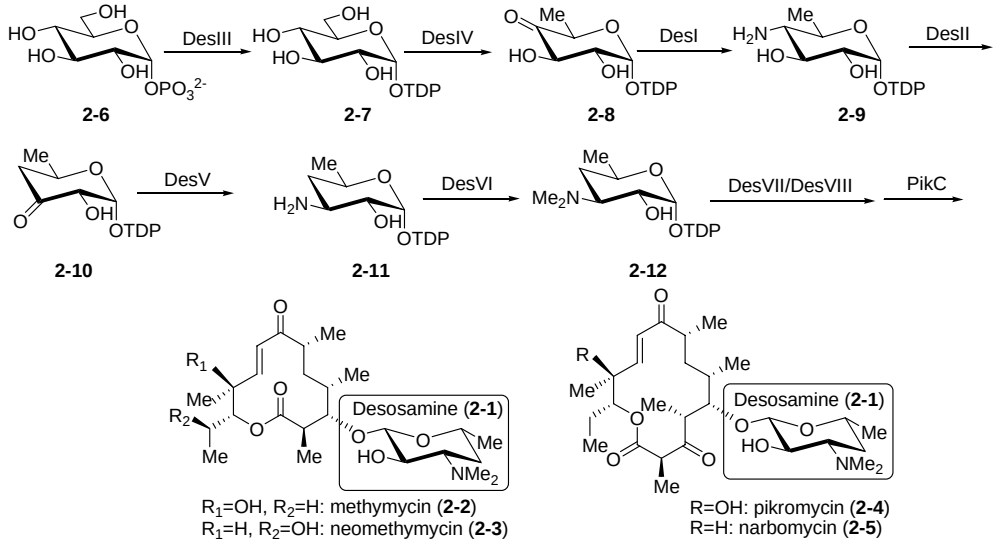

Figure 2-1. TDP-D-desosamine biosynthesis in *S. venezuelae*.

Previous genetic studies have shown that among eight open reading frames within the desosamine biosynthetic gene cluster (*desI* to *desVIII*), *desI* and *desII* were determined to be associated with the C4 deoxygenation (*5*). Additionally, previous mechanistic investigation of various deoxyhexose biosynthesis demonstrated that the deoxygenation mechanism correlates with the position of the scissile carbon-oxygen bond, either α or β to an activating group such as a keto moiety (*6*). For example, a stepwise dehydration-reduction sequence catalyzed by a pyridoxamine 5'-phosphate (PMP)-dependent [2Fe-2S]-containing enzyme, E_1 (*7, 8*), and an iron-sulfur flavoprotein reductase, E_3 (*9*), is the prototypical mechanism for α-deoxygenation of a ketosugar substrate (*10, 11*) (Figure 2-2).

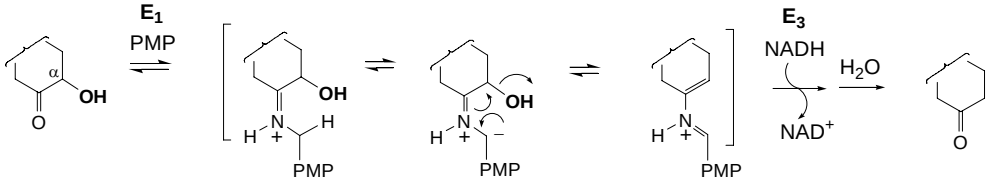

Figure 2-2. A prototypical mechanism for α-deoxygenation of a ketosugar substrate.

Hence, the deoxygenation at C4 in the biosynthesis of D-desosamine could follow the α-deoxygenation path similar to that catalyzed by E_1 and E_3 starting from TDP-3-keto-6-deoxyhexose (**2-13**) to give TDP-3-keto-4,6-dideoxyhexose (**2-10**, Figure 2-3, path A). This possibility is supported by the fact that the translated sequences of two genes, *desI* and *desII*, which are assigned to encode proteins involved in the C4 deoxygenation in the desosamine biosynthetic gene cluster (*3, 4*), are highly similar to B_6-dependent enzymes and those containing an iron-sulfur center, respectively. In the previously proposed

reaction sequence, DesVIII was thought to catalyze 3,4-ketoisomerization of **2-8** (i.e., **2-8→2-13**) preceding C4 deoxygenation.

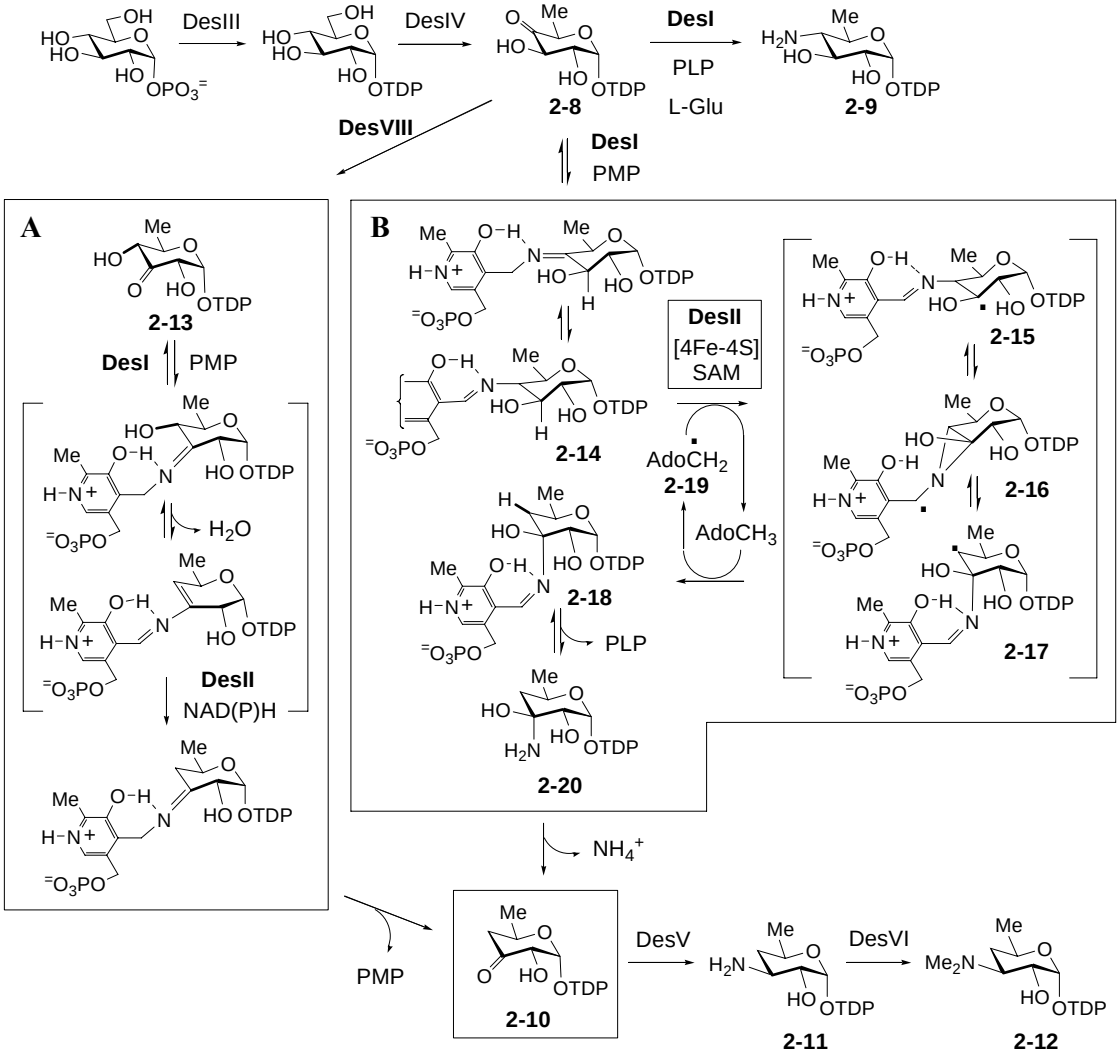

Figure 2-3. Possible mechanisms of deoxygenation at the C-4 position in the biosynthesis of TDP-D-desosamine.

However, recent bichemical studies on DesI showed that it recognizes TDP-4-keto-6-deoxy-glucose (**2-8**) as a substrate, but not **2-13**. Thus, 3,4-ketoisomerization of **2-8** previously thought to be catalyzed by DesVIII is not necessary for DesI activity. Furthermore, DesI is a pyridoxal 5′-phosphate (PLP)-dependent 4-aminotransferase and

catalyzes a transamination reaction to generate TDP-4-amino-4,6-dideoxy-glucose (*5*) (**2-9**, Figure 2-4). DesII, which contains the [4Fe-4S] consensus motif, CXXXCXXC, has been identified as a member of the radical *S*-adenosylmethionine (SAM) superfamily by sequence analysis (*12*). Representative alignments are shown in Figure 2-5. More recently, DesVIII was demonstrated to be an auxiliary protein of D-desosaminyl transferase, DesVII, and participates in the glycosyltransfer reaction, transferring TDP-D-desosamine to its parent aglycones (*13, 14*). These observations prompted a revision of the proposed biosynthetic pathway for TDP-D-desosamine.

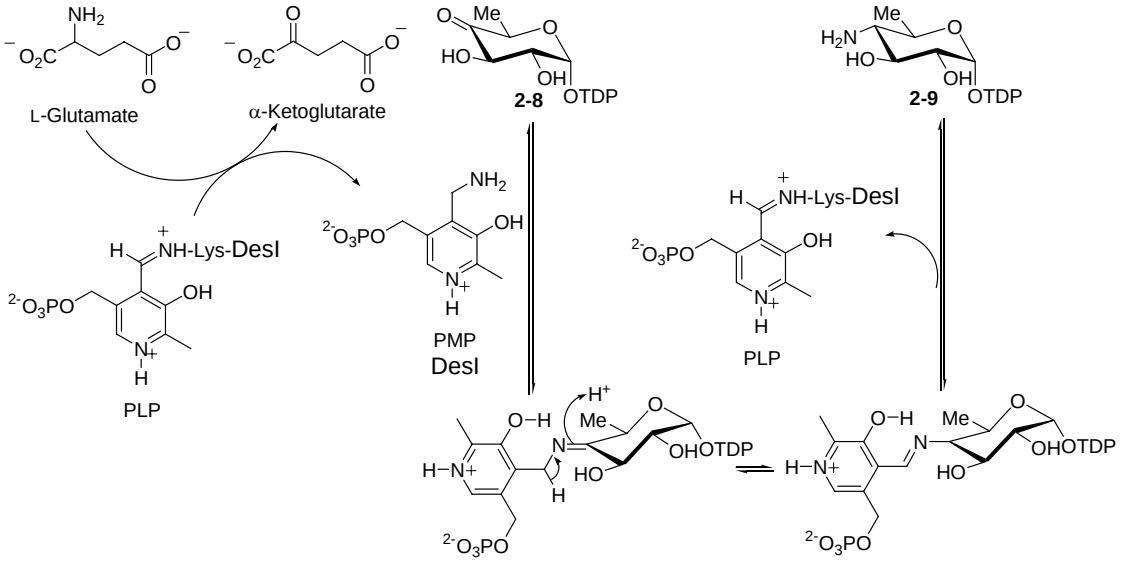

Figure 2-4. The transamination reaction catalyzed by DesI in desosamine biosynthesis.

Lysine 2,3-Aminomutase	VLLLITDMCSMYCRHCTRRRFAGO
Biotin Synthase	LLSIKTGACPEDCKYCPQSSRYKT
Ribonucleotide Reductase Class III	RCTLFVSGCVHECPGCYNKSTWRV
Lipoate Synthase	TFMILGAVCTRACRFCAVKTGLPT
Pyruvate Formate Lyase-Activase	RYVIFTQGCLLRCQGCHNADTWEI
DesII	VGLYPGPTCMFRCHFCVRVTGARY
Consensus Sequence	CXXXCXXC

Figure 2-5. The sequence alignment of radical SAM enzyme superfamily.

On the basis of other established radical enzyme mechanisms (*15, 16*), a possible mechanism for C-4 deoxygenation was proposed, in which DesI and DesII may function together (Figure 2-3, path B). In this mechanism, DesI-DesII catalysis is initiated by the formation of a Schiff base (**2-14**) between DesI-bound PMP and the C-4 position of the sugar substrate **2-8**, followed by an aza-allylic isomerization to form **2-18** (i.e., **2-14→2-15→2-16→2-17→2-18**). Abstraction of the C-3 hydrogen from the Schiff base **2-14** by the 5′-deoxyadenosyl radical (**2-19**) leads to the radical **2-15** and 5′-deoxyadenosine. This is followed by a 1,2-nitrogen shift from C-4 to C-3. Pairing of the unpaired electron in **2-15** with a π-electron of the imine bond forms an azacyclopropylcarbinyl radical **2-16**. Subsequent C4-N bond cleavage gives the C-4-centered radical **2-17**. Abstraction of a hydrogen atom from the methyl group of 5′-deoxyadenosine by C-4-centered radical **2-17** produces the Schiff base **2-18** and regenerates the 5′-deoxyadenosyl radical (**2-19**). Hydrolysis of the Schiff base **2-18** followed by the elimination of ammonia gives the 3-keto sugar product **2-10**.

Such a 1,2-migration of an amino group has been observed in the interconversion of L-lysine and L-β-lysine catalyzed by lysine 2,3-aminomutase (LAM) as described in Chapter 1 (*15*). The LAM from *Clostridium subterminale* SB4 contains a [4Fe-4S] center and requires PLP as well as SAM for its activity. Because DesI is a PLP-dependent enzyme and DesII is a member of the radical SAM superfamily, DesI and DesII may work together to catalyze a 1,2-amino migration and accomplish C-4 deoxygenation. Catalysis by LAM is believed to involve a 5′-deoxyadenosyl radical (**2-19**) which is generated by a reductive cleavage of SAM (*17*). The reduced form of the [4Fe-4S] center

in DesII is expected to donate one electron to initiate the reductive cleavage of SAM to generate the 5′-deoxyadenosyl radical (**2-19**), which then abstracts a C-3 hydrogen atom of the Schiff base **2-14** and initiates the isomerization.

The work described in this chapter was initially intended to test the aforementioned hypothesis (i.e., Figure 2-3, path B). The experiments begun with the heterologous expression and purification of the recombinant DesI and DesII in *E. coli*, followed by experiments carried out to characterize the purified enzymes. The basic properties of DesI were confirmed as previously reported (*5*). The DesI substrate was prepared following literature procedures and the identity of the DesI substrate was verified by NMR spectroscopy (*5*). An anaerobic reconstitution method was developed to reconstitute the $[4Fe\text{-}4S]^{+}$ cluster of DesII *in vitro*. The reducing agent sodium dithionite was added to reduce the $[4Fe\text{-}4S]^{2+}$ cluster to the $[4Fe\text{-}4S]^{+}$ state, which is the EPR-sensitive catalytic form. The iron-sulfur cluster in both the as-purified and reconstituted DesII was characterized by EPR spectroscopy. An HPLC assay was developed to demonstrate the converstion of TDP-4-keto-6-deoxy-D-glucose (**2-8**, Figure 2-1) to TDP-3-keto-4,6-dideoxy-D-glucose (**2-10**) by DesI and DesII. Furthermore, the HPLC assay was also carried out to show the conversion of TDP-4-amino-4,6-dideoxy-D-glucose (**2-9**) to TDP-3-keto-4,6-dideoxy-D-glucose (**2-10**) in the presence of DesII alone. In addition to high-resolution mass spectrometry analysis, a coupled assay including DesII and DesV, the C-3 aminotransferase converting TDP-3-keto-4,6-dideoxy-D-glucose (**2-10**) to TDP-3-amino-4,6-dideoxy-D-glucose (*18*) (**2-11**, Figure 2-1), was also performed to further demonstrate the formation of the DesII product. The result showed that DesII can recognize the DesI product (**2-9**, Figure 2-1) as a substrate, clearly indicating that

DesI and DesII function independently to carry out C-4 deoxygenation. A revision of the proposed mechanisms to account for these observations is presented in the discussion section of this chapter (Figure 2-39). The steady-state kinetic parameters for the DesII-catalyzed reaction were determined and compared with those of other radical SAM enzymes. A possible biological reducing system, flavodoxin, flavodoxin reductase, and NADPH, for the reduction of the $[4Fe\text{-}4S]^{2+}$ cluster, was cloned, expressed, and purified in *E. coli*. DesII activity was established in the presence of this reducing system. Additionally, the substrate specificity of DesI and DesII was also investigated. The substrate flexibility of DesII opened the possibilities to synthesize potential mechanistic probes to elucidate C-4 deoxygenation, which will be discussed in Chapter 3.

2.2 MATERIALS AND METHODS

General. Protein concentrations were determined by the method of Bradford (*19*) using bovine serum albumin as the standard. The relative molecular mass and purity of enzyme samples were determined using SDS-PAGE as described by Laemmli (*20*). The native molecular mass of DesII was determined by the gel filtration method of Andrews (*21*). NMR spectra were acquired on either a Varian Unity 300 or 500 MHz spectrometer, and chemical shifts (δ in parts per million) are given relative to those for the corresponding solvent peaks (for ^{1}H and ^{13}C) and aqueous 85% H_3PO_4 (external, for ^{31}P), with coupling constants reported in hertz (Hz). DNA sequencing was performed by the Core Facilities of the Institute of Cellular and Molecular Biology at the University of Texas at Austin. Mass spectra were obtained by the Mass Spectrometry Core Facility in

the Department of Chemistry and Biochemistry at the University of Texas at Austin. The general methods and protocols for recombinant DNA manipulations followed those described by Sambrook *et al*. (*22*) . Kinetic data were analyzed by nonlinear fit using Grafit5 (Erithacus Software Ltd.).

Materials. Vectors pET24b(+) and pET28b(+) were purchased from Novagen (Madison, WI). Enzymes and molecular weight standards used for molecular cloning experiments were products of Invitrogen (Carlsbad, CA) or New England Biolabs (Ipswich, MA). Ni-NTA agarose and kits for DNA gel extraction and spin miniprep were obtained from Qiagen (Valencia, CA). *Pfu* DNA polymerase was purchased from Stratagene (La Jolla, CA), and growth medium components were acquired from Becton Dickinson (Sparks, MD). Antibiotics and chemicals were products of Sigma-Aldrich Chemical Co. (St. Louis, MO) or Fisher Scientific (Pittsburgh, PA). All chemicals were analytical grade or the highest quality commercially available. Oxygen free argon, nitrogen, and gas mixture (5% hydrogen and 95% nitrogen) were obtained from Airgas (Austin, TX). Bio-gel P2 resin and all reagents for sodium dodecyl sulfate-polyacrylamide gel electrophoresis (SDS-PAGE) were purchased from Bio-Rad (Hercules, CA), with the exception of the prestained protein molecular weight marker, which was obtained from New England Biolabs. Amicon YM-10 filtration products were purchased from Millipore (Billerica, MA). Sephadex G-25 resin was acquired from Amersham (GE Healthcare). Oligonucleotide primers for cloning were prepared by Integrated DNA Technologies (Coralville, IA) or Invitrogen (Carlsbad, CA). The plasmid, pDB1282, encoding genes for iron-sulfur cluster biosynthesis was a generous gift from Professor Dennis Dean at Virginia Polytechnic Institute and State University.

The genomic DNA of *Streptomyces venezuelae*, the Tyl1a and TylB enzymes were provided by Dr. Charles E. Melancüon III of this labrotory. The genomic DNA of *E. coli* K-12 used to clone *flavodoxin* and *flavodoxin reductase* was prepared by Dr. Wei-luen Allen Yu of this labrotory. The plasmid pET28b(+) containing the *desI* gene was previously constructed by Dr. Lishan Zhao of this group (*5*). The products of DesII and DesV enzymes were previously prepared using a combination of synthetic and enzymatic methods by Dr. Lishan Zhao and Dr. Cheng-wei Chang of this laboratory, respectively (*18, 23*).

Bacterial Strains. E. coli DH5α from Invitrogen (Carlsbad, CA) was used as the host for routine cloning. *E. coli* BL21 Star (DE3) and BL21(DE3) from Novagen (Madison, WI) were used as the hosts for the overexpression of recombinant proteins.

Instrumentation. The pH values were measured using a Corning pH meter 240 from Fisher Scientific. Agarose gel electrophoresis was conducted using a mini-sub cell GT apparatus from Biorad (Richmond, CA) which was powered by either a FB600 or a FB300 power supply from Fisher Scientific. Centrifugation procedures were performed using either an Avanti J-25 or Avanti JE-25 unit from Beckman-Coulter (Arlington Heights, IL) for large volumes, or using an Eppendorf 5415C microcentrifuge from Brinkmann Instruments (Westbury, NY) for small volumes. Photography of agarose gels was carried out with a Kodak EDAS 290 apparatus connected to a PC running Kodak 1D 3.5 software using a FBTIV-88 transilluminator from Fisher Scientific. PCR was performed using an Eppendorf Mastercycler Gradient from Brinkman Instruments. HPLC separations were performed using a Beckman 366 instrument (Beckman Instruments, Fullerton, CA). Analytical (4 × 250 mm) and semi-preparative (9 × 250 mm) CarboPac™

PA1 HPLC columns were obtained from Dionex (Sunnyvale, CA). FPLC was acquired from Amersham Biosciences, and Mono-Q H/R 16/10 FPLC columns were purchased from Pharmacia (Uppsala, Sweden). Mini-PROTEAN II vertical system used for SDS-PAGE, Mini Trans-Blot Cell used for blotting transfer, GelAir gel drying system, and the accessories were products of BioRad. Ultraviolet–visible spectra were obtained using a Beckman DU-650 spectrophotometer. Cell disruption was performed using a Fisher 550 Sonic Dismembrator. A Schlenk line used for anaerobic experiments was purchased from ACE Glass, Inc. (Vineland, NJ). All the anaerobic experiments were performed in the glovebox (Coy Laboratory Products, Inc. Grass Lake, MI) under the atmosphere consisting of 95% N_2 and 5% H_2 at oxygen levels <5 ppm. The catalysis used to remove the oxygen was regenerated every month by heating at 120 °C for 2 h. EPR spectra were recorded at liquid helium temperature on a Bruker EMX EPR spectrometer at the University of Texas at Houston Medical School.

Preparation of Competent Cells. Competent cells were prepared using the rubidium chloride (RbCl) method (*22*). Specifically, a single fresh colony of the appropriate *E. coli* strain was used to inoculate 2 mL of Luria-Bertani (LB) liquid medium and the resulting culture was grown overnight at 37 °C with constant shaking at 250 rpm. A 250 μL aliquot of an overnight culture was transferred to 50 mL of the LB medium in a 250 mL Erlenmeyer flask. Cells were grown at 37 °C to an OD_{600} of approximately 0.4, at which time the culture was transferred into a pre-cooled polypropylene tube and incubated on ice for 30 min. After centrifugation at 3,000*g* for 12 min at 4 °C, the supernatant was discarded, and the cell pellet was gently resuspended in one-third (15 mL) the original culture volume of ice-cold RF1 solution (100 mM RbCl,

15% glycerol, 50 mM $MnCl_2$, 30 mM potassium acetate, 10 mM $CaCl_2$, pH 5.8, filter sterilized by passage through a 0.22 μm membrane). After subsequent incubation on ice for 15 min, the cell suspension was centrifuged again at 3,000*g*, 4 °C for 12 min, and the resulting cell pellet was resuspended in two twenty-fifths (4 mL) of the original culture volume of ice-cold RF2 solution (10 mM RbCl, 10 mM MOPS, 75 mM $CaCl_2$, 15% glycerol, pH 6.8). The cell suspension was then aliquoted into 100 μL portions in sterilized pre-cooled microcentrifuge tubes and frozen at –80 °C.

PCR Primers. Two oligonucleotide primers complementary to the sequences at each end of the DNA fragment to be amplified were designed and the appropriate restriction enzyme sites were incorporated when appropriate. Several primer design rules were obeyed. First, each primer must have at least 18 base pairs exactly matching the bases of the template (genome) sequences. Second, the melting temperatures (T_m) of the portion of the primer pair complementary to the target sequence and of the entire primer sequence of the primer pair were matched as closely as possible to ensure efficient annealing throughout the reaction. If restriction enzyme recognition sites were engineered into the primers, a two to four base pair variable sequence was added to the 5' end of the primer, depending on the restriction enzyme. Additionally, primer pairs were checked using NetPrimer® available on the PREMIER Biosoft Int. Website (http://www.premierbiosoft.com/) to ensure that stable secondary structures, self-dimers and hetero-dimers do not occur in the chosen sequences. The primer pairs used to clone *desII*, *flavodoxin* (*fld*), and *flavodoxin reductase* (*fpr*) genes are listed in Table 2-1.

Gene	Cloning Sites	Primer Sequence
desII	*Nde*I	5′-CGCG**CATATG**ACCGCCCCCGCCCTTTCC-3′ (forward)
	*Xho*I	5′-GCGC**CTCGAG**GCGCAGGAAGCC-3′ (reverse)
fld	*Nde*I	5′-TCGC**CATATG**AACAGCTGCGTATTAATAA-3′ (forward)
	*Xho*I	5′-GCAA**CTCGAG**TTAATAAAAACGTGGACA-3′ (reverse)
fpr	*Nco*I	5′-AAAA**CCATGG**CTGATTGGGTAAC-3′ (forward)
	*Xho*I	5′-AAGT**CTCGAG**CCAGTAATGCTCCGCTGT-3′ (reverse)

Table 2-1. Primer pairs for cloning *desII*, *flavodoxin* (*fld*), and *flavodoxin reductase* (*fpr*) genes.

Polyacrylamide Gel Electrophoresis. The subunit molecular mass and the purity of the protein samples were assessed by SDS-PAGE. The separation gel and the stacking gel for electrophoresis were 12% and 4%, respectively. Prior to electrophoresis, protein samples were mixed with 10 μL of loading buffer (62.5 mM Tri-HCl buffer, pH 6.8, containing 10% glycerol, 2% SDS, 5% β-mercaptoethanol, and 0.0025% bromophenol blue) and heated in boiling water for 5 min except for the His_6-tagged proteins. For proteins with either N- or C-terminal His_6-tag, the corresponding mixtures were incubated at 37 °C for 10 min. Electrophoresis was performed using 25 mM Tris·HCl buffer containing 192 mM glycine, and 0.1% SDS (pH 8.3) at 25 mA. Gels were stained with Coomassie blue and destained with acetic acid/methanol/water (15:29:165 by volume). Protein standards for SDS-PAGE include α-lactalbumin (14 kDa), trypsinogen (24 kDa), carbonic anhydrase (29 kDa), glyceraldehyde-3-phosphate dehydrogenase (36 kDa), egg albumin (45 kDa), and bovine serum albumin (66 kDa).

Analysis of Poly-Histidine-Tagged Recombinant Protein Using Western Blotting. After SDS-PAGE was complete, the polyacrylamide gel was removed carefully and

equilibrated in transfer buffer (25 mM Tris•HCl, 192 mM glycine, 20% (v/v) methanol, pH 8.3) at room temperature for 10 min with gentle shaking. The equilibrated gel and blotting membrane were assembled into the gel-transfer cassette and placed within the Mini Trans-Blot Cell apparatus. The protein transfer was performed at 100 V for 1 h using an internal icepack to cool apparatus. After transfer, the membrane with immobilized proteins was rinsed with TBST buffer (100 mM Tris•HCl, 0.9% (w/v) NaCl, 0.1% (v/v) Tween 20, pH 7.5), and then blocked with 5% non-fat milk/TBST buffer (w/v) at room temperature for 1 h. The blocked membrane was hybridized with mouse monoclonal anti-polyHistidine antibody (3,000 × dilution in 5% non-fat milk/TBST) at room temperature for 1 h or at 4 °C overnight. After washing three times with TBST buffer, the membrane was incubated with alkaline-phosphatase-conjugated anti-mouse IgG Fc-specific secondary antibody (30,000 × dilutions in 5% non-fat milk/TBST) at room temperature for 45 min with gentle agitation. The membrane was then washed three times with TBST buffer, and the immobilized poly-histidine-tagged protein was detected with BCIP/NBT color development substrate in alkaline phosphatase buffer (100 mM Tris•HCl, 100 mM NaCl, 5 mM $MgCl_2$, pH 9.5).

Concentrating Purified Proteins and Protein Dialysis. The protein eluates, from either Ni-NTA or FPLC-MonoQ chromatography, were concentrated with Amicon Ultra-15 Centrifugal Filter Units (Membrane NMWL, 10,000 kDa) until the total volume of the eluate was reduced to approximately 5 mL and then dialyzed to remove imidazole. The centrifugation operations were carried out at 4 °C. The dialysis buffer was exchanged for fresh buffer at least three times, and for each round, the dialysis was performed with gentle stirring for at least 6 h. After dialysis, protein concentrations were determined by

either Bradford assay (*19*) with bovine serum albumin (BSA) as the standard, or the UV absorbance at 280 nm. The proteins were aliquoted into 1 mL fractions and stored at -80 °C.

Molecular Mass Determination of DesII. The native molecular mass of DesII was determined by gel filtration performed on a FPLC system equipped with a Superdex 200 HR 10/30 column. The proteins were eluted isocratically using 50 mM NaH_2PO_4 buffer with 150 mM NaCl (pH 7.0) at a flow rate of 0.5 mL/min. The system was calibrated with protein standards (Sigma), and the void volume (V_0) was measured using blue dextran. The data were analyzed by the method of Andrews (*21*).

Iron Titration. The standard curve was determined using $Fe(NH_4)_2(SO_4)_2$. Protein samples (1 mL each) for iron titration analysis (*24*) were mixed with 500 μL of reagent A (1:1 of 4.5% $KMnO_4$:1.2 N HCl) and incubated at 60 °C for 2 h. To these samples were added 100 μL of reagent B (8.8 g of ascorbic acid, 9.7 g of ammonium acetate, 80 mg of ferrozine, 80 mg of neocuproine, and ddH_2O to 25 mL total volume) followed by immediate vortexing. The absorbance of the samples was determined at 562 nm after the samples had incubated for 1 h at room temperature.

Sulfur Content Determination. The labile sulfur content of DesII was determined by quantitating the sulfide released following protein denaturation by guanidine hydrochloride in the presence of dithiothreitol (*25*). First, the inorganic sulfur S^{2-} was absorbed on zinc as zinc sulfide. The S^{2-} was released in acidic solution, treated with *p*-aminodimethylamine, and the resulting methylene blue was assayed at 670 nm. This assay allows the quantitation of 1-3 nmol of inorganic sulfur. All glassware was

previously acid-washed and all solutions were prepared with metal free distilled H_2O. Approximately 75 μg of protein (1.5 nmol, in duplicate) was diluted with water or 20 mM Tris•HCl buffer, pH 7.6 to a total volume of 200 μL. A freshly prepared deoxygenated 1% zinc acetate solution (600 μL) was quickly added immediately followed by an addition of 30 μL of 12% NaOH. The mixture was stirred until the color became homogeneous. After the reaction was incubated at room temperature for 1 h, 150 μL of DMPD solution (0.1% *N*,*N*-dimethyl-*p*-phenylenediamine monohydrochloride in 5N HCl) was added followed by gentle stirring until only the top 2-mm layer retained undissolved zinc hydroxide as observed by the presence of pink color. A volume of 30 μL of $FeCl_3$ (23 mM $FeCl_3$ in 1.2 N HCl) solution was added and mixed rapidly to generate a colorless solution. The mixture was incubated for 30 min and the color of the solution changed to blue. This blue solution was centrifuged to precipitate protein, and the absorbance determined at 670 nm (ε = 34,500 M^{-1} cm^{-1}). A blank (in the absence of DesII) and a series of standard (Na_2S) were run in parallel with the DesII sample. The actual sulfur content was determined by comparison to a standard curve determined by different concentrations of Na_2S. The Na_2S standrads were prepared by dissolving appropriate amounts of Na_2S in 0.03% NaOH aqueous solution.

Preparation of Anaerobic Reagents and Buffers. All buffers and reaction components used for anaerobic experiments were degassed using a Schlenk line (ACE Glass, Inc. Vineland, NJ) and oxygen-free argon (Airgas, Austin, TX). Small volumes (approximately 150 μL) were made anaerobic by bubbling argon into the solution for 20-30 min, and large volumes (>1 mL) were degassed for 2 h. All solid chemical reagents

were made anaerobic by alternating cycles of vacuum (30 s) and argon purging (30 s) for twenty times. Purifed DesII protein was made anaerobic by alternating cycles of vacuum (3 s) and argon purging (20 s) for thirty times. Following degassing, all anaerobic components were immediately transferred to a Coy Laboratories anaerobic chamber (Grass Lakes, MI) under an atmosphere consisting of 95% N_2 and 5% H_2 (O_2 < 5 ppm).

Preparation of Degassed Buffers for the Aerobic Purification of DesII. All buffers used for the aerobic purification of DesII were degassed under vacuum for 1 h and purged with nitrogen for 1 h. This vacuum and purge process was repeated twice for small volumes (less than 500 mL) and three times for large volumes (approximately 500 mL to 1 L).

Preparation of Large Quantity of Anaerobic Buffers for DesII Reconstitution. Large quantity of buffers were made anaerobic using Airfree® flasks (Chemglass Inc. Vineland, NJ) and a Schlenk line. The Airfree® flasks were filled with buffers up to half of their maximum capacity. The buffers were frozen by immersing into liquid nitrogen for 30 min. The buffers were thawed under vacuum with occasional agitation to remove air bubbles. Following degassing, all anaerobic buffers were immediately transferred to a Coy Laboratories anaerobic chamber under an atmosphere composed of 95% N_2 and 5% H_2 (O_2 < 5 ppm).

*Anaerobic Test with Resazurin (**2-20**).* This dye is known to be an oxidation-reduction indicator (*26*). 1 mL of 5% (w/v) sodium carbonate, 5 mg of cysteine, and 10 μL of 0.2% (w/v) resazurin were mixed together in a final volume of 10 mL of water. This solution was left to stand inside the glovebox

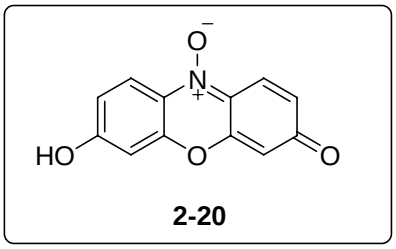

2-20

and turned colorless. When freshly prepared, the dye is in its oxidized state and is blue in color. After 3 h, due to the presence of cysteine in the solution, it was converted to the semireduced state, which is pink in color. In the absence of oxygen, the dye was completely reduced and turned colorless.

Construction of the Expression Plasmid for desII. The *desII* gene was cloned into pET24b(+) vector at the *Nde*I and *Xho*I restriction sites. Two primers were designed to amplify the *desII* gene from *Streptomyces venezuelae* genomic DNA. The forward primer, 5′-CGCGCATATGACCGCCCCCGCCCTTTCC-3′, contained an *Nde*I restriction site (underlined), and the reverse primer, 5′-GCGCCTCGAGGCGCAGGAAGCC-3′, contained an *Xho*I restriction site (underlined). The PCR mixture (100 μL) contained 59.5 μL of ddH_2O, 8.0 μL of deoxyribonucleotidyltriphosphate mixture (dNTP, 2.5 mM each), 10.0 μL DMSO, 2.5 μL 40% glycerol, 4 μL of each of the two primers (20 μM), 1.0 μL template DNA (pLZ4, 0.1 μg), 10.0 μL *Pfu* polymerase buffer (10X) and 1.0 μL cloned *Pfu* polymerase (2.5 units) (Stratagene, La Jolla, CA). The PCR consisted of 30 cycles, plus a 3-min incubation period at 95 °C preceding the 30 cycles, and a 5-min incubation period at 72 °C following the 30 cycles. Each cycle consisted of three steps: denaturation at 95 °C for 30 sec, annealing at 55 °C for 30 sec, and elongation at 72 °C for 30 sec. The PCR product was purified from agarose gel (Gibco BRL) using a DNA Gel Extraction kit (Qiagen, La Jolla, CA), digested by the appropriate enzymes, and ligated into the *Nde*I/*Xho*I sites of the vector pET24b(+). This recombinant plasmid was used to transform *E. coli* DH5α cells and subjected to antibiotic selection to screen for uptake of

recombinant plasmid. Plasmids were extracted from colonies that grew in the presense of kanamycin (50 μg/mL) using alkaline lysis (*22*). Positive clones were identified by digestion of the plasmid DNA with *Nde*I/*Xho*I and the excised insert was observed by staining an agarose gel of the DNA with ethidium bromide. The plasmid DNA from positive clones was used to transform *E. coli* BL21 Star (DE3) cells for gene overexpression and subsequent protein purification. The sequence of the resulting construct was further confirmed by DNA sequencing. The general methods and protocols for recombinant DNA manipulations followed those described by Sambrook *et al*. (*22*).

Construction of the Expression Plasmid for flavodoxin (fld). The *fld* gene was cloned into pET24b(+) vector (Novagen, Madison, WI) at the *Nde*I and *Xho*I restriction sites. Two primers were designed to amplify the *fld* gene. The forward primer, 5′-TCGCCATATGAACAGCTGCGTATTAATAA-3′, contained an *Nde*I restriction site (underlined), and the reverse primer, 5′-GCAACTCGAGTTAATAAAAACGTGGACA-3′, contained an *Xho*I restriction site (underlined). The remaining procedures were identical to those used for the construction of the *desII* expression plasmid.

Construction of the Expression Plasmid for flavodoxin reductase (fpr). The *fpr* gene was cloned into pET28b(+) vector (Novagen, Madison, WI) at the *Nco*I and *Xho*I restriction sites. Two primers were designed to amplify the *fpr* gene. The forward primer, 5′-AAAACCATGGCTGATTGGGTAAC-3′, contained an *Nco*I restriction site (underlined), and the stop primer, 5′-AAGTCTCGAGCCAGTAATGCTCCGCTGT-3′, contained an *Xho*I restriction site (underlined). The remaining procedures were identical to those used for the construction of the *desII* expression plasmid.

Co-transformation of desII/pET24b(+) and pDB1282 into E. coli BL21 Star (DE3). Plasmid pDB1282 contains the gene cluster involved in the iron-sulfur cluster biosynthesis including iscS, iscU, iscA, hscB, hscA, and fdx (*27*) (Figure 2-6). Equal concentration of *desII/pET24b(+)* and pDB1282 were added to 50 μL of *E. coli* BL21 Star (DE3) competent cells, which were prepared as described above. The 1.5-mL eppendorf tube containing the competent cells and plasmids were incubated on ice for 20 min. Subsequently, the cells were heated at 42 °C for 45 sec. The cells were chilled on ice for 2 min and 800 μL of LB medium was added to the cells. The cells were incubated at 37 °C with shaking at 200 rpm for 45 min. The cells were centrifuged to collect the cell pellets for 30 sec at maximum speed in a tabletop microcentrifuge, and 800 μL of supernatant was removed by aspiration. The cell pellets were resuspended in the remaining LB medium and then used to spread a LB plate containing both kanamycin (50 μg/mL) and ampicillin (100 μg/mL). The resulting LB plate was incubated at 37 °C for 16 h.

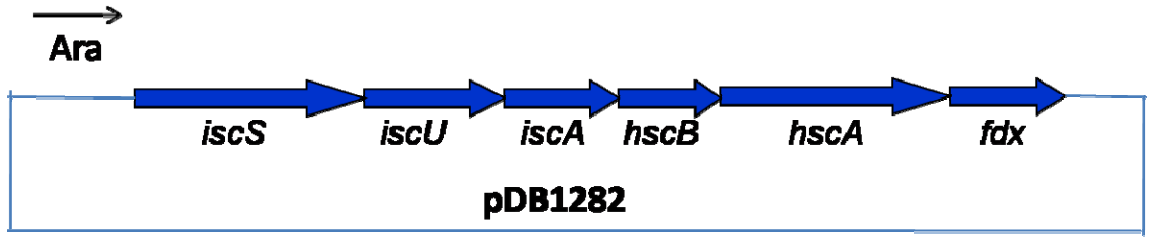

Figure 2-6. pDB1282 encodes a gene cluster required for iron-sulfur cluster biosynthesis including *iscS, iscU, iscA, hscB, hscA, and fdx*.

Expression and Purification of DesII, DesI, DesV, Flavodoxin, and Flavodoxin Reductase. The expression conditions for DesII, DesI, DesV, flavodoxin, and flavodoxin reductase are listed in Table 2-2.

Plasmid	Host Strain	Gene	Vector	His_6-tag	Antibiotic Selection	IPTG (mM)	Growth Conditions
desII/pET24b(+)	*BL21 Star*	*desII*	pET24b(+)	*C*-teminal	Kan	0.1	18 °C, 18 h
desI/pET28b(+)	BL21	*desI*	pET28b(+)	*N*-teminal	Kan	0.1	20 °C, 21 h
desV/pET28b(+)	BL21	*desV*	pET28b(+)	*C*-teminal	Kan	0.1	20 °C, 21 h
fld/pET24b(+)	BL21	*fld*	pET24b(+)	*C*-teminal	Kan	0.1	37 °C, 6 h
fpr/pET28b(+)	BL21	*fpr*	pET28b(+)	*N*-teminal	Kan	0.1	37 °C, 6 h

Table 2-2. Plasmid constructs and expression conditions for DesI, DesII, DesV, flavodoxin, and flavodoxin reductase.

Expression and Purification of DesII in E. coli. All buffers were degassed and saturated with nitrogen before use as previoulsy described. The general purification procedure is a modified version of that described in the QIAexpressionist handbook provided by Qiagen for use with Ni-NTA agarose resin (*28*). All protein purification operations were carried out at 4 °C, except for the FPLC step, which was performed at room temperature, with buffers and the collected fractions stored at 4 °C.

Step 1: Growth of E. coli BL21 Star (DE3)-desII/pET24b(+) Cells. An overnight culture of *E. coli* BL21 Star (DE3)-*desII*/pET24b(+) grown at 37 °C in Luria-Bertani (LB) medium containing kanamycin (50 μg/mL) was used, in a 200-fold dilution, to inoculate 6 L of the same medium. When the OD_{600} reached 0.4-0.6, the incubation

temperature was lowered to 18 °C and isopropyl β-D-thiogalactoside (IPTG) was added to a final concentration of 0.1 mM to induce gene expression. $Fe(NH_4)_2(SO_4)_2$ was added to a final concentration of 0.2 mM to provide the iron source for the iron-sulfur cluster biosynthesis. After incubation for an additional 18 h at 18 °C, cells were harvested by centrifugation (4000*g*, 10 min) at 4 °C, washed with potassium phosphate buffer (50 mM, pH 7.5), collected again by centrifugation (4000*g*, 10 min), and stored at -80 °C. The typical yield was 6 g of wet cells per liter of culture.

Step 2: Crude E. coli Extract Preparation. The harvested cells were thawed, resuspended in 100-150 mL of cell lysis buffer (10% glycerol (w/v), 50 mM sodium phosphate, 150 mM NaCl, 10 mM imidazole, pH 8.0), and disrupted with eight 45 sec sonication bursts (30% intensity of 400 W/20 kHz) with intermittent 1 min cooling periods on ice. Cell lysates were centrifuged at 30,000*g* for 30 min at 4 °C, and the supernatants were filtered through a 0.45 μm membrane. The filtrate was then subjected to Ni-NTA resin purification.

Step 3: Ni-NTA Affinity Chromatography. The total soluble cell lysate was added to 10 mL of Ni-NTA slurry, and the mixture was incubated for 1 h with gentle shaking at 4 °C. The total mixture was then loaded onto an empty liquid chromatography column. In an alternative procedure, the filtrate was loaded onto a column pre-packed with 10 mL Ni-NTA resin which was pre-equilibrated with 50 mL lysis buffer (10% glycerol (w/v), 50 mM sodium phosphate, 150 mM NaCl, 10 mM imidazole, pH 8.0). The cell lysate was allowed to flow through the resin by gravity and the resultant flow-through was collected. The column was then washed with 30 mL of lysis buffer, followed by 50 mL of washing buffer (20% glycerol (w/v), 50 mM sodium phosphate, 150 mM NaCl, 20 mM imidazole,

pH 8.0). The washing buffer eluting unbound proteins from the resin was also collected. After washing, 25 mL of elution buffer (10% glycerol (w/v), 50 mM sodium phosphate, 150 mM NaCl, 250 mM imidazole, pH 8.0) was used to elute the resin-bound protein. The unbound lysate, washing buffer flow-through, and the final elution fractions were subjected to SDS-PAGE analysis (12% acrylamide gel) with Coomassie blue staining and Western Blotting with anti-His-tag monoclonal antibody.

Step 4: FPLC-MonoQ chromatography of DesII Protein. The DesII eluate obtained from step 3 was further purified by FPLC with a MonoQ HR (16/10) column using buffers A (10% glycerol (w/v), 20 mM Tris•HCl, pH 7.5) and B (10% glycerol (w/v), 20 mM Tris•HCl, 500 mM NaCl, pH 7.5). The elution gradient started from 10% buffer B at 15 min to 100% buffer B at 55 min. The flow rate was 5.0 mL/min and the detector was set at 280 nm. The DesII protein, eluted at approximately the 70% buffer B, was collected. All the fractions containing DesII protein were subjected to SDS-PAGE analysis.

Expression of pDB1282 in E. coli BL21 Star (DE3). An overnight culture of *E. coli* BL21 Star (DE3) containing pDB1282 grown at 37 °C in LB medium containing ampicillin (100 μg/mL) was used, in a 100-fold dilution, to inoculate 1 L of the same medium. This culture was allowed to grow at 37 °C. When the OD_{600} reached 0.3, arabinose was added at a final concentration of 0.05% (w/v). After incubation for an additional 6 h at 37 °C, cells were harvested and crude *E. coli* extract was prepared following the procedures previously established for DesII. A 10 μL aliquot of the supernatant was subjected to SDS-PAGE analysis.

Expression of desII/pET24b(+) and pDB1281 in E. coli BL21 Star (DE3) at 37 °C. An overnight culture of *E. coli* BL21 Star (DE3) containing *desII*/pET24b(+) and pDB1282 grown at 37 °C in LB medium containing kanamycin (50 μg/mL) and ampicillin (100 μg/mL) was used, in a 100-fold dilution, to inoculate 1 L of the same medium. The culture was grown at 37 °C. When the OD_{600} reached 0.3, arabinose was added to a final concentration of 0.05% (w/v). At an OD_{600} of 0.6, IPTG and $Fe(NH_4)_2(SO_4)_2$ were added to final concentrations of 100 and 200 μM, respectively. After incubation for an additional 4 h at 37 °C, cells were harvested and crude *E. coli* extract was prepared following the procedures previously established for DesII. A 10 μL aliquot of the supernatant was subjected to SDS-PAGE analysis. In case that DesII formed inclusion bodies under the expression condition, cell debris was resuspended in 8 M urea and then subjected to SDS-PAGE analysis.

Expression of desII/pET24b(+) and pDB1281 in E. coli BL21 Star (DE3) at 18 °C. An overnight culture of *E. coli* BL21 Star (DE3) containing *desII*/pET24b(+) and pDB1282 grown at 37 °C in LB medium containing kanamycin (50 μg/mL) and ampicillin (100 μg/mL) was used, in a 100-fold dilution, to inoculate 1 L of the same medium. The culture was allowed to grow at 37 °C. When the OD_{600} reached 0.3, arabinose was added to a final concentration of 0.05% (w/v). At an OD_{600} of 0.6, IPTG and $Fe(NH_4)_2(SO_4)_2$ were added to final concentrations of 100 and 200 μM, respectively. After incubation for an additional 17 h at 18 °C, cells were harvested and crude *E. coli* extract was prepared following the procedures previously established for DesII. A 10 μL

aliquot of the supernatant and cell debris resuspended in 8 M urea were subjected to SDS-PAGE analysis.

Expression and Purification of DesII in E. coli. Grown in M9 Minimal Medium. Mössbauer spectroscopy is a useful technique that enables the evaluation of the composition of the iron-sulfur cluster in DesII. The common approach to prepare the Mössbauer samples is to grow cells in M9 minimal medium to obtain the purified apo-protein and then to reconstitute the iron-sulfur cluster using ^{57}Fe (which is Mössbauer sensitive) and sodium sulfide. Some metalloenzymes produced inclusion bodies when they were grown in the absense of metals, such as in M9 minimal medium. Therefore, the expression and purification of DesII in M9 minimal medium was tested. M9 minimal medium was prepared following a literature procedure (*22*). The medium contained 45.4 mM phosphate buffer, pH 7.3, 10 mM NaCl, 20 mM NH_4Cl, 2 mM $MgSO_4$, 0.4% glucose, 0.1 mM $CaCl_2$, and 50 μg/mL of kanamycin. The phosphate buffer and glucose were filtered through Corning sterile syringe filters with 0.22 μm membrane (Corning, NY) prior to media preparation. An overnight culture of *E. coli* BL21 Star (DE3)-*desII*/pET24b(+) grown at 37 °C in Luria-Bertani (LB) medium containing kanamycin (50 μg/mL) were collected by centrifugation (4000*g*, 10 min) at 4 °C. The supernatant was removed and the cell pellets were washed with M9 minimal medium three times and collected again by centrifugation (4000*g*, 10 min). Subsequently, the cell pellets resuspended in M9 medium were used, in a 50-fold dilution, to inoculate 6 L of the same medium containing kanamycin (50 μg/mL). The remaining expression and purification steps were identical to those used for cells grown in the LB medium except that

$Fe(NH_4)_2(SO_4)_2$ was omitted. Since cell growth in M9 minimal medium is slower than in LB medium, extended growth time was required. Resultant enzyme was purified by the procedure established for DesII grown in LB medium and analyzed by SDS-PAGE. In case that DesII formed inclusion bodies and was absent from the supernatant, cell debris resuspended in 8 M urea was also subjected to SDS-PAGE analysis.

Expression and Purification of DesII in E. coli Grown in Iron-depleted Medium. The difference between M9 minimal medium and iron-depleted medium is that iron-depleted medium contains trace amounts of metals, such as calcium, zinc, copper, manganese, and cobalt, to help cell growth. Iron-depleted medium (*29*) contained 45.4 mM phosphate buffer, pH 7.3, 7.57 mM $(NH_4)_2SO_4$, 0.4% glucose, 610 μM L-leucine, 406 μM MgSO4, 50 μM EDTA, 5 μM $CaCl_2$, 0.6 M $ZnCl_2$, 60 μM $CuSO_4$, 0.6 μM $MnCl_2$, 0.75 μM $CoC1_2$, 5.9 μM thiamin dichloride, and 50 μg/mL kanamycin. The phosphate buffer, $(NH_4)_2SO_4$, glucose, and leucine solutions were sterilized by filtering through a 0.22 μM membrane. An overnight culture of *E. coli* BL21 Star (DE3)-*desII*/pET24b(+) grown at 37 °C in Luria-Bertani (LB) medium containing kanamycin (50 μg/mL) were collected by centrifugation (4000*g*, 10 min) at 4 °C. The supernatant was removed and the cell pellets were washed with iron-depleted medium three times and collected again by centrifugation (4000*g*, 10 min). Subsequently, the cell pellets resuspended in iron-depleted medium were used, in a 50-fold dilution, to inoculate 6 L of the same medium containing kanamycin (50 μg/mL). The remaining expression and purification steps were identical to those used for cells grown in LB medium except that $Fe(NH_4)_2(SO_4)_2$ was omitted. Since cell growth in iron-depleted medium is slower than in

LB medium, extended growth time was required. Resultant enzyme was purified by the procedure established for DesII grown in LB medium and analyzed by SDS-PAGE. Cell debris resuspended in 8 M urea was also subjected to SDS-PAGE analysis.

Expression and Purification of DesII in E. coli Grown in Iron-deplete Medium with Supplemental $Fe(NH_4)_2(SO_4)_2$. Supplemental $Fe(NH_4)_2(SO_4)_2$ is likely to increase the yield of soluble DesII obtained from iron-depleted medium. In the preparation of samples for Mössbauer spectroscopy studies, $Fe(NH_4)_2(SO_4)_2$ can be replaced by $^{57}Fe(NH_4)_2(SO_4)_2$. Iron-depleted medium was prepared as described above (*29*). An overnight culture of *E. coli* BL21 Star (DE3)-*desII*/pET24b(+) grown at 37 °C in Luria-Bertani (LB) medium containing kanamycin (50 μg/mL) was collected by centrifugation (4000*g*, 10 min) at 4 °C. The cell pellets were washed with iron-depleted medium as described above. Subsequently, cell pellets resuspended in iron-depleted medium were used, in a 50-fold dilution, to inoculate 6 L of the same medium containing kanamycin (50 μg/mL). When the OD_{600} reached 0.4-0.6, the incubation temperature was lowered to 18 °C and IPTG was added to a final concentration of 0.1 mM to induce gene expression and $Fe(NH_4)_2(SO_4)_2$ was added to a final concentration of 0.2 mM to provide the iron source for iron-sulfur cluster biosynthesis. After incubation for an additional 48 h at 18 °C, cells were harvested by centrifugation (4000*g*, 10 min) at 4 °C, washed with potassium phosphate buffer (50 mM, pH 7.5), collected again by centrifugation (4000*g*, 10 min), and stored at -80 °C. The typical yield was 2 g of cells per liter of culture. The enzyme produced was purified by the procedure established for DesII grown in LB

medium and analyzed by SDS-PAGE. Cell debris resuspended in 8 M urea was also subjected to SDS-PAGE analysis.

Expression and Purification of DesI in E. coli. An overnight culture of *E. coli* BL21 (DE3)-*desI*/pET28b(+) grown at 37 °C in Luria-Bertani (LB) medium containing kanamycin (50 μg/mL) was used, in a 200-fold dilution, to inoculate 6L of the same medium. When the OD_{600} reached 0.4-0.6, the incubation temperature was lowered to 20 °C and IPTG was added to a final concentration of 0.1 mM to induce gene expression. After incubation for an additional 21 h at 20 °C, cells were harvested by centrifugation (4000*g*, 10 min) at 4 °C, washed with potassium phosphate buffer (50 mM, pH 7.5), collected again by centrifugation (4000*g*, 10 min), and stored at -80 °C. The typical yield was 6 g of cells per liter of culture. The following procedures including crude *E. coli* extract preparation and Ni-NTA affinity chromatography were identical to those used for DesII purification.

Expression and Purification of DesV in E. coli. An overnight culture of *E. coli* BL21 (DE3)-*desV*/pET28b(+) grown at 37 °C in Luria-Bertani (LB) medium containing kanamycin (50 μg/mL) was used, in a 200-fold dilution, to inoculate 6L of the same medium. When the OD_{600} reached 0.4-0.6, the incubation temperature was lowered to 20 °C and IPTG was added to a final concentration of 0.1 mM to induce gene expression. After incubation for an additional 21 h at 20 °C, cells were harvested by centrifugation (4000*g*, 10 min) at 4 °C, washed with potassium phosphate buffer (50 mM, pH 7.5), collected again by centrifugation (4000*g*, 10 min), and stored at -80 °C. The typical yield was 6 g of cells per liter of culture. The following procedures including crude *E. coli*

extract preparation and Ni-NTA affinity chromatography were identical to those used for DesII purification.

Expression and Purification of E. coli Flavodoxin (FLD) and Flavodoxin Reductase (FPR). Overnight cultures of *E. coli* BL21(DE3)-*fld*/pET24b(+) and *fpr*/pET28b(+) grown at 37 °C in LB medium containing kanamycin (50 μg/mL) was used, in a 100-fold dilution, to inoculate 6 L of the same medium, respectively. These cultures were incubated at 37 °C until OD_{600} reached 0.5-0.6. Protein expression was then induced by addition of IPTG to a final concentration of 0.1 mM, and the cells were allowed to grow at 37 °C for an additional 6 h. After this time, the cells were harvested by centrifugation (4000*g*, 10 min) at 4 °C, washed with potassium phosphate buffer (50 mM, pH 7.5), collected again by centrifugation (4000*g*, 10 min), and stored at -80 °C. The typical yield was 6 g of wet cells per liter of culture. The following procedures including crude *E. coli* extract preparation and Ni-NTA affinity chromatography were identical to those used for DesII purification.

*Preparation of Enzymes Used in Enzymatic Synthesis of **2-8**.* The thymidine kinase (TK), thymidylate kinase (TMK), and nucleotide diphosphate kinase (NDK) used in this synthesis were prepared following the method reported by Takahashi *et al*. (*30*). Rabbit muscle pyruvate kinase was purchased from Sigma Chemical Co. as a 400-800 units/mg ammonium sulfate precipitate. This ammonium sulfate precipitate was dissolved in water to a concentration of 2500 units/mL, dialyzed against 50 mM potassium phosphate buffer, 300 mM NaCl, pH 8.0, to remove ammonium sulfate, and stored at -80 °C. RfbA was prepared by Dr. Yung-nan Liu of this laboratory as follows. The *rfbA* gene was amplified from *Salmonella enterica serovar* Typhimurium LT2 genomic DNA using

PCR. The start primer contained an engineered *Bam*HI restriction site (in italics), ribosomal binding sequence (underlined), and AT rich region upstream of the native start codon (shown in bold), with sequence 5'-CGGGATCCGAAGGAGATATATAA**ATG**AA-AACGCGTAAGGGC-3'; and the stop primer contained an engineered *Pst*I restriction site (in italics) and a *C*-terminal His_5-tag (underlined) immediately downstream of the stop codon (in bold), with sequence 5'-CTTGCATGCCTGCAG**TTA**ATGATGATGAT-GATGTAAACCTTTCACCATC-3'. The PCR-amplified gene was purified, digested with *Bam*HI and *Pst*I, and ligated into *Bam*HI/*Pst*I digested pUC18. The resulting construct was used to transform *E. coli* BL21(DE3). Overexpression was achieved by growth of the transformed host in LB media in the presence of 100 μg/mL ampicillin at 37 °C overnight. Protein was purified from the harvested cells by Ni-NTA affinity chromatography in an identical manner to that used for the purification of DesI. The 4,6-dehydratase RfbB used in the synthesis of **14** was prepared by Dr. Yung-nan Liu of this laboratory in the following manner. The *rfbB* gene was amplified from *Salmonella enterica serovar* Typhimurium LT2 genomic DNA by PCR. The start primer contained an engineered *Eco*RI restriction site (in italics), ribosomal binding sequence (underlined), and AT rich region upstream of the native start codon (shown in bold), with sequence 5'-GGAATTCGAAGGAGATATATAA**ATG**GTGAAGATACTTATTACTGG-3'. The stop primer contained an engineered *Bam*HI restriction site (in italics) and a His_5-tag sequence (underlined) immediately downstream of the stop codon (in bold), with sequence 5'-CGGGATCC**TTA**ATGATGATGATGATGCTGGCGTCCTTCATAGTTC-3'. The PCR-amplified gene was purified, digested with *Eco*RI and *Bam*HI, and ligated into *Eco*RI/*Bam*HI digested pUC18. The resulting construct was used to transform *E. coli*

BL21(DE3). Overexpression was achieved by growth of the transformed host in LB medium supplemented with 100 μg/mL ampicillin at 37 °C overnight. Protein was purified from the harvested cells by Ni-NTA affinity chromatography in an identical manner to that used for the purification of DesII.

*Enzymatic Synthesis of TDP-4-keto-6-deoxy-D-glucose (**2-8**).* The large-scale enzymatic preparation of DesI substrate (**2-8**) was initiated by coupling thymidine with glucose-1-phosphate (**2-6**) to make TDP-D-glucose (**2-7**), which was then converted to TDP-4-keto-6-deoxy-D-glucose (**2-8**, Figure 2-1). Preparation of TDP-D-glucose (**2-7**) from thymidine and glucose-1-phosphate (**2-6**) was conducted in a two-stage, "one-pot" reaction (*30*). In the first stage, a mixture containing 76.2 mM phosphoenolpyruvate (PEP), 24 mM thymidine, 1.6 mM ATP, 27 mM $MgCl_2$, 25 μM thymidine kinase (TK), 25 μM thymidylate kinase (TMK), 25 μM nucleoside diphosphate kinase (NDK), and 1000 units of rabbit muscle pyruvate kinase (PK) in 15 mL of 50 mM Tris•HCl buffer, pH 7.5, was incubated at 37 °C for 4 h, generating thymidine triphosphate (TTP). The enzymes were removed by filtration through a YM10 Diaflo membrane (Amicon), and glucose-1-phospate (**2-6**), $MgCl_2$, and α-D-glucose-1-phosphate thymidylyltransferase (RfbA) from *S. enterica* LT2 were added to the filtrate to give final concentrations of 28 mM, 50 mM, and 36 μM, respectively. The mixture was incubated for 16 h at 37 °C, centrifuged at 5,000*g* for 10 min to remove precipitate, and filtered through an Amicon YM-10 membrane to remove enzymes. The crude product (**2-7**), with a theoretical yield of 228 mg, was stored at 4 °C. The enzyme-free filtrate from the previous step was loaded onto a Bio-gel P2 column (25 mm × 100 cm) pre-washed with water, and run at a flow rate of 12 mL/h with water as the eluant, with 8 mL fractions collected. Fractions

demonstrating UV absorption at 267 nm were lyophilized, and the identity and purity of the compounds in each fraction assessed by ^{1}H and ^{31}P NMR spectroscopy. TDP-D-glucose (**2-7**) containing fractions (total weight 170 mg), which varied in purity from 25-70%, were pooled according to their purities. Further purification of TDP-D-glucose was performed by FPLC equipped with a Mono Q 16/10 column. A linear gradient of 0 to 40% of a solution of 400 mM NH_4HCO_3 in water was used as the eluant. The detector was set at 280 nm, and the flow rate was 5 mL/min. Fractions containing the major peak were lyophilized individually, redissolved in water, and lyophilized again to remove NH_4HCO_3. The purities of these fractions (total weight 123 mg), which ranged from 50-90%, were assessed by ^{1}H and ^{31}P NMR spectroscopy. From these fractions, 23 mg of 90% pure TDP-D-glucose (**2-7**) was obtained.

TDP-D-glucose (**2-7**, 23 mg) obtained from the previous step was dissolved in 50 mM potassium phosphate buffer, pH 7.5, to give a final concentration of 29 μM. This solution was incubated with TDP-D-glucose 4,6-dehydratase (RfbB) from *S. enterica* LT2 (18 μM) at 37 °C for 2 h, after which RfbB was removed by filtration through a YM10 Diaflo membrane (Amicon). The filtrate was loaded onto a Sephadex G-10 column pre-washed with water and run at a flow rate of 1 mL/min using water as the eluant, with 10 mL fractions collected. Those fractions exhibiting absorption at 267 nm were lyophilized and their purities assessed by ^{1}H and ^{31}P NMR spectroscopy. Those fractions containing pure TDP-4-keto-6-deoxy-D-glucose (**2-8**, 12.3 mg, >90% purity) were combined and the concentration of **2-8** in the solution was determined spectrophotometrically at 267 nm, ($\varepsilon = 9600\ M^{-1}cm^{-1}$).

*Preparation of TDP-4-amino-4,6-dideoxy-D-glucose (**2-9**).* The TDP-4-amino-4,6-dideoxy-D-glucose (**2-9**) was prepared by incubation of TDP-D-glucose (46.2 mg, 8.2 mM) and RfbB (0.028 mM) in 10 mL of 50 mM potassium phosphate buffer, pH 7.5, at 37 °C for 1 h, followed by addition of L-glutamate (5 mM), pyridoxal 5′-phosphate (PLP) (0.8 mM), and DesI (0.026 mM). The mixture was incubated at 25 °C for 1 h. The enzymes were removed using a YM10 Diaflo membrane (Amicon), and the filtrate was separated by FPLC using a MonoQ HR (16/10) column. The flow rate was 3 mL/min and the detector was set at 280 nm. A linear gradient of 0-350 mM NH_4HCO_3 over 25 min followed by a gradient of 350-500 mM NH_4HCO_3 over 5 min separated the product from the other components of the reaction mixture. The TDP-4-amino-4,6-dideoxy-D-glucose (**2-9**), which eluted at 250 mM NH_4HCO_3, was collected, lyophilized, and subjected to analysis by NMR spectroscopy.

*Preparation of CDP-4-keto-6-deoxy-D-glucose (**2-21**).*

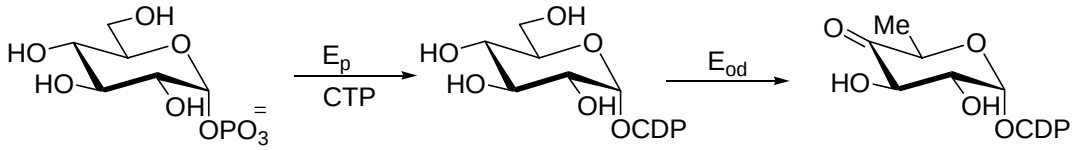

2-6 **2-21**

Figure 2-7. Biosynthesis of CDP-4-keto-6-deoxy-D-glucose (**2-21**) from glucose-1-phosphate (**2-6**) and CTP, catalyzed by E_p and E_{od}.

Preparation of CDP-4-keto-6-deoxy-D-glucose (**2-21**), was achieved following a literature procedure (*31*) using glucose-1-phosphate (**2-6**) as the starting material (Figure 2-7). In this preparation, glucose-1-phosphate (16 mg, 44.6 μmol), cytidine triphosphate

(CTP) (22 mg, 44.6 μmol), and nicotinamide adenine dinucleotide (NAD^+) (5 mg, 7.5 μmol) were dissolved in 50 mM potassium phosphate buffer, which also contained 10 mM $MgCl_2$ (pH 7.5). To this solution were added glucose-1-phosphate cytidylyltransferase (E_p, 0.32 mg) and CDP-D-glucose 4,6-dehydratase (E_{od}, 0.90 mg) to a final volume of 3 mL. The mixture was incubated at 37 °C for 1 h. The desired product was isolated by FPLC with a MonoQ 10/10 column using the published protocol (*32*). The concentration of this substrate was determined spectrophotometrically (*33*). The E_p and E_{od} were purified from *E. coli* HB101-pJT12 (*34*) and HB101-pJT8 (*32*), respectively, as previously reported.

*Preparation of TDP-D-quinovose (**2-22**) and TDP-D-fucose (**2-23**).* TDP-D-quinovose (**2-22**) and TDP-D-fucose (**2-23**) were prepared following a literature procedure (*35*) (Figure 2-8). First, TDP-4-keto-4,6-dideoxy-D-glucose (**2-8**) was prepared by incubation of TDP-D-glucose (**2-7**, 46.2 mg, 8.2 mM) and RfbB (0.028 mM) in 10 mL of 50 mM potassium phosphate buffer, pH 7.5, at 37 °C for 1 h.

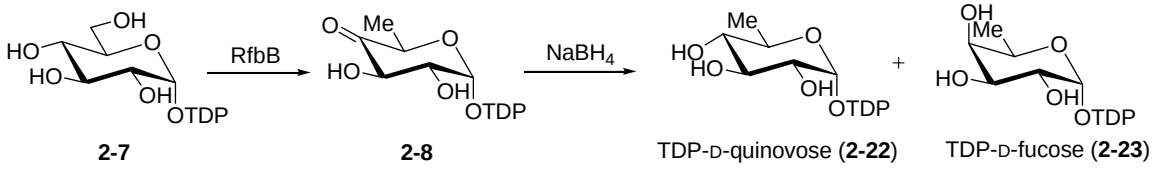

Figure 2-8. Reduction of the C-4 keto group in TDP-4-keto-6-deoxy-D-glucose (**2-8**) leads to the formation of TDP-D-quinovose (**2-22**) and TDP-D-fucose (**2-23**).

The enzyme was removed by filtration through an Amicon ultrafiltration unit equipped with a YM10 membrane. To the filtrate was added $NaBH_4$ (10 μM) and the

reaction was monitored by HPLC using a Dionex CarboPac PA1 column (4 × 250 mm). The flow rate was 1.0 mL/min and the detector was set at 267 nm. A linear gradient from 2.5% to 10% solvent B (1 M ammonium acetate, pH 7.0) in solvent A (ddH_2O) over 20 min, followed by a second linear gradient from 10% to 30% solvent B in solvent A over 20 min gave a satisfactory separation between TDP-D-quinovose (**2-22**) and TDP-D-fucose (**2-23**) (the ratio of **2-22** : **2-23** = 3:1). The peaks of both epimers could be assigned by comparison with the elution profile of the 4-epimers UDP-glucose/UDP-galactose, which are separated by the same gradient as described above. Both peaks were collected, lyophilized to dryness, and then subjected to NMR spectroscopy analysis.

*Preparation of TDP-3-amino-3,6-dideoxy-D-glucose (TylB Product, **2-24**).*

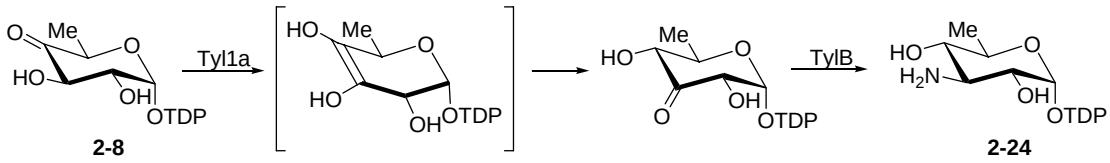

Figure 2-9. Enzymatic synthesis of TDP-3-amino-3,6-dideoxy-D-glucose (TylB product, **2-24**).

The 3,4-ketoisomerase Tyl1a and the C-3 aminotransferase TylB used in this assay were provided by Dr. Charles E. Melançon, III of this laboratory. The TylB product, TDP-3-amino-3,6-dideoxy-D-glucose (**2-24**), was prepared according to a published procedure (*36*) (Figure 2-9). Briefly, the reaction mixture (1 mL) contained 28.5 μM Tyl1a, 10 μM TylB, 1 mM TDP-4-keto-6-deoxy-D-glucose (**2-8**), 10 mM L-glutamate, and 50 μM pyridoxal 5'-phosphate (PLP), in 50 mM potassium phosphate

buffer (pH 7.5). The reaction mixture was incubated at 25 °C for 70 min, and then quenched by flash-freezing in liquid nitrogen. The mixture was thawed on ice, and enzymes were removed by ultrafiltration through a YM10 Diaflo membrane (Amicon) at 4 °C. The sample was then separated using a semipreparative Dionex CarboPac PA-1 column and a gradient elution program identical to that used for the analytical Dionex CarboPac PA-1 column described above, with a flow rate of 5 mL/min. Compound **2-24**, which eluted at 12.5 min, was collected manually and lyophilized to near dryness. HPLC analysis showed 35% conversion of **2-8** to **2-24**. Compound **2-24** was resuspended in water to a concentration of 0.1 mg/mL for hign-resolution ESI-MS (electrospray ionization mass spectrometry) analysis.

Reconstitution of the [4Fe-4S] Cluster in vitro. All procedures including the apoprotein preparation, reconstitution, reduction of the iron-sulfur cluster, and activity assay were performed anaerobically inside a glovebox (Coy Laboratory Products, Grass Lake, MI) in an N_2 atmosphere, containing less than 5 ppm O_2. All solutions were deoxygenated prior to use by repeated freeze-vacuum-thaw cycles under argon, and all solids were deoxygenated prior to use by vacuum and argon cycles.

Step 1: Preparation of the Apoprotein Forms of DesII. Protein-bound iron was removed by incubating the enzyme in the presence of 100 mM EDTA and 2 mM sodium dithionite in 100 mM Tris•HCl buffer, pH 8, for 1 h at room temperature. The solutions became colorless after 30 min of reduction with sodium dithionite. Protein was loaded onto a Sephadex G-25 column (column volume: 50 mL) pre-equilibrated and eluted with 100 mM Tris•HCl buffer, pH 8, and concentrated to approximately 8 mg/mL by ultrafiltration through a YM10 Diaflo membrane (Amicon) (80% recovery).

Step 2: Reconstitution of [4Fe-4S] Center. The apoprotein was incubated with a 10-fold molar excess of Na_2S and $Fe(NH_4)_2(SO_4)_2$ in 1 mL of 100 mM Tris•HCl buffer, pH 8 containing 5 mM dithiothreitol (DTT), for 6 h at room temperature. A deaerated solution of EDTA (2 mM final concentration) was then added to the protein. The resulting solution was incubated for 30 min. Protein was loaded onto a 50 mL Sephadex G-25 column equilibrated and eluted with 100 mM Tris•HCl buffer, pH 8. Green-gray fractions were collected and concentrated to approximately 10 mg/mL by ultrafiltration through a YM10 Diaflo membrane (Amicon) (75-80% recovery). This preparation was then analyzed for iron and sulfur content by iron titration and sulfur determination, respectively, and the iron-sulfur cluster was characterized by UV-vis and EPR spectroscopy.

Step 3: Reduction of [4Fe-4S] Center. Reduction of the [4Fe-4S] center of the reconstituted protein was monitored by UV-vis spectroscopy. The reducing agent was sodium dithionite prepared freshly in 100 mM Tris•HCl buffer, pH 8 prior to the reduction procedure. A 0.19 mM protein solution was reduced with a 6-fold molar excess of sodium dithionite over 1 h. Reduction was monitored by the decrease of the absorption band at 420 nm.

HPLC Programs on a CarboPac PA1 column (4 × 250 mm) for Activity Assays. Three different HPLC programs were used to analyze different assay mixtures. The detector was set at 267 nm. The flow rate was 0.6 mL/min for program A, whereas the flow rate was 1.0 mL/min for programs B and C. Program A is composed of a linear gradient from 20 to 35% solvent B (1 M ammonium acetate, pH 7.0) in solvent A

(ddH_2O) over 30 min. Program B consists of a linear gradient from 2.5 to 15% solvent B (1 M ammonium acetate, pH 7.0) in solvent A (ddH_2O) over 20 min, followed by a second linear gradient from 15 to 20% solvent B in solvent A over 20 min. Program C contains a linear gradient from 2.5 to 10% solvent B (1 M ammonium acetate, pH 7.0) in solvent A (ddH_2O) over 20 min, followed by a second linear gradient from 10 to 30% solvent B in solvent A over 20 min.

DesI and DesII Coupled Activity Assay. The activity assay was carried out anaerobically by mixing TDP-4-keto-6-deoxy-D-glucose (**2-8**, Figure 2-1; 0.6 mM), L-glutamate (0.5 mM), pyridoxal 5′-phosphate (PLP; 0.14 mM), DesI (0.026 mM), reduced DesII (0.1 mM), and SAM (0.1 mM) in 100 mM Tris•HCl buffer (pH 8) in the presence of DTT (2 mM). The final reaction volume was 1 mL. The reaction mixture was incubated at 25 °C for 3 h, and the reaction was quenched by filtering through an ultrafiltration unit equipped with a YM10 Diaflo membrane (Amicon) to remove the enzymes. The reaction progress was monitored by HPLC on a CarboPac PA1 column (4 × 250 mm) obtained from Dionex Corporation (Sunnyvale, CA). Program A was used to analyze the assay mixture. The desired product**,** which eluted at 28.2 min, was collected and subjected to mass spectrometry analysis.

DesII Activity Assay. Activity assays were carried out in 100 mM Tris•HCl buffer, pH 8 with 2 mM DTT in the presence of 0.5 mM substrate (TDP-4-amino-4,6-dideoxy-D-glucose, **2-9**), 0.1 mM reduced DesII protein, and 0.1 mM SAM. The final volume of the assay mixture was 1 mL. The reaction mixture was incubated at 25 °C for 1 h, and was quenched by removing the enzymes by ultrafiltration through YM10 Diaflo membrane

(Amicon). The reaction progress was monitored by HPLC on a CarboPac PA1 column (4 × 250 mm). Program A was used to analyze the reaction mixture. The desired product, which eluted at 28.2 min, was collected and subjected to mass spectrometry analysis.

DesV Activity Assay.

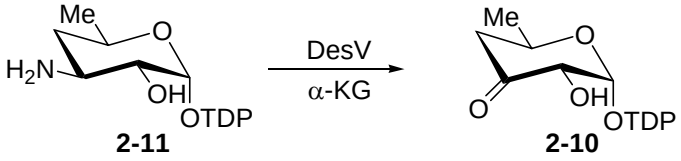

2-11 **2-10**

Figure 2-10. The reverse reaction catalyzed by DesV in desosamine biosynthesis.

The activity of DesV was confirmed by running the reaction in the reverse direction following a previously established procedure (*18*) (Figure 2-10). The DesV product (**2-11**) was purified and characterized by Dr. Hiroshi Yamase of this laboratory (*18*). A typical assay mixture of 500 μL contained 0.64 mM of substrate (**2-11**), 25 mM of α-ketoglutarate, 5 μM of DesV protein, and 40 μM PLP in 50 mM potassium phosphate buffer (pH 7.5). Aliquots of 20 μL were withdrawn at the appropriate time and the DesV enzyme was removed by ultrafiltration through a YM 10 membrane. The reaction progress was monitored by HPLC on a CarboPac PA1 column (4 × 250 mm). Program A was applied to analyze the reaction mixture. The new product, which eluted at 28.2 min was collected and subjected to mass spectrometry analysis.

DesII and DesV Coupled Activity Assay. Coupled DesII and DesV activity assays were carried out in 100 mM Tris•HCl buffer, pH 8 with 2 mM DTT in the presence of 0.5 mM substrate (TDP-4-amino-4,6-dideoxy-D-glucose, **2-9**), 0.1 mM reduced DesII protein,

and 0.1 mM SAM. The final volume of the assay mixture was 1 mL. After incubation of DesII assay mixture at 25 °C for 1 h, 10 mM L-glutamate, 0.8 mM PLP, and 0.1 mM DesV enzyme were added to the assay mixture, and then incubated at 25 °C for 30 min. The reaction was stopped by removing the enzymes by ultrafiltration through a YM10 Diaflo membrane (Amicon). The reaction progress was monitored by HPLC using program A. The DesV product, which eluted at 3.7 min, was collected and subjected to mass spectrometry analysis.

*DesII Activity Assay Using TDP-D-quinovose (**2-22**).* Assays were carried out in 100 mM Tris•HCl buffer, pH 8 with 2 mM DTT in the presence of 0.5 mM TDP-D-quinovose (**2-22**), 0.1 mM reduced DesII protein, and 0.1 mM SAM. The final volume of the assay mixture was 1 mL. The reaction mixture was incubated at 25 °C for 3 h, and was then stopped by removing the enzymes by ultrafiltration through a YM10 Diaflo membrane. The reaction progress was monitored by HPLC on a CarboPac PA1 anion exchange column (4 × 250 mm). A linear gradient using program B resulted in a satisfactory separation between substrate **2-22** (at the retention time of 18.9 min) and the new product **2-10** (at the retention time of 27.8 min). The new product, which eluted at 27.8 min, was collected and subjected to mass spectrometry analysis.

*Activity Assay Using TDP-D-fucose (**2-23**).* Assays were carried out in 100 mM Tris•HCl buffer, pH 8 with 2 mM DTT in the presence of 0.5 mM TDP-D-fucose (**2-23**), 0.1 mM reduced DesII protein, and 0.1 mM SAM. The final volume of the assay mixture was 1 mL. The reaction mixture was incubated at 25 °C for 24 h, and was then stopped by removing the enzymes by ultrafiltration through a YM10 Diaflo membrane. The

reaction progress was monitored by HPLC using program B.

*DesII Activity Assay with TylB Product (**2-24**).* Assays were carried out in 100 mM Tris•HCl buffer, pH 8 with 2 mM DTT in the presence of 0.5 mM TylB product (**2-24**), 50 μM reduced DesII protein, and 50 μM SAM. The final volume of the assay mixture was 1 mL. The reaction mixture was incubated at 25 °C for 3 h, and was then quenched by removing the enzymes by ultrafiltration through a YM10 Diaflo membrane (Amicon). The reaction progress was monitored by HPLC on a CarboPac PA1 column as described above. A linear gradient using program C resulted in a satisfactory separation between substrate **2-24** (at the retention time of 18.1 min) and the new product (at the retention time of 37.2 min). The new product, which eluted at 37.2 min, was collected and subjected to mass spectrometry analysis.

*Coupled DesII and DesV Assays with TylB Product (**2-24**).* Coupled DesII and DesV ctivity assays were carried out in 100 mM Tris•HCl buffer, pH 8, with 2 mM DTT in the presence of 0.5 mM TylB product (**2-24**), 0.1 mM reduced DesII protein, and 0.1 mM SAM. The final volume of the assay mixture was 1 mL. After incubation of DesII assay mixture at 25 °C for 3 h, 10 mM of L-glutamate, 0.8 mM of PLP, and 0.1 mM DesV enzyme were added to the assay mixture, and subsequently incubated at 25 °C for 30 min. The reaction was quenched by removing the enzymes by ultrafiltration through a YM10 Diaflo membrane (Amicon). The reaction progress was monitored by HPLC using program C. The new product, which eluted at 9.5 min, was collected and subjected to mass spectrometry analysis.

*DesII Activity Assay with the Substrate Isostere (**2-25**)* The substrate isostere (**2-25**) was chemically synthesized by Dr. Qingquan Wu of this laboratory. The activity assay was carried out anaerobically by mixing the substrate isostere (**2-25**, 0.6 mM), reduced DesII (0.1 mM), and SAM (0.1 mM) in 100 mM Tris•HCl buffer (pH 8) in the presence of DTT (2 mM). The final assay volume was 1 mL. The reaction mixture was incubated at 25 °C for 3 h, and the reaction was quenched by ultrafiltration through an Amicon ultrafiltration unit equipped with a YM10 membrane to remove the enzymes. The reaction progress was monitored by HPLC on a CarboPac PA1 column (4 × 250 mm). Program A was utilized to analyze the reaction mixture. However, no formation of expected 3-keto sugar product was observed. The DesII activity assay was performed in the presence of the natural substrate (TDP-4-amino-4,6-dideoxy-D-glucose, **2-9**, Figure 2-1) to confirm the anaerobic condition for this assay. In the presence of the natural substrate, the formation of TDP-3-keto-4,6-dideoxy-D-glucose (**2-10**, Figure 2-1) was observed.

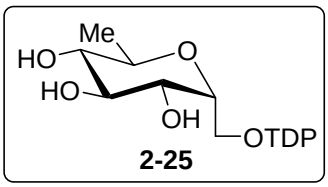

2-25

*DesI Activity Assay with CDP-4-keto-6-deoxy-D-glucose (**2-21**).* Activity assays were carried out in 50 mM potassium phosphate buffer, pH 7.5 in the presence of 1 mM substrate (CDP-4-keto-6-deoxy-D-glucose, **2-21**), 50 μM DesI enzyme, 1.5 mM PLP, and 4.5 mM L-glutamate. The final volume of the assay mixture was 0.5 mL. The reaction mixture was incubated at 25 °C and the reaction terminated at different time points by removing the enzymes through centrifugal filtration using a YM10 Diaflo membrane (Amicon). A linear gradient using program C resulted a satisfactory separation between

substrate **2-21** and a new product, which eluted at 10 min. The new product was collected and subjected to mass spectrometry analysis.

NAD(P)H:DCPIP Oxidoreductase Activity Assay of Flavodoxin and Flavodoxin Reductase.

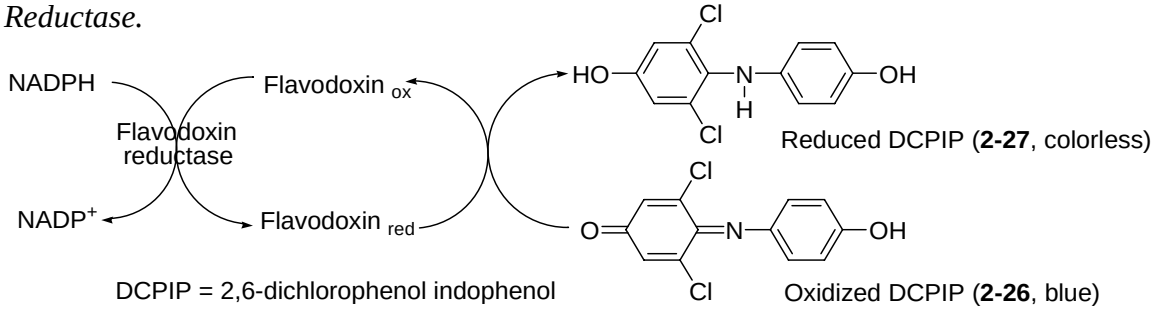

Figure 2-11. NAD(P)H:DCPIP oxidoreductase activity assay of flavodoxin and flavodoxin reductase.

The activity of purified FLD and FPR was determined by performing an assay previously reported by Davis (*37*). In this coupled assay, 2,6-dichlorophenolindophenol (DCPIP) is used as a common 2-electron acceptor. As shown in Figure 2-11, the enzyme is reduced by NAD(P)H, which then transfers electrons to reduce DCPIP **2-26**. Oxidized DCPIP (**2-26**) has a strong absorbance at 600 nm with an extinction coefficient (ε) of 22,000 M^{-1} cm^{-1}, whereas reduced DCPIP **2-27** has negligible absorption at this wavelength. Thus the reduction of DCPIP can be monitored by the decrease in the absorption at 600 nm during turnover. The 1 mL assay solution contained 1.4 mM NAD(P)H, 42 μM DCPIP, 12.0 μM flavodoxin in 20 mM Tris•HCl buffer (pH 7.5), and 6.0 μM flavodoxin reductase in 20 mM Tris•HCl buffer (pH 7.5). The reaction was initiated by the addition of NAD(P)H. Absorbance at 600 nm was monitored over a 3 min period and used to calculate the rate of DCPIP reduction. A control assay without enzyme was used to determine the background reduction of DCPIP by NAD(P)H. Sample and

control assays were carried out in triplicate using averaged values used to calculate specific activity. All assays were performed at room temperature.

Using a Biological Reducing System, Flavodoxin, Flavodoxin Reductase, and NADPH to Assay DesII Activity. Activity assays were carried out in 100 mM Tris•HCl buffer, pH 8, with 2 mM DTT in the presence of 0.5 mM substrate (TDP-4-amino-4,6-dideoxy-D-glucose, **2-9**), 0.1 mM reconstituted DesII protein, 0.1 mM SAM, 1 mM NADPH, 12 μM flavodoxin (FLD), and 6 μM flavodoxin reductase (FPR) (Figure 2-12). The final reaction volume of the assay mixture was 1 mL. The reaction mixture was incubated at 25 °C for 3 h, and was then stopped by removing the enzymes by ultrafiltration through a YM10 Diaflo membrane (Amicon). The reaction progress was monitored by HPLC on a CarboPac PA1 anion exchange column (4 × 250 mm). A linear gradient using program C resulted in a satisfactory separation between substrate **2-9** (at the retention time of 18.1 min) and the product **2-10**, which eluted at 37.2 min. The new product was collected and subjected to mass spectrometry analysis.

Coupled DesII and DesV Assay Using a Biological Reducing System. Activity assays were carried out in 100 mM Tris•HCl buffer, pH 8.0, with 2 mM DTT in the presence of 0.5 mM substrate (TDP-4-amino-4,6-dideoxy-D-glucose, **2-9**), 50 μM reconstituted DesII protein, 50 μM SAM, 1 mM NADPH, 12 μM flavodoxin (FLD), and 6 μM flavodoxin reductase (FPR) (Figure 2-12). The final reaction volume of the assay mixture was 1 mL. After incubation of the DesII assay mixture at 25 °C for 3 h, 10 mM L-glutamate, 0.8 mM PLP, and 0.1 mM DesV enzyme were added to the assay mixture, and followed by incubation at 25 °C for 1 h. The reaction was quenched by removing the

enzymes by ultrafiltration through a YM10 Diaflo membrane. The reaction progress was monitored by HPLC on a CarboPac PA1 column (4 × 250 mm). A linear gradient using program C resulted in a satisfactory separation between substrate **2-9** (with the retention time of 18.1 min) and the DesV product, TDP-3-amino-4,6-dideoxy-D-glucose (**2-11**), which eluted at 9.5 min. The flow rate was 0.6 mL/min and the detector was set at 267 nm. The DesV product was collected and subjected to mass spectrometry analysis.

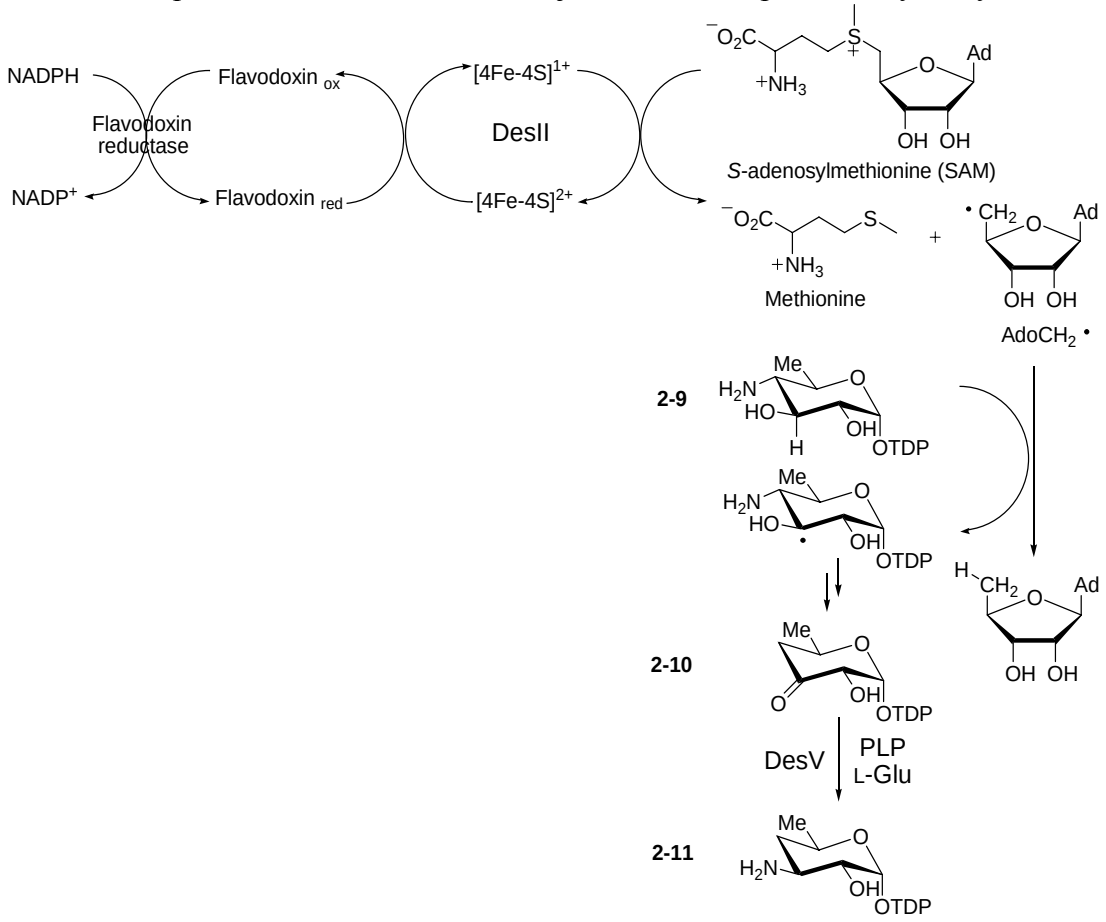

Figure 2-12. The function of the biological reducing system, flavodoxin, flavodoxin reductase, and NADPH in the DesII-catalyzed reaction.

Determination of Kinetic Parameters for the DesII-catalyzed Reaction. The steady state kinetic parameters of the DesII-catalyzed reaction were determined by the HPLC activity assay as described above. Reaction mixtures containing 3 μM

reconstituted and reduced DesII, 0.1 mM SAM, and varied amounts of substrate, TDP-4-amino-6-deoxy-D-glucose (3 μM to 1 mM) in 100 mM Tris•HCl buffer (pH 8.0) were incubated at 25 °C. Larger reaction volumes were used for the lower substrate concentrations to facilitate HPLC analysis. Aliquots were taken at four different time points for each of the 16 substrate concentrations. Incubation mixtures with lower substrate concentrations were monitored for shorter periods of time (2-3 min), and those with higher substrate concentrations were monitored for periods as long as 7 min. Since the substrate concentration in each sample was known, the percent conversion as determined by HPLC could be used to calculate the micromoles of product formed for each time point. The amounts of product formed at the four time points for a given substrate concentration were plotted against time, and the slope of each line was plotted versus substrate concentration. The resulting data were fit to the Michaelis-Menten equation by nonlinear regression using Grafit 5 to determine the k_{cat} and K_m values.

Preparation of EPR Samples. All samples were prepared anaerobically inside a glovebox under a N_2 atmosphere, containing less than 5 ppm O_2. In addition, all samples were freshly made prior to the EPR measurements. The purification and reconstitution of DesII protein were carried out as described above. In the preparation of EPR samples for reduction with dithionite, the following were added in the order given and to the specified concentrations: dithionite to 2 mM, SAM to 1.5 mM, and 200 μM DesII enzyme in 100 mM Tris•HCl buffer, pH 8.0, containing 1 mM DTT. In the preparation of samples in the absence of dithionite, it was replaced with 100 mM Tris•HCl at pH 8.0, containing 1 mM DTT. The final sample volume was 500 μL. The samples were mixed, transferred to EPR

tubes, and frozen by immersion of the tubes in cold isopentane (approximately – 140 °C) within 30 sec after mixing. The samples were stored in liquid nitrogen until analysis.

EPR Spectroscopy. EPR spectra were recorded at liquid helium temperature on a Bruker EMX EPR spectrometer. A GFS600 transfer line and an ITC503 temperature controller were used to maintain the temperature. An Oxford ESR900 cryostat was used to accommodate the sample. Data analysis was conducted using WinEPR provided by Bruker.

2.3 RESULTS

Purification and Characterization of DesII Protein. C-terminal His_6-tagged DesII enzyme was purified to near homogeneity using a Ni-NTA column (Qiagen) followed by FPLC on a MonoQ (16/10) column. The desired fractions were detected by SDS-PAGE (Figure 2-13). After aerobic purification, DesII was slightly brown in color. A 6-liter culture yielded 15 mg of homogeneous DesII protein. The *N*-terminal peptide sequencing analysis confirmed that the first 10 amino acid residues (TAPALSATAP) of the purified protein were identical to the translated DesII sequence except for the initiating methionine residue, which was removed during protein synthesis in *E. coli.* The subunit molecular mass of DesII was estimated to be 54 kDa as judged by SDS-PAGE, which correlates well with the calculated molecular weight of 54,265 Da (including the His_6 tag). Analysis by gel filtration chromatography revealed a M_r of 48.4 kDa for DesII suggesting that DesII exists as a monomer in solution.

UV-vis Spectroscopy of Purified DesII. The UV-vis spectrum of the purified

protein exhibits a broad shoulder between 400 and 500 nm, which is characteristic for iron-sulfur cluster containing proteins, such as the anaerobic *E. coli* ribonucleotide reductase. The approximate extinction coefficients are $\varepsilon_{420} = 4000\ M^{-1} \cdot cm^{-1}$ for DesII and $\varepsilon_{420} = 3700\ M^{-1}\ cm^{-1}$ for the anaerobic *E. coli* ribonucleotide reductase (*38*) (Figure 2-14).

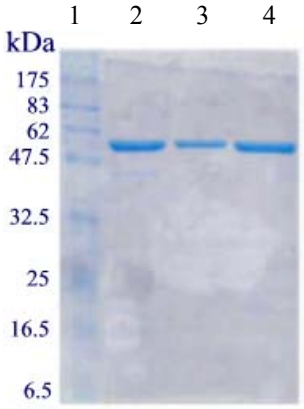

Figure 2-13. SDS-PAGE of purified DesII isolated from *E. coli* BL21 Star (DE3): lane 1, the molecular mass standards: MBP-β-galactosidase (175 kDa), MBP-paramyosin (83 kDa), glutamic dehydrogenase (62 kDa), aldolase (47.5 kDa), triosephosphate isomerase (32.5 kDa), β-lactoglobulin A (25 kDa), lysozyme (16.5 kDa), and aprotinin (6.5 kDa), lane 2-4, fractions of DesII purified using a Ni-NTA column followed by FPLC on a MonoQ HR (16/10) column.

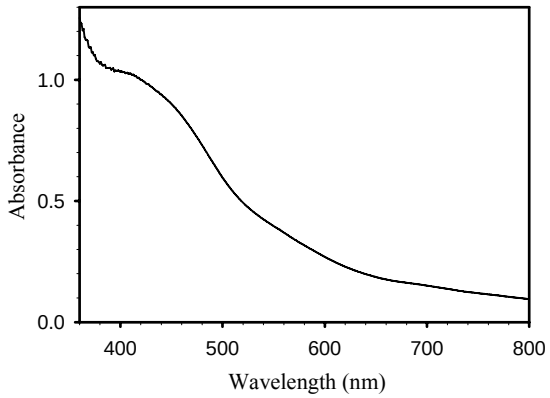

Figure 2-14. UV-vis absorption spectrum of aerobically purified DesII in 50 mM Tris•HCl buffer, pH 7.5. The protein concentration is 0.35 mM.

Purification and Characterization of DesI Protein. *N*-terminal His_6-tagged DesI enzyme was purified to near homogeneity using a Ni-NTA column (Qiagen). The desired fractions were detected by SDS-PAGE (Figure 2-15). A 6-liter culture yielded 30 mg of homogeneous DesI protein. The subunit molecular mass of DesI was estimated to be 45 kDa as judged by SDS-PAGE, which correlates well with the calculated molecular weight of 45,765 Da (including the His_6 tag). All the biochemical properties of DesI were identical to those previously reported (*5*).

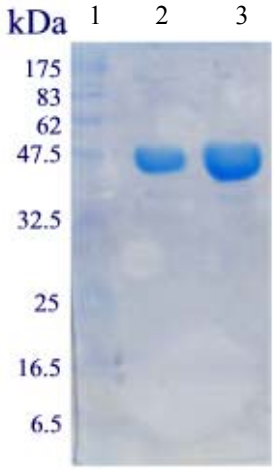

Figure 2-15. SDS-PAGE of purified DesI isolated from *E. coli* BL21(DE3): lane 1, the molecular mass standards, lane 2-3, fractions of DesI purified using a Ni-NTA column.

UV-vis Spectroscopy of Purified DesI. The UV-vis spectrum of the purified protein exhibits characteristic peaks at 330 and 420 nm, suggesting that DesI contains PLP as a cofactor (Figure 2-16).

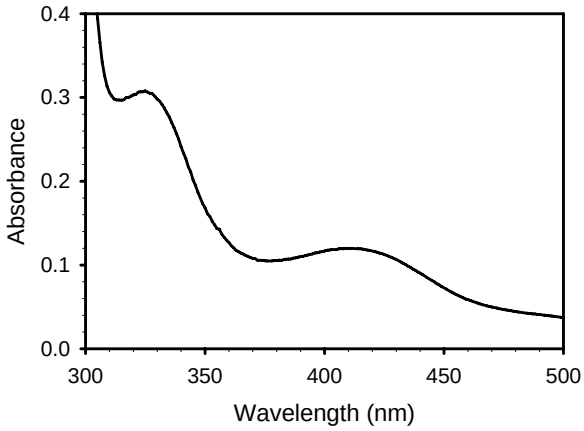

Figure 2-16. UV-vis absorption spectrum of purified DesI in 50 mM potassium phosphate buffer, pH 7.5. The protein concentration is 0.1 mM.

Purification and Characterization of DesV Protein. *C*-terminal His_6-tagged DesV enzyme was purified to near homogeneity using a Ni-NTA column (Qiagen). The desired fractions were detected by SDS-PAGE (Figure 2-17). A 6-liter culture yielded 90 mg of nearly homogeneous DesV protein. The subunit molecular mass of DesII was estimated to be 42 kDa as judged by SDS-PAGE, which correlates well with the calculated molecular weight of 42,104 Da (including the His_6 tag). The UV-vis spectrum of the purified protein exhibits characteristic peaks at 330 and 420 nm, suggesting that DesV contains PLP as a cofactor. All the biochemical properties of DesV were identical to those previously reported (*18*).

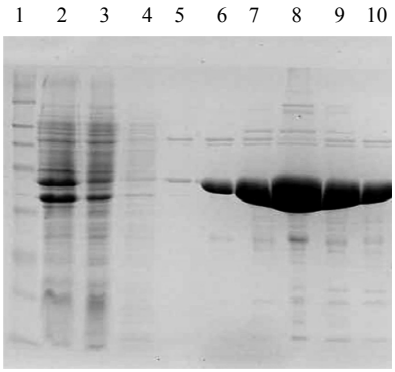

Figure 2-17. SDS-PAGE of purified DesV isolated from *E. coli* BL21(DE3): lane 1, the molecular mass standards: MBP-β-galactosidase (175 kDa), MBP-paramyosin (83 kDa), glutamic dehydrogenase (62 kDa), aldolase (47.5 kDa), triosephosphate isomerase (32.5 kDa), β-lactoglobulin A (25 kDa), lysozyme (16.5 kDa), and aprotinin (6.5 kDa); lane 2, supernatant after lysis, lane 3, supernatant after incubation with Ni-NTA resin, lane 4, washing fraction (20 mM imidazole), lanes 5-10, elution fractions containing DesV.

Purification and Characterization of E. coli Flavodoxin (FLD). *C*-terminal His_6-tagged flavodoxin (FLD) was purified to near homogeneity using a Ni-NTA column (Qiagen). The desired fractions were detected by SDS-PAGE (Figure 2-18). A 6-liter culture yielded 90 mg of homogeneous FLD protein. The subunit molecular mass of FLD was estimated to be 22 kDa as judged by SDS-PAGE, which correlates well with the calculated molecular weight of 22,765 Da (including the His_6 tag). The UV-vis spectrum of the purified FPR exhibits characteristic peaks at 360 and 460 nm as well as a shoulder at approximately 500 nm (Figure 2-19). The observed UV-vis spectrum suggested that FPR contains flavin mononucleotide (FMN) as a cofactor.

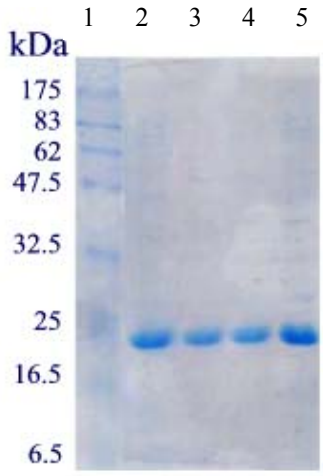

Figure 2-18. SDS-PAGE of purified flavodoxin (FLD) isolated from *E. coli* BL21 (DE3): lane 1, the molecular mass standards, lane 2-5, fractions of FLD purified using a Ni-NTA column.

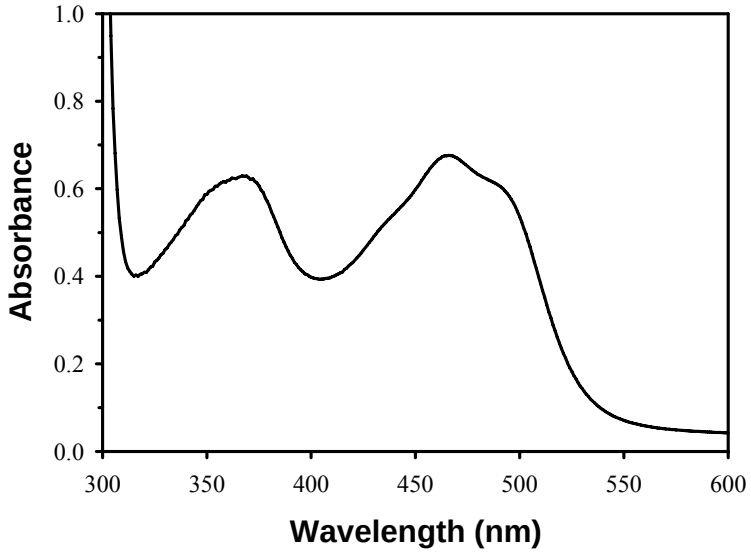

Figure 2-19. UV-vis absorption spectrum of purified flavodoxin in 20 mM Tris•HCl buffer, pH 7.5. The protein concentration is 0.3 mM.

Purification and Characterization of E. coli Flavodoxin Reductase (FPR). *N*-terminal His_6-tagged flavodoxin reductase (FPR) was purified to near homogeneity using

a Ni-NTA column (Qiagen). The desired fractions were detected by SDS-PAGE (Figure 2-20). A 6-liter culture yielded 100 mg of homogeneous FPR protein. The subunit molecular mass of FPR was estimated to be 29 kDa as judged by SDS-PAGE, which correlates well with the calculated molecular weight of 29,765 Da (including the His_6 tag). The UV-vis spectrum of the purified FPR exhibits characteristic peaks at 400 and 465 nm as well as a shoulder at approximately 480 nm (Figure 2-21). The observed UV-vis spectrum suggested that FPR contains flavin adenine dinucleotide (FAD) as a cofactor.

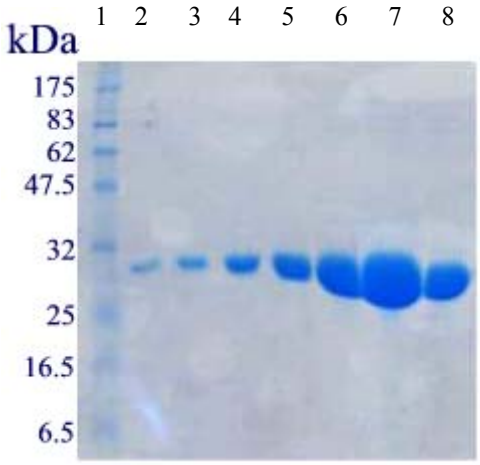

Figure 2-20. SDS-PAGE of purified flavodoxin reductase (FPR) isolated from *E. coli* BL21(DE3): lane 1, the molecular mass standards, lane 2-8, fractions of FPR purified using a Ni-NTA column.

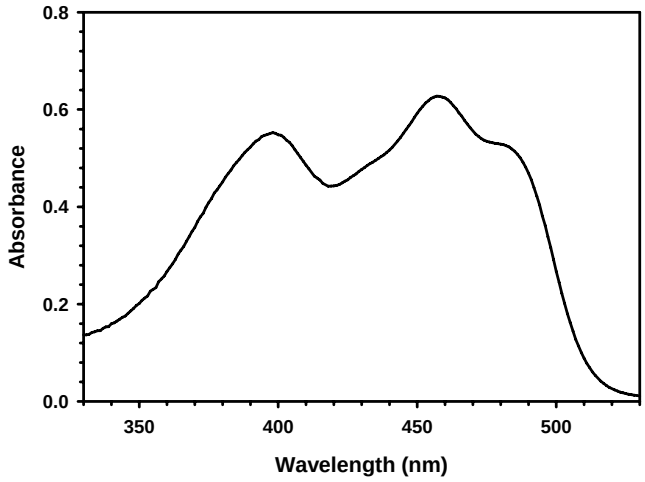

Figure 2-21. UV-vis absorption spectrum of purified FPR in 20 mM Tris•HCl buffer, pH 7.5. The protein concentration is 0.3 mM.

Expression of pDB1282 in E. coli BL21 Star (DE3). The SDS-PAGE (Figure 2-22) showed that the supernatant contained HscA, IscS, Fdx, HscB, IscU, and IscA, which are encoded in pDB1282.

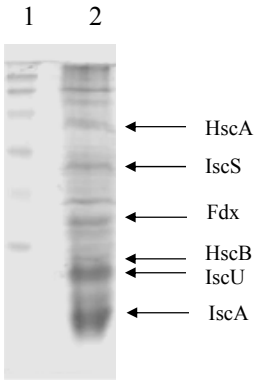

Figure 2-22. SDS-PAGE of cell lysate isolated from *E. coli* BL21 Star (DE3) containing pDB1282: lane 1, the molecular mass standards, lane 2, cell lysate containing HscA, IscS, Fdx, HscB, IscU, and IscA.

Expression of desII/pET24b(+) and pDB1281 in E. coli BL21 Star (DE3) at 37 °C. The SDS-PAGE (Figure 2-23) showed that the supernatant (lane 2) contained

HscA, IscS, Fdx, HscB, IscU, and IscA, which are encoded in pDB1282. However, there is no DesII protein present in the supernatant. It was likely that DesII formed inclusion bodies when grown at 37 °C. In order to determine whether DesII formed inclusion bodies, cell debris resuspended in 8 M urea was subjected to SDS-PAGE analysis (Figure 2-23, lane 3). The SDS-PAGE clearly showed that the major protein band in the cell debris was DesII. Since DesII formed inclusion bodies at 37 °C, the temperature was lowered to 18 °C to test whether DesII expression could yield soluble protein.

Expression of desII/pET24b(+) and pDB1281 in E. coli BL21 Star (DE3) at 18 °C. The SDS-PAGE for the supernatant (Figure 2-23, lane 4) and the cell debris in 8M urea (Figure 2-23, lane 5) showed that neither cell fractions contained the DesII protein. Moreover, neither these cell fractions contained HscA, IscS, Fdx, HscB, IscU, and IscA, which are encoded in pDB1282. Thus, neither DesII nor the proteins required for iron-sulfur cluster assemble were found to be expressed under this condition.

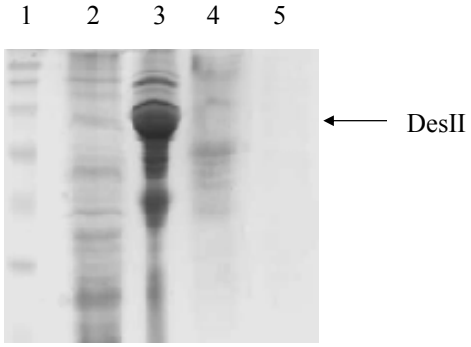

Figure 2-23. SDS-PAGE of expression of *desII*/pET24b(+) and pDB1282 in *E. coli* BL21 Star (DE3): lane 1, the molecular mass standards, lane 2, supernatant when culture was grown at 37 °C, lane 3, cell debris in 8 M urea when culture was grown at 37 °C, lane 4, supernatant when culture was grown at 18 °C, lane 5, cell debirs in 8 M urea when culture was grown at 18 °C.

Expression of DesII in E. coli in M9 minimal Medium. In order to isolate apo DesII for future preparation of Mössbauer samples, M9 minimal medium in lieu of LB medium to express the DesII protein. As judged by SDS-PAGE, the majority of DesII presented in the cell debris (Figure 2-24, lane 2) and was not soluble in the supernatant. Thus, it was concluded that DesII formed an inclusion bodies when the recombinant strain was grown in M9 minimal medium. As previously described, iron-depleted medium was used to express the DesII protein, which contains some trace metals and is likely to assist cell growth.

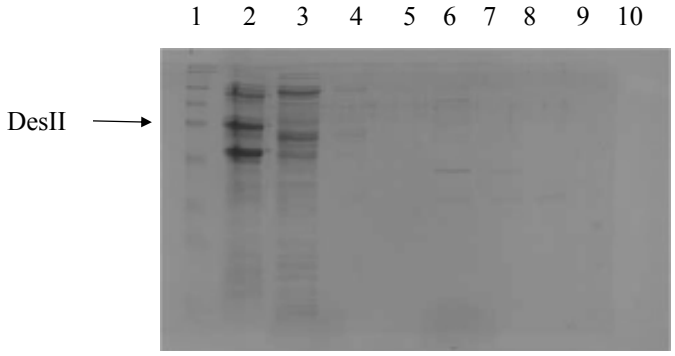

Figure 2-24. SDS-PAGE of DesII expression in M9 minimal medium: lane 1, the molecular mass standards; lane 2, cell debris in 8 M urea, lane 3, supernatant, lanes 4-5, washing fractions (20 mM imidazole), lanes 6-10, elution fractions (250 mM imidazole).

Expression of DesII in E. coli in Iron-depleted Medium. As judged by SDS-PAGE, trace amounts of soluble DesII protein was present in the supernatant (Figure 2-25, lane 2). The solubility of DesII improved slightly when the culture was grown in iron-depleted medium. To increase the yield of the DesII protein, $Fe(NH_4)_2(SO_4)_2$ was added to the culture, which can be replaced by $^{57}Fe(NH_4)_2(SO_4)_2$ in the purification of the DesII protein for Mössbauer samples.

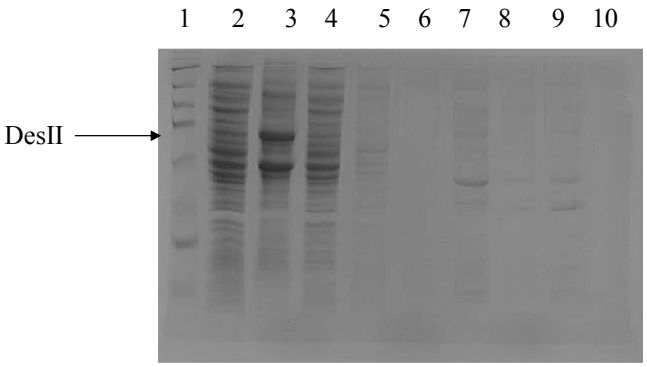

Figure 2-25. SDS-PAGE of DesII expression in iron-depleted medium: lane 1, the molecular mass standards, lane 2, supernatant, lane 3, cell debris in 8 M urea, lanes 4-5, washing fractions (20 mM imidazole), lanes 6-10, elution fractions (250 mM imidazole).

Expression of DesII in E. coli in Iron-depleted Medium with Supplemental $Fe(NH_4)_2(SO_4)_2$. When DesII was cultured in iron-depleted medium, 0.2 mM $Fe(NH_4)_2(SO_4)_2$ was added to provide the iron source for the iron-sulfur cluster biosynthesis. As judged by SDS-PAGE, in the presence of $Fe(NH_4)_2(SO_4)_2$ an increased amount of soluble DesII protein was present in the elution fractions (Figure 2-26, lanes 7 and 8). Therefore, the purified DesII protein for Mössbauer samples could be prepared by growing the culture in iron-depleted medium with supplemental $^{57}Fe(NH_4)_2(SO_4)_2$. After aerobic purification, the [4^{57}Fe-4S] cluster can be anaerobically reconstituted *in vitro* using $^{57}Fe(NH_4)_2(SO_4)_2$ by a previously established procedure.

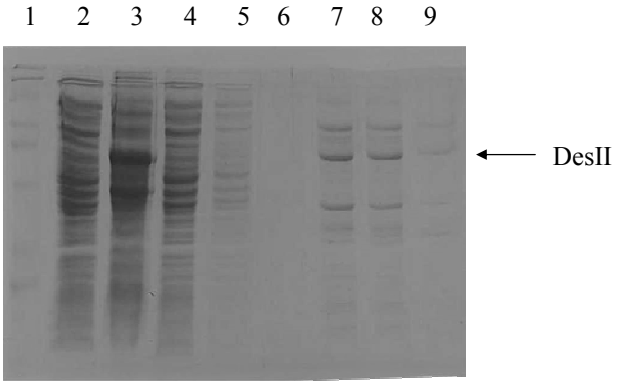

Figure 2-26. SDS-PAGE of DesII expression in iron-depleted medium with supplemental $Fe(NH_4)_2(SO_4)_2$: lane 1, the molecular mass standards, lane 2, supernatant, lane 3, cell debris in 8 M urea, lanes 4-5, washing fractions (20 mM imidazole), lanes 6-9, elution fractions (250 mM imidazole).

Reconstitution and Reduction of the Iron Sulfur Center of DesII. The purified enzyme was anaerobically converted into the colorless apoprotein by incubating with ethyl diamine tetetric acid (EDTA) in the presence of the reducing agent, sodium dithionite. Subsequent reconstitution was achieved by incubating the enzyme with an excess of ferrous iron and sodium sulfide in the presence of DTT for 3 h at 25 °C. After anaerobic reconstitution, the color of the reconstituted protein changed to green-gray. The reconstituted DesII exhibits a broad absorption band at 420 nm (ε_{420} = 9200 $M^{-1}\cdot cm^{-1}$) and absorption across the entire UV-vis spectrum, which are characteristic features of the $[4Fe\text{-}4S]^{2+}$ cluster found in biotin synthase (*39*) and other $[4Fe\text{-}4S]^{2+}$ containing enzymes (*40, 41*) (Figure 2-27). The differences in UV-vis spectrum between purified DesII and fully reconstituted DesII suggest that aerobically purified DesII may not contain an intact $[4Fe\text{-}4S]^{2+}$ cluster. This implication is consistent with the fact that $[4Fe\text{-}4S]^{1+/2+}$ clusters

are oxygen sensitive and may degrade to a $[2Fe\text{-}2S]^{2+}$ cluster upon exposure to oxygen (*39*).

The catalytic form of $[4Fe\text{-}4S]^{1+}$ cluster was generated by anaerobic reduction of $[4Fe\text{-}4S]^{2+}$ cluster with sodium dithionite. The $[4Fe\text{-}4S]^{2+}$ cluster reduction was monitored by following the decrease of absorbance at 420 nm. The decrease in absorbance in the 400 to 550 nm range is associated with the reduction of the $[4Fe\text{-}4S]^{2+}$ cluster to $[4Fe\text{-}4S]^{1+}$ state (*42*) (Figure 2-27).

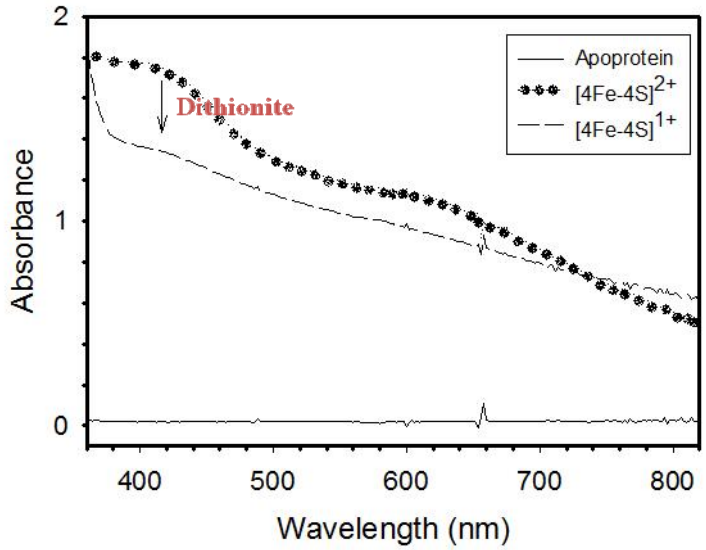

Figure 2-27. UV-vis absorption spectra of apoprotein (solid line), reconstituted protein before (dotted line) and after (dashed line) reduction with 1.14 mM sodium dithionite. The protein concentration is 0.19 mM in 100 mM Tris•HCl buffer, pH 8.0.

Difference of Iron Content in Purified DesII and Reconstituted DesII. Purified DesII contained approximately 0.6 iron molecules per monomer, which may reflect the loss of iron during aerobic purification. Fully reconstituted DesII contained approximately 4 iron molecules per monomer, consistent with DesII containing a [4Fe-4S] cluster as suggested by UV-vis spectrum (Figure 2-28).

Difference of Sulfur Content in Purified DesII and Reconstituted DesII. Purified DesII contained approximately 0.5 sulfur molecules per monomer. Fully reconstituted DesII contained approximately 4 sulfur molecules per monomer, consistent with DesII containing a [4Fe-4S] cluster as suggested by UV-vis spectrum (Figure 2-27).

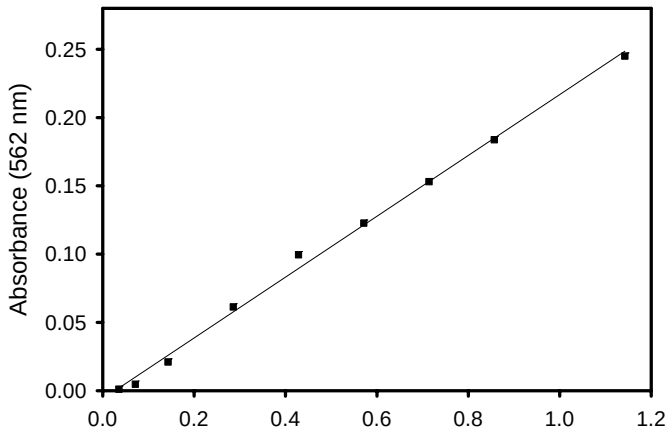

DesII	DesII (μmole)	A_{562}	Iron Conc. (μg/mL)	Iron (μmole)	Iron/DesII
Purified	0.0047	0.0312	0.1673	0.0029	**0.633**
Purified	0.0094	0.0573	0.2844	0.0050	**0.539**
Reconstituted	0.0023	0.1118	0.5287	0.0094	**4.079**
Reconstituted	0.0046	0.2247	1.0353	0.0184	**4.002**

Figure 2-28. The determination of iron content of purified DesII and reconstituted DesII by iron titration analysis. The standard curve was determined by $Fe(NH_4)_2(SO_4)_2$.

Characterization of $[3Fe\text{-}4S]^{1+}$ Cluster in Aerobically Purified DesII by EPR Spectroscopy. The EPR spectrum of the as-purified DesII protein in the absence of dithionite recorded at 9.6 GHz and 10 K is shown in Figure 2-29. The aerobically purified DesII exhibits a strong, nearly isotropic EPR signal with *g* value (definition shown below) centered at 2.009. This EPR singal is similar to that for a $[3Fe\text{-}4S]^{+}$ cluster (with *S* (spin states) = ½) previously observed in other as-isolated radical SAM enzymes.

For example, as-isolated spore photoproduct lyase exhibits an isotropic EPR signal arising from a $[3Fe\text{-}4S]^{+}$ cluster, which has a *g* value centered at 2.02 (*43*). Likewise, anaerobic ribonucleotide reductase-activase upon exposure to air exhibits a similar isotropic EPR signals arising from a $[3Fe\text{-}4S]^{+}$ cluster, having a *g* value centered at 2.015 (*44*). The $[3Fe\text{-}4S]^{+}$ cluster is the oxidation product of $[4Fe\text{-}4S]^{3+}$ cluster upon exposure to air and is not functional in catalysis. No EPR signal was observed in the as-purified DesII protein in the presence of dithionite recorded under the same conditions (data not shown), suggesting the iron-sulfur cluster is in an EPR-silent form, $[3Fe\text{-}4S]^{0}$ with $S = 2$.

$$g = \frac{h\upsilon}{\beta_e B}$$

h = Plank's constant
υ= Frequency
β_e = Bohr magneton
B = Applied magnetic field

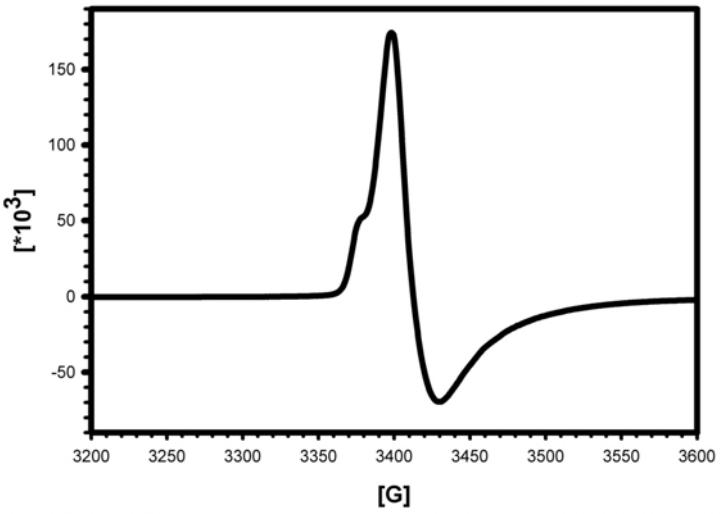

Figure 2-29. EPR spectrum of as-purified DesII containing a $[3Fe\text{-}4S]^{1+}$ cluster with a *g* value centered at 2.009. The protein concentration is 0.2 mM.

Characterization of [4Fe-4S]$^{1+}$ Cluster in Anaerobically Reconstituted DesII by EPR Spectroscopy. Previously, the EPR spectrum of the DesII protein in the absence of dithionite recorded at 9.6 GHz and 10 K displayed a very weak, nearly axial signal with the *g*-value centered at 2.004 (data not shown). This signal centered at 2.004 is similar to that centered at 2.007 arising from [4Fe-4S]$^{3+}$ in lysine 2,3-aminomutase (*45*). However, the [4Fe-4S]$^{3+}$ cluster is not functional in catalysis and is easily degraded to the [3Fe-4S]$^{1+}$ cluster upon oxidation. In order to avoid the accumulation of the [4Fe-4S]$^{3+}$ cluster in the EPR samples, freshly reconstituted DesII was prepared to acquire the EPR spectra. The EPR spectrum of the freshly reconstituted DesII protein in the presence of cofactor SAM and reducing agent, dithionite, recorded at 9.6 GHz and 10 K is shown in Figure 2-30. The reconstituted DesII, which is reduced by dithionite in the presence of SAM, exhibits a nearly rhombic EPR signal with *g* values at 2.01, 1.95, and 1.86 (g_{av} = 1.94). This EPR signal is similar to that for a [4Fe-4S]$^{1+}$ cluater observed in anaerobic ribonucleotide reductase-activase. Anaerobic ribonucleotide reductase-activase reduced by dithionite in the presence of SAM exhibits a rhombic EPR signal with *g* values at 2.00, 1.92, and 1.86 (g_{av} = 1.93) (*46*). No EPR signal was observed in the reconstituted DesII protein in the absence of dithionite recorded under the same conditions (data not shown), suggesting the iron-sulfur cluster is in its EPR-silent form, [4Fe-4S]$^{2+}$ with $S = 0$.

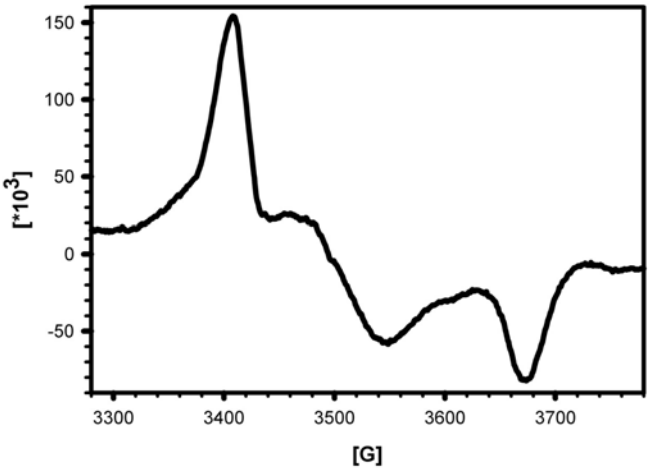

Figure 2-30. EPR spectrum of reconstituted DesII containing a $[4Fe\text{-}4S]^{1+}$ cluster with *g* values at 2.00, 1.92, and 1.86 (g_{av} = 1.93). The protein concentration is 0.2 mM.

*Characterization of TDP-D-glucose (**2-7**).* TDP-D-glucose (**2-7**) was prepared from glucose-1-phosphate and thymidine in the presence of thymidine kinase (TK), thymidylate kinase (TMK), nucleoside diphosphate kinase (NDK), pyruvate kinase, and α-D-glucose-1-phosphate thymidylyltransferase (RfbA). The identity of TDP-D-glucose (8) was established by ^{1}H NMR spectroscopy. The spectral data are comparable to those reported for **2-7** in the literature (*47*). The product was recovered in 70% yield. **2-7:** ^{1}H NMR (300 MHz, D_2O) δ 1.78 (3H, s, 5"-Me), 2.22 (2H, m, 2'-Hs), 3.28-3.40 (2H, m, 2-H, 3-H), 3.59-3.78 (2H, m, 4-H, 5-H), 3.95-4.06 (3H, m, 4'-H, 5'-Hs), 4.45 (1H, m, 3'-H), 5.44 (1H, dd, *J* = 6.9, 3.3 Hz, 1-H), 6.20 (1H, t, *J* = 6.9 Hz, 1'-H), 7.59 (1H, s, 6"-H).

*Characterization of TDP-4-keto-6-deoxy-D-glucose (**2-8**).* TDP-4-keto-6-deoxy-D-glucose (**2-8**) was generated from TDP-D-glucose (**2-7**) in the presence of RfbB. The identity of TDP-4-keto-6-deoxy-D-glucose (**2-8**) was established by ^{1}H NMR spectroscopy. The spectral data are comparable to those reported for **2-8** in the literature

(*47*). The product was recovered in 60% yield. ^{1}H NMR (300 MHz D_2O) of **2-8** (a mixture of hydrate and keto forms): δ 1.08 (3H, d, *J* = 6.5 Hz, 5-Me of hydrate form), 1.12 (3H, d, *J* = 6.5 Hz, 5-Me of keto form), 1.79 (3H, s, 5"-Me), 2.09-2.26 (2H, m, 2'-Hs), 3.48 (1H, m, 2-H of hydrate form), 3.64 (1H, d, *J* = 10.0 Hz, 3-H of hydrate form), 3.68 (1H, m, 2-H of keto form), 3.96 (1H, q, *J* = 6.5 Hz, 5-H of hydrate form), 4.01-4.07 (3H, m, 4'-H, 5'-Hs), 4.48 (1H, m, 3'-H), 5.41 (1H, dd, *J* = 7.3, 3.8 Hz, 1-H of hydrate form), 5.59 (1H, dd, *J* = 7.0, 3.0 Hz, 1-H of keto form), 6.20 (1H, t, *J* = 6.9 Hz, 1'-H), 7.60 (1H, s, 6"-H).

*Characterization of TDP-D-quinovose (**2-22**).* TDP-D-quinovose (**2-22**, Figure 2-8) was generated from TDP-4-keto-6-deoxy-D-glucose by the reduction of the C-4 keto group using $NaBH_4$ as a major product. The identity of TDP-D-quinovose (**2-22**) was established by ^{1}H and ^{31}P NMR spectroscopy. The spectral data are comparable to those reported for **2-22** in the literature (*35*). The product was recovered in 40% yield. TDP-D-quinovose (**2-22**): ^{1}H NMR (300 MHz, D_2O): ^{1}H NMR (300 MHz, D_2O) δ 0.80 (3H, d, *J* = 5.7 Hz, 5-Me), 1.52 (3H, s, 5′′-Me), 1.98-2.08 (2H, m, 2′-Hs), 2.84 (1H, dd, $J_{3,4} = J_{4,5}$ = 9.9 Hz, 4-H), 3.22-3.31 (1H, m, 2-H), 3.28 (1H, dd, $J_{2,3}$ = 9.3, $J_{3,4}$ = 9.9 Hz, 3-H), 3.53 (1H, m, 5-H), 3.75-3.88 (3H, m, 4′-H, 5′-Hs), 4.18-4.22 (1H, m, 3′-H), 5.15 (1H, dd, $J_{1,p}$ = 6.8, $J_{1,2}$ = 3.1 Hz, 1-H), 5.94 (1H, t, *J* = 6.7 Hz, 1′-H), 7.29 (1H, s, 6′′-H); ^{31}P NMR (121 MHz, D_2O) δ -11.79 (d, *J* = 18.3 Hz), -10.34 (d, *J* = 18.3 Hz).

*Characterization of TDP-D-fucose (**2-23**).* TDP-D-fucose (**2-23**, Figure 2-8) was generated from TDP-4-keto-6-deoxy-D-glucose by the reduction of the C-4 keto group using $NaBH_4$ as a minor product. The identity of TDP-D-fucose (**2-23**) was established by

^{1}H and ^{31}P NMR spectroscopy. The spectral data are comparable to those reported for **2-23** in the literature (*35*). The product was recovered in 13% yield. TDP-D-fucose (**2-23**): ^{1}H NMR (300 MHz, D_2O) δ 1.21 (3H, d, *J* = 6.6 Hz, 5-Me), 1.93 (3H, s, 5″-Me), 2.36 (2H, m, 2'-Hs), 3.74 (1H, dt, *J* = 10.5, 3.2 Hz, 2-H), 3.81 (1H, *J* = 3.2 Hz, 4-H), 3.91 (1H, dd, *J* = 10.5, 3.2 Hz, 3-H), 4.17 (3H, m, 4'-H and 5'-Hs), 4.28 (1H, *J* = 6.6 Hz, 5-H), 4.62 (1H, m, 3'-H), 5.56 (1H, dd, *J* = 6.8, 3.6 Hz, 1-H), 6.34 (1H, t, *J* = 7.0 Hz, 1'-H), 7.74 (1H, s, 6"-H); ^{31}P NMR (121 MHz, D_2O) δ -11.75 (d, *J* = 18.3 Hz), -10.39 (d, *J* = 18.3 Hz).

*Characterization of TDP-4-amino-4,6-dideoxy-D-glucose (**2-9**, DesII Substrate).* TDP-4-amino-4,6-dideoxy-D-glucose (**2-9**, Figure 2-1) was generated from TDP-D-glucose (**2-7**, Figure 2-1) in the presence of RfbB, DesI, PLP, and L-glutamate. The identity of TDP-4-amino-4,6-dideoxy-D-glucose (**2-9**) was established by ^{1}H and ^{31}P NMR spectroscopy. The spectral data are comparable to those reported for **2-9** in the literature (*5*). The product was recovered in 39% yield. **2-9**: ^{1}H NMR (300 MHz, D_2O) δ 0.80 (3H, d, *J* = 5.7 Hz, 5-Me), 1.52 (3H, s, 5″-Me), 1.98-2.08 (2H, m, 2′-Hs), 2.84 (1H, dd, $J_{3,4} = J_{4,5}$ = 9.9 Hz, 4-H), 3.22-3.31 (1H, m, 2-H), 3.28 (1H, m, *J* = 9.9, 9.3 Hz, 3-H), 3.53 (1H, m, 5-H), 3.75-3.88 (3H, m, 4′-H, 5′-Hs), 4.18-4.22 (1H, m, 3′-H), 5.15 (1H, dd, *J* = 6.8, 3.1 Hz, 1-H), 5.94 (1H, t, *J* = 6.7 Hz, 1′-H), 7.29 (1H, s, 6″-H); ^{31}P NMR (121 MHz, D_2O) δ -11.79 (d, *J* = 18.3 Hz), -10.34 (d, *J* = 18.3 Hz).

NAD(P)H:DCPIP Oxidoreductase Activity of Flavodoxin and Flavodoxin Reductase. Flavodoxin and flavodoxin reducatse together have NAD(P)H:DCPIP oxidoreductase activity. They reduce DCPIP at a rate of 4.8 nmol mg^{-1} min^{-1} in the presence of 1.4 mM NADPH. This rate decreases to 1.9 nmol mg^{-1} min^{-1} when NADH is

used as the reducing agent. From these results it was concluded that the purified flavodoxin and flavodoxin reductase from *E. coli* are active.

Catalytic Activity of DesI. TDP-4-keto-6-deoxy-D-glucose (**2-8**, Figure 2-1) was used as a substrate to assay the activity of purified DesI. Consumption of **2-8** (with a retention time of 13.8 min) and the concomitant formation of a new product (with a retention time of 6.1 min) were observed. This new compound was purified by FPLC equipped with a MonoQ column and characterized by NMR spectroscopy and high resolution mass spectrometry. The spectral data of DesI product were comparable to those previously reported for **2-9** (*5*).

Catalytic Activity of DesV. Incubation of purified DesV with TDP-3-amino-3,4-6-trideoxy-D-glucose (**2-11**, Figure 2-1) in the presence of α-ketoglutarate resulted in a new product observed by HPLC with a retention time of 28.2 min, which is identical to that of TDP-3-keto-4,6-dideoxy-D-glucose (**2-10**, Figure 2-1). Thus, the catalytic activity of DesV was comparable to those previously established (*18*).

DesI and DesII Coupled Activity. After anaerobic incubation of substrate (**2-8**, Figure 2-1), DesI, reduced DesII enzyme, the cofactors PLP and SAM, and L-glutamate, the formation of TDP-3-keto-4,6-dideoxy-D-glucose (**2-10**) was observed by HPLC. The product had a retention time of 28.2 min, which is identical to that of the standard (Figure 2-31). The identity of the product was verified by the high resolution mass spectrometry. High-resolution FAB-MS calcd for $C_{16}H_{24}N_2O_{14}P_2$ $[M-H]^-$ 529.0625, found 529.0629.

Previous studies have shown that TDP-3-keto-4,6-dideoxy-D-glucose (**2-10**) is the substrate for the next enzyme, DesV, in the TDP-D-desosamine biosynthetic pathway (*18*). Therefore, DesV was used to further confirm the identity of TDP-3-keto-4,6-

dideoxy-D-glucose (**2-10**) as follows. The DesII reaction mixture was incubated for 3 h, followed by the addition of DesV and the cofactors PLP and L-glutamate to convert TDP-3-keto-4,6-dideoxy-D-glucose (**2-10**) to TDP-3-amino-4,6-dideoxy-D-glucose (**2-11**). The formation of **2-11** was confirmed by HPLC, as a new peak with a retention time of 3.7 min was observed. The retention time is identical to that of the standard (Figure 2-31). The identity of the product was confirmed by high resolution mass spectrometry. High-resolution FAB-MS calcd for $C_{16}H_{27}N_3O_{13}P_2$ $[M-H]^-$ 530.0941, found 530.0945. These results provided compelling evidence supporting the formation of TDP-3-keto-4,6-dideoxy-D-glucose (**2-10**) and the activity of *in vitro* reconstituted DesII.

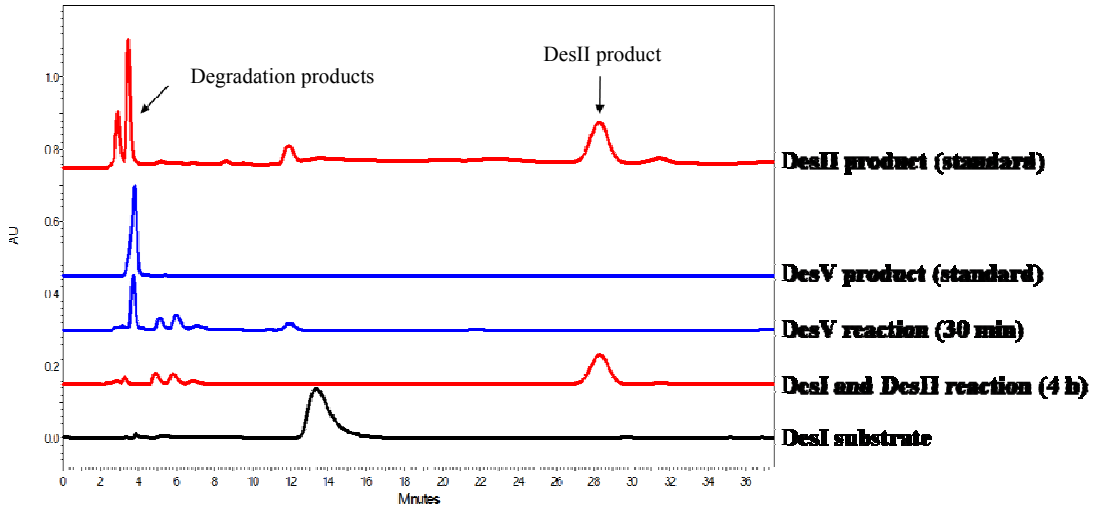

Figure 2-31. HPLC traces demonstrating coupled DesI and DesII activity.

In vitro Reconstitution of DesII Activity. After anaerobic incubation of substrate (**2-9**), reduced DesII enzyme, and the cofactor SAM, the formation of TDP-3-keto-4,6-dideoxy-D-glucose (**2-10**) was observed by HPLC. The product had a retention time of 28.2 min, which is identical to that of the standard (Figure 2-32). The identity of the

product was verified by the high resolution mass spectrometry. High-resolution FAB-MS calc for $C_{16}H_{24}N_2O_{14}P_2$ $[M-H]^-$ 529.0625, found 529.0621. The DesII reaction mixture was incubated for 3 h, followed by the addition of DesV and the cofactors PLP and L-glutamate to convert TDP-3-keto-4,6-dideoxy-D-glucose (**2-10**) to TDP-3-amino-4,6-dideoxy-D-glucose (**2-11**). The formation of **2-11** was confirmed by HPLC, as a new peak with retention time of 3.7 min was observed. The retention time is identical to that of the standard (Figure 2-32). The identity of the product was further confirmed by high resolution mass spectrometry. High-resolution FAB-MS calcd for $C_{16}H_{27}N_3O_{13}P_2$ $[M-H]^-$ 530.0941, found 530.0951. These results provided complelling evidence supporting the formation of TDP-3-keto-4,6-dideoxy-D-glucose (**2-10**) and the activity of *in vitro* reconstituted DesII.

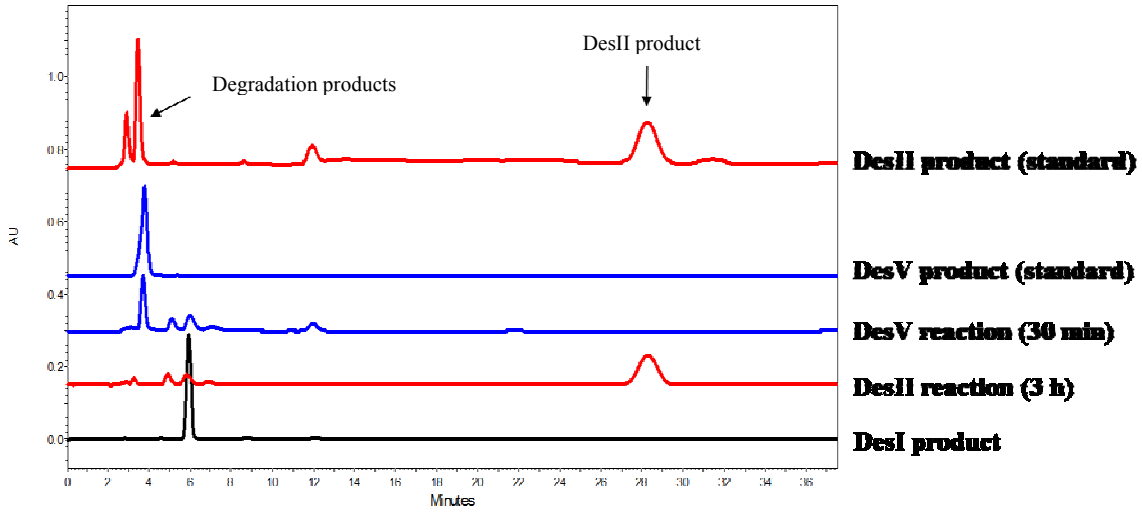

Figure 2-32. HPLC traces demonstrating DesII activity in the absence of DesI.

Determination of Kinetic Parameters for DesII-Catalyzed Reaction. To determine the steady state kinetic parameters for the DesII-catalyzed conversion of **2-9** to **2-10**

(Figure 2-1), a discontinuous HPLC assay was developed. The plot of v_0 (initial velocity) versus [S] (3 μM to 1 mM) (Figure 2-33) was fitted to the Michaelis-Menten equation by nonlinear regression to yield a k_{cat} of 0.99 ± 0.07 min^{-1} and a K_m of 49.45 ± 1.73 μM for **2-9**.

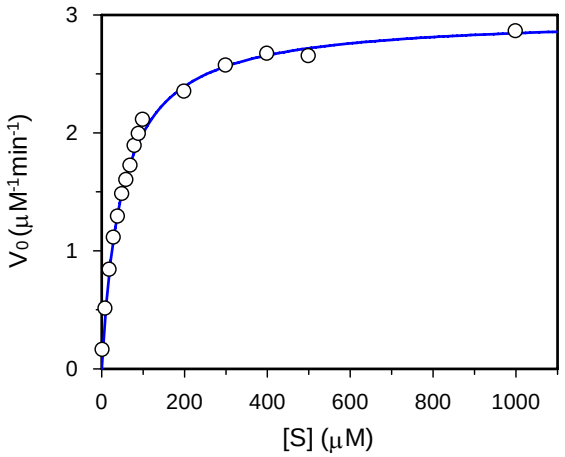

Figure 2-33. Plot of v_o vs [S] determined by an HPLC assay from which the steady state kinetic constants for the DesII-catalyzed reaction were determined.

Characterization of a Biological Reducing System for DesII. After anaerobic incubation of substrate (**2-9**), reconstituted DesII enzyme, SAM, flavodoxin, flavodoxin reducatse, and NADPH, the formation of TDP-3-keto-4,6-dideoxy-D-glucose (**2-10**) was observed by HPLC. The product had a retention time of 37.2 min, which is identical to that of the chemoenzymatically synthesized standard (Figure 2-34). The identity of the product was confirmed by the high resolution mass spectrometry. High-resolution FAB-MS calcd for $C_{16}H_{24}N_2O_{14}P_2$ $[M-H]^-$ 529.0625, found 529.0620. The DesII reaction mixture was incubated for 3 h, followed by the addition of DesV, PLP and L-glutamate to convert TDP-3-keto-4,6-dideoxy-D-glucose (**2-10**) to TDP-3-amino-4,6-dideoxy-D-glucose (**2-11**). The formation of **2-11** was confirmed by HPLC, as a new peak with a

retention time of 9.5 min was observed. The retention time is identical to that of the standard (Figure 2-34). The identity of the product was further confirmed by high resolution mass spectrometry. High-resolution FAB-MS calcd for $C_{16}H_{27}N_3O_{13}P_2$ $[M-H]^-$ 530.0941, found 530.0949. Thymidine monophosphate (TMP), a TDP-sugar degradation product was observed at retention time of 30.1 min in the DesV reaction. These results provided strong evidence for the formation of TDP-3-keto-4,6-dideoxy-D-glucose (**2-10**). Accordingly, a possible *in vivo* reducing system consisting of flavodoxin, flavodoxin reductase, and NADPH was identified and used to replace the chemical reductant, dithionite, to assay DesII activity. The $[4Fe\text{-}4S]^{2+}$ of DesII is reduced to $[4Fe\text{-}4S]^{1+}$ by an electron transferred from NADPH through flavodoxin and flavodoxin reductase.

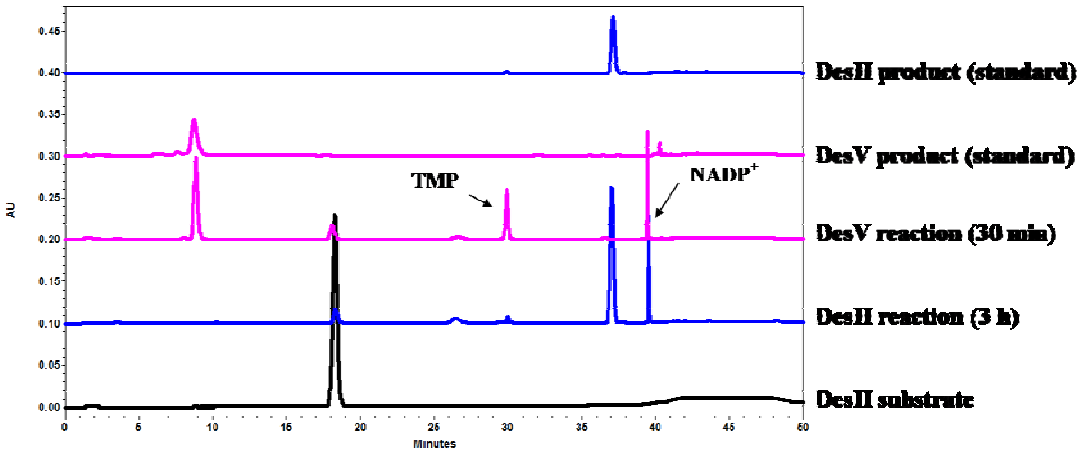

Figure 2-34. HPLC traces demonstrating DesII activity using flavodoxin, flavodoxin reductase, and NADPH as a reducing system.

*DesII Activity with the Substrate Isostere (**2-25**).* After anaerobic incubation of the substrate isostere (**2-25**), reduced DesII enzyme, and the cofactor SAM, the formation of the expected 3-keto sugar product (**2-28**, Figure 2-35) was not observed by HPLC. The DesII activity assay in the presence of the natural substrate (TDP-4-amino-4,6-dideoxy-

D-glucose, **2-9**, Figure 2-1) was carried out in parallel to confirm the anaerobic condition for this assay. In the presence of the natural substrate, the formation of TDP-3-keto-4,6-dideoxy-D-glucose (**2-10**) was observed. The results showed that this substrate isostere (**2-25**) was not turned over by DesII. It is likely that this substrate isostere (**2-25**) with one extra carbon at the C-1 position did not bind to DesII active site.

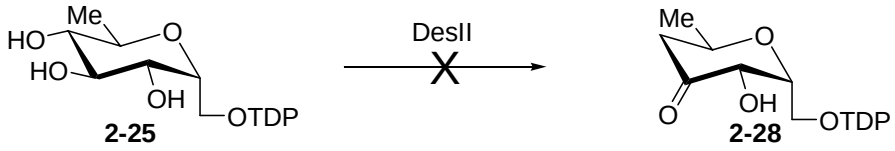

Figure 2-35. The expected reaction catalyzed by DesII using the DesII substrate isostere (**2-25**).

DesII Activity with TDP-D-quinovose (2-22). After anaerobic incubation of TDP-D-quinovose (**2-22**), reconstituted and reduced DesII enzyme, and the cofactor SAM, the formation of TDP-3-keto-4,6-dideoxy-D-glucose (**2-10**) was observed by HPLC (Figure 2-36). The product had a retention time of 26.8 min, which is identical to that of the standard. The identity of the product was further confirmed by the high resolution mass spectrometry. High-resolution FAB-MS calcd for $C_{16}H_{24}N_2O_{14}P_2$ $[M\text{-}H]^-$ 529.0625, found 529.0615. To compare DesII activity towards TDP-D-quinovose with that of the natural substrate, the activity assay in the presence of the natural substrate (TDP-4-amino-4,6-dideoxy-D-glucose) was carried out in parallel. The percent conversions measured at different time points are summarized in Table 2-3. The results showed that DesII can process TDP-D-quinovose as an alternate substrate to form TDP-D-3-keto-4,6-dideoxy glucose (**2-10**) at a similar rate as the natural substrate.

Time (min)	Percent Conversion (%)	
	Natural Substrate (**2-9**)	TDP-D-Quinovose (**2-22**)
0	0	0
15	14	12
30	19	17
60	33	30
90	65	60
120	65	60

Table 2-3. The comparison of percent conversion between TDP-D-quinovose (**2-22**) and the natural substrate (**2-9**) catalyzed by DesII.

*DesII Activity with TDP-D-fucose (**2-23**).* After anaerobic incubation of TDP-D-fucose (**2-23**), with reconstituted and reduced DesII enzyme, and the cofactor SAM, the expected formation of TDP-3-keto-4,6-dideoxy-D-glucose (**2-10**) was not observed by HPLC (Figure 2-36). This result suggests that DesII cannot recognize TDP-D-fucose (**2-23**) as an alternate substrate. Thus, the stereochemistry of the C-4 amino group in DesII substrate **2-9**, which is equatorially positioned on the hexose ring, may be important in the DesII-catalyzed reaction.

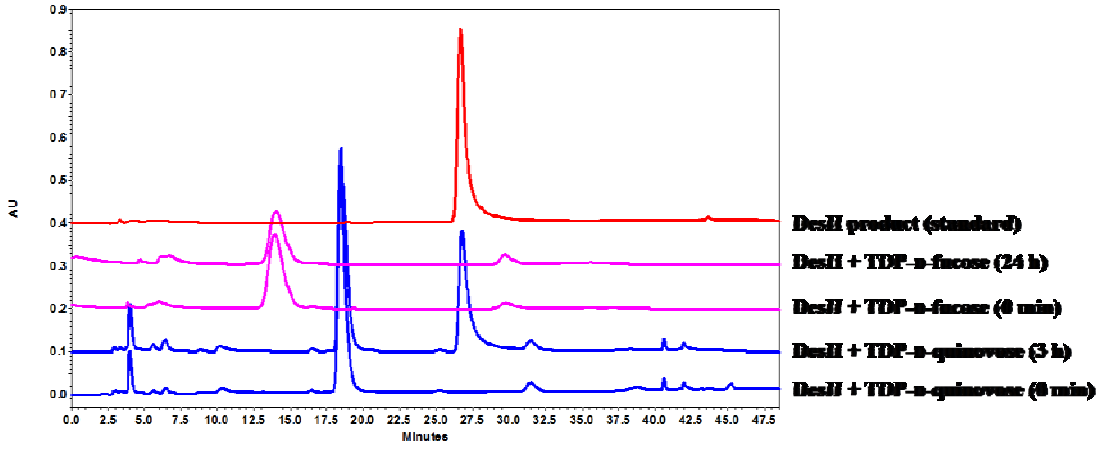

Figure 2-36. HPLC traces demonstrating DesII substrate specificity using TDP-D-quinovose (**2-22**) and TDP-D-fucose (**2-23**).

*DesII Activity with TylB Product (**2-24**).* After anaerobic incubation of TylB product (**2-24**), with reconstituted and reduced DesII enzyme, the cofactor SAM, the formation of TDP-3-keto-4,6-dideoxy-D-glucose (**2-10**) was observed by HPLC. The product had a retention time of 37.2 min, which is identical to that of the chemoenzymatically synthesized standard (Figure 2-37). The identity of the product was further confirmed by high resolution mass spectrometry. High-resolution FAB-MS calcd for $C_{16}H_{24}N_2O_{14}P_2$ $[M-H]^-$ 529.0625, found 529.0616. The DesII reaction mixture was incubated for 3 h, followed by the addition of DesV and the cofactors PLP and L-glutamate to convert TDP-3-keto-4,6-dideoxy-D-glucose (**2-10**) to TDP-3-amino-4,6-dideoxy-D-glucose (**2-11**). The formation of **2-11** was indicated by HPLC, as a new peak with a retention time of 9.5 min was observed. The retention time is identical to that of the standard (Figure 2-37). The identity of the product was confirmed by high resolution mass spectrometry. High-resolution FAB-MS calcd for $C_{16}H_{27}N_3O_{13}P_2$ $[M-H]^-$ 530.0941, found 530.0931. These results provided confirmatory evidence for the formation of TDP-3-keto-4,6-dideoxy-D-glucose (**2-10**). Interestingly, this result demonstrats that DesII can recognize TylB product from the macrolide antibiotic tylosin as an alternate substrate, but with lower conversion efficiency. The percent conversion for TylB product was 25%, as compared to natural substrate conversion, which was found to be approximately 65% under the assay conditions. TylB contains a C-3 amino group and a C-4 hydroxyl group, whereas DesII substrate contains a C-3 hydroxyl group and a C-4 amino group. Possible mechanisms that provide support for the formation of TDP-3-keto-4,6-dideoxy-D-glucose are presented in section 2.4.

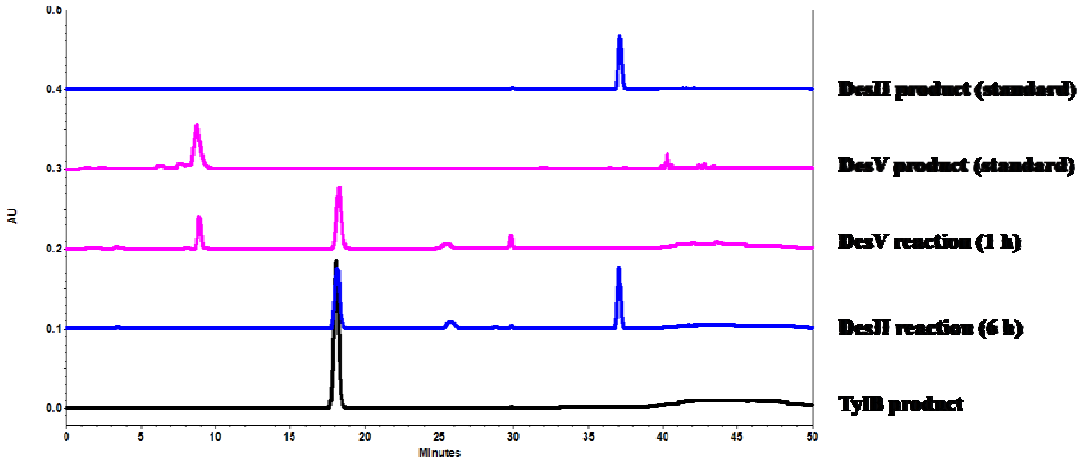

Figure 2-37. HPLC traces demonstrating DesII substrate specificity using TylB product (**2-24**).

*DesI Activity with CDP-4-keto-6-deoxy-D-glucose (**2-21**).* To test DesI substrate flexibility, CDP-4-keto-6-deoxy-D-glucose (**2-21**, Figure 2-38A) was used to replace TDP-4-keto-6-deoxy-D-glucose (DesI natural substrate) in the activity assay. The formation of a new peak at 16.5 min was observed by HPLC assay after incubation for 2 h at 25 °C (Figure 2-38B). It was collected, lyophilized to dryness, resuspended in water, and submitted for ESI mass spectrometry analysis (MS). High resolution MS consistent with CDP-4-amino-4,6-dideoxy-D-glucose (**2-29**, Figure 2-38A) was obtained: high-resolution ESI-MS calcd for $C_{15}H_{25}N_4O_{14}P_2$ $[M-H]^-$ 547.0843, found 547.0841. Cytidine monophosphate (CMP), a CDP-sugar degradation product was observed at retention time of 30.1 min in the reaction. The percent conversion for CDP-4-keto-6-deoxy-D-glucose was 42%, while the percent conversion for the natural substrate was 75%. The only difference between CDP-4-keto-6-deoxy-D-glucose (**2-21**) and the natural substrate (**2-9**)

for DesI is the nucleotide to which it is tethered. Thus, DesI is flexible toward a cytidine diphosphate attached to C-1 of the hexose ring.

(A)

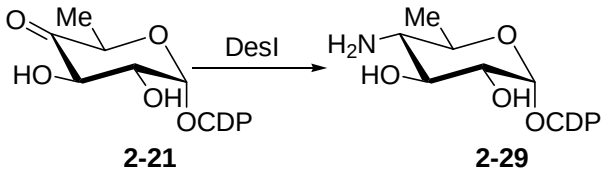

2-21 **2-29**

(B)

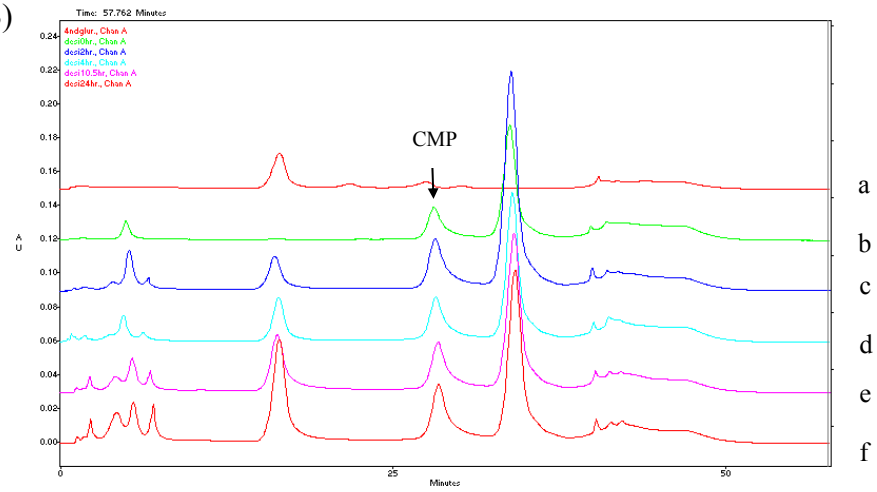

Figure 2-38. (A) The conversion of CDP-4-keto-6-deoxy-D-glucose (**2-21**) to CDP-4-amino-4,6-dideoxy-D-glucose (**2-29**) catalyzed by DesI. (B) HPLC traces demonstrating DesI substrate specificity using CDP-4-keto-6-deoxy-D-glucose (**2-21**): (a) The chemically synthesized standard for CDP-4-amino-4,6-dideoxy-D-glucose (**2-29**), (b) reaction for 0 h, 0% conversion, (c) reaction for 2 h, 12% conversion, (d) reaction for 4 h, 18% conversion, (e) reaction for 10.5 h, 25% conversion, (f) reaction for 24 h, 42% conversion.

2.4 DISCUSSION

At the time when the function of DesII from *Streptomyces venezuelae* was first established in 2005 (*48*), DesII was the first radical SAM enzyme involved in secondary

metabolite biosynthesis to be characterized at the enzymatic level. DesII was identified as a member of radical SAM enzyme superfamily based on the sequence analysis in 2001 (*12*). At that time, this enzyme superfamily was composed of about 600 members, whereas it currently contains more than 2800 proteins and is growing fast (*49*). Enzymes within this superfamily catalyze diverse and unusual transformations as described in Chapter 1. Previous genetic studies suggested that DesI and DesII are involved in C-4 deoxygenation, a key step in desosamine biosynthesis (*5*). In order to test the proposed mechanism shown in Figure 2-3 (path B), the DesII protein was heterologously overexpressed in *E. coli* to near homogeneity. On the basis of the well established reconstitution procedures for other radical SAM enzymes, such as lysine 2,3-aminomutase (*15*), biotin synthase and lipoyl synthase (*50*), an anaerobic method was developed to reconstitute the [4Fe-4S] cluster *in vitro* from the aerobically purified DesII protein. The proposed substrate for DesI/DesII reaction, TDP-4-keto-6-dideoxy-D-glucose (**2-8**), was prepared by the procedure established by Dr. Lishan Zhao of this laboratory (*5*). The conversion of TDP-4-keto-4,6-dideoxy-D-glucose (**2-8**) to TDP-3-keto-4,6-dideoxy-D-glucose (**2-10**) in the presence of DesI, DesII, and required cofactors was observed by HPLC. The expected turnover product **2-10** was characterized by high resolution mass spectrometry. Interestingly, the consumption of TDP-4-amino-4,6-dideoxy-D-glucose (**2-9**) and the formation of TDP-3-keto-4,6-dideoxy-D-glucose (**2-10**) was also observed in the presence of DesII alone. This result suggests that DesII can recognize TDP-4-amino-4,6-dideoxy-D-glucose (DesI product, **2-9**) as a substrate and function independently in the absence of DesI. In this scenario, DesI functions solely as a C4-aminotransferase to generate TDP-4-amino-4,6-dideoxy-D-glucose (**2-9**) and DesII

carries out the C-4 deamination to yield TDP-3-keto-4,6-dideoxy-D-glucose (**2-10**). Additionally, the lack of evidence for a DesI-DesII interaction from previously performed yeast two-hybrid assay results (carried out by Dr. Xuemei He of this labrotory) also supports this observation. The new biochemical characterization of DesII prompted a revision of the proposed mechanism for C-4 deoxygenation involved in desosamine biosynthesis. To account for these results, two possible mechanisms for the DesII-catalyzed reaction can be envisioned. As depicted in Figure 2-39, generation of the 5′-deoxyadenosyl radical (**2-19**) is expected to be the first part of the reaction facilitated by the reduced $[4Fe\text{-}4S]^{+}$ center as found in other radical SAM dependent enzymes (*15*, *49*).

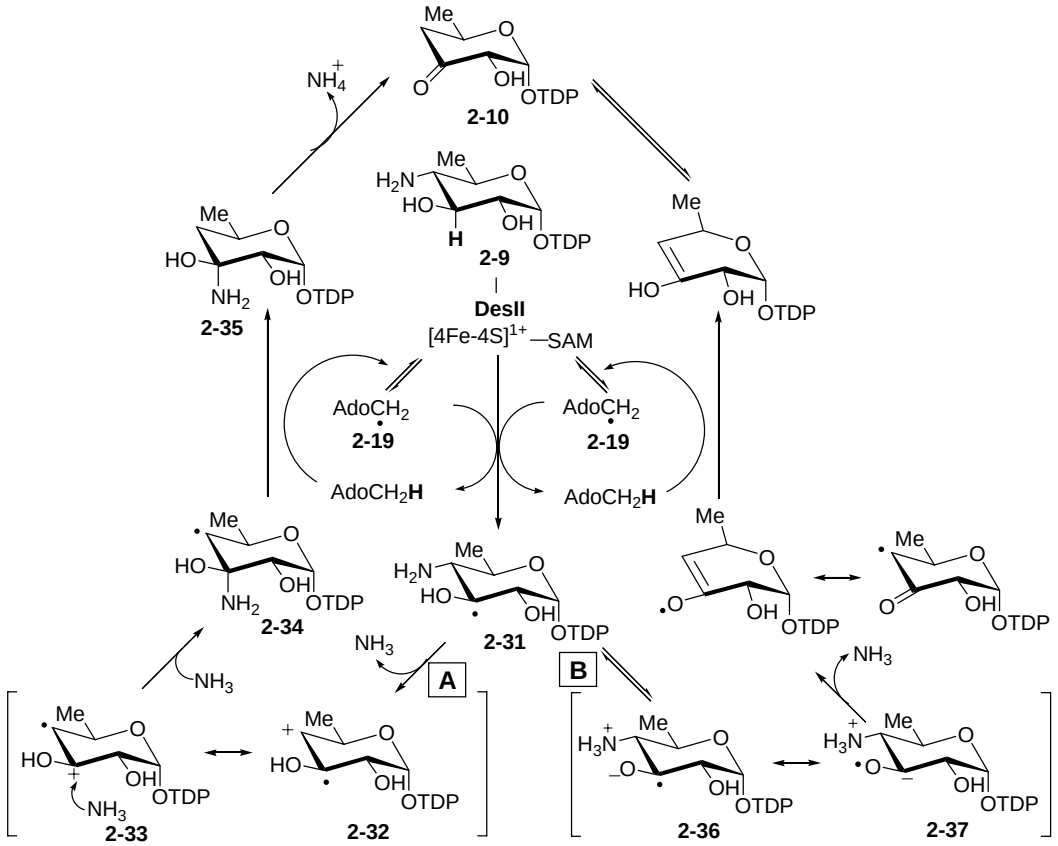

Figure 2-39. The revised mechanisms of C4 deoxygenation catalyzed by DesI and DesII.

The actual chemical conversion may be triggered by abstraction of a hydrogen atom at C3 of **2-9** by **2-19** to give **2-31**. The mechanism for the subsequent transformation is less obvious, but may parallel the reaction catalyzed by the coenzyme B_{12} dependent ethanolamine ammonia-lyase, which converts ethanolamine into ammonia and acetaldehyde (*51-53*). The proposed mechanism for the reaction catalyzed by ethanolamine ammonia-lyase will be reviewed in chapter 3. As shown in Figure 2-39 (path A), the key step may be a radical-induced deamination followed by the readdition of ammonia to the resulting cation radical intermediate (**2-32**/**2-33**), which is effectively a 1,2-amino shift (**2-31**→**2-32**/**2-33**→**2-34**), to form an aminol radical **2-34**. Reclaiming a hydrogen atom from 5′-deoxyadenosine results in the formation of **2-35** and the regeneration of **2-19**, or more likely the reduced $[4Fe\text{-}4S]^{+}$-SAM complex. Elimination of an ammonium ion from **2-35** would afford the desired product **2-10**. The reaction may also involve deprotonation of the 3-hydroxy group of **2-31** to yield a ketyl radical anion **2-36**, whose resonance form **2-37** facilitates the β-elimination of the 4-amino group (Figure 2-29, path B). The reaction catalyzed by (*R*)-2-hydroxyacyl-CoA dehydratase (*54-57*) in the fermentation of α-amino acids by anaerobic bacteria provides a precedent. The key step of the latter reaction involves ketyl radical anion induced carbon-oxygen bond cleavage to expel a hydroxy group. Representative enzymatic mechanisms involving ketyl radical anions will be reviewed in Chapter 3. Experiments to study and potentially distinguish these mechanistic proposals are also presented in Chapter 3.

After the establishment of DesII's catalytic function *in vitro*, the reaction sequence of desosamine biosynthesis has now been completely determined. TDP-D-

desosamine is biosynthesized from glucose-1-phosphate (**2-6**) by a series of enzymes participating in the following sequence: DesIII, α-D-glucose-1-phosphate thymidylytransferase, DesIV, NAD^+-dependent nucleotidyldiphosphohexose 4,6-dehydratase, DesI, a PLP-dependent C-4 aminotranferase (*5*), DesII, a radical SAM-dependent C-4 deaminase (*48*), DesV, a PLP-dependent C-3 aminotransferase (*18*), and DesVI, a SAM-dependent *N*,*N*-dimethylase (*23, 58*). Desosamine is a trideoxy sugar with deoxygenation occurring sequentially; at C-6, C-4, and finally C-3. These three deoxygenation events were performed by DesIII, catalyzing C-6 deoxygenation, DesII, catalyzing C-4 deamination, followed by DesV, catalyzing C-3 aminotransfer.

The UV-vis spectrum of the reconstituted DesII exhibits a broad absorption band at 420 nm, which is a characteristic feature of the $[4Fe\text{-}4S]^{2+}$ cluster. The iron and sulfur content determination showed that DesII contains approximately four iron and four sulfur molecules per monomer. The EPR spectrum of as-purified DesII demonstrated that it contains a $[3Fe\text{-}4S]^{1+}$ cluster, which is an oxidation product of $[4Fe\text{-}4S]^{3+}$ cluster upon exposure to air. The initial EPR studies of the reconstituted DesII showed that it contains a $[4Fe\text{-}4S]^{3+}$ cluster, whereas the $[4Fe\text{-}4S]^{3+}$ cluster is not a catalytic form (*15*). Significant efforts were devoted to obtain the EPR spectrum of the catalytically active $[4Fe\text{-}4S]^{1+}$ cluster. This task was eventually accomplished by preparing freshly reconstituted DesII for EPR studies. The EPR spectrum of the reconstituted DesII exhibits a nealy rhombic signal with g values at 2.01, 1.95, and 1.86 (g_{av} = 1.94). The EPR spectrum is similar to that for a $[4Fe\text{-}4S]^{1+}$ cluster observed in anaerobic ribonucleotide reductase-activase (ARR-activase) reduced by dithionite in the presence of SAM (*46*). EPR studies of ARR-activase demonstrated that the addition of SAM alters

the axial EPR signal to the rhombic signal. Additionally, the presence of different reducing agents (i.e., 5′-deazaflavin or dithionite) also alters the EPR signals (*46*). However, the EPR spectrum of DesII in the absence of SAM could be obtained. One possible reason is that the $[4Fe\text{-}4S]^{2+/1+}$ cluster in DesII is unstable in the absence of SAM binding to one of its open iron sites. The $[4Fe\text{-}4S]^{2+/1+}$ cluster is likely to lose one iron and then degrades to the $[3Fe\text{-}4S]^{1+}$ cluster. Subsequently, the $[3Fe\text{-}4S]^{1+}$ cluster is reduced to the EPR-silent $[3Fe\text{-}4S]^{0+}$ cluster in the presence of reducing agent dithionite. Second, the $[4Fe\text{-}4S]^{2+}$ cluster in DesII may be difficult to reduce to the $[4Fe\text{-}4S]^{1+}$ cluster in the absence of SAM. The second possibility has been demonstrated in lysine 2,3-aminomutase, where SAM binding elevates the reduction potential of the $[4Fe\text{-}4S]^{2+/1+}$ cluster by 86 mV (*59*). Thus, a similar comparison between EPR spectra of DesII in the presense and absence of SAM cannot be made. When the goal to obtain the EPR spectrum of the catalytically active $[4Fe\text{-}4S]^{1+}$ cluster was accomplished, the preparation of the Mössbauer samples launched. Mössbauer spectroscopic studies will provide more insights into the composition of the iron-sulfur clusters in DesII. The preliminary results showed that DesII can be expressed in iron-depleted media and the yield can be increased by adding $Fe(NH_4)_2(SO_4)_2$, which can be replaced by $^{57}Fe(NH_4)_2(SO_4)_2$ for the preparation of Mössbauer samples. The samples for those spectroscopic studies (i.e., EPR, Mössbauer, and ENDOR spectrocopies) usually require significant amounts of protein. For example, one EPR sample usually requires 5 mg of DesII protein but a 6-liter culture produces approximately 15 mg nearly homogeneous DesII. The low yield and solubility are common problems for actinomycetes enzymes when being overexpressed heterologously in *E. coli*. Previous studies of other radical SAM enzymes, such as lipoyl

synthase, revealed that the co-expression of radical SAM enzymes and pDB1282, which encodes the gene cluster required for the iron-sulfur cluster biosynthesis (Figure 2-6), increased the yield and solubility of purified enzymes (*60*). The proteins encoded in pDB1282 include IscS, a pyridoxal 5'-phosphate-dependent cysteine desulfurase, IscU and IscA, the assembly scaffords, HscA, a molecular chaperone, HscB, a co-chaperone, and Fdx, a [2Fe-2S]-type ferredoxin (*27*). With the hope that the yield of purified DesII could be improved by a similar approach, coexpression of *desII*/pET24b(+) and pDB1282 in *E. coli* BL21 Star (DE3) was carried out. Unfortunately, DesII was found to express poorly in the presence of pDB1282 either at 37 °C or 18 °C.

The kinetic parameters for the DesII-catalyzed reaction were determined by a discontinuous HPLC assay. The results show a k_{cat} of 1.0 ± 0.1 min^{-1} and a K_m of 49.5 ± 1.7 μM with respect to the sugar substrate, **2-9**. The literature reported kinetic parameters for other radical SAM enzymes are summarized in Table 2-4. Among these six examples, the k_{cat} ranges from 33.5 min^{-1} (lysine 2,3-aminomutase) to 0.175 min^{-1} (lipoyl synthase). Additionally, the K_m ranges from 1.4 μM (pyruvate formate lyase-activase) to 8.0 mM (lysine 2,3-aminomutase). In biotin synthase, lipoyl synthase, and BtrN, SAM serves as a co-substrate but not a cofactor. Accordingly, the kinetic parameters for these three enzymes were also determined with respect to the co-substrate, SAM (not shown in Table 2-4).

Enzymes	K_m	k_{cat}	References
Lysine 2,3-aminomutase	8.0 mM	Specific Activity = 620 m-units•mg^{-1} (= 33.5 min^{-1})	Wu, W. *et al. (61)*
Pyruvate formate lyase-activase	1.4μM	1 min^{-1}	Wagner, A. F. *et al.* (*62*)
Anaerobic ribonucleotide reductase-activase	ND	ND	
Biotin Synthase	30 μM	ND	Picciocchi, A. *et al*. (*63*)
Lipoyl Synthase	37 μM	0.175 min^{-1}	Cicchillo, R. M. *et al*. (*60*)
BtrN	22 μM	2.2 ± 0.22 min^{-1}	Yokoyama, K. *et al*. (*64*)

Table 2-4. The kinetic parameters reported in the literature for the reactions catalyzed by radical SAM enzymes under the assay conditions with saturating SAM.

Although chemical reductants such as dithionite or 5′-deazaflavin are commonly applied to reduce the $[4Fe\text{-}4S]^{2+}$ cluster in radical SAM enzymes, flavodoxin, flavodoxin reductase, and NADPH are a more likely reducing system under physiological conditions. In fact, flavodoxin, flavodoxin reductase, and NADPH have been identified as the reducing system in a few radical SAM enzymes including pyruvate formate lyase-activase, anaerobic ribonucleotide reductase-activase, and biotin synthase (*15*). NADPH serves as an electron donor and the electron transfers to the $[4Fe\text{-}4S]^{2+}$ cluster by relaying through flavodoxin and flavodoxin reductase (Figure 2-40). The $[4Fe\text{-}4S]^{2+}$ cluster is reduced to the $[4Fe\text{-}4S]^{1+}$ state after accepting an electron from the reduced form of flavodoxin. The DesII activity in the presence of flavodoxin, flavodoxin reductase plus NADPH demonstrated that DesII could also employ such a biological reducing system similar to other radical SAM enzymes. Additionally, *in vivo* studies of TDP-D-desosamine biosynthesis in erythromycin demonstrated that coexpression of flavodoxin

and flavodoxin reductatse from *E. coli* as an additional electron carrier increased DesI/DesII activity *in vivo (65)*. This result reinforces that the *in vivo* reducing system for DesII is flavodoxin, flavodoxin reducatse, and NADPH.

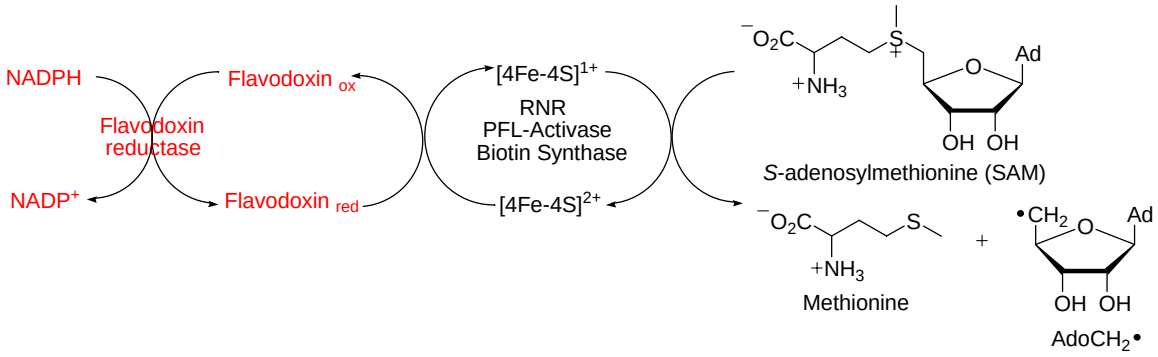

Figure 2-40. Reductive cleavage of SAM by the reduced $[4Fe\text{-}4S]^{1+}$ cluster, which is reduced by the reducing system, flavodoxin, flavodoxin reductase, and NADPH.

TDP-D-quinovose (**2-22**) contains a C-4 hydroxyl group, whereas the DesII natural substrate, TDP-4-amino-4,6-dideoxy-D-glucose (**2-9**, Figure 2-1), contains a C-4 amino group. Interestingly, DesII can turn over TDP-D-quinovose (**2-22**) at a similar rate as compared to the natural substrate. Both proposed mechanisms for DesII shown in Figure 2-39 can be applied to explain the conversion of TDP-D-quinovose (**2-22**) to TDP-3-keto-4,6-D-dideoxy glucose (**2-10**, Figure 2-1). If the reaction mechanism proceeds through route A, the migration of the hydroxyl group is similar to the proposed mechanisms for the long-known coenzyme B_{12}-dependent enzyme glycerol dehydratase and diol dehydratase, which catalyzes the conversion of glycerol to 3-hydroxypropanal and 1,2-ethanediol to acetaldehyde, respectively (*66*) (Figure 2-41).

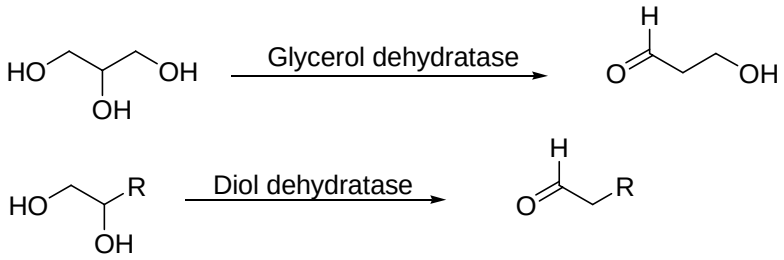

Figure 2-41. The reactions catalyzed by the coenzyme B_{12}-dependent glycerol dehydratase and diol dehydratase.

However, an alternative pathway for glycerol dehydratase to generate the 5′-deoxyadenosyl radical was recently found in the anaerobic bacterium *Clostridium butyricum* (*67*). This dehydratase contains a glycyl radical at the active site, which is formed by the action of the 5′-deoxyadenosyl radical on a specific glycine residue of the protein. The 5′-deoxyadenosyl radical is generated not from coenzyme B_{12}, but by a one-electron reduction of the much simpler molecule *S*-adenosylmethionine (SAM). If the reaction mechanism for DesII proceeds through route B, the key step is still the deprotonation of the 3-hydroxyl group to yield a ketyl radical anion, whose resonance form facilitates the β-elimination of the 4-hydroxyl group instead of the 4-amino group to afford an enol radical. Interestingly, TDP-D-fucose, which contains a C-4 hydroxyl group in the axial position on the hexose ring, is not an alternate substrate for DesII. This result indicates that the stereochemistry of the C-4 hydroxyl group plays a role in DesII catalysis. The turnover of TDP-D-quinovose (**2-22**) by DesII opened the possibility to synthesize mechanistic probes with a C-4 hydroxyl substitute. As such, the synthetic strategy can be simplified without the need to incorporate an amino functional group at the C-4 position. For example, substrate analogs with different functional groups at the

C-3 position could act as mechanism probes to potentially distinguish between these two proposed mechasims. A detailed discussion including the synthesis of potential substrate analogues and their respective mechanistic studies will be presented in Chapter 3.

TylB product (**2-24**) carries a C-3 amino group and a C-4 hydroxyl group, in contrast to the natural substrate, which contains a C-3 hydroxyl group and a C-4 amino group. The turnover of TylB product (**2-24**) can likely proceed through either route A or B as proposed in Figure 2-42. If the reaction proceeds through route A, the migration of C-4 hydroxyl group in **2-38** with concomitant radical rearrangement generates the aminol radical intermediate **2-41** (i.e., **2-38**→**2-39**/**2-40**→**2-41**). The aminol radical intermediate **2-41** reabstracts a hydrogen atom from the 5′-deoxyadenosine, generating **2-42** and regenerating the 5′-deoxyadenosyl radical **2-19**. Elimination of ammonia in **2-42** leads to the formation TDP-3-keto-4,6-dideoxy-D-glucose **2-10**. Alternatively, the reaction proceeding through route B involves the key step, the deprotonation of the 3-amino group of **2-38**, to yield a radical anion **2-43**. The resonance form of the radical anion **2-43** facilitates the β-elimination of the 4-hydroxyl group instead of the 4-amino group in the natural substrate (**2-9**), affording **2-45**. Tautomerization of **2-45** leads to an imine radical intermediate **2-46**. The imine radical intermediate **2-46** reabstracts a hydrogen atom from the 5′-deoxyadenosine, generating the imime intermediate **2-47** and regenerating the 5′-deoxyadenosyl radical **2-19**. Hydrolysis of the labile imine intermediate **2-47** affords the final product, **2-10**.

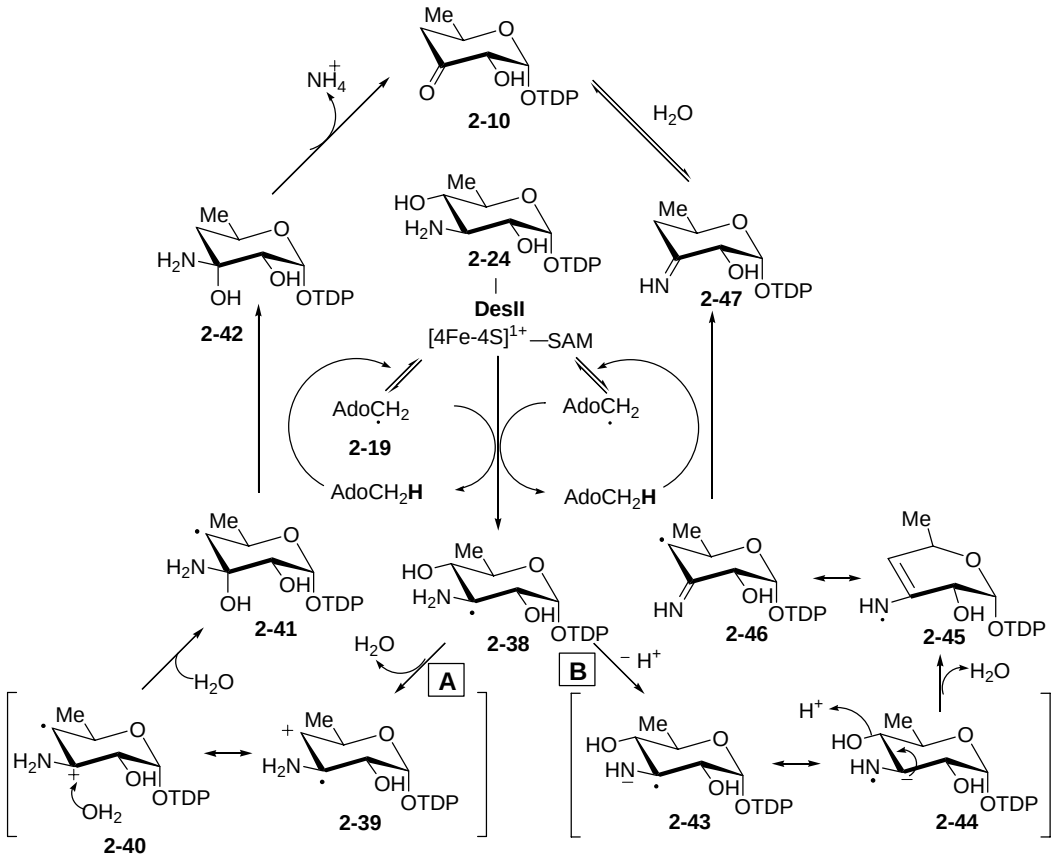

Figure 2-42. Proposed mechanisms for conversion of TylB product (**2-24**) to DesII product (**2-10**).

The conclusion drawn from the substrate specificity studies is twofold. First, DesII can tolerate alternate substitutes at the C-4 position with correct stereochemistry (i.e., TDP-D-quinovose (**2-22**) v.s. TDP-D-fucose (**2-23**)). Second, DesII also can accept alternate substrates with moieties exchanged at the C-3 and C-4 positions of the hexose ring (i.e., TylB product (**2-23**)). These results suggest that DesII is able to eliminate different substitutes at the C-4 position after the formation of the C3-centered radical intermediate (**2-31** in Figure 2-39 or **2-38** in Figure 2-42), although whether route A or B

is involved in the real mechanism remain elusive.

While most deoxy sugar intermediates involved in the secondary metabolite biosynthesis are TDP-hexoses, deoxy sugars activated by CDP, GDP, and UDP groups are not uncommon. Although previous studies have demonstrated that the sugar thymidylyltransferase RmlA (E_p) from *Sa. enterica* can take UTP as an alternate substrate (*68*), not much is known about the ability of other deoxy sugar biosynthetic enzymes to use substrates with alternate nucleotides. Identification of deoxy sugar biosynthetic enzymes that have flexible specificity with respect to the nucleoside portion of their NDP-sugar substrates would be useful for preparing NDP-activated sugars.

In this chapter, it was demonstrated that DesI is capable of turnover of CDP-4-keto-6-deoxy-D-glucose (**2-21**, Figure 2-38), the CDP version of its natural substrate, but at a reduced percent conversion. It was approximately 2-fold lower than that of the natural substrate, TDP-4-keto-6-deoxy-D-glucose (**2-8**). However, large quantities of DesI can be readily purified so that *in vitro* synthesis of CDP-sugars involving C-4 aminotransfer reaction in their biosynthesis may be feasible using DesI. In addition, as more X-ray crystal structures of deoxysugar biosynthetic enzymes have been determined, a structure-based rational design may be used to engineer NDP-promiscuous enzymes for the combinatorial biosynthesis of a variety of NDP-activated deoxysugars.

In conclusion, based on the biochemical characterization of DesII presented here, DesII was clearly established to be a radical SAM-dependent C-4 deaminase involved in C-4 deoxygenation, a key step in TDP-D-desosamine (**2-12**, Figure 2-1) biosynthesis. After the function of DesII established, the key reaction sequence involved in TDP-D-desosamine biosynthesis from *Streptomyces venezuelae* was confirmed. DesI functions as

a C-4 aminotransferase and DesII is directly responsible for the production of the key intermediate **2-10** (Figure 2-1) in the biosynthesis of TDP-D-desosamine. DesII requires a $[4Fe\text{-}4S]^{1+}$ center and *S*-adenosylmethionine (SAM) for activity. It catalyzes the oxidative deamination of a C-4 amino sugar (**2-9**) to generate a C-3 ketosugar **2-10** (Figure 2-1). A possible biological reducing system, flavodoxin, flavodoxin reductase, and NADPH, for the reduction of $[4Fe\text{-}4S]^{2+}$ cluster, was identified. Additionally, DesII is flexible towards TDP-D-quinovose (**2-22**) and TDP-3-amino-4,6-dideoxy-D-glucose (TylB product, **2-24**). DesII's ability to tolerate alternate substrates has allowed the design of strategies to prepare potential substrate analogues, which are presented in Chapter 3.

2.5 REFERENCE

1. Thorson, J. S., Hosted, T. J., Jr., Jiang, J., Biggins, J. B., and Ahlert, J. (2001) Nature's carbohydrate chemists: the enzymatic glycosylation of bioactive bacterial metabolites, *Curr. Org. Chem. 5*, 139-167.

2. Kren, V., and Martinkova, L. (2001) Glycosides in medicine: "the role of glycosidic residue in biological activity", *Curr. Med. Chem. 8*, 1303-1328.

3. Zhao, L., Sherman, D. H., and Liu, H.-w. (1998) Biosynthesis of desosamine: Molecular evidence suggesting b-glucosylation as a self-resistance mechanism in methymycin/neomethymycin producing strain, *Streptomyces venezuelae*, *J. Am. Chem. Soc. 120*, 9374-9374.

4. Xue, Y., Zhao, L., Liu, H.-w., and Sherman, D. H. (1998) A gene cluster for macrolide antibiotic biosynthesis in *Streptomyces venezuelae*: architecture of metabolic diversity, *Proc. Natl. Acad. Sci. USA. 95*, 12111-12116.

5. Zhao, L., Borisova, S., Yeung, S.-M., and Liu, H.-w. (2001) Study of C-4 deoxygenation in the biosynthesis of desosamine: evidence implicating a novel mechanism, *J. Am. Chem. Soc. 123*, 7909-7910.

6. He, X., H.-w. (2002) Formation of unusual sugars: mechanistic studies and biosynthetic applications, *Annu. Rev. Biochem. 71*, 701-754.

7. Lei, Y., Ploux, O., and Liu, H.-w. (1995) Mechanistic studies of CDP-6-deoxy-D-*glycero*-L-*threo*-4-hexulose-3-dehydrase: identification of His220 as the active-site base by chemical modification and site-directed mutagenesis, *Biochemistry 34*, 4643-4654.

8. Thorson, J. S., and Liu, H.-w. (1993) Characterization of the first PMP dependent iron-sulfur containing enzyme which is essential for the biosynthesis of 3,6-dideoxyhexoses, *J. Am. Chem. Soc. 115*, 7539-7540.

9. Miller, V. P., Thorson, J. S., Ploux, O., Lo, S. F., and Liu, H.-w. (1993) Cofactor characterization and mechanistic studies of CDP-6-deoxy-$\Delta^{3,4}$-glucoseen reductase: Exploration into a novel enzymic carbon-oxygen bond cleavage event, *Biochemistry 32*, 11934-11942.

10. Chang, C.-W. T., Johnson, D. A., Bandarian, V., Zhou, H., LoBrutto, R., Reed, G. H., and Liu, H.-w. (2000) Characterization of a unique coenzyme B_6 radical in the ascarylose biosynthetic pathway, *J. Am. Chem. Soc. 122*, 4239-4240.

11. Johnson, D. A., Gassner, G. T., Bandarian, V., Ruzicka, F. J., Ballou, D. P., Reed, G. H., and Liu, H.-w. (1996) Kinetic characterization of an organic radical in the ascarylose biosynthetic pathway, *Biochemistry 35*, 15846-15856.

12. Sofia, H. J., Chen, G., Hetzler, B. G., Reyes-Spindola, J. F., and Miller, N. E. (2001) Radical SAM, a novel protein superfamily linking unresolved steps in familiar biosynthetic pathways with radical mechanisms: functional characterization using new analysis and information visualization methods, *Nucleic Acids Research 29*, 1097-1106.

13. Borisova, S. A., Zhang, C., Takahashi, H., Zhang, H., Wong, A. W., Thorson, J. S., and Liu, H.-w. (2005) Substrate specificity of the macrolide-glycosylating enzyme pair DesVII/DesVIII: opportunities, limitations, and mechanistic hypotheses, *Angew. Chem. Int. Ed. 45*, 2748-2753.

14. Borisova, S. A., Zhao, L., Melancon, C. E., III , Kao, C.-L., and Liu, H.-w. (2004) Characterization of the glycosyltransferase activity of DesVII: analysis of and implications for the biosynthesis of macrolide antibiotics, *J. Am. Chem. Soc. 126*, 6534-6535.

15. Frey, P. A., and Magnusson, O. T. (2003) *S*-adenosylmethionine: A wolf in sheep's clothing, or a rich man's adenosylcobalamin?, *Chem. Rev. 103*, 2129-2148.

16. Toraya, T. (2003) Radical catalysis in coenzyme B_{12}-dependent isomerization (eliminating) reactions, *Chem. Rev. 103*, 2095-2128.

17. Chen, D., Walsby, C., Hoffman, B. M., and Frey, P. A. (2003) Coordination and mechanism of reversible cleavage of *S*-adenosylmethionine by the [4Fe-4S] center in lysine 2,3-aminomutase, *J. Am. Chem. Soc. 125*, 11788-11789.

18. Zhao, L. (2000) Biosynthetic Studies of D-desosamine and Engineered Biosynthesis of Methmycin/Pikromycin Analogs Carrying Modified Deoxysugars, in *Department of Chemistry*, p 238, University of Minnesota, Twin Cities.

19. Bradford, M. M. (1976) A rapid and sensitive method for the quantitation of microgram quantities of protein utilizing the principle of protein-dye binding, *Anal. Biochem. 72*, 248-254.

20. Laemmli, U. K. (1970) Cleavage of structural proteins during the assembly of the head of bacteriophage T4, *Nature 227*, 680-685.

21. Andrews, P. (1964) Estimation of the molecular weights of proteins by Sephadex gel-filtration, *Biochem. J. 91*, 222-233.

22. Sambrook, J., and Russell, D. W. (2001) *Molecular cloning: A laboratory manual*, 3rd ed., Cold Spring Harbor Laboratory Press, Plainview, NY.

23. Chang, C.-w., Zhao, L., Yamase, H., and Liu, H.-w. (2000) DesVI: a new member of the sugar *N*,*N*-dimethyltransferase family involved in the biosynthesis of desosamine, *Angew. Chem. In. Ed. 39*, 2160-2163.

24. Fish, W. W. (1988) Rapid colorimetric micromethod for the quantitation of complexed iron in biological samples, *Methods Enzymol. 158*, 357-364.

25. Beinert, H. (1983) Semi-micro methods for analysis of labile sulfide and of labile sulfide plus sulfane sulfur in unusually stable iron-sulfur proteins, *Anal. Biochem. 131*, 373-378.

26. Carter, R. A., Ericsson, S. A., Corn, C. D., Weyerts, P. R., Dart, M. G., Escue, S. G., and Mesta, J. (1998) Assessing the fertility potential of equine semen samples using the reducible dyes methylene green and resazurin, *Arch. Androl. 40*, 59-66.

27. Johnson, D. C., Dean, D. R., Smith, A. D., and Johnson, M. K. (2005) Structure, function, and formation of biological iron-sulfur clusters, *Annu. Rev. Biochem. 74*, 247-281.

28. QIAGEN (2003) *The QIAexpressionist: A handbook for high-level expression and purification of 6xHis-tagged proteins*, 5th ed., QIAGEN GmbH, Germany.

29. Aberg, A., Ormo, M., Nordlund, P., and Sjöberg, B. M. (1993) Autocatalytic generation of dopa in the engineered protein R2 F208Y from *Escherichia coli* ribonucleotide reductase and crystal structure of the dopa-208 protein, *Biochemistry 32*, 9845-9850.

30. Takahashi, H., Liu, Y.-n., and Liu, H.-w. (2006) A two-stage one-pot enzymatic synthesis of TDP-L-mycarose from thymidine and glucose-1-phosphate, *J. Am. Chem. Soc. 128*, 1432-1433.

31. Agnihotri, G., Liu, Y.-n., Paschal, B. M., and Liu, H.-w. (2004) Identification of an unusual [2Fe-2S]-binding motif in the CDP-6-deoxy-D-*glycero*-L-*threo*-4-hexulose-3-dehydrase from *Yersinia pseudotuberculosis*: implication for C-3 deoxygenation in the biosynthesis of 3,6-dideoxyhexoses, *Biochemistry 43*, 14265-14274.

32. Thorson, J. S., Lo, S. F., Ploux, O., He, X., and Liu, H.-w. (1994) Studies of the biosynthesis of 3,6-dideoxyhexoses: molecular cloning and characterization of the *asc* (ascarylose) region from *Yersinia pseudotuberculosis* serogroup VA, *J Bacteriol. 176*, 5463-5493.

33. Yu, Y., Russell, R. N., Thorson, J. S., Liu, L.-D., and Liu, H.-w. (1992) Mechanistic studies of the biosynthesis of 3,6-dideoxyhexoses in *Yersinia pseudotuberculosis*. Purification and stereochemical analysis of CDP-D-glucose oxidoreductase, *J. Biol. Chem. 267*, 5868-5875.

34. Thorson, J. S., Kelly, T. M., and Liu, H.-w. (1994) Cloning, sequencing, and overexpression in *Escherichia coli* of the α-D-glucose-1-phosphate cytidylyltransferase gene isolated from *Yersinia pseudotuberculosis*, *J Bacteriol. 176*, 1840-1849.

35. Elling, L., Rupprath, C., Guenther, N., Roemer, U., Verseck, S., Weingarten, P., Draeger, G., Kirschning, A., and Piepersberg, W. (2005) An enzyme module system for the synthesis of dTDP-activated deoxysugars from dTMP and sucrose, *ChemBioChem 6*, 1423-1430.

36. Melancon, C. E., III, Hong, L., White, J. A., Liu, Y.-n., and Liu, H.-w. (2007) Characterization of TDP-4-keto-6-deoxy-D-glucose-3,4-ketoisomerase from the D-mycaminose biosynthetic pathway of *Streptomyces fradiae*: *in vitro* activity and substrate specificity studies, *Biochemistry 46*.

37. Davis, D. J., and Pietro, A. S. (1977) Evidence for the role of sulfhydryl groups in a pH-dependent transition of ferredoxin:NADP oxidoreductase, *Arch. Biochem. Biophys. 184*, 572-577.

38. Ollagnier, S., Mulliez, E., Gaillard, J., Eliasson, R., Fontecave, M., and Reichard, P. (1996) The anaerobic *Escherichia coli* ribonucleotide reductase. Subunit structure and iron sulfur center, *J. Biol. Chem. 271*, 9410-9416.

39. Ugulava, N. B., Gibney, B. R., and Jarrett, J. T. (2000) Iron-sulfur cluster interconversions in biotin synthase: dissociation and reassociation of iron during conversion of [2Fe-2S] to [4Fe-4S] clusters, *Biochemistry 39*, 5206-5214.

40. Ollagnier, S., Meier, C., Mulliez, E., Gaillard, J., Schuenemann, V., Trautwein, A., Mattioli, T., Lutz, M., and Fontecave, M. (1999) Assembly of 2Fe-2S and 4Fe-4S clusters in the anaerobic ribonucleotide reductase from *Escherichia coli*, *J. Am. Chem. Soc. 121*, 6344-6350.

41. Külzer, R., Pils, T., Kappl, R., Hüttermann, J., and Knappe, J. (1998) Reconstitution and characterization of the polynuclear iron-sulfur cluster in pyruvate formate-lyase-activating enzyme. Molecular properties of the holoenzyme form, *J. Biol. Chem. 273*, 4897-4903.

42. Duin, E. C., Lafferty, M. E., Crouse, B. R., Allen, R. M., Sanyal, I., Flint, D. H., and Johnson, M. K. (1997) [2Fe-2S] to [4Fe-4S] cluster conversion in *Escherichia coli* biotin synthase, *Biochemistry 36*, 11811-11820.

43. Buis, J. M., Cheek, J., Kalliri, E., and Broderick, J. B. (2006) Characterization of an active spore photoproduct lyase, a DNA repair enzyme in the radical *S*-adenosylmethionine superfamily, ***J. Biol. Chem. 281***, 25994-26003.

44. Torrents, E., Buist, G., Liu, A., Eliasson, R., Kok, J., Gibert, I., Graslund, A., and Reichard, P. (2000) The anaerobic (class III) ribonucleotide reductase from *Lactococcus lactis*. Catalytic properties and allosteric regulation of the pure enzyme system., ***J. Biol. Chem. 275***, 2463-2471.

45. Petrovich, R. M., Ruzicka, F. J., Reed, G. H., and Frey, P. A. (1992) Characterization of iron-sulfur clusters in lysine 2,3-aminomutase by electron paramagnetic resonance spectroscopy, ***Biochemistry 31***, 10774-10781.

46. Liu, A., and Graslund, A. (2000) Electron paramagnetic resonance evidence for a novel interconversion of $[3Fe\text{-}4S]^{+}$ and $[4Fe\text{-}4S]^{+}$ clusters with endogenous iron and sulfide in anaerobic ribonucleotide reductase activase ***in vitro***, ***J. Biol. Chem. 275***, 12367-12373.

47. Melancon, C. E., III, Hong, L., White, J. A., Liu, Y.-n., and Liu, H.-w. (2007) Characterization of TDP-4-Keto-6-deoxy-D-glucose-3,4-ketoisomerase from the D-Mycaminose Biosynthetic Pathway of Streptomyces fradiae: In Vitro Activity and Substrate Specificity Studies, ***Biochemistry 46***, 577-590.

48. Szu, P.-h., He, X., Zhao, L., and Liu, H.-w. (2005) Biosynthesis of TDP-D-desosamine: Identification of a strategy for C4 deoxygenation, ***Angew. Chem. Int. Ed. 44***, 6742-6746.

49. Frey, P. A., Hegeman, A. D., and Ruzicka, F. J. (2008) The radical SAM superfamily, ***Crit. Rev. Biochem. Mol. Biol. 43***, 63-88.

50. Ollagnier-de Choudens, S., Sanakis, Y., Hewitson, K. S., Roach, P., Baldwin, J. E., Munck, E., and Fontecave, M. (2000) Iron-sulfur center of biotin synthase and lipoate synthase, ***Biochemistry 39***, 4165-4173.

51. Bandarian, V., and Reed, G. H. (1999) ***Ethanolamine ammonia-lyase***.

52. LoBrutto, R., Bandarian, V., Magnusson, O. T., Chen, X., Schramm, V. L., and Reed, G. H. (2001) 5'-Deoxyadenosine contacts the substrate radical intermediate in the active site of ethanolamine ammonia-lyase: ^{2}H and ^{13}C electron nuclear double resonance studies, ***Biochemistry 40***, 9-14.

53. Sandala, G. M., Smith, D. M., and Radom, L. (2005) Divergent mechanisms of suicide inactivation for ethanolamine ammonia-lyase, ***J. Am. Chem. Soc. 127***, 8856-8864.

54. Buckel, W. (1996) Unusual dehydrations in anaerobic bacteria: considering ketyls (radical anions) as reactive intermediates in enzymic reactions, *FEBS Lett. 389*, 20-24.

55. Buckel, W. (2001) Unusual enzymes involved in five pathways of glutamate fermentation, *Appl. Microbiol. Biotechnol. 57*, 263-273.

56. Buckel, W., and Golding, B. T. (1998) Radical species in the catalytic pathways of enzymes from anaerobes, *FEMS Microbiol. Rev. 22*, 523-541.

57. Kim, J., Hetzel, M., Boiangiu, C. D., and Buckel, W. (2004) Dehydration of (*R*)-2-hydroxyacyl-CoA to enoyl-CoA in the fermentation of α-amino acids by anaerobic bacteria, *FEMS Microbiol. Rev. 28*, 455-468.

58. Chen, H., Yamase, H., Murakami, K., Chang, C.-w., Zhao, L., Zhao, Z., and Liu, H.-w. (2002) Expression, purification, and characterization of two *N*,*N*-dimethyltransferases, TylM1 and DesVI, involved in the biosynthesis of mycaminose and desosamine, *Biochemistry 41*, 9165-9183.

59. Hinckley, G. T., and Frey, P. A. (2006) Cofactor dependence of reduction potentials for $[4Fe\text{-}4S]^{2+/1+}$ in lysine 2,3-aminomutase, *Biochemistry 45*, 3219-3225.

60. Cicchillo, R. M., Iwig, D. F., Jones, A. D., Nesbitt, N. M., Baleanu-Gogonea, C., Souder, M. G., Tu, L., and Booker, S. J. (2004) Lipoyl synthase requires two equivalents of *S*-adenosyl-L-methionine to synthesize one equivalent of lipoic acid, *Biochemistry 43*, 6378-6386.

61. Wu, W., Lieder, K. W., Reed, G. H., and Frey, P. A. (1995) Observation of a second substrate radical intermediate in the reaction of lysine 2,3-aminomutase: A radical centered on the β-carbon of the alternative substrate, 4-thia-L-lysine, *Biochemistry 34*, 10532-10537.

62. Wagner, A. F., Demand, J., Schilling, G., Pils, T., and Knappe, J. (1999) A dehydroalanyl residue can capture the 5'-deoxyadenosyl radical generated from *S*-adenosylmethionine by pyruvate formate-lyase-activating enzyme, *Biochem. Biophys. Res. Commun. 254*, 306-310.

63. Picciocchi, A., Douce, R., and Alban, C. (2001) Biochemical characterization of the Arabidopsis biotin synthase reaction. The importance of mitochondria in biotin synthesis, *Plant Physiology 127*, 1224-1233.

64. Yokoyama, K., Numakura, M., Kudo, F., Ohmori, D., and Eguchi, T. (2007) Characterization and mechanistic study of a radical SAM dehydrogenase in the biosynthesis of butirosin, *J. Am. Chem. Soc. 129*, 15147-15155.

65. Lee, H. Y., and Khosla, C. (2007) Bioassay-guided evolution of glycosylated macrolide antibiotics in *Escherichia coli*, *PLoS Biology 5*, 243-250.

66. Buckel, W., Kratky, C., and Golding, B. T. (2006) Stabilisation of methylene radicals by cob(II)alamin in coenzyme B_{12} dependent mutases, *Chem. Eur. J. 12*, 352-262.

67. O'Brien, J. R., Raynaud, C., Croux, C., Girbal, L., Soucaille, P., and Lanzilotta, W. N. (2004) Insight into the mechanism of the B_{12}-independent glycerol dehydratase from *Clostridium butyricum*: Preliminary biochemical and structural characterization, *Biochemistry 43*, 4635-4645.

68. Jiang, J., Biggins, J. B., and Thorson, J. S. (2000) A general enzymatic method for the synthesis of natural and "unnatural" UDP- and TDP-nucleotide sugars, *J. Am. Chem. Soc. 122*, 6803-6804.

Chapter 3: Mechanistic Studies of DesII in the Biosynthesis of TDP-D-desosamine from *Streptomyces venezuelae*

3.1 INTRODUCTION

DesII has previously been identified as a member of the radical SAM enzyme superfamily based on sequence analysis (*1*). Biochemical characterization presented in Chapter 2 clearly establishes that DesII is a radical SAM-dependent deaminase, but not a deoxygenase as previously surmised (Figure 2-3, path A). Additionally, DesI and DesII function independently to carry out an overall C-4 deoxygenation reaction in desosamine biosynthesis. Revised mechanisms that support these results have been proposed (Figure 3-1). DesII contains the conserved sequence motif, CXXXCXXC, which coordinates three iron sites of the [4Fe-4S] cluster (*2*). The cofactor, SAM, is proposed to coordinate the unique iron site of the [4Fe-4S] cluster through the N/O chelate. The electron transfer from the reduced $[4Fe\text{-}4S]^{1+}$ cluster to the carbon-sulfur bond of SAM induces reductive cleavage to generate the 5′-deoxyadenosyl radical (**3-2**) and methionine with a concomitant oxidation of the $[4Fe\text{-}4S]^{1+}$ cluster to the $[4Fe\text{-}4S]^{2+}$ cluster. The chemical conversion may be triggered by abstraction of a hydrogen atom at C3 of **3-1** by **3-2** to give **3-3**. The mechanism for the subsequent transformation is less obvious, but may parallel the reaction catalyzed by the coenzyme B_{12} dependent ethanolamine ammonia-lyase, which converts ethanolamine (**3-13**) into ammonia and acetaldehyde (**3-17**, Figure 3-2) (*3, 4*).

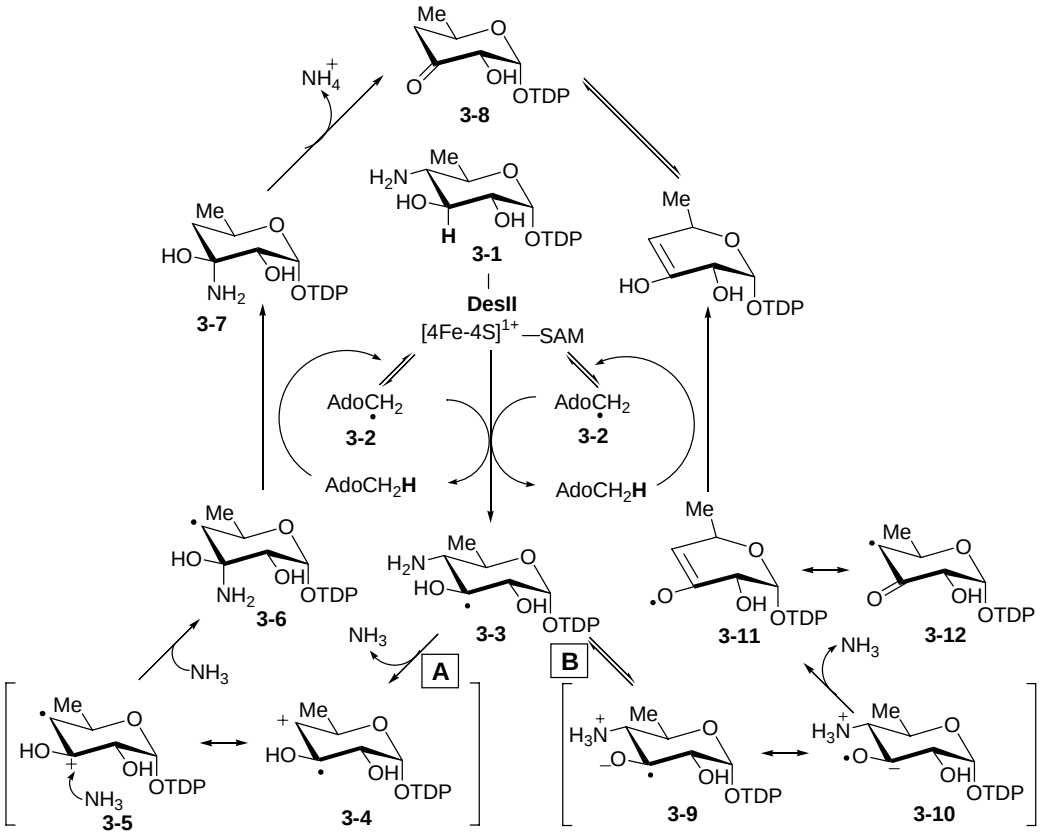

Figure 3-1. The proposed mechanisms of C-4 deamination catalyzed by radical SAM-dependent DesII.

The generally accepted mechanism proposed for the rearrangement catalyzed by ethanolamine ammonia-lyase involves five steps (*3, 4*) (Steps A-E, Figure 3-2). The first step (step A), initiated upon substrate binding, is the homolytic cleavage of the Co-C bond of adenosylcobalamin (AdoCbl, **3-18**), generating the cob(II)alamin and the 5′-deoxyadenosyl radical (**3-2**). In step B, the 5′-deoxyadenosyl radical (**3-2**) abstracts a hydrogen atom from the C1 of the substrate, ethanolamine (**3-13**) to form the the 5′-deoxyadenosine and substrate radical intermediate (**3-14**). The radical rearrangement, concomitant with 1,2-amino rearrangement affords the product radical **3-15** (step C). In

step D, the product radical **3-15** reabstracts a hydrogen atom from the 5′-deoxyadenosine to yield an aminol intermediate **3-16** and regenerate the 5′-deoxyadenosyl radical (**3-2**), which can subsequently recombine with cob(II)alamin to form adenosylcobalamin (AdoCbl, **3-18**). The final step (step E) involves the elimination of the ammonia, yielding the product, aldehyde **3-17**. The first possible mechanism for the DesII-catalyzed reaction has been proposed to be analogous to the reaction catalyzed by ethanolamine ammonia-lyase (Figure 3-1, path A). As shown in Figure 3-1 (path A), the key step may be a radical-induced deamination followed by the readdition of ammonia to the resulting cation radical intermediate (**3-5**), which is effectively a 1,2-amino shift (**3-3**→**3-4**/**3-5**→**3-6**), to form an aminol radical **3-6**. This 1,2-migration may be a stepwise transfer (**3-3**→**3-4**/**3-5**→**3-6**) or a direct transfer (**3-3**→**3-6**). Reclaiming a hydrogen atom from 5′-deoxyadenosine results in the formation of **3-7** and the regeneration of **3-2**, or more likely the reduced $[4Fe\text{-}4S]^{+}$-SAM complex. Reclaiming a hydrogen atom from $AdoCH_3$ by **3-6** (or **3-11**/**3-12** in path B) is energetically unfavorable, thus stabilization of the resulting 5′-deoxyadenosyl radical (**3-2**) by reforming the $[4Fe\text{-}4S]^{+}$-SAM complex may provide the driving force to complete the catalytic cycle. A similar argument which invokes reversible cleavage of SAM by the [4Fe-4S] center has been proposed for the lysine 2,3-aminomutase reaction (*2*). Elimination of an ammonium ion from **3-7** would afford the desired product **3-8**.

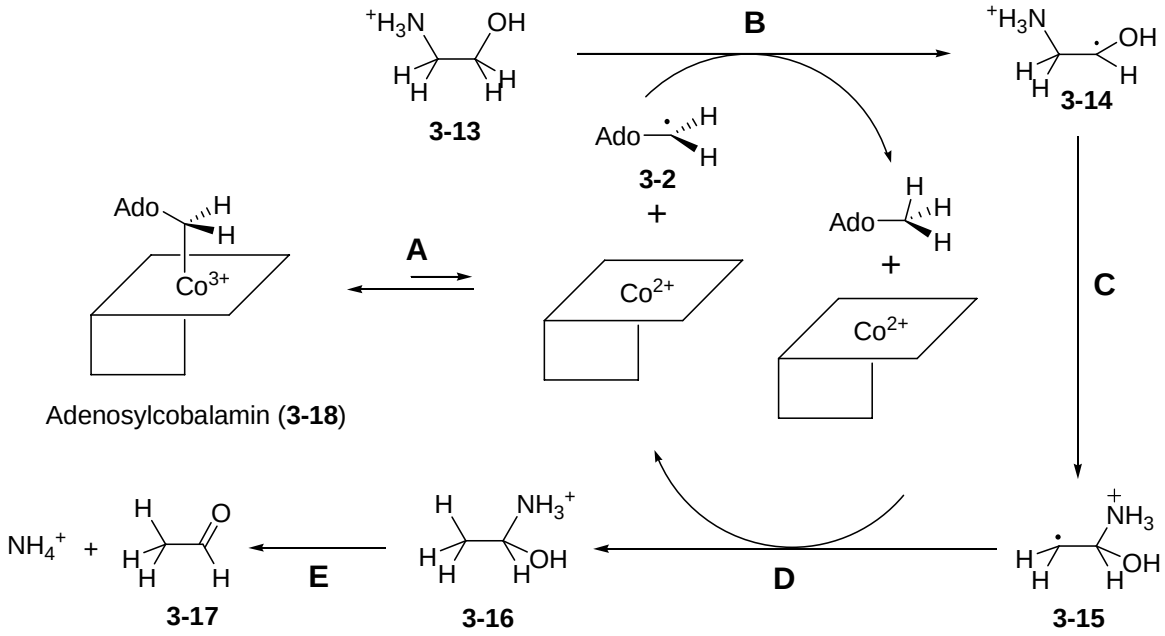

Figure 3-2. Generally accepted mechanism for the rearrangement catalyzed by ethanolamine ammonia-lyase (*3, 4*).

Alternatively, the reaction may involve deprotonation of the 3-hydroxy group of **3-3** to yield a ketyl radical anion **3-9**, whose resonance form **3-10** facilitates the β-elimination of the 4-amino group (Figure 3-1, path B). The pK_a value of the hydroxyl group in a ketyl radical (**3-3**) is lower by approximately five units than that of the corresponding alcohol (*5*). The reaction catalyzed by (*R*)-2-hydroxyacyl-CoA dehydratase (*6-10*) in the fermentation of α-amino acids by anaerobic bacteria provides a precedent. For example, (*R*)-2-hydroxy-4-methylpentanoyl-CoA dehydratase catalyzes the dehydration of (*R*)-2-hydroxy-4-methylpentanoyl-CoA (**3-19**) to 4-methylpent-2-enoyl-CoA (**3-23**) by *syn*-elinimation as shown in Figure 3-3a. In addition to the heterodimeric dehydratase, a homodimeric activator is also required for the overall

dehydration. Both dehydratase and activator are oxygen-sensitive. Activation proceeds through ATP-hydrolysis-driven electron transfer from the $[4Fe\text{-}4S]^{1+}$ cluster of the activator to the [Fe-S] cluster of the dehydratase. The dehydratase subsequently transfers electron to the substrate, (*R*)-2-hydroxy-4-methylpentanoyl-CoA (**3-19**), to generate the substrate ketyl radical anion **3-20**, which facilitates the elimination of the hydroxyl group to generate **3-21**. The β-hydrogen in the substrate **3-19** which is later eliminated as a proton is not activated (p$K \approx$ 40-50). The β-hydrogen in the resulting enoxyradical **3-21** is activated (p$K \approx$ 14) and the elimination of this β-hydrogen generates the product ketyl radical anion (**3-22**). One electron from the product ketyl radical anion (**3-22**) is transferred to the next incoming substrate (**3-19**) without further hydrolysis of ATP, affording the product, 4-methylpent-2-enoyl-CoA (**3-23**). This example clearly demonstrates that the formation of the ketyl radical anion induces a carbon-oxygen bond cleavage to expel a hydroxyl group. Very recently, a product-related ketyl radical (**3-22a** or **3-22b**) bound to the enzyme, which is kinetically competent, has been characterized by EPR spectroscopy using isotope-labelled (*R*)-2-hydroxy-4-methylpentanoyl-CoA (**3-19**) (*11*). Additionally, this study also demonstrates that (*R*)-2-hydroxy-4-methylpentanoyl-CoA dehydratase produces the stabilized pentadienoyl ketyl radical (**3-24**) from the substrate analogue, 2-hydroxypent-4-enoyl-CoA (Figure 3-3b). These EPR studies provide the spectroscopic evidence for the involvement of a ketyl radical anion intermediate in the reaction catalyzed by (*R*)-2-hydroxy-4-methylpentanoyl-CoA dehydratase.

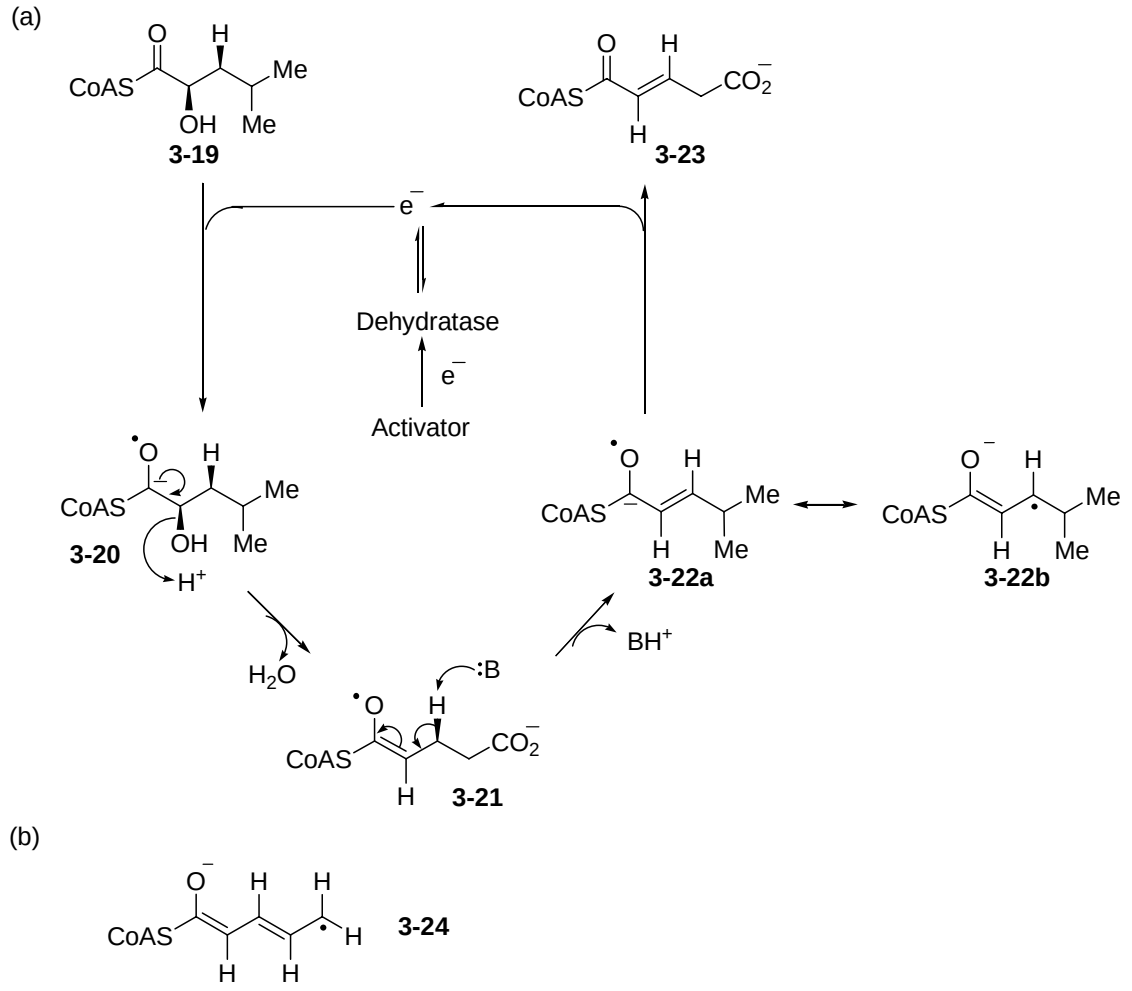

Figure 3-3. (a) The reaction catalyzed by (*R*)-2-hydroxy-4-methylpentanoyl-CoA dehydratase demonstrating the ketyl radical anion as a reactive intermediate (*11*). (b) The structure of 2-hydroxypent-4-enoyl-CoA ketyl radical.

Previously, deuterium incorporation generating monodeuterated 5′-deoxyadenosine was demonstrated for three radical SAM enzymes using deuterium-labeled substrates. These examples include biotin synthase (*12*), pyruvate formate lyase-activase (*13*), and lipoyl synthase (*14*). It should be noted that SAM serves as a cosubstrate rather than a cofactor in these three enzymes, where stoichiometric amounts

of SAM are consumed and corresponding amounts of 5′-deoxyadenosine are formed. Recently, mechanistic studies of BtrN form the butirosin biosynthetic pathway have shown that the BtrN reaction using deuterium-labeled substrate generated nondeuterated and dideuterated 5′-deoxyadenosine, which suggests that the hydrogen atom abstraction is reversible (*15*). This chapter describes the synthesis of TDP-[3-^{2}H]-4-amino-4,6-dideoxy-D-glucose (**3-25**, Figure 3-4) to study the first step, C-3 hydrogen atom abstraction by the 5'-deoxyadenosyl radical (**3-2**, Figure 3-4), in the proposed mechanism. The expectation is that the C3-deuterium of the substrate **3-25** will be transferred to SAM after the DesII enzyme turns over **3-25**, as depicted in Figure 3-4. Accordingly, this chapter also describes the assays carried out to characterize the deuterium incorporation into SAM by mass spectrometry.

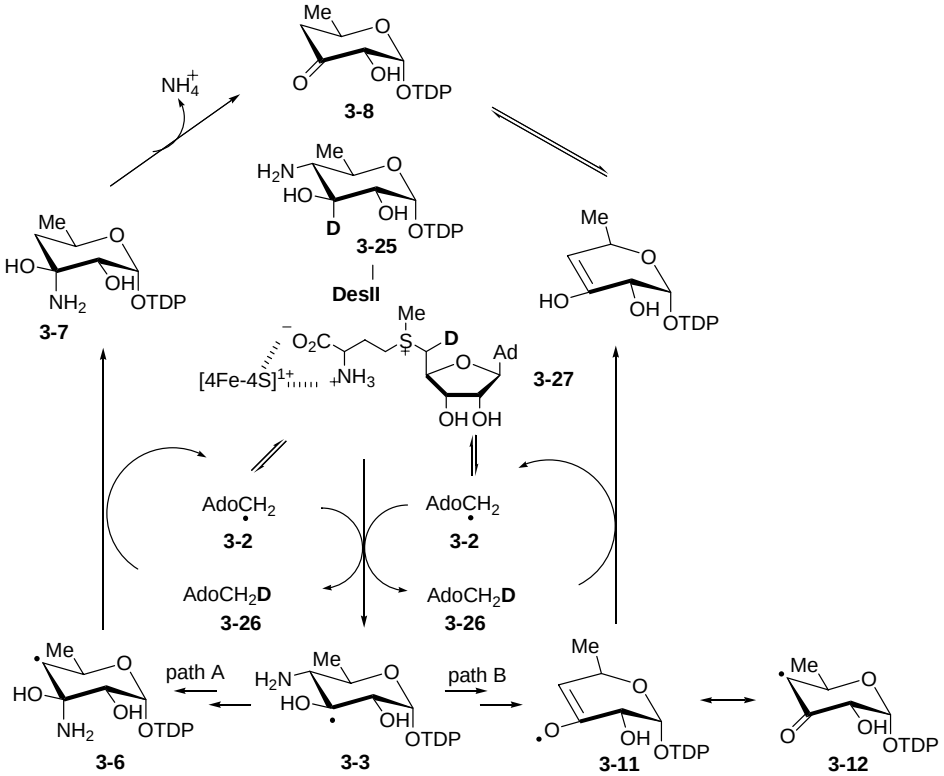

Figure 3-4. The expected results of deuterium incorporation into SAM using TDP-[3-^{2}H]-4-amino-4,6-dideoxy-D-glucose (**3-25**) as a substrate.

Fluorinated substrate analogues are commonly used as mechanistic probes to study enzymatic catalyses, since fluorine is an effective hydroxyl group mimic and can also be used to replace a hydrogen atom (*16*). The electronegativity and van der Waals radii of fluorine (4.0, 1.47 Å) compare favorably with those of oxygen (3.5, 1.57 Å) allowing fluorine to serve as an effective hydroxyl group mimic (*17*). The use of fluorine as a hydrogen surrogate is somewhat less intuitive, since the van der Waals radii of hydrogen (1.2 Å) is much smaller than that of fluorine. However, analysis of monofluorinated stearic acids deposited on graphite reveals a smooth two-dimensional packing suggesting a very close isosteric relationship between hydrogen and fluorine (*18*). Thus, fluorine has also been used to replace hydrogen atoms in designing enzyme probes and inhibitors. Previous studies have shown that fluorinated substrate analogues are useful for probing a variety of enzymatic mechanisms. Examples include enzymes involving cationic mechanisms, such as prenyltransferases (*19*), isopentenyl pyrophosphate Type I isomerase (*19-23*), glycosidases (*24, 25*), UDP-*N*-acetylglucosamine enolpyruvyl transferase (MurZ) (*26*), thiamine phosphate synthase (*27*), and cyclopropane fatty acid synthase (*28*). Examples involving oxidation/reduction mechanisms include thymidylate synthase (*29*), estrogen synthetase (aromatase) (*30*), CDP-D-glucose 4,6-dehydratase (E_{od}) (*31*), (*S*)-hydroxypropylphosphonic acid expoxidase (*32*), and TDP-L-rhamnose synthase (*33*). Examples involving radical mechanisms include chorismate synthase (*34-36*) and CDP-6-deoxy-L-*threo*-D-*glycero*-4-hexulose-3-dehydrase (E_1)/CDP-6-deoxy-L-*threo*-D-*glycero*-4-hexulose-3-dehydrase reductase (E_3). The enzymatic mechanism for C-3 deoxygenation catalyzed by E_1/E_3 has been reviewed in Chapter 1 (Section 1.2.3). One unique feature of the reaction

mechanism catalyzed by E_1/E_3 is the formation of a cofactor-based radical (**1-38**, Figure 1-8). The fluorinated pyridoxamine 5′-phosphate analogue (F-PMP, **3-28**, Figure 3-5), which contains 3′-F instead of 3′-OH in PMP, was synthesized to gain further insight into the involvement of a cofactor-based radical (*37*). Other examples include CDP-D-tyvelose 2-epimerase (*38*), YerE (*39*), and UDP-galactopyranose mutase (*40*) in which fluorinated substrate analogues were used to study the stereochemical models/rearrangement mechanisms.

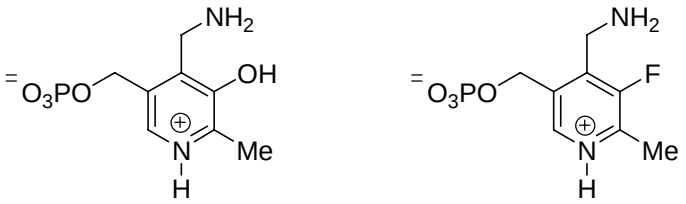

Figure 3-5. The structures of pyridoxamine 5′-phosphate (PMP) and the fluorinated pyridoxamine 5′-phosphate analogue (F-PMP, **3-28**).

This chapter describes the synthesis of TDP-3-fluoro-3,6-dideoxy-D-glucose (**3-29**, Figure 3-6) to study whether deprotonation of the 3-hydroxyl group (**3-3** to **3-9**, Figure 3-1) is a part of the reaction mechanism. This analogue contains a hydroxyl group at C4 similar to TDP-D-quinovose (**3-30**, Figure 3-6), which is a competent substrate comparable to the natural substrate as described in Chapter 2. If the reaction proceeds through path A, the free fluoride ion will be released which could be detected by ^{19}F NMR spectroscopy. The formation of the expected product **3-8** could also be monitored by the HPLC assay as described in Chapter 2 (Figure 3-6, path A). Alternatively, if the reaction proceeds through path B, the substitution of the C3-hydroxyl group with a

fluorine will prevent the deprotonation of the C3-hydroxyl group, a key step in the proposed mechanism B (Figure 3-6, path B). The results of these studies are presented in this chapter. The HPLC assay demonstrated that DesII did not take TDP-3-fluoro-3,6-dideoxy-D-glucose (**3-29**) as a substrate. Instead, the subsequent inhibition studies demonstrated that this fluorinated analogue **3-29** functions as a competitive inhibitor for the DesII enzyme.

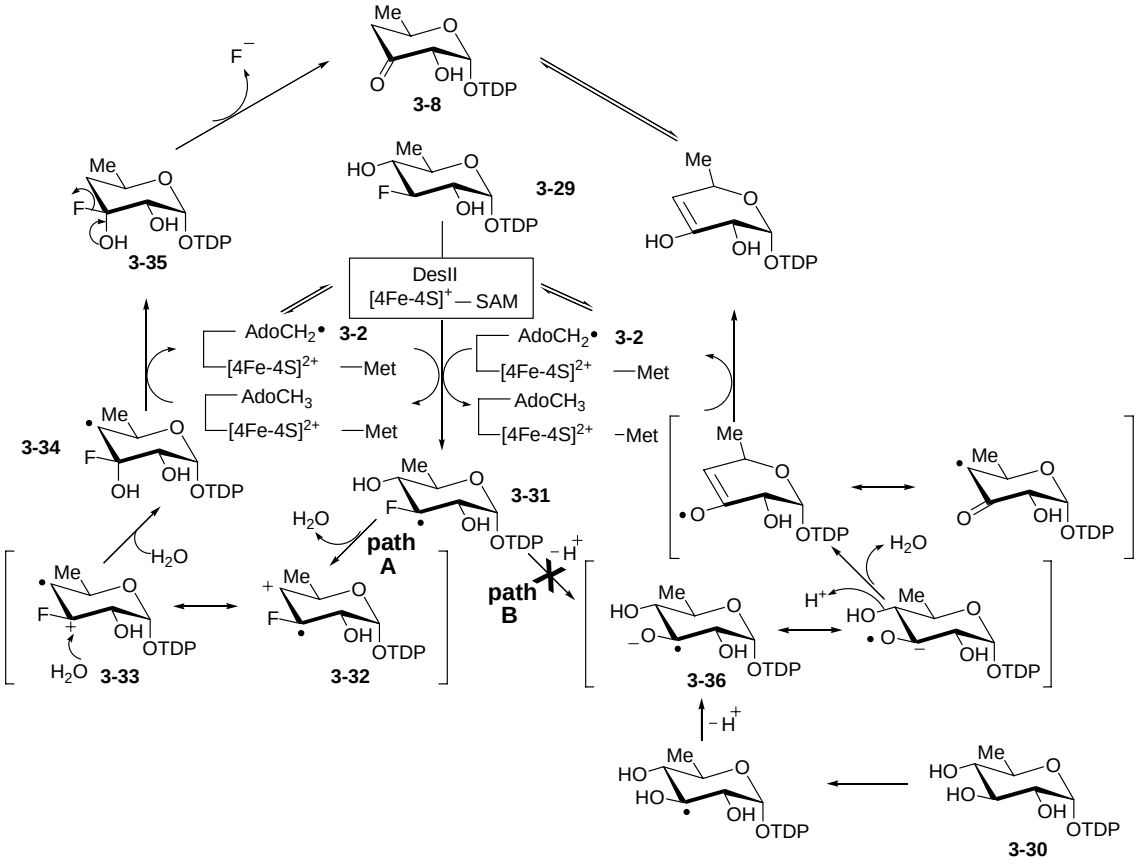

Figure 3-6. The predicted results using TDP-3-fluoro-3,6-dideoxy-D-glucose (**3-29**) as the substrate analogue.

3.2 MATERIALS AND METHODS

General. In addition to those described in Chapter 2, ^{1}H, ^{13}C, ^{31}P, ^{19}F NMR spectra were recorded using either Varian Unity Plus 300 or 500 MHz instrument. Chemical shifts (δ in ppm) are given relative to those for the corresponding solvent peak with coupling constants reported in hertz (Hz). Mass spectra were recorded by the MS facility at the Department of Chemistry and Biochemistry of the University of Texas at Austin. All reagents and solvents were purchased from commercial sources and were used without further purification unless otherwise noted. Analytical thin layer chromatography (TLC) was carried out on precoated TLC glass plates (silica gel, grade 60, F_{254}, 0.25 mm layer thickness) purchased from EMD chemicals (Madison, WI). The spots on TLC plates were visualized first under UV light and then by heating plates previously stained with solutions of vanillin/ethanol/H_2SO_4 (1:98:1) or phosphomolybdic acid (7% in EtOH). Flash column chromatography was performed on silica gel (230-400 mesh, grade 60) obtained from Sorbent Technologies (Atlanta, GA) by elution with the specified solvents. Celite 545 Filter Aid (Powder) was a product of Fisher Scientific Inc. (Pittsburgh, PA). All reactions were carried out in oven-dried glassware (100 °C) under an atmosphere of dry argon unless indicated otherwise. Kinetic data were analyzed by nonlinear fit using Grafit5 (Erithacus Software Ltd.).

Materials. Most materials used in these experiments were identical to those described in Chapter 2. The new materials are listed below: hexokinase (from *Saccharomyces cerevisiae*) and phosphoglucomutase (from rabbit muscle) are products of Sigma-Aldrich Chemical Co. (St. Louis, MO).

Instrumentation. All instruments used in these experiments were identical to those described in Chapter 2. The analytical Microsorb-MV C_{18} column (4.5 × 250 mm, 5 μm) was purchased from Alltech (Deerfield, IL).

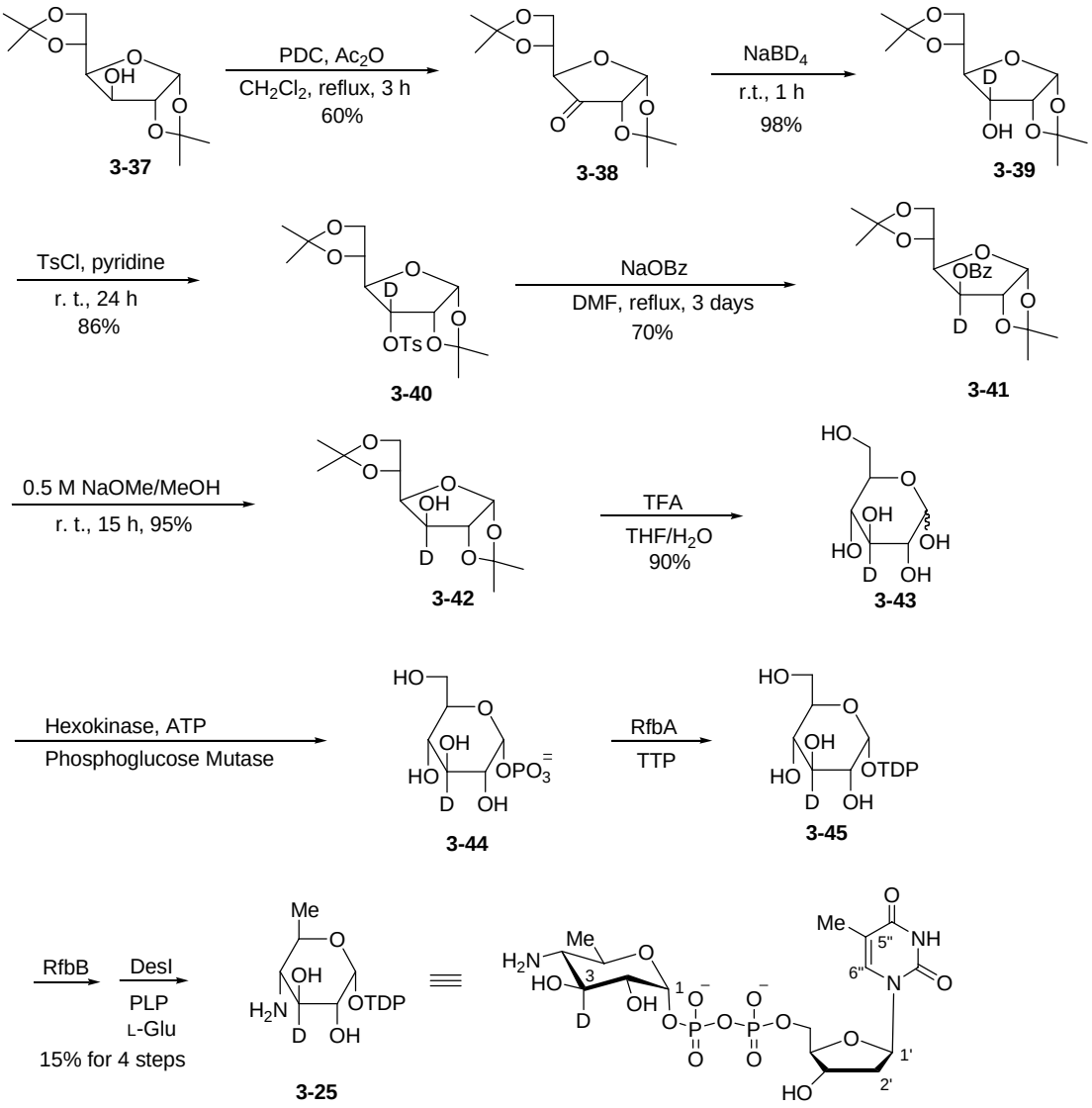

Figure 3-7. The chemoenzymatic synthesis of TDP-[3-^{2}H]-4-amino-4,6-dideoxy-D-glucopyranose (**3-25**).

*Synthesis of TDP-[3-^{2}H]-4-amino-4,6-dideoxy-D-glucose (**3-25**)*. The synthetic strategy used to make TDP-[3-^{2}H]-4-amino-4,6-dideoxy-D-glucose (**3-25**) is presented in Figure 3-7. The preparation of [3-^{2}H]-1-phosphoryl-α-D-glucopyranose (**3-44**), starting from 1,2:5,6-di-*O*-isopropylidene-α-D-glucofuranose (**3-37**), was performed following the same synthetic schemes previously developed by Dr. Patricia A. Pieper of this laboratory (*41*). The conversion of [3-^{2}H]-1-phosphoryl-α-D-glucopyranose (**3-44**) to TDP-[3-^{2}H]-4-amino-4,6-dideoxy-D-glucose (**3-25**) was carried out following the identical procedure used to make TDP-4-amino-4,6-dideoxy-D-glucose (**3-1**) as described in Chapter 2. The drying agent used in the workup was anhydrous sodium sulfate unless specified otherwise.

*1,2:5,6-Di-O-isopropylidene-α-D-ribo-hexofuranos-3-ulose (**3-38**)*. A solution of 1,2:5,6-di-*O*-isopropylidene-α-D-glucofuranose (**3-37**, 13 g, 49.9 mmol), pyridinium dichromate (PDC, 11.3 g, 30 mmol), and acetic anhydride (16 mL, 169.2 mmol) in anhydrous dichloromethane (300 mL) was heated under reflux for 3 h, and then concentrated to approximately half its volume. Chromium salts were precipitated by the addition of ethyl acetate (approximately 300 mL) and then removed by filtration through a celite pad (Fisher Scientific Inc., Pittsburgh, PA). The resultant dark filtrate was then concentrated. Purification by flash column chromatography (1:1 EtOAc in hexanes) yielded 7.7 g (60%) of **3-38** as a colorless, viscous oil: ^{1}H NMR (300 MHz, $CDCl_3$) δ 1.31 (3H, s), 1.32 (3H, s), 1.41 (3H, s), 1.44 (3H, s), 4.01 (2H, d, J = 6.3 Hz, 6-Hs), 4.32-4.38 (3H, m, 2-H, 4-H, and 5-H), 6.12 (1H, d, J = 4.5 Hz, 1-H); ^{13}C NMR (75 MHz,

$CDCl_3$) δ 25.2, 25.9, 27.1, 27.4, 64.2, 76.3, 76.6, 78.8, 103.0, 110.2, 114.2, 208.8; CI-HRMS calcd for $C_{12}H_{20}O_6$ $[M + H]^+$ 261.1333, found 261.1325.

*1,2:5,6-Di-O-isopropylidene-[3-^{2}H]-α-D-allofuranose (**3-39**).* Compound **3-38** (7.7 g, 29.8 mmol) was dissolved in 95% aqueous tetrahydrofuran (200 mL). Subsequently, 1.25 g (29.8 mmol) sodium borodeuteride was divided into 3 portions and added over a period of 20 min at 0 °C. The resulting mixture was stirred at room temperature for 1 h. The solution was diluted with water (100 mL) and extracted with chloroform three times (3 × 30 mL). The combined organic extracts were dried using $MgSO_4$ and evaporated to a colorless syrup. The residual syrup was purified by flash column chromatography (1:3 EtOAc in hexanes) to give **3-39** (7.6 g, 98%). ^{1}H NMR (300 MHz, $CDCl_3$) δ 1.11 (3H, s), 1.12 (3H, s), 1.19 (3H, s), 1.31 (3H, s), 2.88 (1H, s, exch.), 3.59 (1H, d, *J* = 3.6 Hz, 4-H), 3.78 (2H, m, 6-Hs), 4.05 (1H, q, *J* = 4.2 Hz, 5-H), 4.33 (1H, d, *J* = 3.6 Hz, 2-H), 5.52 (1H, d, *J* = 3.9 Hz, 1-H); ^{13}C NMR (75 MHz, $CDCl_3$) δ 25.3, 26.3, 26.5, 26.6, 65.5, 71.9 (t, *J* = 20 Hz), 75.5, 79.2, 79.4, 103.8, 109.6, 112.6; CI-HRMS calcd for $C_{12}H_{20}DO_6$ $[M + H]^+$ 262.1401, found 262.1399.

*1,2:5,6-Di-O-isopropylidene-[3-^{2}H]-3-O-(p-toluenesulfonyl)-α-D-allofuranose (**3-40**).* *p*-Toluenesulfonyl chloride (6.1 g, 32.0 mmol) was added to a solution of **3-39** (7.6 g, 29.1 mmol) in pyridine (51 mL) at 0 °C under nitrogen. The resulting mixture was stirred at room temperature for 24 h, and then water (50 mL) was added to quench the reaction. After stirring for 30 min, the aqueous and organic layers were separated and the organic layer was washed with 1M HCl (50 mL) to remove remaining pyridine and then with brine twice (2 × 50 mL). The combined organic layers were dried and filtered. The

filtrate was concentrated under vacuum. The mixture was purified by flash column chromatography (1:3 EtOAc in hexanes) to yield 12.1 g (86%) of **3-40**: ^{1}H NMR (300 MHz, $CDCl_3$) δ 1.28 (3H, s), 1.30 (3H, s), 1.33 (3H, s), 1.53 (3H, s), 2.45 (3H, s, PhC*H*$_3$), 3.78 (1H, dd, *J* = 6.6, 2.1 Hz, 6a-H), 3.93 (1H, dd, *J* = 6.9, 1.5 Hz, 6b-H), 4.17 (2H, m, 4-H and 5-H), 4.64 (1H, d, *J* = 3.6 Hz, 2-H), 5.76 (1H, d, *J* = 3.6 Hz, 1-H), 7.37 (2H, d, *J* = 8.1 Hz, Ar-H's), 7.81 (2H, d, *J* = 8.1 Hz, Ar-H's); ^{13}C NMR (75 MHz, $CDCl_3$) δ 21.6, 25.0, 26.0, 26.4, 26.5, 65.1, 74.5, 76.8 (t, *J* = 20 Hz), 77.4, 77.8, 103.7, 109.8, 113.5, 128.0, 129.9, 132.3, 145.1; CI-HRMS calcd for $C_{19}H_{26}DO_8S$ $[M + H]^+$ 416.1484, found 416.1478.

1,2:5,6-Di-O-isopropylidene-[3-^{2}H]-3-O-benzoyl-α-D-glucofuranose (***3-41***). Compound **3-40** (9.1 g, 21.9 mmol) was dissolved in anhydrous *N*,*N*-dimethylformamide (300 mL), and then sodium benzoate (3.3 g, 22.9 mmol) was added. The suspension was heated under reflux for 3 days. Subsequently, water (50 mL) was added to dissolve remaining sodium benzoate, and the solution was extracted with chloroform (60 mL). The chloroform extract was then washed five times with water (5 × 60 mL) to remove *N*,*N*-dimethylformamide. After drying with $MgSO_4$ and filtering, the resulting filtrate was concentrated to a colorless syrup. Purification by flash column chromatography (1:3 EtOAc in hexanes) yielded 5.7 g (70%) of **3-41** as a white solid: ^{1}H NMR (300 MHz, $CDCl_3$) δ 1.28 (3H, s), 1.30 (3H, s), 1.33 (3H, s), 1.53 (3H, s), 4.13 (2H, dd, *J* = 6.6, 2.1 Hz, 6-Hs), 4.37 (2H, m, 4-H and 5-H), 4.65 (1H, d, *J* = 3.6 Hz, 2-H), 5.97 (1H, d, *J* = 3.6 Hz, 1-H), 7.48 (2H, d, *J* = 7.8 Hz, Ar-H's), 7.61 (1H, d, *J* = 4.0 Hz, Ar-H's), 7.81 (2H, d, *J* = 7.8 Hz, Ar-H's); ^{13}C NMR (75 MHz, $CDCl_3$) δ 25.0, 26.0, 26.4, 26.5, 67.2, 72.6, 76.8

(t, J = 20 Hz), 79.9, 83.3, 105.1, 109.4, 112.4, 128.0, 129.9, 133.5, 145.1, 172.0; CI-HRMS calcd for $C_{19}H_{24}DO_7$ $[M + H]^+$ 366.1658, found 366.1651.

*1,2:5,6-Di-O-isopropylidene-[3-^{2}H]-α-D-glucofuranose (**3-42**)*. To **3-41** (5.7 g, 15.6 mmol) dissolved in 35 mL anhydrous methanol, 180 mL sodium methoxide solution (0.5 M in methanol, 93.6 mmol) was added dropwise at 0 °C. The resulting reaction mixture was stirred at room temperature for 15 h. The reaction mixture was poured cautiously into 200 mL water. To this mixture was slowly added 15% H_2SO_4 solution at 0 °C until the pH was adjusted to approximately 6.5. The solution was subsequently extracted with dichloromethane (3 × 100 mL). The organic extracts were washed with water (3 × 60 mL), and dried ($MgSO_4$). The solvent was evaporated under reduced pressure to give a light-yellow, semi-crystalline product. Purification by flash column chromatography (1:3 to 1:1 EtOAc in hexanes) yielded 3.8 g (95%) of **3-42** as a white solid: ^{1}H NMR (300 MHz, $CDCl_3$) δ 1.32 (3H, s), 1.37 (3H, s), 1.45 (3H, s), 1.50 (3H, s), 2.65 (1H, s, exch.) 4.01 (2H, dd, J = 6.6, 2.1 Hz, 6-Hs), 4.17 (1H, d, J = 7.8 Hz, 4-H), 4.35 (1H, q, J = 6 Hz, 5-H), 4.53 (1H, d, J = 3.9 Hz, 2-H), 5.94 (1H, d, J = 3.6 Hz, 1-H); ^{13}C NMR (75 MHz, $CDCl_3$) δ 25.1, 26.1, 26.7, 26.8, 67.6, 72.4, 73.7 (t, J = 23 Hz), 81.00, 85.0, 105.1, 109.4, 111.8; CI-HRMS calcd for $C_{12}H_{20}DO_6$ $[M + H]^+$ 262.1401, found 262.1404.

*[3-^{2}H]-α/β-D-glucopyranose (**3-43**)*. A mixture of tetrahydrofuran, water, and trifluoroacetic acid (1:1:4 v/v, 50 mL in total) was added to **3-42** (3.8 g, 14.56 mmol) and the solution was stirred for 8 h at room temperature. The solvent was then removed to yield **3-43** (3.42 g, 90%). The product was used for the next step without further

purification. Spectral data of **3-43**: ^{1}H NMR (500 MHz, D_2O) δ 3.12 (1H, d, *J* = 4.8 Hz, 4-H), 3.3-3.8 (3H, m, 5-H and 6-Hs), 4.52 (1H, d, *J* = 4.8 Hz, 2-H), 5.11 (1H, d, *J* = 2.4 Hz, 1-H); ^{13}C NMR (125 MHz, D_2O) δ 62.2, 64.2, 66.2 (t, *J* = 22 Hz), 71.3, 72.5, 95.0; CI-HRMS calcd for $C_6H_{12}DO_6$ $[M + H]^+$ 182.0775, found 182.0780.

*TDP-[3-^{2}H]-α-D-glucopyranose (**3-45**).* Reaction mixtures containing 100 mM [3-^{2}H]-α/β-D-glucopyranose (**3-43**), 50 μM hexokinase, 500 mM ATP in 20 mM Tris•HCl buffer, pH 8.0 with 13.3 mM $MgCl_2$ were incubated at 30 °C for 1 h. The final reaction volume was 10 mL. Subsequently, 50 μM of phosphoglucomutase and 100 μM of glucose-1,6-bisphosphate were added to generate [3-^{2}H]-glucose-1-phosphate (**3-44**). The reaction was incubated at 30 °C for 1 h. The coupling of [3-^{2}H]-glucose-1-phosphate (**3-44)** with thymidine to generate TDP-[3-^{2}H]-D-glucopyranose (**3-45**) was carried out following the procedure established for the preparation of TDP-D-glucose described in Chapter 2. The enzymes were removed using a Centricon-10 centrifugal filter unit prior to HPLC analysis. The formation of TDP-[3-^{2}H]-D-glucopyranose (**3-45**) was monitored by HPLC on a CarboPac anion exchange column using the program applied to examine the TDP-D-glucose formation. TDP-[3-^{2}H]-D-glucopyranose (**3-45**) eluted at 36.2 min, which is identical to that of TDP-D-glucose. TDP-[3-^{2}H]-D-glucose (**3-45**) was purified by size exclusion chromatography using a Bio-Gel P-2 column (2 × 140 cm) as described in Chapter 2.

*TDP-[3-^{2}H]-4-amino-4,6-dideoxy-D-glucopyranose (**3-25**).* TDP-[3-^{2}H]-4-amino-4,6-dideoxy-D-glucopyranose (**3-25**) was prepared by incubation of 46.2 mg (8.2 mM) of TDP-[3-^{2}H]-D-glucopyranose (**3-45**) and 0.028 mM RfbB in 10 mL of 50 mM potassium

phosphate buffer, pH 7.5, at 37 °C for 1 h, followed by addition of 5 mM L-glutamate, 0.8 mM PLP, and 0.026 mM DesI, and then incubated at 25 °C for 2 h. The enzyme was removed using a Centricon-10 centrifugal filter unit, and the filtrate was separated by FPLC using a MonoQ HR (10/10) column. The flow rate was 3 mL/min, and the detector was set at 280 nm. A linear gradient of 0-350 mM NH_4HCO_3 over 25 min followed by a gradient of 350-500 mM NH_4HCO_3 over 5 min provided a satisfactory separation of the product from other reagents. The desired product (**3-25**), which was eluted at 250 mM NH_4HCO_3, was collected, lyophilized, and subjected to analysis by NMR spectroscopy. Spectral data of **3-25** (10 mg, 15% yield for four enzymatic steps): ^{1}H NMR (500 MHz, D_2O) δ 0.80 (3H, d, *J* = 5.7 Hz, 5-Me), 1.52 (3H, s, 5″-Me), 1.98-2.03 (2H, m, 2′-Hs), 2.84 (1H, d, *J* = 9.9 Hz, 4-H), 3.28 (1H, d, *J* = 3.6 Hz, 2-H), 3.53 (1H, m, 5-H), 3.75-3.88 (3H, m, 4′-H, 5′-Hs), 4.18-4.22 (1H, m, 3′-H), 5.48 (1H, dd, *J* = 6.8, 3.1 Hz, 1-H), 5.94 (1H, t, *J* = 6.7 Hz, 1′-H), 7.29 (1H, s, 6″-H); ^{13}C NMR (125 MHz, D_2O) δ 12.8, 17.6, 39.7, 55.9, 66.6 (d, *J* = 6.0 Hz), 70.1 (t, *J* = 20 Hz), 70.6 (d, *J* = 8.4 Hz), 72.1, 73.3, 86.2, 86.4 (d, *J* = 9.2 Hz), 95.6 (d, *J* = 6.1 Hz), 112.8, 138.5, 153.0, 167.9; ^{31}P NMR (202 MHz, D_2O) δ -13.47 (d, *J* = 20.7 Hz), -11.75 (d, *J* = 20.7 Hz); ESI-HRMS calcd for $C_{16}H_{25}DN_3O_{14}P_2$ $[M - H]^-$ 547.0958, found 547.0951.

*Synthesis of TDP-3-fluoro-3,6-dideoxy-D-glucose (**3-29**).* The synthetic strategy used to make TDP-3-fluoro-3,6-dideoxy-D-glucose (**3-29**) is presented in Figure 3-8. The drying agent used in the workup was anhydrous sodium sulfate unless otherwise specified.

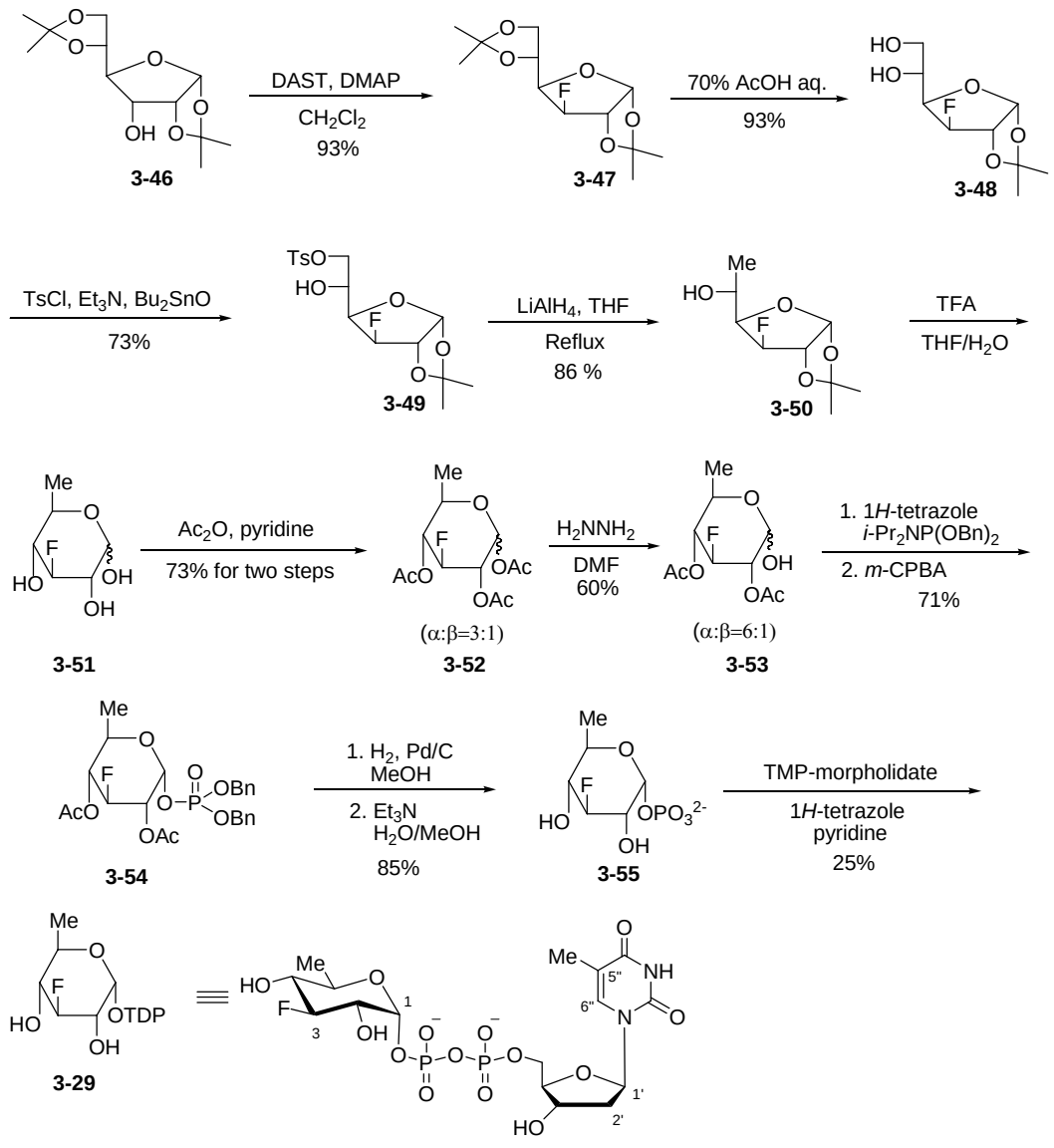

Figure 3-8. The chemical synthesis of TDP-3-fluoro-3,6-dideoxy-D-glucopyranose (**3-29**).

*3-Deoxy-3-fluoro-1,2:5,6-di-O-isopropylidene-α-D-glucofuranose (**3-47**).* To a solution of 1,2:5,6-di-*O*-isopropylidene-α-D-allofuranose (**3-46**) (3 g, 11.5 mmol) in anhydrous CH_2Cl_2 (15 mL) was added 4-dimethylaminopyridine (DMAP, 3 g, 24.6

mmol) followed by the dropwise addition of diethylaminosulfur trifluoride (DAST, 3 mL, 15.3 mmol) at 0 °C (*42*). The mixture was stirred at room temperature for 15 h and then carefully poured into a saturated $NaHCO_3$ solution (20 mL) to quench the reaction. The organic layer was separated, washed with brine (2 × 20 mL), dried, and concentrated. The resulting residue was purified by flash column chromatography (1:10 EtOAc in hexanes) and yielded 2.9 g (93%) of **3-47** as a colorless oil: ^{1}H NMR (300 MHz, $CDCl_3$) δ 1.33 (3H, s), 1.37 (3H, s), 1.45 (3H, s), 1.51 (3H, s), 4.4-4.0 (5H, m, 2-H, 5-H, and 6-Hs), 4.71 (1H, dd, *J* = 6.9, 3.6 Hz, 4-H), 5.02 (1H, dd, *J* = 47.7, 2.1 Hz, 3-H), 5.96 (1H, d, *J* = 3.6 Hz, 1-H); ^{13}C NMR (75 MHz, $CDCl_3$) δ 25.1, 26.2, 26.7, 26.8, 67.1, 71.9 (d, *J* = 7.1 Hz), 80.6 (d, *J* = 18.5 Hz), 82.5 (d, *J* = 32.8 Hz), 93.8 (d, *J* = 183 Hz), 105.2, 109.5, 112.4; ^{19}F NMR (282 MHz, $CDCl_3$) δ -208 (ddd, *J* = 45, 29, 11 Hz); CI-HRMS calcd for $C_{12}H_{19}FO_6$ $[M + H]^+$ 263.1289, found 263.1294.

*3-Deoxy-3-fluoro-l,2-O-isopropylidene-α-D-glucofuranose (**3-48**).* A solution of **3-47** (2.9 g, 11.1 mmol) in aqueous 70% AcOH (73 mL) was stirred at room temperature for 15 h (*43*). The solvents were evaporated under vacuum and the residue was purified by flash column chromatography (1:1 EtOAc in hexanes), yielding 2.3 g (93%) of **3-48** as a colorless syrup: ^{1}H NMR (300 MHz, $CDCl_3$) δ 1.33 (3H, s), 1.52 (3H, s), 2.24 (1H, s, exch.), 2.89 (1H, s, exch.), 3.66 (1H, dd, *J* = 11.7, 4.5 Hz, 6-H), 3.78 (1H, dd, *J* = 11.7, 3.9 Hz, 6-H), 3.86 (1H, dddd, *J* = 7.5, 4.5, 3.9, 0.9 Hz, 5-H), 4.31 (1H, dddd, *J* = 24.0, 7.5, 1.8, 0.9 Hz, 4-H), 4.78 (1H, dd, *J* = 15.3, 4.2 Hz, 2-H), 5.00 (1H, dd, *J* = 51.0, 1.8 Hz, 3-H), 5.98 (1H, d, *J* = 4.2 Hz, 1-H); ^{13}C NMR (75 MHz, $CDCl_3$) δ 25.9, 26.5, 63.4, 69.9 (d, *J* = 9 Hz), 84.4 (d, *J* = 32 Hz), 85.9 (d, *J* = 25 Hz), 95.3 (d, *J* = 182 Hz), 105.6,

113.5; ^{19}F NMR (282 MHz, $CDCl_3$) δ -208 (ddd, *J* = 45, 29, 11 Hz); CI-HRMS calcd for $C_{12}H_{19}FO_6$ $[M + H]^+$ 263.1289, found 263.1294.

*3-Deoxy-3-fluoro-6-O-tosyl-l,2-O-isopropylidene-α-D-glucofuranose (**3-49**).* To a solution of **3-48** (2.2 g, 10 mmol) in CH_2Cl_2 (20 mL) were added Bu_2SnO (0.2 mmol), *p*-TsCl (10 mmol), and Et_3N (10 mmol) (*44*). The reaction mixture was stirred at room temperature for 18 h. The reaction was quenched with water, and the layers were separated. The aqueous layer was extracted with CH_2Cl_2 (2 × 50 mL), the combined organic layers were washed sequentially with water and brine. The washed extract was then dried, and filtered, and the filtrate was concentrated under vacuum. Purification by flash column chromatography (1:3 EtOAc in hexanes) yielded 2.6 g (73%) of monotosylated compound (**3-49**) as a white solid: ^{1}H NMR (300 MHz, $CDCl_3$) δ 1.32 (3H, s), 1.48 (3H, s), 2.47 (3H, s, PhC*H*$_3$), 4.05-4.13 (3H, m, 5-H and 6-Hs), 4.33 (1H, dd, *J* = 3, 2.7 Hz, 4-H), 4.68 (1H, dd, *J* = 6.3, 3.9 Hz, 2-H), 5.08 (1H, dd, *J* = 48.6, 2.1 Hz, 3-H), 5.91 (1H, d, *J* = 3.9 Hz, 1-H), 7.37 (2H, d, *J* = 8.1 Hz, Ar-H's), 7.81 (2H, d, *J* = 8.1 Hz, Ar-H's); ^{13}C NMR (75 MHz, $CDCl_3$) δ 21.6, 26.2, 26.6, 66.5 (d, *J* = 8.8 Hz), 72.2, 78.9 (d, *J* = 19.3 Hz), 82.1 (d, *J* = 32.4 Hz), 93.6 (d, *J* = 184.7 Hz), 105.1, 112.5, 128.0, 129.9, 132.3, 145.1; ^{19}F NMR (282 MHz, $CDCl_3$) δ -208.8 (ddd, *J* = 44, 29, 10 Hz); CI-HRMS calcd for $C_{16}H_{22}FO_7S$ $[M + H]^+$ 377.1065, found 377.1061.

*3-Fluoro-3,6-dideoxy-l,2-O-isopropylidene-α-D-glucofuranose (**3-50**).* Powered **3-49** (2.5 g, 7.3 mmol) was slowly added to a suspension of $LiAlH_4$ (720 mg, 20 mmol) in anhydrous THF at 0 °C (*45*). After the resulting mixture was boiled under reflux for 1 hr, it was cooled to 0 °C and the excess hydride was destroyed by the addition of H_2O

(0.7 mL), aqueous 15% NaOH (0.7 mL), and H_2O (2.2 mL) with caution. Solids were filtered through a Celite pad and the filtrates were dried and evaporated to yield the crude product. Purification by flash column chromatography (1:2 EtOAc in hexanes) yielded 1.2 g (86%) of **3-50** as white crystals: ^{1}H NMR (300 MHz, $CDCl_3$) δ 1.33 (3H, s), 1.37 (3H, d, *J* = 6.6 Hz, 5-Me), 1.51 (3H, s), 1.98 (1H, s, exch.), 3.90-4.10 (2H, m, 4-H and 5-H), 4.66 (1H, dd, *J* = 7.5, 3.9 Hz, 2-H), 5.08 (1H, dd, *J* = 47.7, 2.4 Hz, 3-H), 5.87 (1H, d, *J* = 3.6 Hz, 1-H); ^{13}C NMR (75 MHz, $CDCl_3$) δ 20.7, 26.2, 26.6, 64.8 (d, *J* = 8 Hz), 82.6 (d, *J* = 33 Hz), 83.7 (d, *J* = 19 Hz), 94.0 (d, *J* = 184 Hz), 105.0, 112.1; ^{19}F NMR (282 MHz, $CDCl_3$) δ -208 (ddd, *J* = 44, 29, 10 Hz); CI-HRMS calcd for $C_9H_{16}FO_4$ $[M + H]^+$ 207.1027, found 207.1021.

*3-Fluoro-3,6-dideoxy-α/β-D-glucopyranose (**3-51**).* A mixture of tetrahydrofuran, water, and trifluoroacetic acid (1:1:4 v/v, 20 mL) was added to **3-50** (1.2 g, 5.82 mmol). The resulting solution was stirred at room temperature for 10 h, and then evaporated to yield **3-51** (0.97 g). The product was used for the next step without further purification.

*1,2,4-Tri-O-acetyl-3-fluoro-3,6-dideoxy-α/β-D-glucopyranose (**3-52**).* A solution of 3-fluoro-3-deoxy-α/β-D-glucopyranose (0.97 g, 5.84 mmol) in 11 mL of dry pyridine was acetylated by the addition of 6 mL of acetic anhydride at 0 °C. After the addition, the ice bath was removed and the resulting solution was stirred at room temperature for 2 h. The reaction solution was concentrated and then diluted with CH_2Cl_2. The reaction mixture was successively washed with 1M HCl (30 mL), H_2O (50 mL) and brine (50 mL). The organic phase was dried over anhydrous $MgSO_4$, filtered, and then concentrated in vacuum. The residual syrup was subjected to chromatography on silica

gel with EtOAc/hexanes (1:3) to give **3-52** (740 mg, 73% for two steps) as a 3:1 (α/β) mixture of anomers. ^{1}H NMR (300 MHz, $CDCl_3$) δ 1.22, 1.26 (3H, d, *J* = 6 Hz, 5-Me (α and β anomers)), 2.10, 2.12, 2.13, 2.14, 2.16, 2.17 (9H, s, 3 × OAc (α and β anomers)), 3.56, 3.94 (1H, m, 5-H (α and β anomers)), 4.56, 4.78 (1H, dt, *J* = 53, 9.3 Hz, 3-H (α and β anomers)), 4.94-5.28 (2H, m, 2-H and 4-H (α and β anomers)), 5.63 (0.25H, d, *J* = 8.4 Hz, 1β-H), 6.29 (0.75H, t, *J* = 3.9 Hz, 1α-H); ^{13}C NMR (75 MHz, $CDCl_3$) δ 17.1, 20.5, 20.7, 20.8, 67.6 (d, J = 7 Hz, C-5), 70.0 (d, J = 18 Hz), 72.9 (d, *J* = 18 Hz), 88.9 (d, *J* = 189 Hz), 89.3 (d, *J* = 10 Hz), 168.8, 169.4, 169.6; ^{19}F NMR (282 MHz, $CDCl_3$) δ -200 (dt, *J* = 52, 13 Hz), -196 (dt, *J* = 52, 13 Hz); CI-HRMS calcd for $C_{12}H_{18}FO_7$ $[M + H]^+$ 293.1031, found 293.1024.

*2,4-Di-O-acetyl-3-fluoro-3,6-dideoxy-α/β-D-glucopyranose (**3-53**).* **3-52** (740 mg, 2.53 mmol) was dissolved in *N*,*N*-dimethylformamide (10 mL). Hydrazine acetate (284 mg, 3.1 mmol) was added, and the resulting solution was stirred at 50 °C for 30 min (*46*). The reaction progress was monitored by TLC (EtOAc : hexanes = 1:1) until the complete consumption of the starting material was observed. The solvent was subsequently evaporated under vacuum. The mixture was diluted with ethyl acetate (50 mL) and washed with brine (30 mL). The organic layer was dried using anhydrous $MgSO_4$, filtered, and concentrated. The crude product was purified by flash column chromatography on silica gel and eluted with EtOAc/hexanes (2:3) to give **3-53** (380 mg. 60%) as a 6:1 (α/β) mixture of anomers. ^{1}H NMR (300 MHz, $CDCl_3$) δ 1.19, 1.25 (3H, d, *J* = 6.3 Hz, 5-Me (α and β anomers)), 2.13, 2.14, 2.15, 2.16 (6 H, s, 2 × OAc (α and β anomers)), 3.40 (1H, s, exch.), 3.52, 4.10 (1H, m, 5-H (α and β anomers)), 4.50, 4.68

(1H, dt, J = 32.4, 9.3 Hz, 3-H (α and β anomers)), 4.76 (0.17H, d, J = 9.6 Hz, 1β-H) 4.88-5.00 (2H, m, 2-H and 4-H (α and β anomers)), 5.40 (0.83H, t, J = 3.6 Hz, 1α-H); ^{13}C NMR (75 MHz, $CDCl_3$) δ 17.0, 20.7, 20.8, 64.7 (d, J = 7 Hz, C-5), 71.9 (d, J = 17 Hz, C-2), 73.6 (d, J = 17 Hz, C-4), 88.9 (d, J = 174 Hz, C-3), 90.2 (d, J = 4.4 Hz, C-1), 169.9, 170.4; ^{19}F NMR (282 MHz, $CDCl_3$) δ -200 (dt, J = 51, 13 Hz), -196 (dt, J = 51, 13 Hz); CI-HRMS calcd for $C_{10}H_{16}FO_6$ $[M + H]^+$ 251.0931, found 251.0936.

*2,4-Di-O-acetyl-1-dibenzylphosphosphoryl-3-fluoro-3,6-dideoxy-α-D-glucopyranose (**3-54**).* Under nitrogen 1*H*-tetrazole (84 mg, 1.20 mmol) was suspended in dry dichloromethane (1.5 mL). After the addition of dibenzyl diisopropylphosphoramidite (206 mg, 0.60 mmol), the mixture was stirred at room temperature for 15 min in order to form the tetrazolide intermediate. Then a solution of **3-53** (70 mg, 0.24 mmol) in dry dichloromethane (1.5 mL) was added and the mixture was stirred for an additional 3 h at room temperature before being cooled to 0 °C. *m*-Chloroperoxybenzoic acid (MCPBA, 3 equivalents) was added and stirring continued for 1 h (*47*). Purification was performed by flash column chromatography with ethyl acetate/petroleum ether (1:3 to 1:2) to give **3-54** (80 mg, 71%). Spectral data of **3-54**: ^{1}H NMR (500 MHz, $CDCl_3$) δ 1.14, (3H, d, J = 6.3 Hz, 5-Me), 1.99 (3H, s, OAc), 2.14 (3H, s, OAc), 3.93 (1H, J = 10, 6.3 Hz, 5-H), 4.69 (1H, dt, J = 34.5, 9.3 Hz, 3-H), 4.91-5.02 (2H, m, 2-H and 4-H), 5.06-5.12 (4H, m, 2 × PhCH_2), 5.86 (1H, ddd, $J_{1\text{-H, P}}$ = 6.6 Hz, $J_{1\text{-H, 2-H}}$ = $J_{1\text{-H, 3-F}}$ = 3.3 Hz, 1-H); ^{13}C NMR (125 MHz, $CDCl_3$) δ 16.9, 20.4, 20.7, 67.5 (d, J = 5.5 Hz), 69.7 (d, J = 5.5 Hz), 70.6 (dd, J = 17, 9.9 Hz), 72.6 (d, J = 17 Hz), 88.4 (d, J = 189 Hz), 94.1 (dd, J = 5.5, 4.4 Hz), 127.9-135.3 (Ph*C*s), 169.4, 169.8; ^{19}F NMR (470

MHz, $CDCl_3$) δ -201 (ddt, J = 25, 12, 4.0 Hz); ^{31}P NMR (202 MHz, $CDCl_3$) δ –1.58; CI-HRMS calcd for $C_{24}H_{29}FO_9P$ $[M + H]^+$ 511.1528, found 511.1521.

*3-Fluoro-3,6-dideoxy-1-phosphoryl-α-D-glucopyranose (**3-55**).* To the solution of **3-54** (1.9 g, 2.92 mmol) in methanol (40 mL) was added 20% palladium on carbon (200 mg). Hydrogenation was carried out under atmospheric pressure of hydrogen gas for 24 h. The reaction mixture was filtered through a Celite pad, and solvent was removed by rotary evaporation to give the crude product. Without further purification, the crude product was dissolved in a mixture of methanol and water (MeOH : H_2O = 50 mL : 50 mL) and 20 mL Et_3N was added. The resulting solution was stirred at room temperature for 48 h. The solvent was then removed under vacuum to give **3-55** as a triethylammonium salt with an estimated 85% combined yield (414 mg, 1.5 mmol). The content of triethylamine in the sample was estimated to be 1.35 equivalents as judged by ^{1}H NMR. **3-55**: ^{1}H NMR (300 MHz, CD_3OD) δ 1.14, (3H, d, J = 6.3 Hz, 5-Me), 3.93 (1H, J = 10, 6.3 Hz, 5-H), 4.69 (1H, dt, J = 34.5, 9.3 Hz, 3-H), 4.91-5.02 (2H, m, 2,4-H), 5.86 (1H, ddd, $J_{1\text{-H,P}}$ = 6.6 Hz, $J_{1\text{-H, 2-H}} = J_{1\text{-H,3-F}}$ = 3.3 Hz, 1-H); ^{13}C NMR (75 MHz, CD_3OD) δ 16.9, 20.7, 70.6 (dd, J = 17, 9.9 Hz), 72.6 (d, J = 17 Hz), 88.4 (d, J = 189 Hz), 94.1 (dd, J = 5.5, 4.4 Hz); ^{19}F NMR (282 MHz, CD_3OD) δ -201 (ddt, J = 25, 12, 4.0 Hz); ^{31}P NMR (121 MHz, CD_3OD) δ –1.51.

Preparation of Thymidine 5′-monophosphate (Free Acid Form). Commercial thymidine 5′-monophosphate is available as the disodium salt. The free acid form of thymidine 5′-monophosphate is required for its coupling to morpholine. The free acid form can be generated by passing the disodium form through Dowex resin (50W × 8,

hydrogen form), which was pre-equilibrated with 1N HCl. The acid fractions (judged by pH test papers) containing thymidine 5′-monophosphate were collected and lyophilized to dryness.

Thymidine 5′-monophosphoromorpholidate. A solution of *N*,*N*′-dicyclohexylcarbodiimide (824 mg, 4 mmol) in *t*-butyl alcohol (15 mL) was added dropwise to a refluxing solution of the thymidine 5′-monophosphate (1 mmol of free acid) in a mixture of water (10 mL), *t*-butyl alcohol (10 mL) and purified morpholine (0.34 mL, 4 mmol). The addition was completed in 5-6 h and the resulting mixture was further refluxed for 4 h. The mixture was then cooled to room temperature and crystallized solid was removed by filtration and washed with *t*-butyl alcohol. The filtrate was evaporated under reduced pressure until the *t*-butyl alcohol was mostly removed. The remaining aqueous solution was extracted with ether (3 × 50 mL). The combined clear aqueous solution was lyophilized to dryness and subjected to analysis by NMR spectroscopy. The NMR data was comparable to that reported in the literature (*48*).

*TDP-3-fluoro-3,6-dideoxy-α-D-glucopyranose (**3-29**).* The triethylammonium salt of **3-55** (63.9 mg, 225 μmol) and thymidine 5'-monophosphomorpholidate 4-morpholine-*N*,*N*′-dicyclohexylcarboxamidine salt (246 mg, 360 μmol) were coevaporated with anhydrous pyridine (3 mL) three times. To this dry mixture were added 1*H*-tetrazole (47 mg, 675 μmol) and anhydrous pyridine (5 mL), and the resulting solution was stirred at room temperature for 3 days (*49*). The solvent was removed, and the solid residue was coevaporated with water (2 × 2 mL). The residue was purified by size exclusion chromatography using a Bio-Gel P-2 column (2 × 140 cm). The elution buffer was 20

mM ammonium bicarbonate (pH 7.0), and the flow rate was 6.0 mL/h. Fractions containing the desired product as judged by UV-vis spectroscopy and HPLC on a CarboPac column were pooled and lyophilized to give **3-29** in 25% yield (20.7 mg, 47.25 μmol): ^{1}H NMR (500 MHz, D_2O) δ 1.10 (3H, d, *J* = 6.3 Hz, 5-Me), 1.74 (3H, s, 5″-Me), 2.17-2.22 (2H, m, 2'-Hs), 3.18 (1H, m, 4-H), 3.24 (1H, t, *J* = 10.2 Hz, 3-H), 3.61 (1H, ddd, *J* = 10.2, 3.3, 3.1 Hz, 2-H), 3.77-3.87 (1H, m, 5-H), 3.99-4.01 (3H, m, 4'-H, 5'-Hs), 4.41-4.44 (1H, m, 3'-H), 4.59 (1H, dt, *J* = 34.5, 9.3 Hz, 3-H), 5.40 (1H, dd, *J* = 7.2, 3.3 Hz, 1-H), 6.17 (1H, dd, *J* = 7.2, 6.9 Hz, 1'-H), 7.55 (1H, s, 6″-H); ^{13}C NMR (125 MHz, D_2O) δ 12.8, 17.6, 39.7, 55.9, 66.6 (d, *J* = 6.0 Hz), 70.1, 70.6 (d, *J* = 8.4 Hz), 73.3, 86.2, 86.4 (d, *J* = 9.2 Hz), 89.4 (d, *J* = 189 Hz), 95.6 (d, *J* = 6.1 Hz), 112.8, 138.5, 153.0, 167.9; ^{19}F NMR (470 MHz, D_2O) δ -201 (ddt, *J* = 25, 12, 4.0 Hz); ^{31}P NMR (202 MHz, D_2O) δ -13.47 (d, *J* = 20.7 Hz), -11.75 (d, *J* = 20.7 Hz); ESI-HRMS calcd for $C_{16}H_{25}FN_2O_{14}P_2$ $[M - H]^-$ 549.0692, found 549.0685.

*Large-scale Enzymatic Synthesis of TDP-3-amino-3,4.6-trideoxy-D-glucose (DesV product, **3-56**, Figure 3-10a).* The large quantity of DesV product (**3-56**) was prepared from TDP-4-amino-4,6-dideoxy-D-glucose (**3-1**) using the DesII and DesV enzymes. The assay contained 0.5 mM substrate (TDP-4-amino-4,6-dideoxy-D-glucose, **3-1**), 0.1 mM reconstituted and reduced DesII protein, and 0.1 mM SAM in 100 mM Tris•HCl buffer, pH 8.0 containing 1 mM DTT. The final reaction volume of the assay mixture was 6 mL. After incubation of the assay mixture at 25 °C for 3 h, 10 mM L-glutamate, 0.8 mM PLP, and 0.1 mM DesV enzyme were added to the assay mixture followed by incubation at 25 °C for 1 h. The reaction was quenched by filtration through

a YM10 Diaflo membrane (Amicon) to remove the enzymes. The reaction mixture was then purified using a semipreparative CarboPac PA-1 column obtained from Dionex Inc. A gradient elution program identical to that used for the analytical CarboPac PA-1 column described in Chapter 2, was employed with a flow rate of 5 mL/min. Compound **3-56**, which eluted at 3.7 min, was collected manually and lyophilized to near dryness. HPLC analysis showed 40% conversion of **3-1** to **3-56**.

Deuterium Incorporation into S-adenosylmethionine (SAM). The incorporation of the deuterium atom of TDP-[3-^{2}H]-4-amino-4,6-dideoxy-D-glucose (**3-25**) into *S*-adenosylmethionine (SAM) was determined following literature procedures (*12-15*) with minor modifications. Specifically, the assay contained 500 μM TDP-[3-^{2}H]-4-amino-4,6-dideoxy-D-glucose (**3-25**), 100 μM AdoMet, and 100 μM reconstituted DesII in 100 mM Tris•HCl buffer, pH 8.0, containing 1 mM DTT. The final reaction volume of the assay was 1 mL. The reaction was initiated by the addition of AdoMet and reconstituted DesII after incubation of the other components of the assay mixture at 25 °C for 5 min. After incubation at 25 °C for 3 h, the reaction was quenched by ultrafiltration through a YM10 Diaflo membrane (Amicon) to remove the enzyme. The reaction progress was monitored by HPLC with the UV detector set at 260 nm on an analytical Microsorb-MV C_{18} column (4.5 × 250 mm, 5 μm, Varian). Solvent A consisted of 0.1% trifluoroacetic acid (TFA) and solvent B consisted of acetonitrile containing 0.1% TFA. The column was pre-equilibrated in 100% solvent A and subsequently eluted with a 20-min linear gradient of 0 to 45% solvent B at a flow rate of 1 mL/min. *S*-adenosylmethionine (SAM), which

eluted at 5.1 min, was collected, concentrated, and subjected to analysis by ESI mass spectrometry.

*DesII Activity Assay Using TDP-3-fluoro-3,6-dideoxy-D-glucose (**3-29**).* The assay solution (1 mL) contained the fluorinated substrate analogue **3-29** (0.5 mM), reconstituted and reduced DesII (0.1 mM), and SAM (0.1 mM) in 100 mM Tris•HCl buffer (pH 8.0), containing 1 mM DTT. The assay mixture was incubated anaerobically at room temperature, and the reaction was quenched at different time points by ultrafiltration through a YM10 Diaflo membrane (Amicon) to remove the enzyme. The reaction progress was monitored by HPLC on an analytical CarboPac PA1 column (4 × 250 mm). A linear gradient from 2.5% to 10% solvent B (1 M ammonium acetate, pH 7.0) in solvent A (ddH_2O) over 20 min, followed by a second linear gradient from 10% to 30% solvent B in solvent A over 30 min was employed to analyze the reaction mixtures. The assay mixture was also subjected to analysis by ^{19}F NMR spectroscopy.

*Inhibition Studies of the DesII Enzyme Using TDP-3-fluoro-3,6-dideoxy-D-glucose (**3-29**).* The inhibition studies of the DesII enzyme using TDP-3-fluoro-3,6-dideoxy-D-glucose (**3-29**) were performed using the HPLC activity assay as described in Chapter 2. Reaction mixtures containing 5 μM reconstituted and reduced DesII, 50 μM SAM, and various concentrations of TDP-4-amino-4,6-dideoxy-D-glucose (10 to 100 μM) in 100 mM Tris•HCl buffer (pH 8.0), containing 1 mM DTT were incubated at 25 °C. To these reaction mixtures was added 50 μM TDP-3-fluoro-3,6-dideoxy-D-glucose (**3-29**). Aliquots were taken at four different time points for each of four substrate concentrations. Since the substrate concentration in each sample was known, the percent

conversion as determined by HPLC could be used to calculate the micromoles of product formed for each time point. The amounts of product formed at the four time points for a given substrate concentration were plotted against time, and the slope of each line was the reaction rate at various substrate concentrations. The assay was repeated using various concentrations of the fluorinated substrate analogue (**3-29**). The final concentrations of **3-29** used ranged from 0 to 300 μM. The resulting data were fitted by nonlinear regression data analysis using the equation for competitive inhibition provided within the Grafit program to determine the K_i value.

*Preparation of EPR Samples Using the Natural Substrate (**3-1**), the Fluorinated Substrate Analogue (**3-29**), and the DesV Product (**3-56**).* All samples were prepared anaerobically inside a glovebox under a nitrogen atmosphere, containing less than 5 ppm O_2. In addition, all samples were freshly made prior to the EPR measurements. The purification and reconstitution of DesII protein were carried out as described in Chapter 2. In the preparation of EPR samples, the following were added in the order given and to the specified concentrations: dithionite to 2 mM, SAM to 1.5 mM, 200 μM DesII enzyme, and 200 mM of the natural substrate in 100 mM Tris•HCl buffer, pH 8.0, containing 1 mM DTT. The samples containing either the fluorinated substrate analogue (**3-29**) or the DesV product (**3-56**) were prepared in identical manner and concentration. The final sample volume was 500 μL. The samples were mixed, transferred to EPR tubes, and frozen by immersion of the tubes in cold isopentane (approximately – 140 °C) within 30 sec after mixing. The samples were stored in liquid nitrogen until analysis.

EPR Spectroscopy. EPR spectra were recorded at either 77 K or 100 K on a Bruker EMX EPR spectrometer. A GFS600 transfer line and an ITC503 temperature controller were used to maintain the temperature. An Oxford ESR900 cryostat was used to accommodate the sample. Data analysis was conducted using WinEPR provided by Bruker.

3.3 RESULTS

*Synthesis of TDP-[3-^{2}H]-4-amino-4,6-dideoxy-D-glucose (**3-25**).* TDP-[3-^{2}H]-4-amino-4,6-dideoxy-D-glucose (**3-25**) was synthesized from 1,2:5,6-di-*O*-isopropylidene-α-D-glucofuranose (**3-37**) as shown in Figure 3-7. The deuterium was incorporated into 1,2:5,6-di-*O*-isopropylidene-α-D-*ribo*-hexofuranos-3-ulose (**3-38**) by the reduction of the C3-keto group using $NaBD_4$. The configuration at C-3 of **3-40** was inverted by the S_N2 displacement reaction with a benzoyl group. The isopropylidene protecting groups were removed under acidic conditions with concomitant conversion of [3-^{2}H]-glucofuranose to [3-^{2}H]-glucopyranose (**3-43**). The following steps converting **3-43** to **3-25** were carried out enzymatically. The phosphate group at C-1 of **3-44** was incorporated using hexokinase and phophoglucose mutase in the presence of ATP. [3-^{2}H]-glucose-1-phosphate (**3-44**) was converted to TDP-[3-^{2}H]-4-amino-4,6-dideoxy-D-glucose (**3-25**) using RfbA, RfbB, and DesI enzymes following the procedures established for the preparation of TDP-4-amino-4,6-dideoxy-D-glucose (**3-1**) as described in Chapter 2.

*Synthesis of TDP-3-fluoro-3,6-dideoxy-D-glucose (**3-29**).* TDP-3-fluoro-3,6-dideoxy-D-glucose (**3-29**) was synthesized from 1,2:5,6-di-*O*-isopropylidene-α-D-allofuranose (**3-46**) as shown in Figure 3-8. The fluorine at C-3 was incorporated into **3-**

46 using DASF reagent. The configuration at C-3 of **3-46** was inverted by the S_N2 displacement reaction with a fluoride ion from DASF. The C-6 deoxygenation to make **3-50** was accomplished by selective tosylation of C6-hydroxyl group of **3-48** in the presence of Bu_2SnO. Subsequent hydride reduction of the C6-tosyl group yielded **3-50**. The isopropylidene protecting group at C1 and C2 was removed under acidic conditions. After acetylation of **3-51**, the anomeric carbon was selectively deprotected using H_2NNH_2, affording **3-53**. Benzylphosphorylation of **3-53** generated **3-54**, which was deprotected by hydrogenation followed by basic hydrolysis. The final step involves coupling of **3-55** with TMP-morpholidate, which was prepared following a previously published procedure.

*Deuterium Incorporation into S-adenosylmethionine (SAM) from TDP-[3-^{2}H]-4-amino-4,6-dideoxy-D-glucose (**3-25**).* After anaerobic incubation of the deuterium-labeled substrate (**3-25**), reconstituted and reduced DesII enzyme, and the cofactor SAM for 3 h, the reaction was quenched by ultrafiltration through a YM10 Diaflo membrane (Amicon) to remove the enzyme. The reaction mixture was analyzed by HPLC on an analytical C_{18} column. The SAM cofactor, which eluted at 5.1 min, was collected, concentrated, and then subjected to ESI-MS analysis. ESI-HRMS calcd for $C_{15}H_{21}D_2N_6O_5S$ $[M+H]^+$ 401.1571, found 401.1562. The DesII activity assay using the non-labeled substrate was carried out in parallel. Similarly, the SAM cofactor, which eluted at 5 min, was collected, lyophilized to near dryness, and then subjected to ESI-MS analysis. ESI-HRMS calcd for $C_{15}H_{23}N_6O_5S$ $[M+H]^+$ 399.1450, found 399.1452. The molecular weight increase of two clearly demonstrates that two deuterium atoms were incorporated into SAM. These

results are consistent with the assay conditions where a catalytic amount of SAM was used so that each molecule of SAM was employed multiple times in DesII catalysis.

*DesII Activity Using TDP-3-fluoro-3,6-dideoxy-D-glucose (**3-29**).* After anaerobic incubation of the fluorinated substrate analogue (**3-29**), reconstituted and reduced DesII enzyme, the cofactor SAM, the reaction was quenched at different points by ultrafiltration through a YM10 Diaflo membrane (Amicon) to remove the enzyme. The reaction mixture was analyzed by HPLC on a CarboPac anion exchange column. No formation of the expected product **3-8** (if the DesII reaction proceeds through route A) was observed. Furthermore, ^{19}F NMR spectrum also failed to detect any released fluoride ion. The DesII activity assay in the presence of the natural substrate (TDP-4-amino-4,6-dideoxy-D-glucose, **3-1**, Figure 3-1) was carried out in parallel as a positive control. In the presence of the natural substrate (**3-1**), the formation of TDP-3-keto-4,6-dideoxy-D-glucose (**3-8**) was observed. On the basis of these results, it was concluded that this fluorinated substrate analogue (**3-29**) is not a substrate for the DesII enzyme. The inhibition studies were subsequently performed to determine whether this fluorinated analogue (**3-29**) serves as a competitive inhibitor for the DesII enzyme.

*Inhibition Studies Using TDP-3-fluoro-3,6-dideoxy-D-glucose (**3-29**).* The inhibition data for TDP-3-fluoro-3,6-dideoxy-D-glucose (**3-29**) in the presence of the natural substrate were fitted by nonlinear regression data analysis using the equation for competitive inhibition provided within the Grafit program (Erithacus Software Ltd., Staines, U.K., version 5.0). Lineweaver−Burk plot is shown in the insert of Figure 3-9. Lineweaver−Burk analysis confirms the competitive nature of the inhibition and reveals a K_i of 94.1 ± 5.3 μM.

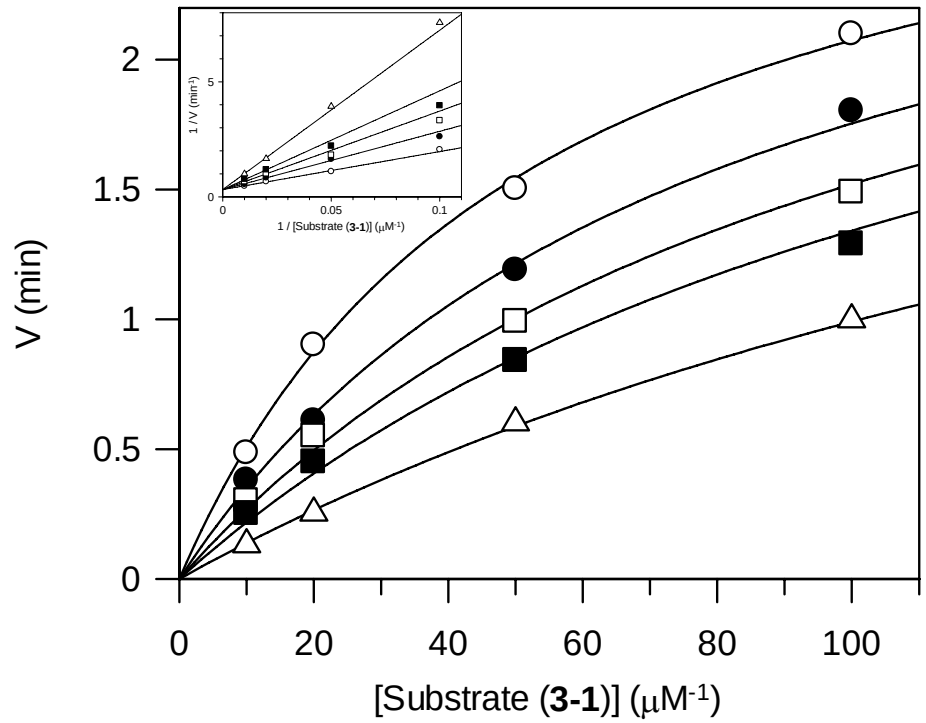

Figure 3-9. Inhibition of DesII by varying amounts of the fluorinated analogue (**3-29**) (○, 0 μM; ●, 50 μM; □, 100 μM; ■, 150 μM; ∆, 300 μM). Insert, Lineweaver−Burk plot showing the competitive nature of the inhibition.

*EPR Studies Using the Natural Substrate (**3-1**), the Fluorinated Substrate Analogue (**3-29**), and the DesV Product (**3-56**).* The EPR spectra in the presence of the natural substrate (**3-1**), the fluorinated substrate (**3-29**), and the DesV product recorded (**3-56**, Figure 3-10) at 9.6 GHz and either 77 K or 100 K displayed no signals for organic radicals. It is likely the lifetime of the radical intermediates is too short to be observed in hand-mixed samples. Rapid freeze-quench EPR spectroscopy will be applied to trap radical intermediates in the future.

3.4 DISCUSSION

Biochemical characterization of DesII presented in Chapter 2 has clearly established that DesII is a radical SAM-dependent C-4 deaminase involved in desosamine biosynthesis. Two possible mechanisms for DesII catalysis have been proposed. The deviation between these two proposed mechanisms occurs after the formation of C3-centered radical intermediate (**3-3**, Figure 3-1). To investigate the C-3 hydrogen atom abstraction by the 5′-deoxyadenosyl radical (**3-2**), TDP-[3-^{2}H]-4-amino-4,6-dideoxy-D-glucose (**3-25**, Figure 3-4) was chemoenzymatically synthesized following the previously established procedures in this laboratory with minor modifications. Deuterium incorporation into SAM using this deuterium-labeled substrate provided the evidence for the first step, the C-3 hydrogen atom abstraction by the 5′-deoxyadenosyl radical (i.e., **3-1**→**3-3**, Figure 3-1), in the proposed mechanisms. The deuterium atom abstraction by the 5′-deoxyadenosyl radical (**3-2**) yields [5′-^{2}H]-5′-deoxyadenosine (**3-26**, Figure 3-4). After either path A or path B, the aminol radical intermediate (**3-6**) in path A or the enol radical intermediate (**3-11**/**3-12**) in path B can reabstract a hydrogen atom or a deuterium atom from the methyl group of [5′-^{2}H]-5′-deoxyadenosine (**3-26**). The hydrogen atom abstraction may dominate due to the isotope effect, which results in the generation of the [5′-^{2}H]-5′-deoxyadenosyl radical. The C-3 deuterium atom abstraction of another molecule of substrate by the [5′-^{2}H]-5′-deoxyadenosyl radical starts the next catalytic cycle and generates [5′-^{2}H$_2$]-5′-deoxyadenosine. The aminol radical intermediate (**3-6**) in path A or the enol radical intermediate (**3-11**/**3-12**) in path B can reabstract either a hydrogen atom or a deuterium atom from the methyl group of [5′-^{2}H$_2$]-5′-deoxyadenosine. Similarly, the hydrogen atom abstraction may dominate again due to the

isotope effect, which results in the generation of the [5′-$^2H_2$]-5′-deoxyadenosyl radical. As reclaiming a hydrogen atom from the methyl group of AdoCD_2H by **3-6** (or **3-11**/**3-12** in path B) is energetically unfavorable, stabilization of the resulting [5′-$^2H_2$]-5′-deoxyadenosyl radical by reforming the $[4Fe\text{-}4S]^+$-[5′-$^2H_2$]-SAM complex may provide the driving force to complete the catalytic cycle (*2*). The mass spectrometry results suggest the formation of [5′-$^2H_2$]-SAM in the presence of TDP-[3-^{2}H]-4-amino-4,6-dideoxy-D-glucose (**3-25**). This result is consistent with that SAM serves as a cofactor in DesII catalysis so that only a catalytic amount of SAM is required for DesII activity.

TDP-3-fluoro-3,6-dideoxy-D-glucose (**3-29**) contains a C4 hydroxyl group instead of a C4 amino group in the natural substrate (**3-1**). This substitution was based on the findings that the DesII enzyme can utilize TDP-D-quinovose (**3-30**, Figure 3-6) as a comparable substrate, which contains a C4 hydroxyl group. The substitution of the C3 hydroxyl group with a fluorine was designed to prevent the deprotonation of 3-OH to the ketyl radical anion intermediate (**3-36**), a key step in the proposed mechanism B (Figure 3-6). If mechanism B is operating, the deprotonation of 3-fluoro in **3-31** could not occur. Consequently, the elimination of the C-4 hydroxyl group facilitated by the formation of the ketyl radical anion (**3-36**) will be prohibited. Alternatively, if mechanism A is the correct mechanism, the radical formation concomitant with 1,2-hydroxyl rearrangement (i.e., **3-31**→**3-34**) is expected to proceed as usual and will afford the C-4-centered radical intermediate (**3-34**). After reabstaction of a hydrogen atom from the 5′-deoxyadenosine, elimination of the fluoride ion in **3-35** will yield the expected product **3-8**. Accordingly, the released fluoride ion could be detected by ^{19}F NMR spectroscopy. The HPLC assay using this fluorinated analogue (**3-29**) along with the ^{19}F NMR results indicate that the

fluorinated substrate analogue **3-29** could not be processed by the DesII enzyme. The subsequent inhibition studies using the HPLC assay established that the fluorinated substrate analogue **3-29** is a competitive inhibitor. Taken together, the results obtained thus far favor mechanism B; that the deprotonation of C-3 hydroxyl group yielding the ketyl radical anion (**3-3**→**3-9**, Figure 3-1) may be an integral part of DesII catalysis. Nevertheless, the possible reactivity differences between the natural substrate (**3-1**) and the fluorinated substrate analogue (**3-29**) need to be noted. For example, the electronegativity differences between a fluorine (electronegativity = 4.0 in the scale of Pauling (*50, 51*)) and an oxygen (electronegativity = 3.5 in the scale of Pauling (*50, 51*)) might influence the stability of the resulting C3-centered radical intermediates (**3-3** in Figure 3-1 and **3-31** in Figure 3-6). Consequently, the failure of the fluorinated substrate analogue (**3-29**) to serve as a substrate caused by the radical stability differences cannot be completely ruled out. Thus, the synthesis of TDP-[3-^{2}H]-3-fluoro-3,6-dideoxy-D-glucose to investigate whether the C-3 hydrogen atom abstraction indeed occurs in the fluorinated substrate analogue is necessary to provide more solid evidence to support mechanism B.

With the natural substrate (**3-1**), the fluorinated substrate analogue (**3-29**), TDP-3-amino-3,4,6-trideoxy-D-glucose (**3-56**, Figure 3-10a) in hand, the attempt to trap radical intermediates was preliminarily tested using hand-mixed samples by EPR spectroscopy. However, the EPR spectra exhibited no detectable organic radical signals at either 77 K or 100 K. The rapid freeze-quench EPR spectroscopy is a useful technique to trap radical intermediates and can be applied to detect and characterize radical intermediates in the proposed mechanisms. The natural substrate (**3-1**) contains a C-3 hydroxyl group, which

can stabilize the C3-centered radical intermediate (**3-3**) by the non-bonded electron pairs on oxygen (Figure 3-10a). This "three-electron bonding" can be described in terms of resonance theory using ionic structures (Figure 3-10b) (*52*). Similar stabilization effects can be applied to the non-bonded electron pairs on fluorine in **3-31** and nitrogen in **3-57** (Figure 3-10a). Furthermore, after the formation of the C-3-centered radical intermediate **3-57**, no substitute at C-4 on the hexose ring can be eliminated. In this scenario, it is possible that the radical may stay at the C-3 position of **3-57** if it is not quenched by any reactive species in the enzyme.

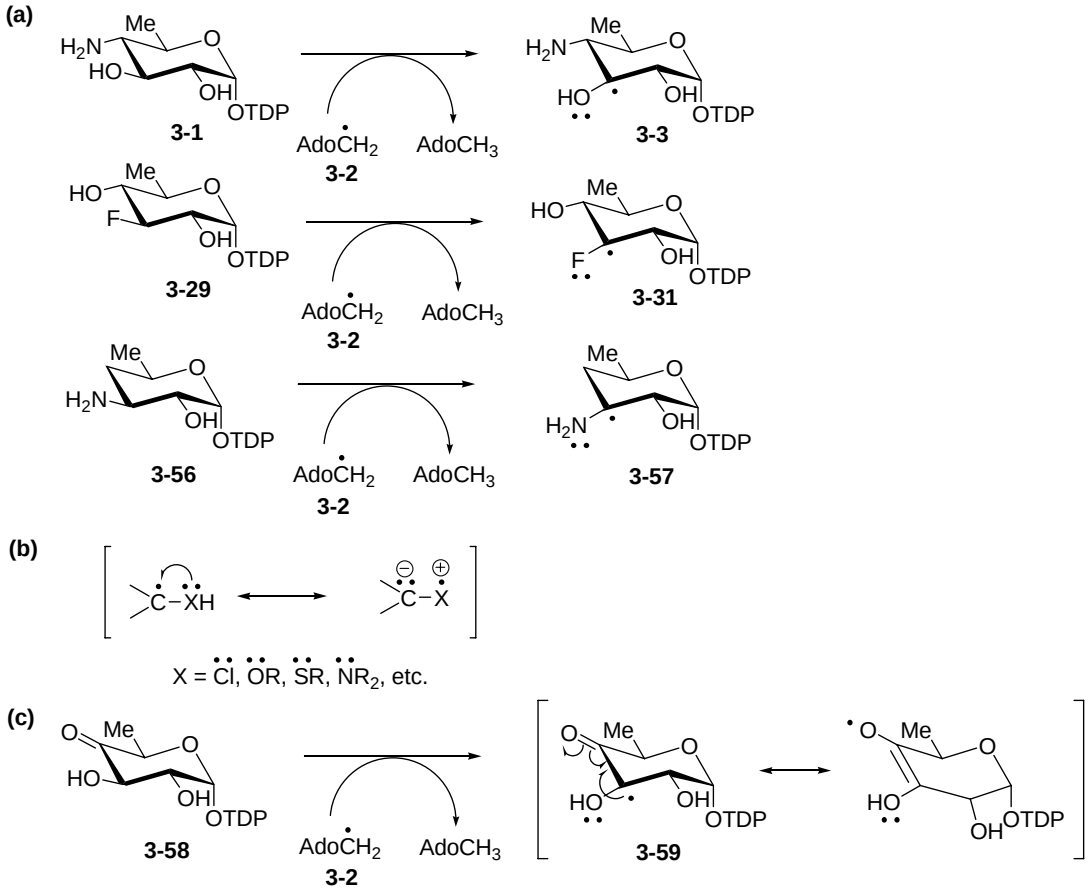

Figure 3-10. (a) The structures of the compounds used in EPR spectroscopic studies. (b) Resonance theoretical description of three-electron bonding (52). (c) The stabilization of the radical intermediate 3-59 through resonance effects.

In addition to the DesV product in desosamine biosynthesis pathway, TDP-4-keto-6-deoxy-D-glucose (**3-58**) may also produce a relatively stable C3-centered radical intermediate (**3-59**, Figure 3-10c). The C3-centered radical on **3-59** can be stabilized by the adjacent carbonyl group through resonance effects (Figure 3-10c). Taken together, the fluorinated substrate analogue (**3-29**), the DesII natural substrate (**3-1**), the DesI substrate (**3-58**), and the DesV product (**3-56**) in desosamine biosynthesis pathway can be potentially employed in future rapid freeze-quench EPR spectroscopic studies.

The conclusion drawn from the initial mechanistic studies presented in this chapter is twofold. First, the studies of deuterium incorporation into SAM using TDP-[3-^{2}H]-4-amino-4,6-dideoxy-D-glucose (**3-25**) provide solid evidence for the first hydrogen atom abstraction step in the proposed mechanism. The preparation of the deuterium-labeled substrate sets the stage for future kinetic isotope effect studies. Second, the inhibition studies using TDP-3-fluoro-3,6-dideoxy-D-glucose (**3-29**) suggest that the deprotonation of the C-3 hydroxyl group is likely important for DesII catalysis. Additionally, the strategy employed to synthesize the C-3 fluorinated substrate may be applied to prepare potential substrate analogues with various functional groups at the C-3 position as shown in Figure 3-11. The turnover of TDP-D-quinovose (**3-30**) by DesII has opened the possibility to synthesize mechanistic probes with a C-4 hydroxyl substitute. As such, the synthetic strategy can be simplified without the need to incorporate an amino functional group at the C-4 position. The preparation of various analogues could be useful for future rapid freeze-quench EPR spectroscopic studies with the potential to trap radical intermediates. Taken together, the initial mechanistic studies pave the road for further mechanistic analysis. The future kinetic studies and characterization of radical

intermediates by rapid freeze-quench EPR spectroscopy will provide further insights into the catalytic mechanism underlying C-4 deoxygenation catalyzed by DesII in desosamine biosynthesis.

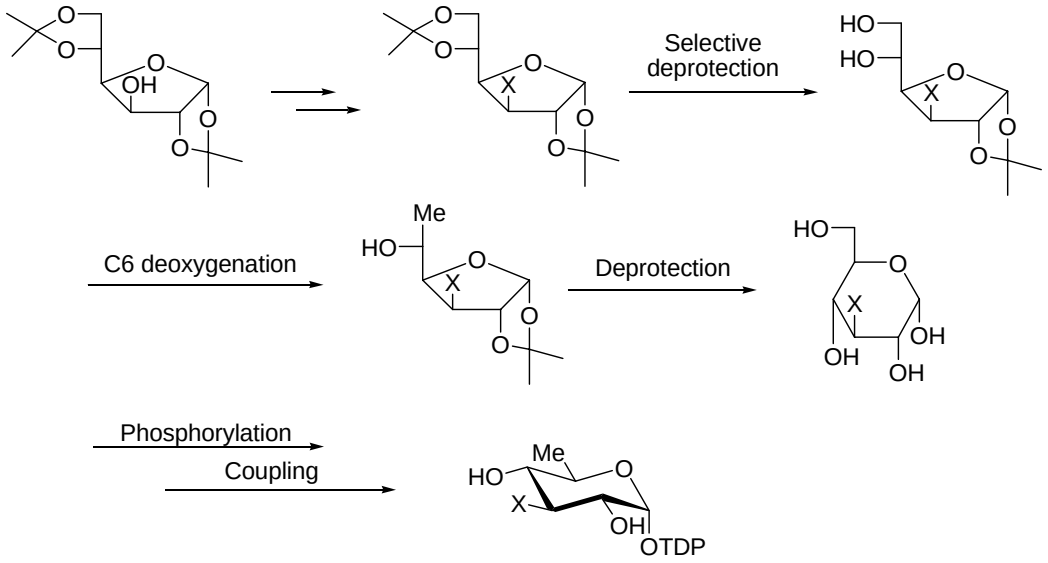

Figure 3-11. Feasible strategies to synthesize the potential substrate analogues with various functional groups at the C-3 position on the hexose ring.

3.5 REFERENCE

1. Sofia, H. J., Chen, G., Hetzler, B. G., Reyes-Spindola, J. F., and Miller, N. E. (2001) Radical SAM, a novel protein superfamily linking unresolved steps in familiar biosynthetic pathways with radical mechanisms: functional characterization using new analysis and information visualization methods, *Nucleic Acids Research 29*, 1097-1106.

2. Chen, D., Walsby, C., Hoffman, B. M., and Frey, P. A. (2003) Coordination and mechanism of reversible cleavage of *S*-adenosylmethionine by the [4Fe-4S] center in lysine 2,3-aminomutase, *J. Am. Chem. Soc. 125*, 11788-11789.

3. LoBrutto, R., Bandarian, V., Magnusson, O. T., Chen, X., Schramm, V. L., and Reed, G. H. (2001) 5'-Deoxyadenosine contacts the substrate radical intermediate in the active site of ethanolamine ammonia-lyase: ^{2}H and ^{13}C electron nuclear double resonance studies, *Biochemistry 40*, 9-14.

4. Sandala, G. M., Smith, D. M., and Radom, L. (2005) Divergent mechanisms of suicide inactivation for ethanolamine ammonia-lyase, *J. Am. Chem. Soc. 127*, 8856-8864.

5. Hayon, E., and Simic, M. (1974) Acid-base properties of free radicals in solution, *Acc. Chem. Res. 7*, 114-121.

6. Buckel, W. (1996) Unusual dehydrations in anaerobic bacteria: considering ketyls (radical anions) as reactive intermediates in enzymic reactions, *FEBS Lett. 389*, 20-24.

7. Buckel, W. (2001) Unusual enzymes involved in five pathways of glutamate fermentation, *Appl. Microbiol. Biotechnol. 57*, 263-273.

8. Buckel, W., and Golding, B. T. (1998) Radical species in the catalytic pathways of enzymes from anaerobes, *FEMS Microbiol. Rev. 22*, 523-541.

9. Buckel, W., Kratky, C., and Golding, B. T. (2006) Stabilisation of methylene radicals by cob(II)alamin in coenzyme B_{12} dependent mutases, *Chem. Eur. J. 12*, 352-262.

10. Kim, J., Hetzel, M., Boiangiu, C. D., and Buckel, W. (2004) Dehydration of (*R*)-2-hydroxyacyl-CoA to enoyl-CoA in the fermentation of α-amino acids by anaerobic bacteria, *FEMS Microbiol. Rev. 28*, 455-468.

11. Kim, J., Darley, D. J., Buckel, W., and Pierik, A. J. (2008) An allylic ketyl radical intermediate in clostridial amino-acid fermentation, *Nature 452*, 239-242.

12. Escalettes, F., Florentin, D., Tse Sum Bui, B., Lesage, D., and Marquet, A. (1999) Biotin synthase mechanism: evidence for hydrogen transfer from the substrate into deoxyadenosine, *J. Am. Chem. Soc. 121*, 3571-3578.

13. Frey, M., Rothe, M., Wagner, A. F. V., and Knappe, J. (1994) Adenosylmethionine-dependent synthesis of the glycyl radical in pyruvate formate-lyase by abstraction of the glycine C-2 *pro-S* hydrogen atom. Studies of [^{2}H]glycine-substituted enzyme and peptides homologous to the glycine 734 site, *J. Biol. Chem. 269*, 12432-12437.

14. Cicchillo, R. M., Iwig, D. F., Jones, A. D., Nesbitt, N. M., Baleanu-Gogonea, C., Souder, M. G., Tu, L., and Booker, S. J. (2004) Lipoyl synthase requires two equivalents of *S*-adenosyl-L-methionine to synthesize one equivalent of lipoic acid, *Biochemistry 43*, 6378-6386.

15. Yokoyama, K., Numakura, M., Kudo, F., Ohmori, D., and Eguchi, T. (2007) Characterization and mechanistic study of a radical SAM dehydrogenase in the biosynthesis of butirosin, *J. Am. Chem. Soc. 129*, 15147-15155.

16. Pongdee, R., and Liu, H.-w. (2004) Elucidation of enzyme mechanisms using fluorinated substrate analogues, *Bioorg. Chem. 32*, 393-437.

17. O'Hagan, D., and Rzepa, H. S. (1997) Some influences of fluorine in bioorganic chemistry, *Chem. Commun.*, 645–652.

18. Stabel, A., Dasaradhi, L., O'Hagan, D., and Rabe, J. P. (1995) Scanning tunneling microscopy imaging of single fluorine atom substitution in stearic acid, *Langmuir 11*, 1427-1430.

19. Poulter, C. D., and Satterwhite, D. M. (1977) Mechanism of the prenyl transfer reaction. Studies with (*E*)- and (*Z*)-3-trifluoromethyl-2-buten-1-yl pyrophosphate, *Biochemistry 16*, 5470-5478.

20. Muehlbacher, M., and Poulter, C. D. (1985) Isopentenyl diphosphate:dimethylallyl diphosphate isomerase. Irreversible inhibition of the enzyme by active-site-directed covalent attachment, *J. Am. Chem. Soc. 107*, 8307-8308.

21. Muehlbacher, M., and Poulter, C. D. (1988) Isopentenyl-diphosphate isomerase: inactivation of the enzyme with active-site-directed irreversible inhibitors and transition state analogs, *Biochemistry 27*, 7315-7328.

22. Poulter, C. D., Muehlbacher, M., and Davis, D. R. (1989) Isopentenyl diphosphate isomerase. Mechanism of active-site-directed irreversible inhibition by 3-(fluoromethyl)-3-butenyl diphosphate, *J. Am. Chem. Soc. 111*, 3740-3742.

23. Reardon, J. E., and Abeles, R. H. (1986) Mechanism of action of isopentenyl pyrophosphate isomerase: evidence for a carbonium ion intermediate, *Biochemistry 25*, 5609-5616.

24. Withers, S. G., Rupitz, K., and Street, I. P. (1988.) 2-Deoxy-2-fluoro-D-glycosyl fluorides. A new class of specific mechanism-based glycosidase inhibitors, *J. Biol. Chem. 263*, 7929-7932.

25. Withers, S. G., Street, I. P., Bird, P., and Dolphin, D. H. (1987) 2-Deoxy-2-fluoroglucosides: a novel class of mechanism-based glucosidase inhibitors, *J. Am. Chem. Soc. 109*, 7530-7531.

26. Kim, D. H., Lees, W. J., Haley, T. M., and Walsh, C. T. (1995) Kinetic characterization of the inactivation of UDP-GlcNAc enolpyruvyl transferase by (*Z*)-3-fluorophosphoenolpyruvate: Evidence for two oxocarbenium ion intermediates in enolpyruvyl transfer catalysis, *J. Am. Chem. Soc. 117*, 1494-1502.

27. Reddick, J. J., Nicewonger, R., and Begley, T. P. (2001) Mechanistic studies on thiamin phosphate synthase: Evidence for a dissociative mechanism, *Biochemistry 40*, 10095-10102.

28. Molitor, E. J., Paschal, B. M., and Liu, H.-w. (2003) Cyclopropane fatty acid synthase from *Escherichia coli*: Enzyme purification and inhibition by vinylfluorine and epoxide-containing substrate analogues, *ChemBioChem 4*, 1352-1356.

29. Santi, D. V., McHenry, C. S., and Sommer, H. (1974) Mechanism of interaction of thymidylate synthetase with 5-fluorodeoxyuridylate, *Biochemistry 13*, 471-481.

30. Marcotte, P. A., and Robinson, C. H. (1982) Inhibition and inactivation of estrogen synthetase (aromatase) by fluorinated substrate analogues, *Biochemistry 21*, 2773-2778.

31. Chang, C.-W. T., Chen, X. H., and Liu, H.-w. (1998) CDP-6-deoxy-6,6-difluoro-D-glucose: A mechanism-based inhibitor for CDP-D-glucose 4,6-dehydratase, *J. Am. Chem. Soc. 120*, 9698-9699.

32. Zhao, Z., Liu, P., Murakami, K., Kuzuyama, T., Seto, H., and Liu, H.-w. (2002) Mechanistic studies of HPP epoxidase: configuration of the substrate governs its enzymatic fate, *Angew. Chem. Int. Ed. 41*, 4529-4532.

33. Leriche, C., He, X., Chang, C.-w. T., and Liu, H.-w. (2003) Reversal of the apparent regiospecificity of NAD(P)H-dependent hydride transfer: The properties of the difluoromethylene group, a carbonyl mimic, *J. Am. Chem. Soc. 125*, 6348-6349.

34. Bornemann, S., Ramjee, M. K., Balasubramanian, S., Abell, C., Coggins, J. R., Lowe, D. J., and Thorneley, R. N. (1995) *Escherichia coli* chorismate synthase catalyzes the conversion of (6*S*)-6-fluoro-5-enolpyruvylshikimate-3-phosphate to 6-fluorochorismate. Implications for the enzyme mechanism and the antimicrobial action of (6*S*)-6-fluoroshikimate, *J. Biol. Chem. 270*, 22811-22815.

35. Lauhon, C. T., and Bartlett, P. A. (1994) Substrate analogs as mechanistic probes for the bifunctional chorismate synthase from *Neurospora crassa*, *Biochemistry 33*, 14100-14108.

36. Ramjee, M. N., Balasubramanian, S., Abell, C., Coggins, J. R., Davies, G. M., Hawkes, T. R., Lowe, D. J., and Thorneley, R. N. F. (1992) Reaction of (6*R*)-6-fluoroEPSP with recombinant *Escherichia coli* chorismate synthase generates a stable flavin mononucleotide semiquinone radical, *J. Am. Chem. Soc. 114*, 3151-3153.

37. Pieper, P. A., Yang, D.-y., Zhou, H.-q., and Liu, H.-w. (1997) 3-Deoxy-3-fluoropyridoxamine 5'-phosphate: synthesis and chemical and biological properties of a coenzyme B_6 analog, *J. Am. Chem. Soc. 119*, 1809-1817.

38. Hallis, T. M., Zhao, Z., and Liu, H.-w. (2000) New insights into the mechanism of CDP-D-tyvelose 2-epimerase: An enzyme-catalyzing epimerization at an unactivated stereocenter, *J. Am. Chem. Soc. 122*, 10493-10503.

39. Zhao, Z., and Liu, H.-w. (2001) Synthesis of a deoxy sugar dinucleotide containing an exo-difluoromethylene moiety as a mechanistic probe for studying enzymes involved in unusual sugar biosynthesis, *J. Org. Chem. 66*, 6810-6815.

40. Zhang, Q., and Liu, H.-w. (2001) Mechanistic investigation of UDP-galactopyranose mutase from *Escherichia coli* using 2- and 3-fluorinated UDP-galactofuranose as probes, *J. Am. Chem. Soc. 123*, 6756-6766.

41. Pieper, P. A., Guo, Z., and Liu, H.-w. (1995) Mechanistic studies of the biosynthesis of 3,6-dideoxy sugars: stereochemical analysis of C-3 deoxygenation, *J. Am. Chem. Soc. 117*, 5158-5159.

42. Kovac, P., and Glaudemans, C. P. J. (1983) Synthesis of methyl 3-deoxy-3-fluoro-β-D-galactopyranoside, *Carbohydr. Res. 123*, 326-331.

43. Jeong, L. S., Lim, B. B., and Marquez, V. E. (1994) Synthesis of a 2,3-dideoxy-2,3-difluorofuranose with the D-*lyxo* configuration. An intramolecular rearrangement of methyl 5-*O*-benzoyl-2,3-dideoxy-2,3-difluoro-D-lyxofuranoside observed during the attempted synthesis of 1-(2,3-dideoxy-2,3-difluoro-β-D-lyxofuranosyl)thymine, *Carbohydr. Res. 262*, 103-114.

44. Martinelli, M. J., Vaidyanathan, R., Pawlak, J. M., Nayyar, N. K., Dhokte, U. P., Doecke, C. W., Zollars, L. M. H., Moher, E. D., Van Khau, V., and Kosmrlj, B. (2002) Catalytic regioselective sulfonylation of α-chelatable alcohols: scope and mechanistic insight, *J. Am. Chem. Soc. 124*, 3578-3583.

45. Valverde, S., Hernandez, A., Herradon, B., Rabanal, R. M., and Martin-Lomas, M. (1987) The synthesis of (-)-anamarine, *Tetrahedron 43*, 3499-3504.

46. Excoffier, G., Gagnare, D., and Utille, J. P. (1975) Synthesis of oligosaccharides on polymeric supports. V. Selective cleavage by hydrazine of the anomeric acetyl groups of acetylated glycosyl residues, *Carbohydr. Res. 39*, 368-373.

47. Chen, H., Yamase, H., Murakami, K., Chang, C.-w., Zhao, L., Zhao, Z., and Liu, H.-w. (2002) Expression, purification, and characterization of two *N*,*N*-dimethyltransferases, TylM1 and DesVI, involved in the biosynthesis of mycaminose and desosamine, *Biochemistry 41*, 9165-9183.

48. Moffatt, J. G., and Khorana, H. G. (1961) Nucleoside polyphosphates. X. The synthesis and some reactions of nucleoside 5'-phosphoromorpholidates and related compounds. Improved methods for the preparation of nucleoside 5'-polyphosphates, *J. Am. Chem. Soc. 83*, 649-658.

49. Wittmann, V., and Wong, C.-H. (1997) 1*H*-Tetrazole as catalyst in phosphoromorpholidate coupling reactions: Efficient synthesis of GDP-fucose, GDP-mannose, and UDP-galactose, *J. Org. Chem. 62*, 2144-2145.

50. Allen, L. C. (1989) Electronegativity is the average one-electron energy of the valence-shell electrons in ground-state free atoms, *J. Am. Chem. Soc. 111*, 9003-9014.

51. Pauling, L. (1960) *The Nature of the Chemical Bond and the Structure of Molecules and Crystals: an Introduction to Modern Structural Chemistry*, 3nd ed. ed., Cornell Univ. Press, Ithaca, NY.

52. Bauld, N. L. (1997) *Radicals, Radical Ions, and Triplets: The Spin-Bearing Intermediates of Organic Chemistry*, Wiley, New York, NY.

Appendix

LIST OF ABBREVIATIONS

5′-dA	5′-Deoxyadenosine
Ado	Adenosine
AdoCbl	Adenosylcobalamin
ARR	Anaerobic ribonucleotide reductase
ATP	Adenosine triphosphate
ATCC	American Type Culture Collection
Bn	Benzyl group
BSA	Bovine serum albumen
Bz	Benzoyl group
CDP	Cytosine diphosphate
CI	Chemical ionization
CMP	Cytosine monophosphate
CoA	Coenzyme A
CTP	Cytosine triphosphate
DAST	Diethylaminosulfur trifluoride
DCPIP	2,6-Dichlorophenolindophenol
DFT	Density functional theory
DMAP	4-Dimethylaminopyridine
DMF	*N*,*N*-Dimethylforaminde
DMSO	Dimethylsulfoxide
DNA	Deoxyribonucleic acid
dUDP	Deoxyuridine triphosphate

DTT	Dithiothreitol
E_1	CDP-6-deoxy-L-*threo*-D-*glycero*-4-hexulose-3-dehydrase
E_3	CDP-6-deoxy-L-*threo*-D-*glycero*-4-hexulose-3-dehydrase reductase
E_{od}	NDP-hexose 4,6-dehydratase
E_p	Glucose-1-phosphate nucleotide transferase
EDTA	Ethylenediaminetetraacetic acid
ENDOR	Electron nuclear double resonance
ESI	Electrospray ionization
EPR	Electron paramagnetic resonance
FAB	Fast atom bombardment
FAD	Flavin adenine dinucleotide
FMN	Flavin mononucleotide
FPLC	Fast protein liquid chromatography
GDP	Guanosine diphosphate
L-Glu	L-Glutamic acid
HPLC	High performance liquid chromatography
IPTG	Isopropyl-β-D-thiogalactoside
KPi	Potassium phosphate
LAM	Lysine 2,3-aminomutase
LB medium	Luria-Bertani medium
LCP	Lipoyl-carrying protein
LPS	Lipopolysaccaride
m-CPBA	*m*-Chloroperoxybenzoic acid

Met	Methionine
MS	Mass spectrometry
NAD+	Nicotinamide adenine dinucleotide, oxidized form
NADH	Nicotinamide adenine dinucleotide, reduced form
NADP	Nicotinamide adenine dinucleotide phosphate, oxidized form
NADPH	Nicotinamide adenine dinucleotide phosphate, reduced form
NDK	Nucleotide diphosphate kinase
NDP	Nucleotide diphosphate
NMR	Nuclear magnetic resonance
OD	Optical density
PAGE	Polyacrylamide gel electrophoresis
PCR	Polymerase chain reaction
PDC	Pyridinium dichromate
PEP	Phosphoenolpyruvate
PFL	Pyruvate formate lyase
PKS	Polyketide synthase
PLP	Pyridoxal 5′-phosphate
PMP	Pyridoxamine 5′-phosphate
RNR	Ribonucleotide reductase
SAM	*S*-Adenosylmethionine
SDS	Sodium dodecyl sulfate
S_N2	Bimolecular nucleophilic substitution

TDP	Thymidine diphosphate
TFA	Trifluoroacetic acid
THF	Tetrahydrofuran
TK	Thymidine kinase
TLC	Thin layer chromatography
TMK	Thymidylate kinase
TMP	Thymidine monophosphate
Tris	Tris(hydroxymethyl)aminomathane
Ts	*p*-Toluenesulfonyl group (tosyl group)
TTP	Thymidine triphosphate
UDP	Uridine diphosphate
UV	Ultraviolet
XAS	X-ray absorption spectroscopy

References

1. Aberg, A., Ormo, M., Nordlund, P., and Sjöberg, B. M. (1993) Autocatalytic generation of dopa in the engineered protein R2 F208Y from *Escherichia coli* ribonucleotide reductase and crystal structure of the dopa-208 protein, *Biochemistry 32*, 9845-9850.

2. Akhtar, M. (1994) The modification of acetate and propionate side chains during the biosynthesis of haem and chlorophills: mechanistic and stereochemical studies, *Ciba Found. Symp. 180*, 131-155.

3. Allard, S. T. M., Beis, K., Giraud, M.-F., Hegeman, A. D., Gross, J. W., Wilmouth, R. C., Whitfield, C., Graninger, M., Messner, P., Allen, A. G., Maskell, D. J., and Naismith, J. H. (2002) Toward a structural understanding of the dehydratase mechanism, *Structure 10*, 81-92.

4. Allen, L. C. (1989) Electronegativity is the average one-electron energy of the valence-shell electrons in ground-state free atoms, *J. Am. Chem. Soc. 111*, 9003-9014.

5. Allen, R. M., Chatterjee, R., Ludden, P. W., and Shah, V. K. (1995) Incorporation of iron and sulfur from NitB cofactor into the iron-molybdenum cofactor of nitrogenase, *J. Biol. Chem. 270*, 26890-26896.

6. Andrews, P. (1964) Estimation of the molecular weights of proteins by Sephadex gel-filtration, *Biochem. J. 91*, 222-233.

7. Ballinger, M. D., Frey, P. A., and Reed, G. H. (1992) Structure of a substrate radical intermediate in the reaction of lysine 2,3-aminomutase, *Biochemistry 31*, 10782-10789.

8. Ballinger, M. D., Frey, P. A., Reed, G. H., and LoBrutto, R. (1995) Pulsed electron paramagnetic resonance studies of the lysine 2,3-aminomutase substrate radical: Evidence for participation of pyridoxal 5'-phosphate in a radical rearrangement, *Biochemistry 34*, 10086-10093.

9. Ballinger, M. D., Reed, G. H., and Frey, P. A. (1992) An organic radical in the lysine 2,3-aminomutase reaction, *Biochemistry 31*, 949-953.

10. Baltz, R. H. (2006) Molecular engineering approaches to peptide, polyketide and other antibiotics, *Nature Biotechnology 24*, 1533 - 1540

11. Bandarian, V., and Reed, G. H. (1999) *Ethanolamine ammonia-lyase*.

12. Bauld, N. L. (1997) *Radicals, Radical Ions, and Triplets: The Spin-Bearing Intermediates of Organic Chemistry*, Wiley, New York, NY.

13. Becker, A., Küster, H., Niehaus, K., and Pühler, A. (1995) Extension of the *Rhizobium meliloti* succinoglycan biosynthesis gene cluster: identification of the *exsA* gene encoding an ABC transporter protein, and the *exsB* gene which probably codes for a regulator of succinoglycan biosynthesis, *Mol. Gen. Genet. 249*, 487-497.

14. Begley, T. P., Xi, J., Kinsland, C., Taylor, S., and McLafferty, F. (1999) The enzymology of sulfur activation during thiamin and biotin biosynthesis, *Curr. Opin. Chem. Biol. 3*, 623-629.

15. Beinert, H. (1983) Semi-micro methods for analysis of labile sulfide and of labile sulfide plus sulfane sulfur in unusually stable iron-sulfur proteins, *Anal. Biochem. 131*, 373-378.

16. Berkovitch, F., Nicolet, Y., Wan, J. T., Jarrett, J. T., and Drennan, C. L. (2004) Crystal structure of biotin synthase, an *S*-adenosylmethionine-dependent radical enzyme, *Science 303*, 76-80.

17. Bianchi, V., Haggaard-Ljungquist, E., Pontis, E., and Reichard, P. (1995) Interruption of the ferredoxin (flavodoxin) $NADP^+$ oxidoreductase gene of *Escherichia coli* does not affect anaerobic growth but increases sensitivity to paraquat, *J. Bacteriol. 177*, 4528-4531.

18. Boll, R., Hofmann, C., Heitmann, B., Hauser, G., Glaser, S., Koslowski, T., Friedrech, T., and Bechthold, A. (2006) The active conformation of avilamycin A is conferred by AviX12, a radical AdoMet enzyme, *J. Biol. Chem. 281*, 14756-14763.

19. Booker, S. J., Cicchillo, R. M., and Grove, T. L. (2007) Self-sacrifice in radical *S*-adenosylmethionine proteins, *Curr. Opin. Chem. Biol. 11*, 543-552.

20. Borisova, S. A., Zhang, C., Takahashi, H., Zhang, H., Wong, A. W., Thorson, J. S., and Liu, H.-w. (2005) Substrate specificity of the macrolide-glycosylating enzyme pair DesVII/DesVIII: opportunities, limitations, and mechanistic hypotheses, *Angew. Chem. Int. Ed. 45*, 2748-2753.

21. Borisova, S. A., Zhao, L., Melancon, C. E., III , Kao, C.-L., and Liu, H.-w. (2004) Characterization of the glycosyltransferase activity of DesVII: analysis of and implications for the biosynthesis of macrolide antibiotics, *J. Am. Chem. Soc. 126*, 6534-6535.

22. Bornemann, S., Ramjee, M. K., Balasubramanian, S., Abell, C., Coggins, J. R., Lowe, D. J., and Thorneley, R. N. (1995) *Escherichia coli* chorismate synthase catalyzes the conversion of (6*S*)-6-fluoro-5-enolpyruvylshikimate-3-phosphate to 6-fluorochorismate. Implications for the enzyme mechanism and the antimicrobial action of (6*S*)-6-fluoroshikimate, *J. Biol. Chem. 270*, 22811-22815.

23. Bradford, M. M. (1976) A rapid and sensitive method for the quantitation of microgram quantities of protein utilizing the principle of protein-dye binding, *Anal. Biochem. 72*, 248-254.

24. Brede, D. A., Faye, T., Johnsborg, O., Odegard, I., Nes, I. F., and Holo, H. (2004) Molecular and genetic characterization of propionicin F, a bacteriocin from *Propionibacterium freudenreicii*, *Appl. Environ. Microbiol. 70*, 7303-7310.

25. Broach, R. B., and Jarrett, J. T. (2006) Role of the $[2Fe\text{-}2S]^{2+}$ cluster in biotin synthase: mutagenesis of the atypical metal ligand arginine 260, *Biochemistry 45*, 14166-14174.

26. Buckel, W. (1996) Unusual dehydrations in anaerobic bacteria: considering ketyls (radical anions) as reactive intermediates in enzymic reactions, *FEBS Lett. 389*, 20-24.

27. Buckel, W. (2001) Unusual enzymes involved in five pathways of glutamate fermentation, *Appl. Microbiol. Biotechnol. 57*, 263-273.

28. Buckel, W., and Golding, B. T. (1998) Radical species in the catalytic pathways of enzymes from anaerobes, *FEMS Microbiol. Rev. 22*, 523-541.

29. Buckel, W., Kratky, C., and Golding, B. T. (2006) Stabilisation of methylene radicals by cob(II)alamin in coenzyme B_{12} dependent mutases, *Chem. Eur. J. 12*, 352-262.

30. Buis, J. M., Cheek, J., Kalliri, E., and Broderick, J. B. (2006) Characterization of an active spore photoproduct lyase, a DNA repair enzyme in the radical *S*-adenosylmethionine superfamily, *J. Biol. Chem. 281*, 25994-26003.

31. Carter, R. A., Ericsson, S. A., Corn, C. D., Weyerts, P. R., Dart, M. G., Escue, S. G., and Mesta, J. (1998) Assessing the fertility potential of equine semen samples using the reducible dyes methylene green and resazurin, *Arch. Androl. 40*, 59-66.

32. Chang, C. H., Ballinger, M. D., Reed, G. H., and Frey, P. A. (1996) Lysine 2,3-aminomutase: rapid mix-quench electron paramagnetic resonance studies establishing the kinetic competence of a substrate-based radical intermediate, *Biochemistry 35*, 11081-11084.

33. Chang, C.-w., Zhao, L., Yamase, H., and Liu, H.-w. (2000) DesVI: a new member

of the sugar *N*,*N*-dimethyltransferase family involved in the biosynthesis of desosamine, *Angew. Chem. In. Ed. 39*, 2160-2163.

34. Chang, C.-W. T., Chen, X. H., and Liu, H.-w. (1998) CDP-6-deoxy-6,6-difluoro-D-glucose: A mechanism-based inhibitor for CDP-D-glucose 4,6-dehydratase, *J. Am. Chem. Soc. 120*, 9698-9699.

35. Chang, C.-W. T., Johnson, D. A., Bandarian, V., Zhou, H., LoBrutto, R., Reed, G. H., and Liu, H.-w. (2000) Characterization of a unique coenzyme B_6 radical in the ascarylose biosynthetic pathway, *J. Am. Chem. Soc. 122*, 4239-4240.

36. Chen, D., Walsby, C., Hoffman, B. M., and Frey, P. A. (2003) Coordination and mechanism of reversible cleavage of *S*-adenosylmethionine by the [4Fe-4S] center in lysine 2,3-Aminomutase, *J. Am. Chem. Soc. 125*, 11788-11789.

37. Chen, H., Agnihotri, G., Guo, Z., Que, N. L. S., Chen, X. H., and Liu, H.-w. (1999) Biosynthesis of mycarose: isolation and characterization of enzymes involved in the C-2 deoxygenation *J. Am. Chem. Soc. 121*, 8124-8125.

38. Chen, H., Yamase, H., Murakami, K., Chang, C.-w., Zhao, L., Zhao, Z., and Liu, H.-w. (2002) Expression, purification, and characterization of two *N*,*N*-dimethyltransferases, TylM1 and DesVI, involved in the biosynthesis of mycaminose and desosamine, *Biochemistry 41*, 9165-9183.

39. Ching, Y. P., Qi, Z., and Wang, J. H. (2000) Cloning of three neuronal Cdk5 activator binding proteins, *Gene 242*, 285-294.

40. Chirpich, T. P., Zappia, V., Costilow, R. N., and Barker, H. A. (1970) Lysine 2,3-aminomutase. Purification and properties of a pyridoxal phosphate and *S*-adenosylmethionine-activated enzyme, *J. Biol. Chem. 245*, 1778-1789.

41. Cho, K. B., Himo, F., Graslund, A., and Siegbahn, P. E. M. J. (2001) The substrate reaction mechanism of class III anaerobic ribonucleotide reductase, *J. Phys. Chem. B 105*, 6445-6452.

42. Christen, P., and Mehta, P. K. (2001) From cofactor to enzymes. The molecular evolution of pyridoxal 5'-phosphate-dependent enzymes, *Chem. Rec. (New York, NY) 1*, 436-447.

43. Cicchillo, R. M., and Booker, S. J. (2005) Mechanistic investigations of lipoic acid biosynthesis in *Escherichia coli*: Both sulfur atoms in lipoic acid are contributed by the same lipoyl synthase polypeptide, *J. Am. Chem. Soc. 127*, 2860-2861.

44. Cicchillo, R. M., Iwig, D. F., Jones, A. D., Nesbitt, N. M., Baleanu-Gogonea, C., Souder, M. G., Tu, L., and Booker, S. J. (2004) Lipoyl synthase requires two

equivalents of *S*-adenosyl-L-methionine to synthesize one equivalent of lipoic acid, *Biochemistry 43*, 6378-6386.

45. Cicchillo, R. M., Lee, K.-H., Baleanu-Gogonea, C., Nesbitt, N. M., Krebs, C., and Booker, S. J. (2004) *Escherichia coli* lipoyl synthase binds two distinct [4Fe–4S] clusters per polypeptide, *Biochemistry 43*, 11770-11781.

46. Cone, M. C., Yin, X., Grochowski, L. L., Parker, M. R., and Zabriskie, T. M. (2003) The blasticidin S biosynthesis gene cluster from *Streptomyces griseochromogenes*: Sequence analysis, organization, and initial characterization, *ChemBioChem 4*, 821-828.

47. Conradt, H., Hohmann-Berger, M., Hohmann, H. P., Blaschowski, H. P., and Knappe, J. (1984) Pyruvate formate-lyase (inactive form) and pyruvate formate-lyase activating enzyme of *Escherichia coli*: isolation and structural properties, *J. Arch. Biochem. Biophys. 228*, 133-142.

48. Cronan, J. E., Zhao, X., and Jiang, Y. (2005) Function, attachment and synthesis of lipoic acid in *Escherichia coli*, *Adv. Microb. Physiol. 50*, 103–146.

49. Davis, D. J., and Pietro, A. S. (1977) Evidence for the role of sulfhydryl groups in a pH-dependent transition of ferredoxin:NADP oxidoreductase, *Arch. Biochem. Biophys. 184*, 572-577.

50. Douglas, P., Kriek, M., Bryant, P., and Roach, P. L. (2006) Lipoyl synthase inserts sulfur atoms into an octanoyl substrate in a stepwise manner, *Angew. Chem. 118*, 5321-5323.

51. Draeger, G., Park, S.-H., and Floss, H. G. (1999) Mechanism of the 2-deoxygenation step in the biosynthesis of the deoxyhexose moieties of the antibiotics granaticin and oleandomycin, *J. Am. Chem. Soc. 121*, 2611-2612.

52. Duin, E. C., Lafferty, M. E., Crouse, B. R., Allen, R. M., Sanyal, I., Flint, D. H., and Johnson, M. K. (1997) [2Fe-2S] to [4Fe-4S] cluster conversion in *Escherichia coli* biotin synthase, *Biochemistry 36*, 11811-11820.

53. Eliasson, R., Fontecave, M., Jornvall, H., Krook, M., Pontis, E., and Reichard, P. (1990) The anaerobic ribonucleoside triphosphate reductase from *Escherichia coli* requires *S*-adenosylmethionine as a cofactor, *Proc. Natl. Acad. Sci. USA 87*, 3314-3318.

54. Eliasson, R., Pontis, E., Sun, X., and Reichard, P. (1994) Allosteric control of the substrate specificity of the anaerobic ribonucleotide reductase from *Escherichia coli*, *J. Biol. Chem. 269*, 26052-26057.

55. Elling, L., Rupprath, C., Guenther, N., Roemer, U., Verseck, S., Weingarten, P.,

Draeger, G., Kirschning, A., and Piepersberg, W. (2005) An enzyme module system for the synthesis of dTDP-activated deoxysugars from dTMP and sucrose, *ChemBioChem 6*, 1423-1430.

56. Esberg, B., Leung, H. -C. E., Tsui, H. -C. T., Björk, G. R. and Winkler, M. E. (1999) Identification of the *miaB* gene, involved in methylthiolation of isopentenylated A37 derivatives in the tRNA of *Salmonella typhymurium Escherichia coli*, *J. Bacteriol. 181*, 7256-7265.

57. Escalettes, F., Florentin, D., Tse Sum Bui, B., Lesage, D., and Marquet, A. (1999) Biotin synthase mechanism: evidence for hydrogen transfer from the substrate into deoxyadenosine, *J. Am. Chem. Soc. 121*, 3571-3578.

58. Excoffier, G., Gagnare, D., and Utille, J. P. (1975) Synthesis of oligosaccharides on polymeric supports. V. Selective cleavage by hydrazine of the anomeric acetyl groups of acetylated glycosyl residues, *Carbohydr. Res. 39*, 368-373.

59. Fang, Q., Peng, J., and Dierks, T. (2004) Post-translational formylglycine modification of bacterial sulfatases by the radical *S*-adenosylmethionine protein AtsB, *J. Biol. Chem. 279*, 14570-14578.

60. Fish, W. W. (1988) Rapid colorimetric micromethod for the quantitation of complexed iron in biological samples, *Methods Enzymol. 158*, 357-364.

61. Flatt, P. M., and Mahmud, T. (2007) Biosynthesis of aminocyclitol-aminoglycoside antibiotics and related compounds, *Nat. Prod. Rep. 24*, 358-392.

62. Frappier, F., Jouany, M., Marquet, A., Olesker, A., and Tabet, J. C. (1982) On the mechanism of the conversion of dethiobiotin to biotin in *E. coli*. Studies with deuterated precursors using tandem mass spectroscopic (MS-MS) techniques, *J. Org. Chem. 47*, 2257-2261.

63. Frey, M., Rothe, M., Wagner, A. F. V., and Knappe, J. (1994) Adenosylmethionine-dependent synthesis of the glycyl radical in pyruvate formate-lyase by abstraction of the glycine C-2 *pro-S* hydrogen atom. Studies of [^{2}H]glycine-substituted enzyme and peptides homologous to the glycine 734 site, *J. Biol. Chem. 269*, 12432-12437.

64. Frey, P. A. (2001) Radical mechanisms of enzymatic catalysis, *Annu. Rev. Biochem. 70*, 121-148.

65. Frey, P. A., Hegeman, A. D., and Ruzicka, F. J. (2008) The radical SAM superfamily, *Crit. Rev. Biochem. Mol. Biol. 43*, 63-88.

66. Frey, P. A., and Magnusson, O. T. (2003) *S*-adenosylmethionine: A wolf in sheep's clothing, or a rich man's adenosylcobalamin?, *Chem. Rev. 103*, 2129-

2148.

67. Goodwin, P. M., and Anthony, C. (1998) The biochemistry, physiology, and genetics of PQQ and PQQ-containing enzymes, *Adv. Microbiol. Physiol. 40*, 1-80.

68. Graham, D. E., Xu, H., and White, R. H. (2003) Identification of the 7,8-didemethyl-8-hydroxy-5-deazariboflavin synthase required for coenzyme F(420) biosynthesis, *Arch. Microbiol. 180*, 455-464.

69. Grewal, T. S., Genever, P. G., Brabbs, A. C., Birch, M., and Skerry, T. M. (2000) Best5: a novel interferon-inducible gene expressed during bone formation, *FASEB J. 14*, 523-531.

70. Hallis, T. M., Zhao, Z., and Liu, H.-w. (2000) New insights into the mechanism of CDP-D-tyvelose 2-epimerase: An enzyme-catalyzing epimerization at an unactivated stereocenter, *J. Am. Chem. Soc. 122*, 10493-10503.

71. Harder, J., Eliasson, R., Pontis, E., Ballinger, M. D., and Reichard, P. (1992) Activation of the anaerobic ribonucleotide reductase from *Escherichia coli* by *S*-adenosylmethionine, *J. Biol. Chem. 267*, 25548-25552.

72. Hayon, E., and Simic, M. (1974) Acid-base properties of free radicals in solution, *Acc. Chem. Res. 7*, 114-121.

73. He, X. M., and Liu, H.-w. (2002) Mechanisms of enzymatic C-O bond cleavages in deoxyhexose biosynthesis, *Curr. Opin. Chem. Biol. 6*, 590-597.

74. Himo, F. (2000) Stability of protein-bound glycyl radical: a density functional theory study, *Chem. Phys. Lett. 328*, 270-276.

75. Hinckley, G. T., and Frey, P. A. (2006) Cofactor dependence of reduction potentials for $[4Fe\text{-}4S]^{2+/1+}$ in lysine 2,3-aminomutase, *Biochemistry 45*, 3219-3225.

76. Jameson, G. N. L., Cosper, M. M., Hernández, H. L., Johnson, M. K., and Huynh, B. H. (2004) Role of the [2Fe–2S] cluster in recombinant *Escherichia coli* biotin synthase, *Biochemistry 43*, 2022–2031.

77. Jeong, L. S., Lim, B. B., and Marquez, V. E. (1994) Synthesis of a 2,3-dideoxy-2,3-difluorofuranose with the D-*lyxo* configuration. An intramolecular rearrangement of methyl 5-*O*-benzoyl-2,3-dideoxy-2,3-difluoro-D-lyxofuranoside observed during the attempted synthesis of 1-(2,3-dideoxy-2,3-difluoro-β-D-lyxofuranosyl)thymine, *Carbohydr. Res. 262*, 103-114.

78. Jiang, J., Biggins, J. B., and Thorson, J. S. (2000) A general enzymatic method for the synthesis of natural and "unnatural" UDP- and TDP-nucleotide sugars, *J. Am.*

Chem. Soc. 122, 6803-6804.

79. Johnson, D. A., Gassner, G. T., Bandarian, V., Ruzicka, F. J., Ballou, D. P., Reed, G. H., and Liu, H.-w. (1996) Kinetic characterization of an organic radical in the ascarylose biosynthetic pathway, *Biochemistry 35*, 15846-15856.

80. Johnson, D. C., Dean, D. R., Smith, A. D., and Johnson, M. K. (2005) Structure, function, and formation of biological iron-sulfur clusters, *Annu. Rev. Biochem. 74*, 247-281.

81. Jordan, A., and Reichard, P. (1998) Ribonucleotide reductases, *Annu. Rev. Biochem. 67*, 71-98.

82. Kim, D. H., Lees, W. J., Haley, T. M., and Walsh, C. T. (1995) Kinetic characterization of the inactivation of UDP-GlcNAc enolpyruvyl transferase by (*Z*)-3-fluorophosphoenolpyruvate: Evidence for two oxocarbenium ion intermediates in enolpyruvyl transfer catalysis, *J. Am. Chem. Soc. 117*, 1494-1502.

83. Kim, J., Darley, D. J., Buckel, W., and Pierik, A. J. (2008) An allylic ketyl radical intermediate in clostridial amino-acid fermentation, *Nature 452*, 239-242.

84. Kim, J., Hetzel, M., Boiangiu, C. D., and Buckel, W. (2004) Dehydration of (*R*)-2-hydroxyacyl-CoA to enoyl-CoA in the fermentation of α-amino acids by anaerobic bacteria, *FEMS Microbiol. Rev. 28*, 455-468.

85. Knappe, J., Blaschkowski, H. P., Groebner, P., and Schmitt, T. (1974) Pyruvate formate-lyase of *Escherichia coli*. Acetyl-enzyme intermediate, *Eur. J. Biochem. 50*, 253-263.

86. Knappe, J., Neugebauer, F. A., Blaschkowski, H. P., and Gaenzler, M. (1984) Post-translational activation introduces a free radical into pyruvate formate-lyase, *Proc. Natl. Acad. Sci. USA. 81*, 1332-1335.

87. Knappe, J., Schacht, J., Moeckel, W., Hoepner, T., Vetter, H., Jr., and Edenharder, R. (1969) Pyruvate formate-lyase reaction in *Escherichia coli*. The enzymic system converting an inactive form of the lyase into the catalytically active enzyme, *Eur. J. Biochem. 11*, 316-327.

88. Knappe, J. S., T. 1976, 71, 1110. (1976) A novel reaction of *S*-adenosyl-L-methionine correlated with the activation of pyruvate formate-lyase, *Biochem. Biophys. Res. Commun. 71*, 1110-1117.

89. Kovac, P., and Glaudemans, C. P. J. (1983) Synthesis of methyl 3-deoxy-3-fluoro-β-D-galactopyranoside, *Carbohydr. Res. 123*, 326-331.

90. Kren, V., and Martinkova, L. (2001) Glycosides in medicine: "the role of glycosidic residue in biological activity", *Curr. Med. Chem. 8*, 1303-1328.

91. Külzer, R., Pils, T., Kappl, R., Hüttermann, J., and Knappe, J. (1998) Reconstitution and characterization of the polynuclear iron-sulfur cluster in pyruvate formate-lyase-activating enzyme. Molecular properties of the holoenzyme form, *J. Biol. Chem. 273*, 4897-4903.

92. Kuzuyama, T., Hidaka, T., Kamigiri, K., Imai, S., and Seto, H. (1992) Studies on the biosynthesis of fosfomycin. 4. The biosynthetic origin of the methyl group of fosfomycin, *J. Antibiot. 45*, 1812-1814.

93. Kuzuyama, T., Seki, T., Dairi, T., Hidaka, T., and Seto, H. (1995) Nucleotide sequence of fortimicin KL1 methyltransferase gene isolated from *Micromonospora olivasterospora*, and comparison of its deduced amino acid sequence with those of methyltransferases involved in the biosynthesis of bialaphos and fosfomycin, *J. Antibiot. 48*, 1191-1193.

94. Laemmli, U. K. (1970) Cleavage of structural proteins during the assembly of the head of bacteriophage T4, *Nature 227*, 680-685.

95. Lauhon, C. T., and Bartlett, P. A. (1994) Substrate analogs as mechanistic probes for the bifunctional chorismate synthase from *Neurospora crassa*, *Biochemistry 33*, 14100-14108.

96. Lee, H. Y., and Khosla, C. (2007) Bioassay-guided evolution of glycosylated macrolide antibiotics in *Escherichia coli*, *PLoS Biology 5*, 243-250.

97. Leriche, C., He, X., Chang, C.-w. T., and Liu, H.-w. (2003) Reversal of the apparent regiospecificity of NAD(P)H-dependent hydride transfer: The properties of the difluoromethylene group, a carbonyl mimic, *J. Am. Chem. Soc. 125*, 6348-6349.

98. Lindberg, B. (1990) Components of bacterial polysaccharides, *Adv. Carbohydr. Chem. Biochem. 48*, 279-318.

99. Liu, A., and Graslund, A. (2000) Electron paramagnetic resonance evidence for a novel interconversion of $[3Fe\text{-}4S]^{+}$ and $[4Fe\text{-}4S]^{+}$ clusters with endogenous iron and sulfide in anaerobic ribonucleotide reductase activase *in vitro*, *J. Biol. Chem. 275*, 12367-12373.

100. Liu, H.-w., and Thorson, J. S. (1994) Pathways and mechanisms in the biogenesis of novel deoxy sugars by bacteria, *Annu. Rev. Microbiol. 48*, 223-256.

101. LoBrutto, R., Bandarian, V., Magnusson, O. T., Chen, X., Schramm, V. L., and Reed, G. H. (2001) 5'-Deoxyadenosine contacts the substrate radical intermediate

in the active site of ethanolamine ammonia-lyase: ^{2}H and ^{13}C electron nuclear double resonance studies, *Biochemistry 40*, 9-14.

102. Lyutzkanova, D., Distler, J., and Altenbuchner, J. (1997) A spectinomycin resistance determinant from the spectinomycin producer *Streptomyces flavopersicus*, *Microbiology 143*, 2135-2143.

103. Magnusson, O. T., Reed, G. H., and Frey, P. A. (1999) Spectroscopic evidence for the participation of an allylic analogue of the 5'-deoxyadenosyl radical in the reaction of lysine 2,3-aminomutase, *J. Am. Chem. Soc. 121*, 9764-9765.

104. Magnusson, O. T., Reed, G. H., and Frey, P. A. (2001) Characterization of an allylic analogue of the 5'-deoxyadenosyl radical: an intermediate in the reaction of lysine 2,3-aminomutase, *Biochemistry 40*, 7773-7782.

105. Mao, U., Varoglu, M., and Sherman, F. H. (1999) Molecular characterization and analysis of the biosynthetic gene cluster for the antitumor antibiotic mitomycin C from *Streptomyces lavendulae* NRRL2564, *Chem. Biol. 6*, 251-263.

106. Marcotte, P. A., and Robinson, C. H. (1982) Inhibition and inactivation of estrogen synthetase (aromatase) by fluorinated substrate analogues, *Biochemistry 21*, 2773-2778.

107. Marquet, A., Frappier, F., Guillerm, G., Azoulay, M., Florentin, D., and Tabet, J. C. (1993) Biotin biosynthesis: synthesis and biological evaluation of the putative intermediate thiols, *J. Am. Chem. Soc. 115*, 2139-2145.

108. Martinelli, M. J., Vaidyanathan, R., Pawlak, J. M., Nayyar, N. K., Dhokte, U. P., Doecke, C. W., Zollars, L. M. H., Moher, E. D., Van Khau, V., and Kosmrlj, B. (2002) Catalytic regioselective sulfonylation of α-chelatable alcohols: scope and mechanistic insight, *J. Am. Chem. Soc. 124*, 3578-3583.

109. Melancon, C. E., III , Hong, L., White, J. A., Liu, Y.-n., and Liu, H.-w. (2007) Characterization of TDP-4-keto-6-deoxy-D-glucose-3,4-ketoisomerase from the D-mycaminose biosynthetic pathway of *Streptomyces fradiae*: *in vitro* activity and substrate specificity studies, *Biochemistry 46*, 577-590.

110. Miller, J., Bandarian, V., Reed, G. H., and Frey, P. A. (2001) Inhibition of lysine 2,3-aminomutase by the alternative substrate 4-thialysine and characterization of the 4-thialysyl radical intermediate, *Arch. Biochem. Biophys. 387*, 281-288.

111. Miller, V. P., Thorson, J. S., Ploux, O., Lo, S. F., and Liu, H.-w. (1993) Cofactor characterization and mechanistic studies of CDP-6-deoxy-$\Delta^{3,4}$-glucoseen reductase: Exploration into a novel enzymic carbon-oxygen bond cleavage event, *Biochemistry 32*, 11934-11942.

112. Moffatt, J. G., and Khorana, H. G. (1961) Nucleoside polyphosphates. X. The synthesis and some reactions of nucleoside 5'-phosphoromorpholidates and related compounds. Improved methods for the preparation of nucleoside 5'-polyphosphates, *J. Am. Chem. Soc. 83*, 649-658.

113. Möhrle, V., Roos, U., and Bormann, C. (1995) Identification of cellular proteins involved in nikkomycin production in *Streptomyces tendae Tü901*, *Mol. Microbiol. 15*, 561-571.

114. Molitor, E. J., Paschal, B. M., and Liu, H.-w. (2003) Cyclopropane fatty acid synthase from *Escherichia coli*: Enzyme purification and inhibition by vinylfluorine and epoxide-containing substrate analogues, *ChemBioChem 4*, 1352-1356.

115. Morita, M., Tomita, K., Ishizawa, M., Takagi, K., Kawamura, F., Takahashi, H., and Morino, T. (1999) Cloning of oxetanocin A biosynthetic and resistance genes that reside on a plasmid of *Bacillus megaterium* strain NK84-0128, *Biosc. Biotechnol. Biochem. 63*, 563-566.

116. Muehlbacher, M., and Poulter, C. D. (1985) Isopentenyl diphosphate:dimethylallyl diphosphate isomerase. Irreversible inhibition of the enzyme by active-site-directed covalent attachment, *J. Am. Chem. Soc. 107*, 8307-8308.

117. Muehlbacher, M., and Poulter, C. D. (1988) Isopentenyl-diphosphate isomerase: inactivation of the enzyme with active-site-directed irreversible inhibitors and transition state analogs, *Biochemistry 27*, 7315-7328.

118. Mulliez, E., Fontecave, M., Gaillard, J., and Reichard, P. (1993) An iron-sulfur center and a free radical in the active anaerobic ribonucleotide reductase of *Escherichia coli*, *J. Biol. Chem. 268*, 2296-2299.

119. Mulliez, E., Ollagnier, S., Fontecave, M., Eliasson, R., and Reichard, P. (1995) Formate is the hydrogen donor for the anaerobic ribonucleotide reductase from *Escherichia coli*, *Proc. Natl. Acad. Sci. USA. 92*, 8759-8762.

120. Noma, A., Kirino, Y., Icheuchi, Y. and Suzuki, T. (2006) Biosynthesis of wybutosine, a hypermodified nucleoside in eukaryotic phenylalanine tRNA, *EMBO J. 25*, 2142-2215.

121. O'Brien, J. R., Raynaud, C., Croux, C., Girbal, L., Soucaille, P., and Lanzilotta, W. N. (2004) Insight into the mechanism of the B_{12}-independent glycerol dehydratase from *Clostridium butyricum*: preliminary biochemical and structural characterization, *Biochemistry 43*, 4635-4645.

122. O'Hagan, D., and Rzepa, H. S. (1997) Some influences of fluorine in bioorganic

chemistry, *Chem. Commun.*, 645–652.

123. Ollagnier, S., Kervio, W., and Rétey, J. (1998) The role and source of 5'-deoxyadenosyl radical in a carbon skeleton rearrangement catalyzed by a plant enzyme, *FEBS Lett. 437*, 309-312.

124. Ollagnier, S., Meier, C., Mulliez, E., Gaillard, J., Schuenemann, V., Trautwein, A., Mattioli, T., Lutz, M., and Fontecave, M. (1999) Assembly of 2Fe-2S and 4Fe-4S clusters in the anaerobic ribonucleotide reductase from *Escherichia coli*, *J. Am. Chem. Soc. 121*, 6344-6350.

125. Ollagnier, S., Mulliez, E., Gaillard, J., Eliasson, R., Fontecave, M., and Reichard, P. (1996) The anaerobic *Escherichia coli* ribonucleotide reductase. Subunit structure and iron sulfur center, *J. Biol. Chem. 271*, 9410-9416.

126. Ollagnier, S., Mulliez, E., Schmidt, P. P., Eliasson, R., Gaillard, J., Deronzier, C., Bergman, T., Graslund, A., Reichard, P., and Fontecave, M. (1997) Activation of the anaerobic ribonucleotide reductase from *Escherichia coli*. The essential role of the iron-sulfur center for *S*-adenosylmethionine reduction, *J. Biol. Chem. 272*, 24216-24223.

127. Ollagnier-de Choudens, S., Sanakis, Y., Hewitson, K. S., Roach, P., Baldwin, J. E., Munck, E., and Fontecave, M. (2000) Iron-sulfur center of biotin synthase and lipoate synthase, *Biochemistry 39*, 4165-4173.

128. Oppermann, U., Filling, C., Hult, M., Shafqat, N., Wu, X., Lindh, M., Shafqat, J., Nordling, E., Kallberg, Y., Persson, B., and Jornvall, H. (2003) Short-chain dehydrogenases/reductases (SDR): the 2002 update. , *Chem. Biol. Interact. 143-144*, 247-253.

129. Paraskevopoulou, C., Fairhurst, S. A., Lowe, D. J., Brick, P., and Onesti, S. (2006) The Elongator subunit Elp3 contains a Fe_4S_4 cluster and binds *S*-adenosylmethionine, *Mol. Microbiol. 59*, 795-806.

130. Parast, C. V., Wong, K. K., and Kozarich, J. W. (1995) Electron paramagnetic resonance evidence for a cysteine-based radical in pyruvate formate-lyase inactivated with mercaptopyruvate, *Biochemistry 34*, 5712-5717.

131. Parast, C. V., Wong, K. K., Lewisch, S. A., and Kozarich, J. W. (1995) Hydrogen exchange of the glycyl radical of pyruvate formate-lyase is catalyzed by cysteine 419, *Biochemistry 34*, 2393-2399.

132. Parry, R. J. (1983) Biosynthesis of some sulfur-containing natural products. Investigations of the mechanism of carbon–sulfur bond formation, *Tetrahedron 39*, 1215-1238.

133. Pauling, L. (1960) *The Nature of the Chemical Bond and the Structure of Molecules and Crystals: an Introduction to Modern Structural Chemistry*, 3nd ed. ed., Cornell Univ. Press, Ithaca, NY.

134. Petrovich, R. M., Ruzicka, F. J., Reed, G. H., and Frey, P. A. (1992) Characterization of iron-sulfur clusters in lysine 2,3-aminomutase by electron paramagnetic resonance spectroscopy, *Biochemistry 31*, 10774-10781.

135. Picciocchi, A., Douce, R., and Alban, C. (2001) Biochemical characterization of the Arabidopsis biotin synthase reaction. The importance of mitochondria in biotin synthesis, *Plant Physiology 127*, 1224-1233.

136. Pieper, P. A., Guo, Z., and Liu, H.-w. (1995) Mechanistic studies of the biosynthesis of 3,6-dideoxy sugars: stereochemical analysis of C-3 deoxygenation, *J. Am. Chem. Soc. 117*, 5158-5159.

137. Pieper, P. A., Yang, D.-y., Zhou, H.-q., and Liu, H.-w. (1997) 3-Deoxy-3-fluoropyridoxamine 5'-phosphate: synthesis and chemical and biological properties of a coenzyme B_6 analog, *J. Am. Chem. Soc. 119*, 1809-1817.

138. Poehlsgaard, J., and Douthwaite, S. (2005) The bacterial ribosome as a target for antibiotics, *Nat. Rev. Microbiol. 3*, 870-881.

139. Pongdee, R., and Liu, H.-w. (2004) Elucidation of enzyme mechanisms using fluorinated substrate analogues, *Bioorg. Chem. 32*, 393-437.

140. Posewitz, M. C., King, P. W., Smolinski, S. L., Zhang, L., Seibert, M., and Ghirardi, M. L. (2004) Discovery of two novel radical *S*-adenosylmethionine proteins required for the assembly of an active [Fe] hydrogenase, *J. Biol. Chem. 279*, 25711-25720.

141. Poulter, C. D., Muehlbacher, M., and Davis, D. R. (1989) Isopentenyl diphosphate isomerase. Mechanism of active-site-directed irreversible inhibition by 3-(fluoromethyl)-3-butenyl diphosphate, *J. Am. Chem. Soc. 111*, 3740-3742.

142. Poulter, C. D., and Satterwhite, D. M. (1977) Mechanism of the prenyl transfer reaction. Studies with (*E*)- and (*Z*)-3-trifluoromethyl-2-buten-1-yl pyrophosphate, *Biochemistry 16*, 5470-5478.

143. QIAGEN (2003) *The QIAexpressionist: A handbook for high-level expression and purification of 6xHis-tagged proteins*, 5th ed., QIAGEN GmbH, Germany.

144. Ramjee, M. N., Balasubramanian, S., Abell, C., Coggins, J. R., Davies, G. M., Hawkes, T. R., Lowe, D. J., and Thorneley, R. N. F. (1992) Reaction of (6*R*)-6-fluoroEPSP with recombinant *Escherichia coli* chorismate synthase generates a stable flavin mononucleotide semiquinone radical, *J. Am. Chem. Soc. 114*, 3151-

3153.

145. Rawlings, B. J. (2001) Type I polyketide biosynthesis in bacteria (Part B), *Nat. Prod. Rep. 18*, 231-281.

146. Read, J. A., Ahmed, R. A., Morrison, J. P., Coleman, W. G., Jr., and Tanner, M. E. (2004) The mechanism of the reaction catalyzed by ADP-β-L-*glycero*-D-*manno*-heptose 6-epimerase, *J. Am. Chem. Soc. 126*, 8878-8879.

147. Reardon, J. E., and Abeles, R. H. (1986) Mechanism of action of isopentenyl pyrophosphate isomerase: evidence for a carbonium ion intermediate, *Biochemistry 25*, 5609-5616.

148. Rebeil, R., Sun, Y., Chooback, L., Pedraza-Reyes, M., Kinsland, C., Begley, T. P., and Nicholson, W. L. (1998) Spore photoproduct lyase from *Bacillus subtilis* spores is a novel iron-sulfur DNA repair enzyme which shares fratures with proteins such as class III anaerobic ribonucleotide reductases and pyruvate-formate lyases, *J. Bacteriol. 180*, 4879-4885.

149. Reddick, J. J., Nicewonger, R., and Begley, T. P. (2001) Mechanistic studies on thiamin phosphate synthase: Evidence for a dissociative mechanism, *Biochemistry 40*, 10095-10102.

150. Reed, G. H. (2004) Radical mechanisms in adenosylcobalamin-dependent enzymes, *Curr. Opin. Chem. Biol. 8*, 477-483.

151. Reed, K. E., and Cronan Jr., J. E. (1993) Lipoic acid metabolism in *Escherichia coli*: sequencing and functional characterization of the *lipA* and *lipB* genes, *J. Bacteriol. 175*, 1325-1336.

152. Rieder, C., Eisenreich, W., O'Brien, J., Richter, G., Götze, E., Boyle, P., Blanchard, S., Bacher, A., and Simon, H. (1998) Rearrangement reactions in the biosynthesis of molybdopterin: an NMR study with multiply $^{13}C/^{15}N$ labeled precursors, *Eur. J. Biochem. 255*, 24-36.

153. Ruzicka, F. J., and Frey, P. A. (2007) Glutamate 2,3-aminomutase: a new member of the radical SAM superfamily of enzymes, *Biochim. Biophys. Acta. 1774*, 286-296.

154. Ruzicka, F. J., Lieder, K. W., and Frey, P. A. (2000) Lysine 2,3-aminomutase from *Clostridium subterminale SB4*: Mass spectral characterization of cyanogens bromide-treated peptides and cloning, sequencing, and expression of the gene kamA in *Escherichia coli*, *J. Bacteriol. 182*, 469-476.

155. Sambrook, J., and Russell, D. W. (2001) *Molecular cloning: A laboratory manual*, 3rd ed., Cold Spring Harbor Laboratory Press, Plainview, NY.

156. Sandala, G. M., Smith, D. M., and Radom, L. (2005) Divergent mechanisms of suicide inactivation for ethanolamine ammonia-lyase, *J. Am. Chem. Soc. 127*, 8856-8864.

157. Santi, D. V., McHenry, C. S., and Sommer, H. (1974) Mechanism of interaction of thymidylate synthetase with 5-fluorodeoxyuridylate, *Biochemistry 13*, 471-481.

158. Sanyal, I., Cohen, G., and Flint, D. H. (1994) Biotin synthase: purification, characterization as a [2Fe-2S] cluster protein, and *in vitro* activity of the *Escherichia coli bioB* gene product, *Biochemistry 33*, 3625-3631.

159. Schlunzen, F., Zarivach, R., Harms, J., Bashan, A., Tocilj, A., Albrecht, R., Yonath, A., and Franceschi, F. (2001) Structural basis for the interaction of antibiotics with the peptidyl transferase centre in eubacteria, *Nature 413*, 814-821.

160. Smith, P., Lin, A., Szu, P.-H., Liu, H.-w., and Tsai, S. C. (2006) Biosynthesis of a 3,6-dideoxyhexose: crystallization and x-ray diffraction of CDP-6-deoxy-L-*threo*-D-*glycero*-4-hexulose-3-dehydrase (E_1) for ascarylose biosynthesis, *Acta Cryst. F62*, 231-234.

161. Sofia, H. J., Chen, G., Hetzler, B. G., Reyes-Spindola, J. F., and Miller, N. E. (2001) Radical SAM, a novel protein superfamily linking unresolved steps in familiar biosynthetic pathways with radical mechanisms: functional characterization using new analysis and information visualization methods, *Nucleic Acids Research 29*, 1097-1106.

162. Song, K. B., and Frey, P. A. (1991) Molecular properties of lysine-2,3-aminomutase, *J. Biol. Chem. 266*, 7651-7655.

163. Stabel, A., Dasaradhi, L., O'Hagan, D., and Rabe, J. P. (1995) Scanning tunneling microscopy imaging of single fluorine atom substitution in stearic acid, *Langmuir 11*, 1427-1430.

164. Stubbe, J., and van der Donk, W. A. (1998) Protein radicals in enzyme catalysis, *Chem. Rev. 98*, 705-762.

165. Sun, X., Eliasson, R., Pontis, E., Andersson, J., Buist, G., Sjoeberg, B.-M., and Reichard, P. (1995) Generation of the glycyl radical of the anaerobic *Escherichia coli* ribonucleotide reductase requires a specific activating enzyme, *J. Biol. Chem. 270*, 2443-2446.

166. Sun, X., Harder, J., Krook, M., Jornvall, H., and Sjoberg, B.-M. (1993) A possible glycine radical in anaerobic ribonucleotide reductase from *Escherichia coli*: Nucleotide sequence of the cloned *nrdD* gene, *Proc. Natl. Acad. Sci. USA. 90*, 577-581.

167. Suzuki, J. Y., Bollivar, D. W., and Bauer, C. E. (1997) Genetic analysis of chlorophyll biosynthesis, *Annu. Rev. Genet. 31*, 61-89.

168. Szu, P.-h., He, X., Zhao, L., and Liu, H.-w. (2005) Biosynthesis of TDP-D-desosamine: Identification of a strategy for C4 deoxygenation, *Angew. Chem. Int. Ed. 44*, 6742-6746.

169. Takahashi, H., Liu, Y.-n., and Liu, H.-w. (2006) A two-stage one-pot enzymatic synthesis of TDP-L-mycarose from thymidine and glucose-1-phosphate, *J. Am. Chem. Soc. 128*, 1432-1433.

170. Thibodeaux, C. J., Melancon, C. E., III , and Liu, H.-w. (2007) Unusual sugar biosynthesis and natural product glycodiversification, *Nature 446*, 1008-1016.

171. Thompson, C. J., and Seto, H. (1995) *Bialaphos: Genetics and Biochemistry of Antibiotic Production*, Vol. 28, Butterworth-Heinemann.

172. Thorson, J. S., Hosted, T. J., Jr., Jiang, J., Biggins, J. B., and Ahlert, J. (2001) Nature's carbohydrate chemists: the enzymatic glycosylation of bioactive bacterial metabolites, *Curr. Org. Chem. 5*, 139-167.

173. Thorson, J. S., Kelly, T. M., and Liu, H.-w. (1994) Cloning, sequencing, and overexpression in *Escherichia coli* of the α-D-glucose-1-phosphate cytidylyltransferase gene isolated from *Yersinia pseudotuberculosis*, *J Bacteriol. 176*, 1840-1849.

174. Thorson, J. S., Lo, S. F., Ploux, O., He, X., and Liu, H.-w. (1994) Studies of the biosynthesis of 3,6-dideoxyhexoses: molecular cloning and characterization of the *asc* (ascarylose) region from *Yersinia pseudotuberculosis* serogroup VA, *J Bacteriol. 176*, 5463-5493.

175. Toraya, T. (2003) Radical catalysis in coenzyme B_{12}-dependent isomerization (eliminating) reactions, *Chem. Rev. 103*, 2095-2128.

176. Torrents, E., Buist, G., Liu, A., Eliasson, R., Kok, J., Gibert, I., Graslund, A., and Reichard, P. (2000) The anaerobic (class III) ribonucleotide reductase from *Lactococcus lactis*. Catalytic properties and allosteric regulation of the pure enzyme system., *J. Biol. Chem. 275*, 2463-2471.

177. Tse Sum Bui, B., Mattioli, T. A., Florentin, D., Bolbach, G., and Marquet, A. (2006) *Escherichia coli* biotin synthase produces selenobiotin. Further evidence of the involvement of the $[2Fe–2S]^{2+}$ cluster in the sulfur insertion step, *Biochemistry 45*, 3824-2834.

178. Ugulava, N. B., Gibney, B. R., and Jarrett, J. T. (2000) Iron-sulfur cluster interconversions in biotin synthase: dissociation and reassociation of iron during

conversion of [2Fe-2S] to [4Fe-4S] clusters, *Biochemistry 39*, 5206-5214.

179. Ugulava, N. B., Sacanell, C. J., and Jarrett, J. T. (2001) Spectroscopic changes during a single turnover of biotin synthase: destruction of a [2Fe–2S] cluster accompanies sulfur insertion, *Biochemistry 40*, 8352–8358.

180. Unkrig, V., Neugebauer, F. A., and Knappe, J. (1989) The free radical of pyruvate formate-lyase. Characterization by EPR spectroscopy and involvement in catalysis as studied with the substrate-analogue hypophosphite, *Eur. J. Biochem. 184*, 723-728.

181. Valverde, S., Hernandez, A., Herradon, B., Rabanal, R. M., and Martin-Lomas, M. (1987) The synthesis of (-)-anamarine, *Tetrahedron 43*, 3499-3504.

182. Wagner, A. F., Demand, J., Schilling, G., Pils, T., and Knappe, J. (1999) A dehydroalanyl residue can capture the 5'-deoxyadenosyl radical generated from *S*-adenosylmethionine by pyruvate formate-lyase-activating enzyme, *Biochem. Biophys. Res. Commun. 254*, 306-310.

183. Wagner, A. F. V., Frey, M., Neugebauer, F. A., Schaefer, W., and Knappe, J. (1992) The free radical in pyruvate formate-lyase is located on glycine-734, *Proc. Natl. Acad. Sci. USA. 89*, 996-1000.

184. Walsby, C. J., Ortillo, D., Broderick, W. E., Broderick, J. B., and Hoffman, B. M. (2002) An anchoring role for FeS clusters: Chelation of the amino acid moiety of *S*-adenosylmethionine to the unique iron site of the [4Fe-4S] cluster of pyruvate formate-lyase activating enzyme, *J. Am. Chem. Soc. 124*, 11270-11271.

185. Walsh, C. T. (2003) *Antibiotics: Actions, Origins, Resistance*, American Society of Microbiology Press, Washington, DC.

186. Webb, M. E., Marquet, A., Mendel, R. R., Rebeille, F., and Smith, A. G. (2007) Elucidating biosynthetic pathways for vitamins and cofactors, *Nat. Prod. Rep. 24*, 988-1008.

187. Westrich, L., Heide, L., and Li, S. M. (2003) CloN6, a novel methyltransferase catalysing the methylation of the pyrrole-2-carboxyl moiety of clorobiocin, *ChemBioChem 4*, 768-773.

188. Withers, S. G., Rupitz, K., and Street, I. P. (1988.) 2-Deoxy-2-fluoro-D-glycosyl fluorides. A new class of specific mechanism-based glycosidase inhibitors, *J. Biol. Chem. 263*, 7929-7932.

189. Withers, S. G., Street, I. P., Bird, P., and Dolphin, D. H. (1987) 2-Deoxy-2-fluoroglucosides: a novel class of mechanism-based glucosidase inhibitors, *J. Am. Chem. Soc. 109*, 7530-7531.

190. Wittmann, V., and Wong, C.-H. (1997) 1*H*-Tetrazole as catalyst in phosphoromorpholidate coupling reactions: Efficient synthesis of GDP-fucose, GDP-mannose, and UDP-galactose, *J. Org. Chem. 62*, 2144-2145.

191. Wong, K. K., Murray, B. W., Lewisch, S. A., Baxter, M. K., Ridky, T. W., Ulissi-DeMario, L., and Kozarich, J. W. (1993) Molecular properties of pyruvate formate-lyase activating enzyme, *Biochemistry 32*, 14102-14110.

192. Wu, W., Lieder, K. W., Reed, G. H., and Frey, P. A. (1995) Observation of a second substrate radical intermediate in the reaction of lysine 2,3-aminomutase: A radical centered on the β-carbon of the alternative substrate, 4-*thia*-L-lysine, *Biochemistry 34*, 10532-10537.

193. Xue, Y., Zhao, L., Liu, H.-w., and Sherman, D. H. (1998) A gene cluster for macrolide antibiotic biosynthesis in *Streptomyces venezuelae*: architecture of metabolic diversity, *Proc. Natl. Acad. Sci. USA. 95*, 12111-12116.

194. Yokoyama, K., Numakura, M., Kudo, F., Ohmori, D., and Eguchi, T. (2007) Characterization and mechanistic study of a radical SAM dehydrogenase in the biosynthesis of butirosin, *J. Am. Chem. Soc. 129*, 15147-15155.

195. Yu, L., Blaser, M., Andrei, P. I., Pierik, A. J., and Selmer, T. (2006) 4-Hydroxyphenylacetate decarboxylases: properties of a novel subclass of glycyl radical enzyme systems, *Biochemistry 45*, 9584-9592.

196. Yu, Y., Russell, R. N., Thorson, J. S., Liu, L.-D., and Liu, H.-w. (1992) Mechanistic studies of the biosynthesis of 3,6-dideoxyhexoses in *Yersinia pseudotuberculosis*. Purification and stereochemical analysis of CDP-D-glucose oxidoreductase, *J. Biol. Chem. 267*, 5868-5875.

197. Zhang, G., Yan, L. Z., Vederas, J. C., and Zuber, P. (1999) Genes of the *sbo-alb* locus of *Bacillus subtilis* are required for production of the antilisterial bacteriocin subtilosin, *J. Bacteriol. 181*, 7346-7355.

198. Zhang, Q., and Liu, H.-w. (2001) Mechanistic investigation of UDP-galactopyranose mutase from *Escherichia coli* using 2- and 3-fluorinated UDP-galactofuranose as probes, *J. Am. Chem. Soc. 123*, 6756-6766.

199. Zhao, L. (2000) Biosynthetic Studies of D-desosamine and Engineered Biosynthesis of Methmycin/Pikromycin Analogs Carrying Modified Deoxysugars, in *Department of Chemistry*, p 238, University of Minnesota, Twin Cities.

200. Zhao, L., Borisova, S., Yeung, S.-M., and Liu, H.-w. (2001) Study of C-4 deoxygenation in the biosynthesis of desosamine: evidence implicating a novel mechanism, *J. Am. Chem. Soc. 123*, 7909-7910.

201. Zhao, L., Sherman, D. H., and Liu, H.-w. (1998) Biosynthesis of desosamine: Molecular evidence suggesting b-glucosylation as a self-resistance mechanism in methymycin/neomethymycin producing strain, *Streptomyces venezuelae*, *J. Am. Chem. Soc. 120*, 9374-9374.

202. Zhao, S., Miller, J. R., Jiang, Y., Marletta, M. A., and Cronan, J. E. J. (2003) Assembly of the covalent linkage between lipoic acid and its cognate enzymes, *Chem. Biol. 10*, 1293-1302.

203. Zhao, Z., and Liu, H.-w. (2001) Synthesis of a deoxy sugar dinucleotide containing an exo-difluoromethylene moiety as a mechanistic probe for studying enzymes involved in unusual sugar biosynthesis, *J. Org. Chem. 66*, 6810-6815.

204. Zhao, Z., Liu, P., Murakami, K., Kuzuyama, T., Seto, H., and Liu, H.-w. (2002) Mechanistic studies of HPP epoxidase: configuration of the substrate governs its enzymatic fate, *Angew. Chem. Int. Ed. 41*, 4529-4532.

Vita

Ping-Hui (Grace) Szu was born in Taipei, Taiwan, R.O.C. on October 23, 1978, the daughter of Wen-Hwa (William) Szu and Chao-Fang Sun. After completing her secondary education at Taipei Municipal Zhongshan Girls' Senior High School in 1997, Grace took the National College Entrance Examination and received admission to National Chung-Cheng University (NCCU), Department of Chemistry (now Department of Chemistry and Biochemistry). At NCCU, she did undergraduate research supported by a National Science Council Undergraduate Research Fellowship from Sept 1998 to June 2001 under the direction of Professor Yung-Son Hon. Her undergraduate work has resulted in two co-authored research articles. In her undergraduate studies, she also completed educational training courses which include a requirement to teach Chemistry in a high school. She graduated from National Chung-Cheng University with B.S. degree in Chemistry in 2001, as the top one student in the class. The following year, Grace entered Graduate School at the University of Texas at Austin, and joined the research group of Professor Hung-wen (Ben) Liu. During her time at UT-Austin, she completed two years as a teaching assistant. She taught Organic Chemistry Laboratory (CH210C), Principles of Chemistry (CH301), and Organic Chemistry (CH610). Her Ph.D. work on the DesII enzyme, a radical SAM enzyme in desosamine biosynthesis has resulted in a co-authored research article and several manuscripts currently in preparation. Her collaboration with Professor Shiou-Chuan (Sheryl) Tsai at the University of California at Irvine on the biochemical and crystallographic studies of CDP-6-deoxy-L-*threo*-D-

glycero-4-hexulose-3-dehydrase (E_1) in the ascarylose biosynthetic pathway has resulted in a co-authored research article and another article under revision.

Permanent address: 11709 Locust Dale CT, Mitchellville, MD 20721

This dissertation was typed by Ping-Hui Szu.